



DEPARTAMENTO DE ENGENHARIA CIVIL
FACULDADE DE CIÊNCIAS E TECNOLOGIA
UNIVERSIDADE DE COIMBRA

STRUCTURAL EVALUATION OF FLEXIBLE PAVEMENTS USING NON-DESTRUCTIVE TESTS

SIMONA FONTUL

Dissertation developed at *Laboratório Nacional de Engenharia Civil* (LNEC), submitted to the *Universidade de Coimbra* (UC) for the degree of Doctor of Philosophy in Civil Engineering, in the frame of the cooperation between UC and LNEC

Lisbon, November 2004



DEPARTAMENTO DE ENGENHARIA CIVIL
FACULDADE DE CIÊNCIAS E TECNOLOGIA
UNIVERSIDADE DE COIMBRA

STRUCTURAL EVALUATION OF FLEXIBLE PAVEMENTS USING NON-DESTRUCTIVE TESTS

AUTHOR:

Simona Fontul
Master in Civil Engineering

SUPERVISERS:

Maria de Lurdes Baptista Costa Antunes
Ph.D., Senior Research Officer at LNEC

Luís Guilherme de Picado Santos
Ph.D., Professor at DEC-FCTUC

Dissertation developed at *Laboratório Nacional de Engenharia Civil (LNEC)*, submitted to the *Universidade de Coimbra (UC)* for the degree of Doctor of Philosophy in Civil Engineering, in the frame of the cooperation between UC and LNEC

Lisbon, November 2004

**Research funded by *Fundação para a Ciência e a Tecnologia* and European Social Fund in the frame of Objective 3
Operational Programme and by LNEC**

**Trabalho de investigação co-financiado pela Fundação para a Ciência e a Tecnologia e pelo Fundo Social Europeu
no âmbito do Terceiro Quadro Comunitário de Apoio e pelo LNEC**

Structural Evaluation of Flexible Pavements using Non-Destructive Tests

Abstract

The aim of this work is to contribute to the improvement of the methodologies used in structural pavement evaluation, concerning in particular the backcalculation of layer moduli based on Falling Weight Deflectometer (FWD) together with Ground Penetrating Radar (GPR) test results. The main aspects that are dealt with are the application of GPR to pavement evaluation, the use of FWD data together with layer thickness data obtained from GPR and the improvement of the efficiency of the backcalculation of pavement layer moduli using Artificial Neural Networks (ANN).

The advantages in using the GPR equipment, as well as the difficulties that occur during testing and data interpretation are addressed. Procedures to overcome some of the problems associated with this technology and to improve the reliability of GPR use are also recommended.

A methodology for structural pavement evaluation using artificial neural networks, based on both FWD and GPR test results is presented. The sensitivity of the proposed method to variations in pavement thickness or to variations in deflections is also addressed.

An application of the proposed method to a runway pavement evaluation is presented. The analysis of the results showed the suitability and advantages of the proposed methodology for structural pavement evaluation. From the experience gathered some recommendations for use of ANN in pavement structural evaluation were drawn, in view of obtaining reliable results.

Caracterização Estrutural de Pavimentos Flexíveis através de Métodos de Auscultação Não Destrutivos

Resumo

O objectivo do presente trabalho é o de contribuir para o aperfeiçoamento das técnicas de ensaio e metodologias de análise para a caracterização estrutural de pavimentos, em particular no que se refere à interpretação de resultados de ensaios de carga com deflectómetro de impacto (FWD) conjuntamente com os do radar (GPR). Os principais aspectos abordados são a aplicação do equipamento radar para pavimentos, a utilização resultados obtidos com o deflectómetro de impacto conjuntamente com espessuras das camadas medidas com o radar e a optimização da interpretação dos resultados de carga utilizando redes neuronais artificiais (ANN).

Abordam-se as vantagens da utilização do radar e referem-se algumas das dificuldades inerentes à realização de ensaios e interpretação de resultados. São apresentadas recomendações relativas à resolução de alguns problemas relacionados com a utilização deste equipamento, visando a melhoria dos resultados obtidos.

Apresenta-se uma metodologia baseada na utilização de redes neuronais artificiais, para a para a caracterização estrutural de pavimentos com base nos resultados obtidos com do deflectómetro de impacto conjuntamente com os do radar. Analisa-se a influência da variação das espessuras das camadas e das deflexões no comportamento da rede neuronal.

Apresenta-se um exemplo da aplicação da metodologia proposta na avaliação de um pavimento aeroportuário. A interpretação dos respectivos resultados permitiu verificar a adequabilidade da metodologia proposta na caracterização estrutural de pavimentos. A experiência recolhida com a utilização desta metodologia permitiu extrair algumas recomendações relativas ao uso de redes neuronais artificiais, tendo em vista a obtenção de resultados fiáveis.

Acknowledgements

This research work has been developed at *Laboratório Nacional de Engenharia Civil* (LNEC), under the supervision of Dr. Maria de Lurdes Antunes, Senior Research Officer and Head of Transportation Infrastructure Division at LNEC and of Dr. Luís Picado Santos, Associate Professor of *Departamento de Engenharia Civil of Faculdade de Ciências e Tecnologia of Universidade de Coimbra*.

The Institutions who contributed to the completion of this thesis are gratefully acknowledged:

The *Laboratório Nacional de Engenharia Civil* for providing material and financial support for this research, in particular the Board of Directors and the Director of Transportation Department, Mr. António Lemonde Macedo.

The *Fundação para a Ciência e a Tecnologia* and European Social Fund for financial assistance through Grant nº PRAXIS XXI / BD / 16086 / 98.

The *Universidade de Coimbra, Departamento de Engenharia Civil of Faculdade de Ciências e Tecnologia* for the support given to the process.

The author wishes to express her gratitude to all persons who have given help and advice in this research. In particular:

Dr. Maria de Lurdes Antunes, not only for the support given by the Infrastructure Division but especially for her excellent supervision, guidance, support and continued encouragement through the course of this work, and also for her friendship.

Professor Luís Picado Santos, for his guidance, encouragement and continued support during this study.

Mr. António Pinelo, former Director of Transportation Department, for his support, interest and helpful discussions, advices and also for his friendship.

Dr. João Marcelino for his expert advice, support and helpful discussion on artificial neural networks.

The colleagues from Infrastructure Division for their cooperation, support and friendship, in particular to Mr. Carlos Pimentel for his assistance during data processing.

The Edition and Graphic Art Division of LNEC for their support and assistance in printing this thesis.

The author highly acknowledges the assistance, support and almost infinite patience of her family, in particular to Mihail and to her parents. Last but certainly not least, a special thanks goes to all her friends, for the care and encouragement shown during these years and for make her feel like home.

The author wishes to dedicate this work to her grandparents.

Table of Contents

1	Introduction	1
1.1	BACKGROUND	1
1.2	OBJECTIVES	4
1.3	STRUCTURE	5
2	Mechanistic Approach to Pavement Design	7
2.1	INTRODUCTION	7
2.1.1	Pavement deterioration mechanisms	7
2.1.2	Pavement design models	9
2.1.3	Considerations of traffic load in pavement design	12
2.2	RESPONSE MODELS	15
2.2.1	Linear elastic approach	16
2.2.2	Non-linear elastic approach	20
2.2.3	Visco-elastic approach	22
2.2.4	Anisotropy	24
2.2.5	Discrete element method (DEM)	25
2.2.6	Software for pavement analysis	26
2.3	PERFORMANCE MODELS	27
2.3.1	Pavement condition indicators	27
2.3.2	Pavement design criteria	27
2.3.3	Residual life	33
2.4	MATERIAL CHARACTERISTICS	35
2.4.1	General concepts	35
2.4.1	Soil and granular materials	36
2.4.2	Bituminous materials	38
2.5	INCREMENTAL MODELS FOR PAVEMENT DESIGN	39
2.6	CRITICAL REVIEW OF PAVEMENT DESIGN METHODS	40

3	Methodologies for Pavement Evaluation	43
3.1	INTRODUCTION	43
3.2	BACKGROUND INFORMATION	46
3.2.1	Historical data	46
3.2.2	Surface condition assessment	47
3.2.3	Complementary tests	50
3.2.4	Traffic and environmental data	53
3.3	NON-DESTRUCTIVE LOAD TESTS	55
3.3.1	Summary of deflection testing equipment	56
3.3.2	Falling Weight Deflectometer (FWD)	62
3.4	LAYER THICKNESS	74
3.5	DIVISION IN SUBSECTIONS	76
3.5.1	Introduction	76
3.5.2	Cumulative difference method	78
3.5.3	Normal distribution criteria	83
3.5.4	Testing statistical significance of sub-sections	84
3.5.5	Final sub-section identification	85
3.5.6	Selection of representative deflection bowl	85
3.6	INTERPRETATION OF THE RESULTS	86
3.6.1	Introduction	86
3.6.2	Pavement Modelling	87
3.6.3	Backcalculation of pavement layer moduli	92
3.6.4	Climatic effects	97
3.7	SUMMARY	99
4	Use of GPR for structural pavement evaluation	101
4.1	INTRODUCTION	101
4.2	GPR EQUIPMENT	103
4.2.1	Available equipment for measurements on road and airfield pavements	103
4.2.2	LNEC's equipment	105

4.3	OPERATION PRINCIPLES	108
4.3.1	General principles	108
4.3.2	Air coupled antennas functioning	109
4.3.3	Electromagnetic characteristics of materials	110
4.3.4	Signal velocity calculation	114
4.4	SURVEY PROCEDURE	118
4.4.1	Survey preparation	118
4.4.2	Equipment settings	119
4.4.3	Data collection	120
4.5	PROCESSING AND INTERPRETATION OF DATA	120
4.5.1	Automatic interpretation	120
4.5.2	Limitations and troubleshooting	122
4.5.3	Detailed interpretation/ calibration	123
4.6	FURTHER APPLICATIONS OF GPR IN PAVEMENTS	124
4.7	SUMMARY	126
5	Artificial Neural Networks	129
5.1	INTRODUCTION	129
5.1.1	From biological neuron to artificial neuron	129
5.1.2	Historical evolution	132
5.1.3	Applications	133
5.1.4	Neural networks vs. conventional computer algorithms	136
5.2	GENERAL CONCEPTS	137
5.2.1	Artificial neuron	137
5.2.2	Activation functions	138
5.2.3	Neural network types	140
5.3	BACKPROPAGATION NEURAL NETWORKS	143
5.3.1	Structure of ANN	143
5.3.2	Training of ANN	144
5.3.3	Learning rule	145
5.3.4	Training troubleshooting	148
5.3.5	Computer program Redes 3	151
5.4	SUMMARY	153

6	Improved method for pavement evaluation	155
6.1	INTRODUCTION.....	155
6.2	SELECTION OF DATA FOR ANALYSIS.....	156
6.3	PRE-PROCESSING OF FWD AND GPR DATA	159
6.4	DEVELOPMENT OF AN ANN FOR INTERPRETATION OF NDT RESULTS.....	162
6.4.1	Introduction	162
6.4.2	Designing and training of ANN for pavement evaluation.....	162
6.4.3	Use of Redes 3 for backanalysis of FWD test results.....	166
6.5	STUDY OF ANN PERFORMANCE.....	167
6.5.1	Introduction	167
6.5.2	Sensitivity to training database type.....	169
6.5.3	Sensitivity to input variation.....	173
6.6	SUMMARY.....	189
7	Application of the proposed methodology to an airport pavement ..	191
7.1	INTRODUCTION.....	191
7.2	BACKGROUND INFORMATION.....	192
7.2.1	Historical information.....	192
7.2.2	Pavement condition assessment.....	193
7.2.3	Complementary tests.....	194
7.2.4	Traffic information.....	196
7.3	SURVEY PROCEDURE.....	197
7.3.1	Deflections	197
7.3.2	Layer thickness.....	198
7.4	DATA PROCESSING.....	199
7.4.1	Division in homogeneous subsections	199
7.4.2	Detailed GPR interpretation.....	203
7.4.3	Pre-processing of FWD and GPR data.....	204
7.5	APPLICATION OF ANN FOR INTERPRETATION OF NDT RESULTS.....	205
7.5.1	Pavement structure modelling using ANN.....	205

7.5.2	ANN training	205
7.5.3	Results	209
7.6	SUMMARY	216
8	Conclusions and Future Developments	217
8.1	CONCLUSIONS	217
8.2	FUTURE DEVELOPMENTS	220
	References	223
Annexes		
	ANNEX 1 – CURRENT FWD ANALYSIS PROGRAMS	249
	ANNEX 2 – ANN PERFORMANCE, SENSITIVITY TO INPUT VARIATIONS RESULTS	257

List of Figures

Figure 2.1 – Main deterioration mechanisms in pavement structures	7
Figure 2.2 – Pavement response and performance models [Ullidtz, P; 2002].....	11
Figure 2.3 – Example of lateral wander traffic distribution on airport pavements [CROW; 1999].....	13
Figure 2.4 – Example of critical positions considered for airport pavement evaluation, for a given group of design aircrafts.....	15
Figure 2.5 – Pavement response model for flexible pavement structure	16
Figure 2.6 – Boussinesq model for a concentrated load.....	17
Figure 2.7 – Odemark's transformation of a two-layered system into a homogeneous half space	19
Figure 2.8 – Typical behaviour of asphalt during constant stress loading (left) and Burgers rheological model (right) [Freire, A.C.; 2003].....	23
Figure 2.9 – Sample of grains during compaction [Ullidtz, P.; 2002].....	25
Figure 2.10 – The test simulation with disk in a particulate medium [Ferrez, J.; et al; 1996].....	25
Figure 2.11 – Pavement serviceability evolution in time [Almeida, J.R. de; 1993].....	28
Figure 2.12 – Different types of rutting [Freire, A.C.; 2002].....	31
Figure 2.13 – Typical variation of pavement condition in time [Hicks, R. G. et al, 1999].....	33
Figure 2.14 – Seasonal variation of subgrade modulus.....	37
Figure 2.15 – Analytical approach suggested for incremental models [COST 333; 1999].....	40
Figure 2.16 – Rating of observed deterioration mechanisms [COST 333; 1999].....	42
Figure 3.1 – Methodology for structural pavement evaluation.....	44
Figure 3.2 – Fatigue equipment LNEC	51
Figure 3.3 - Uniaxial compression testing equipment.....	52
Figure 3.4 – Wheel Tracking equipment LNEC.....	52

Figure 3.5 – Pavement design variables: material’s elastic moduli variation in time [FHWA, 2004a].....	54
Figure 3.6 – Deflection distribution scheme within the pavement structure under FWD action.....	55
Figure 3.7 – “LNEC deflectograph” during tests.....	57
Figure 3.8 – “LNEC deflectograph” functioning scheme.....	57
Figure 3.9 – The Lacroix deflectograph (http://www.cedex.es/cec/documenti/survey.htm).....	58
Figure 3.10 - View of the Danish High Speed Deflectograph.....	59
Figure 3.11 - The Swedish Road Deflection Tester.....	59
Figure 3.12 – Dynaflect [Geo-Log, Inc. 2004].....	60
Figure 3.13 – FWD operating principles.....	63
Figure 3.14 – LNEC’s Falling Weight Deflectometer.....	65
Figure 3.15 – Deflection bowls for different type of pavements.....	68
Figure 3.16 – Calculation of “equivalent temperature” [Antunes, M.L.; 1993].....	69
Figure 3.17 – Influence of different layers on deflection bowl [Almeida, J. R. de;1993].....	73
Figure 3.18 – Core drilling equipment and extracted core.....	75
Figure 3.19 – Cumulative Difference Concept [AASHTO, 2001].....	80
Figure 3.20 – Deflections variation with distance.....	82
Figure 3.21 - Cumulative difference of deflections variation with distance.....	82
Figure 3.22 – Example of final sub-section identification [COST 336, 2002].....	85
Figure 3.23 – Surface modulus plot for one deflection bowl.....	89
Figure 3.24 – Plot of deflection against the inverse of the geophone offset.....	90
Figure 3.25 – Genetic algorithm representation of information (layer moduli) for a Four-Layer Pavement [Fwa, T.F. et al; 1997].....	95
Figure 3.26 – Genetic algorithm operations [Fwa, T.F. et al; 1997].....	95
Figure 3.27 – Flowchart of genetic algorithm [Fwa, T.F. et al; 1997].....	96

Figure 4.1 – GPR operation	102
Figure 4.2 - Examples of dipole close air coupled antennas used for survey at traffic speed [FORMAT; 2004]	104
Figure 4.3 - Examples of GPR with horn antennas [FORMAT; 2004]	105
Figure 4.4 – GPR equipment (main elements)	106
Figure 4.5 – LNEC’s equipment – initial structure: suspension system	107
Figure 4.6 – LNEC’s equipment – actual structure: general view in testing position	107
Figure 4.7 – Typical air-coupled GPR profile [Berthelot, C. et al; 2001]	109
Figure 4.8 - Typical soil dielectric constant variation with water content [King, M.L., 2004]	112
Figure 4.9 – Common mid-point method for signal velocity in surface layer [Highways Agency, 2001]	115
Figure 4.10 – Schematic representation of a WARR survey [Davis, J.L. and Annan, A.P.; 1989]	116
Figure 4.11 – Amplitude estimation method for signal velocity in surface layer of pavement [Highways Agency, 2001]	117
Figure 5.1 – Network of biological neurons [Faley, C.; 2003]	130
Figure 5.2 – Biological neuron [Intrator, N.; 2004]	131
Figure 5.3 – The neuron model [Stergiou, C.; Siganos, D.; 2004]	131
Figure 5.4 – Artificial neuron	137
Figure 5.5 – Sigmoidal function	138
Figure 5.6 – Hyperbolic tangent function	139
Figure 5.7 – Neural network structure	143
Figure 5.8 – Matricial notation for the neural network	146
Figure 5.9 – Derivate of the activation function [Marcelino, J.; 1996]	147

Figure 5.10 – Typical saturation limits for a neuron output [Craven, M.P., 1997]	149
Figure 5.11 – Aspect of an error surface [Koivo, H.N; 2000]	149
Figure 5.12 – Example of error surface, local and global minima [Marcelino, J.; 1989]	150
Figure 5.13 – Backpropagation Neural Networks program flowchart [Marcelino, J.; 1998]	152
Figure 6.1 – Flowchart for pavement structural evaluation – main contributions	156
Figure 6.2– Layer thickness distribution histograms before the statistical analysis	158
Figure 6.3 – Layer thickness distribution histogram (existence of two layers)	158
Figure 6.4 – Cumulative difference of the layer thickness with distance	160
Figure 6.5 – Example of FWD and GPR results plot	161
Figure 6.6 – Flowchart of ANN training for backcalculation of FWD test results [Fontul, S. et al; 2003]	164
Figure 6.7 a) – ANN sensitivity to training conditions	171
Figure 6.7 b) – ANN sensitivity to training conditions – continuation	172
Figure 6.8 a) – Deviation in E1 – ANN A1: training and testing with variable distance to the “rigid” layer datasets	175
Figure 6.8 b) – Deviation in E1 – ANN A1: training and testing with variable distance to the “rigid” layer datasets – continuation	176
Figure 6.9 a) – Deviation in E1 – ANN B2: training and testing with fixed distance to the “rigid” layer datasets	179
Figure 6.9 b) – Deviation in E1 – ANN B2: training and testing with fixed distance to the “rigid” layer datasets– continuation	180
Figure 6.10 – E2 deviation in road pavement case (above) and airport pavement (below)	184
Figure 6.11 – Example of deviation in E3 – A1	185
Figure 6.12 – Example of localised erroneous ANN B4 response	185

Figure 6.13 – Example of ANN response distributed over the same range for negative and positive variation of inputs	186
Figure 6.14 – Example of ANN response distributed over distinct ranges for negative and positive variation of inputs	186
Figure 6.15 – Example of deviation in E1 with 10% variation in D0 – ANN B1	187
Figure 6.16 – Example of deviation in E1 with 10% variation in thickness – ANN B1	188
Figure 7.1 – Pavement structure sketch	192
Figure 7.2 – Pavement surface condition: longitudinal joint (left) and pothole (right)	194
Figure 7.3 – Example of FWD results file – deflections normalised for 150 kN	197
Figure 7.4 – Example of row GPR file – delimitation between the two different structures	198
Figure 7.5 – Cores extracted – general view	198
Figure 7.6 – Cumulative difference for the three central FWD testing profiles (CL, 3mL and R)	201
Figure 7.7 – Pavement structural model	201
Figure 7.8 - Cumulative difference for FWD testing profile – 3mR	202
Figure 7.9 – Layer thickness - GPR results for testing profile 3mR	202
Figure 7.10 – Aspect of GPR file after automatic interpretation	203
Figure 7.11 – Aspect of final GPR file used for calibration based on core data	204
Figure 7.12 – Results obtained for subgrade thickness h3	207
Figure 7.13 – ANN convergence during training	208
Figure 7.14 – Verification of ANN training	209
Figure 7.15 a) – ANN inputs (D0 to D6 and h1, h2) and outputs (E1, E2, E3 and h3)	210
Figure 7.15 b) – ANN inputs (D0 to D6 and h1, h2) and outputs (E1, E2, E3 and h3) – continuation	211
Figure 7.16 – Deflections measured in situ and calculated using ANN pavement structure	212

Figure 7.17 a) – Deflections comparison and average error per deflection.....213

Figure 7.17 b) – Deflections comparison and average error per deflection – continuation...214

Figure 7.18 – Comparison between ANN results and classic approach.....215

Figure 7.19 – Subgrade thickness results.....216

List of Tables

Table 2.1 – Capabilities of pavement evaluation software - mechanistic approach.....	26
Table 2.2 – Main criteria used in pavement design – fatigue cracking in bituminous layers	30
Table 2.3 – Main criteria used in pavement design – permanent deformation.....	32
Table 3.1 – Summary of existing deflection bowl parameters.....	74
Table 4.1 – Range of dielectric constant (ϵ_r) for various materials.....	113
Table 4.2 – List of references presented in Table 4.1.....	114
Table 6.1 – Variable parameters of pavement structure.....	170
Table 6.2 – Case studies - characteristics of data used for ANN training.....	170
Table 6.3 – Variable parameters of pavement structure – range of variation (case A).....	173
Table 6.4 – Deflections obtained – range of variation (case A).....	173
Table 6.5 – Road pavement structure – ANNs used in sensitivity study to input variation..	174
Table 6.6 – Variable parameters of pavement structure (3L) – range of variation (case B)	177
Table 6.7 – Deflections obtained (3L) – range of variation (case B).....	177
Table 6.8 – Variable parameters of pavement structure (4L) – range of variation (case B)	177
Table 6.9 – Deflections obtained (4L) – range of variation (case B).....	178
Table 6.10 – Airport pavement structure – ANNs used in sensitivity study to input variation.....	178
Table 6.11 – Road pavement structure – ANN sensitivity to input variation.....	181
Table 6.12 – Airport pavement structure 3L – ANN sensitivity to input variation.....	182
Table 6.13 – Airport pavement structure 4L, fixed distance to the “rigid” layer – ANN sensitivity to input variation.....	182

Table 6.14 – Airport pavement structure 3L, fixed distance to the “rigid” layer – ANN sensitivity to input variation-results.....	183
Table 7.1 – Pavement foundation characteristics.....	193
Table 7.2 – Aggregate grading of bituminous mixtures.....	195
Table 7.3 – Bituminous mix composition and recovered bitumen characteristics.....	195
Table 7.4 – Traffic information (1990 – 1999).....	196
Table 7.5 – Layer thickness information.....	199
Table 7.6 – Deflections per homogeneous sub-sections (mean and standard deviation)....	200
Table 7.7 – Variable parameters of pavement structure – range of variation.....	206
Table 7.8 – Deflections obtained – range of variation.....	207

List of abbreviations and symbols

ABBREVIATIONS

ANN - Artificial Neural Network

CBR - California Bearing Ratio

ESAL - Equivalent Standard Axle Load

FILTER - FEHRL Investigation on Longitudinal and Transverse Evenness of Roads

FORMAT - Fully Optimised Road Maintenance

FWD - Falling Weight Deflectometer

GPR - Ground Penetrating Radar

IR - Infra Red

ISAP - International Society for Asphalt Pavements

LNEC - *Laboratório Nacional de Engenharia Civil*

LVDT - Linear Variable Differential Transformer

NCHRP - National Cooperative Highway Research Program

NDT - Non- Destructive Tests

NPMA - Northwest Pavement Management Association

SYMBOLS

E_i - elastic modulus (Young's modulus) of i^{th} layer

$E_0(r)$ – the surface modulus at distance “ r ”

$E_{t_r}^{AC}$ - elastic modulus of asphalt normalised for a reference temperature t_r (MPa)

t_r - reference asphalt layer temperature (°C)

ν_i – the Poisson's ratio of the i^{th} layer

h_i - the thickness of the i^{th} layer

ε , ε_x , ε_y - strain, horizontal strain and vertical strain, respectively

ε_6 - the strain corresponding to a fatigue life of 10^6 cycles

σ_z , σ_r , σ_t , τ_{rz} - vertical, radial, tangential and shear stress, respectively

σ_1 , σ_2 , σ_3 - principal stress

θ - sum of principal stresses

M_R - resilient modulus

$P_a = 100$ kPa is the atmospheric pressure

ε_f - maximum tensile strain at the base of asphalt layers;

ε_{pd} - maximum vertical compressive strain in the subgrade;

N_f , N_{pd} - maximum allowable number of wheel loads for fatigue and permanent deformation, respectively

V_b - the binder volume content;

B – Depth from pavement surface to the rigid layer (m)

$c = 3 \times 10^8$ m/s speed of light in vacuum

D_i – deflection measured at i^{th} sensor from test load (μm)

σ_i - standard deviation of deflections

T_d – pavement temperature at desired depth d ($^{\circ}\text{C}$)

T_{surf} – surface temperature ($^{\circ}\text{C}$)

ε_i – the dielectric constant of layer i .

A_1 – the amplitude of reflection from surface (volts)

A_m – the amplitude of reflection from metal plate (volts)

ε_r - relative dielectric constant

v – GPR wave propagation speed (cm/ns)

η - the ANN learning rate

y_i^{k-1} - the output of neuron i of layer $k-1$

E_i - ANN "target" outputs

E_i^{NN} - values calculated by ANN

e_r - ANN "error" ($E_i - E_i^{NN}$)

F – ANN activation function.

N - combined input of an artificial neuron

N - number of wheel passes

t – time;

w_i^0 - initial assigned connection weight

w_{ij} - the weight of the connection between neuron i and neuron j

w_{ij}^k - the weight of the connection between neuron i of layer k to neuron j of layer $k+1$

x_i - input arriving from i^{th} ANN processing element;

Other symbols are defined in the text if necessarily.

1 Introduction

1.1 Background

Roads and airfields are nowadays the communication means most widely used to "connect people" all over the world. The infrastructure condition is an important parameter for the economic and social health of a country. The increase in road traffic volumes and vehicle loads and the recent changes in the heavy truck wheel configuration, from double axle to super singles, contribute to a faster degradation of road pavements condition. Aircraft main gear wheel configurations and loads have also changed. Better and long lasting pavements are needed to meet the present requirements for transport infrastructure.

Pavement maintenance is becoming an important issue, as the construction of new roads tends to decrease, the aggressiveness of traffic loads is increasing and the functional requirements for the existing roads are becoming more demanding. More efficient methods for pavement monitoring and structural evaluation are required in order to ensure a good serviceability and to provide adequate maintenance solutions for the pavements.

The pavements' structural condition is one of the main factors to be taken into account for pavement maintenance planning. Non-Destructive Testing (NDT) of pavements is increasingly being recognised as an effective way to obtain information about their structural behaviour. In order to evaluate the bearing capacity of a pavement, using a mechanistic approach, a structural model of the pavement is required for the estimation of its residual life. This structural model is obtained through interpretation of non-destructive tests. Using layer thickness data as input, the elasticity moduli (E moduli) of the pavement's layers are "backcalculated" from the deflection basin measured with non-destructive load testing equipment. In this way, the pavement bearing capacity is evaluated, and the remaining pavement life can be estimated, taking into account the future traffic.

Several studies on structural evaluation of pavement, using non-destructive load tests, have been developed at *Laboratório Nacional de Engenharia Civil* (LNEC). Almeida Pereira [Pereira, O. A.; 1969] proposed a methodology for interpretation of Benkelman Beam tests, aiming at the estimation of layer moduli from the deflection influence line measured with an LVDT. More recently, [Antunes, M.L, 1993] addressed the structural evaluation of pavements using dynamic non-destructive tests, where various aspects regarding the use and interpretation of Falling Weight Deflectometer (FWD) tests are studied.

The FWD is presently the deflection testing device most widely used in Europe and U.S.A. [COST 336, 2002]. The standard procedure for bearing capacity evaluation using this type of tests is to measure the deflections in considerable number of points. The test points are chosen in order to provide a uniform coverage of the pavement under study. A division of pavement into homogeneous sub-sections is performed, based on the FWD tests and additional background information. Then, for each subsection the backcalculation is performed for a test point, which is considered as “representative”. For the FWD interpretation a pavement structural model is needed, and therefore the layer thickness is required together with pavement material characteristics.

Currently, the information regarding pavement composition is acquired using construction records and stationary tests, such as core drilling and pits (destructive tests). However, there are difficulties in determining the pavement structure with confidence. On one hand the construction records are generally incomplete or unavailable. On the other hand, cores and pits are destructive tests, which require traffic restrictions and give only local information about the pavement structure.

Due to these difficulties in obtaining thickness data in all FWD test points, a selection of “representative” deflection bowls is made for pavement structural evaluation purpose. In these locations, cores are performed for obtaining the layer thickness information required for pavement modelling.

Only recently Ground Penetrating Radar (GPR) tests (non-destructive tests), have began to be used to obtain continuous information on layer thickness and material's characteristics.

With the drastic increase in traffic over the last years, the stationary or slow moving and destructive test procedures have become, not only dangerous for operators and difficult to perform (time consuming) but also with a significant impact on the road users (traffic flow).

It is a general concern nowadays to provide means that can improve safety of road workers and users, during testing and road maintenance works. The FORMAT project (Fully Optimised Road Maintenance) is an European undergoing project, aiming at improving the

efficiency and safety of the European road network [FORMAT, 2002a]. Pavement condition monitoring is one of the four key topics addressed in this project. In a dedicated Work Package, methods, procedures and equipment for monitoring the road pavement condition at traffic speed are studied and improved for future implementation. The characteristics and performance of GPR for pavement thickness measurements are evaluated, as well as its accuracy, type of data able to collect, reliability, speed of monitoring, method of referencing, etc.

The performance and interpretation of GRP test results it is sensitive to the experience of the engineer, as it demands knowledge and engineering judgement in order to obtain realistic results.

The Ground Penetrating Radar is a non-destructive method that has been applied in geological surveys since the 70's [Ulriksen, P.; 1980]. Later, it has become available for pavement evaluation [Maser, K. and Scullion, T.; 1992; Scullion, T.; 1994; Saarenketo, T.; 1992; Van Leest, A.J.; 1998]. LNEC owns a GPR since 1997 and, at that time, the experience on its application for pavement measurements was limited. In geology, the precision it is not a very important issue and the antennas that are used have, in general, low frequencies, providing in this way a deeper penetration but at the same time lower resolution. The interpretation is slower and, usually the material is considered to have the same (dielectric) properties in depth.

With the development of the high frequency antennas and consequently their application on road surveys, the need for an accurate interpretation increased. Some "commercial" computer softwares have been developed, providing semi-automatic interpretation. As a consequence, the data processing has become faster but, at the same time more susceptible to errors. Therefore, a deep knowledge of the equipment, its functioning, together with material characteristics and above all experience and engineering judgement is essential for obtaining realistic results on the pavement structure. Besides, it is important to have a volume of information adequate to the task. Trying to obtain a lot of "information" (such as material moisture content, unbounded layers, etc.) requires more detailed research and validation of results through crosschecking with other data, otherwise can be tricky and erroneous. The intention in this study is to find a "practical" and reliable use of GPR measurements.

At the same time, the use of FWD combined with GPR and core drilling in target locations, can give a more accurate picture of the pavement's structural condition. Therefore, another aim of this study is to improve the efficiency of backcalculation activities using the FWD data together with layer thickness data obtained from GPR, enabling the interpretation of all FWD test points.

1.2 Objectives

This study aims at contributing for a more confident and efficient use of the GPR equipment, as well as for the improvement of the methodology currently used for bearing capacity evaluation based on FWD test results.

An improved methodology for pavement structural evaluation represents an important tool for maintenance and rehabilitation of pavements.

The main purpose of this research work is to develop a procedure for the interpretation of FWD data together with layer thickness data obtained from GPR and, in this way, to contribute to the improvement of the methodology for structural pavement evaluation.

The study represents a continuation of previous research studies developed at LNEC in the field of structural pavement evaluation [Antunes M.L., 1993], already mentioned above. The research carried out concerns the development of GPR survey and data processing procedures and the improvement of backcalculation methods that allow for an efficient interpretation of load tests obtained with the FWD.

GPR is an important tool for pavement evaluation, since it allows for continuous measurement of layer thickness and therefore, a precise identification of changes in pavement structure.

Combining layer thickness distribution obtained through GPR together with FWD results allows for improvements of pavement evaluation methodologies. An adequate backcalculation of layer moduli in all FWD test results becomes feasible in this way, as the pavement structure is known for each FWD test point.

In fact, many of the problems associated with the application of FWD for backanalysis of pavement layer moduli are related to the fact that the layer thickness, determined through coring and test pits on a limited number of locations, is taken as representative of a whole section where this was performed (homogeneous sections).

Taking this into account, this work also focused on the development of more efficient methods for layer moduli backcalculation that can be used for processing a large amount of data, while giving reasonable results.

Taking into account the above mentioned objectives, the following aspects are addressed in this study:

- Ground Penetrating Radar operation and survey procedures. A better understanding of GPR performance when applied to structural pavement evaluation is aimed. The difficulties associated with GPR application are addressed, troubleshooting and the factors that can affect the operation of the equipment are identified and the importance of the detailed interpretation is highlighted.
- Development of an efficient tool for interpretation of results obtained with FWD combined with GPR. Taking into account the large amount of data generated by GPR tests, appropriate methods for the pre-processing and combination of GPR data with FWD data need to be developed. Furthermore, an efficient and reliable tool to perform the interpretation of test results is needed.

This involves the development of a methodology for backcalculation of layer moduli. Among the most up to date available techniques, Artificial Neuronal Networks (ANN) seems to be a promising tool for this purpose. A methodology using ANN is implemented and validated.

The work also comprises application of the methodology to a test site, on an airfield pavement. Although, references are made to rigid pavements, the research presented herein focused mainly on flexible pavement evaluation, as they represent a very high proportion of the Portuguese road and airport infrastructure.

1.3 Outline of the dissertation

The dissertation is organised in 8 chapters, including the Introduction presented in Chapter 1.

Chapter 2 addresses the mechanistic approach to pavement design and evaluation. The pavement deterioration models are mentioned and the pavement structural design process is described. The response models and the performance models for pavement design are addressed, including reference to the residual life concepts. A review on the available knowledge on pavement modelling and design is also made.

Chapter 3 consists basically of a state-of-the-art review of techniques for structural pavement evaluation using mechanistic approach, with special attention given to procedures developed for the interpretation of non-destructive tests performed using FWD and GPR. This includes a summary of methods used for pavement evaluation and the techniques currently available

for back-calculation of pavement layer moduli from measured deflections. Considerations are made on the influence of external factors such as temperature and moisture content on structural condition of pavement. The available methodologies for division into homogeneous sub-sections are mentioned as well as the procedures for the selection of a structural model for pavement evaluation.

A general presentation of the Ground Penetrating Radar equipment is done in Chapter 4. The operation principles and characteristics of the equipments used for pavement evaluation are discussed. Survey procedures and testing conditions are addressed. The Chapter also focuses on the data processing, and reports the experience gathered up to now on the automatic versus detailed interpretation of the results and their calibration using data from cores and pits.

In Chapter 5 the Artificial Neural Network (ANN) technique is described. First, the basic concepts and classification of different types of ANN and their possible applications are referred. References to the most relevant characteristics of the computer program used in this study are included.

An improved methodology for pavement structural evaluation is proposed in Chapter 6. The new approach includes the use of layer thickness obtained with GPR for interpretation of each FWD test point, together with an ANN technique for the backcalculation of layer moduli. The modification and requirements of the ANN when applied to pavement structural evaluation are also referred. A study of the ANN behaviour, reflecting the response of the proposed method to different training options and input variations, is also presented.

An application of the proposed methodology to structural evaluation of an airport pavement is presented in Chapter 7. The main results are presented and analysed.

Finally, Chapter 8 outlines the main conclusions derived from the study and points some future developments.

2 Mechanistic Approach to Pavement Design

2.1 Introduction

2.1.1 Pavement deterioration mechanisms

Pavements are designed in order to provide an adequate surface for traffic circulation without any major deterioration, at a minimum cost.

Pavement material properties change in time under the effect of traffic, climate and ageing and consequently distresses occur, that eventually affect their functional characteristics (Figure 2.1).

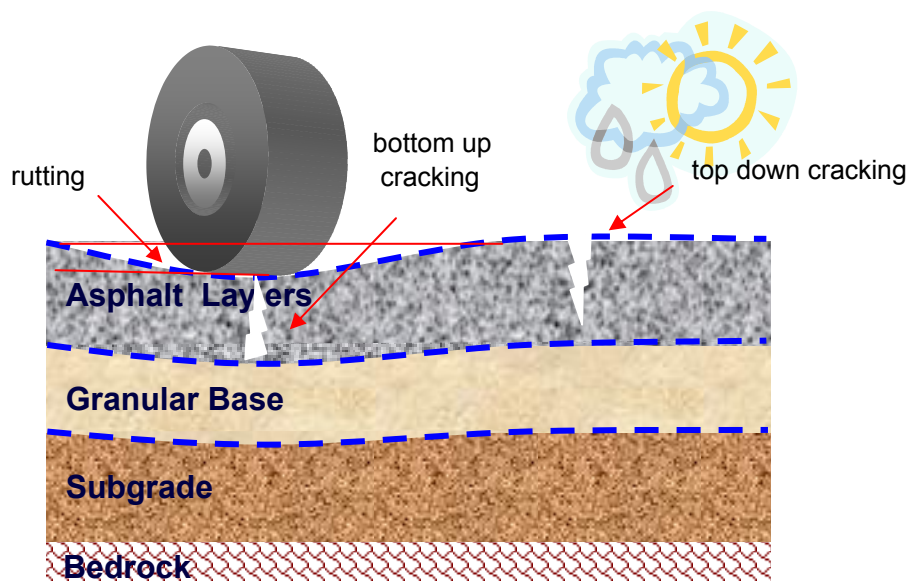


Figure 2.1 – Main deterioration mechanisms in flexible pavement structures

The most relevant deterioration mechanisms specific for each of these factors are briefly presented herein.

2.1.1.1 Traffic associated

Each wheel pass corresponds to a load application in the pavement's surface, inducing a structural damage (elementary damage) in the pavement and "consuming" a small amount of pavement service life. The accumulation of traffic loads during the pavement's life leads to pavement deterioration. The traffic associated deterioration mechanisms are the following:

- ✓ Fatigue of the bound layers due to the repeated application of tensile stresses, which generates cracking at the bottom of these layers ("bottom up" cracking), and eventually propagates upwards to the pavement's surface.
- ✓ Rutting, being a result of the combined effect of permanent deformation of the soil (subgrade), granular materials (base) and bituminous layers, due to repeated traffic loads.
- ✓ Reflective cracking is another type of distress that is traffic associated although other factors, such as temperature variations, also play an important part in this type of deterioration. This phenomenon consists of the propagation of an existing crack or joint, through the bituminous overlay up to the pavement surface. This phenomenon is relevant especially in the case of composite pavements and old cracked bituminous pavements with overlay. The existing cracks in the cementations layers or in the old pavements have vertical movements under the wheel loads and horizontal movements under temperature changes, which cause reflection cracking to the upper layers.

2.1.1.2 Climate associated

The deterioration induced in the pavement's structure depends on the climatic region. In warm countries, the main distresses are rutting of the bituminous layers, bleeding at the surface and bitumen ageing.

Temperature cyclic variations eventually combined with traffic induced stresses lead to micro-cracking of the bituminous bond layers. This distress occurs at pavement surface and

progresses downward to the bottom of the layer, “top down” cracking. This results in water infiltration and crack opening due to freeze-thaw cycles.

In cold climates, the pavement is exposed to degradation due to the freeze-thaw process, resulting in deformation of the subgrade soil and the unbound layers and consequently in cracking of the bound layers [Zang, W. and Macdonald, R.A.; 2000]. In addition, the brittleness of the bitumen and the use of salts for de-icing can cause surface cracking and corrosion. [Salt Institute, 2000]. The use of studded tyres is another distress factor that substantially increases the development of rutting.

In case of unbound materials the main deterioration induced in the pavement structure associated with climate is related with its' sensibility to freeze-thaw cycles and to moisture variation during the year.

2.1.1.3 Time associated

In time the organic structure of bitumen changes, which results in distresses like ageing, hardening, ravelling, chemical alterations. In time, the stiffness of the bitumen increases, the elastic recovery diminishes, the colour becomes lighter and the bond between aggregates and bitumen gets fragile. This leads to loss of aggregates at pavement surface, distress known as ravelling or fretting [FORMAT, 2003]. This phenomenon is more significant in the case of open graded mixtures. The ageing and ravelling can develop into cracking, but in this case from the top of the pavement to the bottom (“top down cracking”). The cracks will result in water infiltration and the consequent unbound layer deterioration.

2.1.2 Pavement design models

In order to design a pavement, or to evaluate the residual life of an existing one, a model is required, which will reproduce as close as possible the real condition of the pavement, in terms of effect of the traffic load in the pavement's structure, under certain climatic conditions.

The modelling is usually performed on a bottom to top base, in other words, starts with the foundation characteristics and successively the sub-base and the base layers and finally the surface layers are considered. The loading is modelled as a vertical pressure uniformly distributed over a circular area on the surface of the pavement.

Historically speaking, the first approach to pavement design was **empirical**. Within this approach, the design is made using the characteristics of the subgrade and the traffic for the design period as input. The pavement layer materials are supposed to have standard performance, and the design thickness is determined through a series of design charts.

These charts were developed from a number of experiments performed on full-scale pavement structures built on different types of subgrade, and under different climatic conditions.

The only criterion considered in empirical pavement methods is the shear failure in the subgrade. Some empirical methods are: U.S Army Corps of Engineers Waterways Experiment Station (WES) which is based on the California Bearing Ratio (CBR) criteria [Yoder, E.J. and Wittczak, M.W.; 1975]; State California Method using stabilometer "R" value [WSDOT Pavement Guide]; Road Note 29 [Road Research Laboratory, 1970].

Traffic evolution in time required changes in design methodologies. New materials were used and different pavement structures were adopted. Consequently, the empirical methods were no longer applicable and the need for more fundamental, **mechanistic** approaches to pavement design was higher. Various forms of distress should be considered within this approach, and the most critical deterioration models should be identified for each type of structure. The response of the pavement to traffic loads must be determined using an appropriate model.

In the 1940's Burmister developed a first theory to solve the two-layered system problem (one layer resting on a linear elastic half-space) and later extended it to a three-layered system [Bursmister, 1943; Bursmister, 1945]. With the technological progress the Bursmister model was extended to deal with multi-layered system, and several computer programmes have been developed, such as ELSYM 5 [Kopperman, S. *et al*, 1985] and BISAR [SHELL, 1995].

The theory is based on the classical theory of elasticity and the following assumptions [Irwin, L.H.; 2002] are made: all materials are homogeneous, isotropic and linear elastic, layers are considered to be continuous and infinite horizontally and to have a finite thickness, the load applied at the surface is uniformly distributed over a circular area and the system is considered axi-symmetric.

This design procedure is generally an iterative one and the final result will be a combination of materials and layer thickness, which insure the required performance under traffic and environmental factors during a certain period of time (service life).

A mechanistic approach is now being widely used in pavement design and evaluation methods. These methods consist of the following steps [Zhang, W. and Ullidtz, P.; 2002]:

1. Set-up a mechanistic model for the pavement, usually a combination of a response model with deterioration models;
2. Calculate the critical stresses and strains under the design load using a response model;
3. Use deterioration models to relate the calculated stresses and strains with the pavements' residual life, e.g. number of load repetitions until failure occurs.

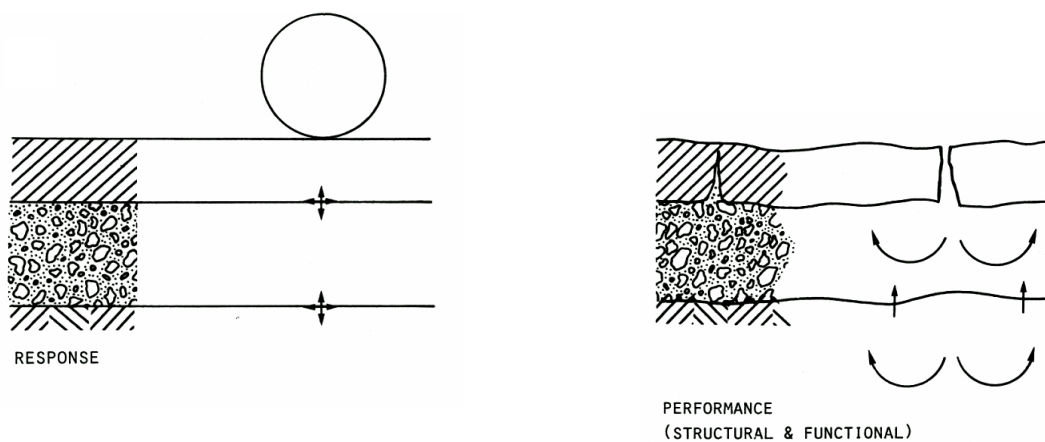


Figure 2.2 – Pavement response and performance models [Ullidtz, P.; 2002]

In order to evaluate the bearing capacity of a pavement, using a mechanistic approach, a structural (response) model of the pavement is required for the estimation of its residual life.

For the design of new pavements, this involves choosing the type of material that will be used in the construction and estimating their mechanical properties according to their nature, and the layer thickness.

When dealing with existing pavements, this task involves the assessment of the actual layer thickness and material characteristics.

2.1.3 Considerations of traffic load in pavement design

2.1.3.1 Road pavements

As already mentioned, heavy vehicles traffic causes damages to the pavement structure that are directly related with the axle weight and configuration. For the design and evaluation purposes, the load is assumed to be a static vertical load stress uniformly distributed over a circular area [Yoder, E.J.; and Witczak, M.W.; 1975; ICAO, 1983; FAA, 1978; ICAO, 1983].

For road pavements, only the effect of heavy vehicle traffic is taken into consideration for designing and evaluation purposes, as it is considered to be the most aggressive. The effect of passenger cars is considered negligible when compared to this one. The wheel loads are often represented by one dual wheel axle configuration so called standard axle load [AASHTO; 2001]. The most commonly used standard axles (expressed in terms of total axle load) are the followings: 80 kN, 100 kN and 130 kN. For each standard axle load there are associated the following characteristics: a vertical load per wheel, a contact radius, a contact pressure, and a distance between wheels. In Portugal [JAE, 1995] the 80 kN standard axle load is usually adopted for flexible pavement design and 130 kN for rigid and composite pavement design. During last years, there is a growing tendency for considering the 130 kN standard axle load in all studies due to changes in heavy vehicle wheel configurations [LCPC, 1997].

The traffic spectrum is converted into equivalent repetitions of standard axle load (ESAL) using the following equation [Yoder, E.J.; and Witczak, M.W.; 1975], which has been developed from the experimental results of the AASHTO Road Trials:

$$N_s = N \left(\frac{L}{L_s} \right)^\alpha \quad (2.1)$$

Where:

- N - number of passes of axle load L ;
- N_s - number of passes of equivalent standard axle load L_s ;
- L - passing axle load;
- L_s - standard axle load;
- α - parameter that depends on the type of pavement ($\alpha = 4$ for flexible pavements tested during the AASHTO Road Test).

In most cases, the value adopted for the parameter α is 4 ("4th Power Damage Law). Recent studies [OECD; 1991] have shown that variations to this rule occur and therefore proposed other coefficients ranging from 2 to 9 for flexible pavements, depending on several issues such as type of design criteria or pavement condition. In case of semi-rigid and rigid

pavements the power coefficient of the above relationship is ranging between 11 and 33 [Quaresma, L.M.; 1992].

In reality, the deterioration process induced by traffic is more complex. Therefore, correction factors are applied for considerations of various factors such as road width, lane distribution, wide base tyre [CROW; 1998].

Usually, the future traffic panorama for all vehicle classes is difficult to predict and only information on the heavy vehicle traffic is available. In this situation, damage factors are applied for calculating the number of equivalent standard axle loads based on the number of heavy traffic (lorry). These damage factors are specific to country and region and depend on the traffic intensity of the road and the type of road [JAE, 1995; LCPC, 1997; Asphalt Institute, 1991; Austroads, 2002; MOPU, 1990]. The Portuguese Road Administration uses different damage factors as a function of the Average Daily Traffic at the beginning of the pavement service life [JAE; 1995]. This organisation has promoted measurements of traffic aggressiveness in the Portuguese main road network [Lima, H. *et al*; 1999]

2.1.3.2 Airport pavements

The main difference on traffic consideration in case of airport pavements is the fact that the traffic is expressed as the number of passes of the main gear of a group of “design” aircrafts. The increased complexity of traffic spectrum, in terms of loads, wheel arrangement and tire pressure would lead to erroneous results if only one standard aircraft would be used, mainly due to the transversal distribution of traffic lanes and traffic lateral wander (see Figure 2.3).

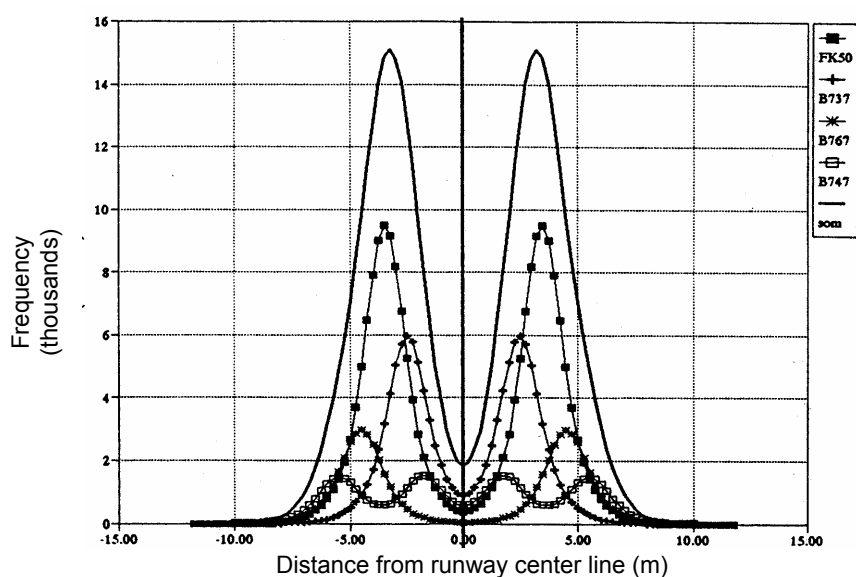


Figure 2.3 – Example of lateral wander traffic distribution on airport pavements [CROW; 1999]

Research studies have shown that aircraft traffic lateral distribution across runways may be represented by a normal (bell shaped) distribution [ICAO, 1983; NATO; 2000]. This aspect is taken into account by converting the number of passes into coverages. The coverage is a measure of the number of maximum stress applications that occur on the surface of the pavement due to traffic loads [ICAO, 1983; FAA, 1978; Antunes, M.L.; 1993; NATO; 2000] and is always lower or equal to the number of passes. Each pass can be converted to coverages using a pass-to-coverage ratio, which is developed assuming a normal distribution of traffic. This ratio depends on the wheel gear characteristics (load, geometry and tire pressure), location on the pavement (runway ends, runway central area or taxiway) and the type of pavement (flexible or rigid).

The consideration of all aircraft that operates in an airport separately is unpractical. Therefore, the methodology generally adopted [ICAO, 1983; FAA, 1978; Antunes, M.L.; 1993] for airport pavement evaluation considers the traffic spectrum divided into main classes, each of them with similar characteristics in terms of load (light, medium and heavy aircrafts). A “design aircraft” is chosen within each of these groups and is used for pavement evaluation.

The following calculations are made for each aircraft group:

- ✓ the landing gear type of all aircrafts is converted to the design aircraft landing gear;
- ✓ the annual departures are converted to equivalent annual departure of the design aircraft. This can be done using the following equation [FAA, 1978; ICAO; 1983]:

$$\log R_1 = \log R_2 \left(\frac{W_2}{W_1} \right)^{\frac{1}{2}} \quad (2.2)$$

Where:

- R_1 - equivalent annual departure by the design aircraft;
 - R_2 - annual departures of the aircraft in question (expressed in designed aircraft landing gear);
 - W_1 - wheel load of the design aircraft;
 - W_2 - wheel load of the aircraft on question.
- ✓ the passes of the design aircraft are converted into coverages using appropriate pass-to coverage ratios.

Finally, critical sections are selected for pavement evaluation taking into account the design aircrafts landing gear configuration. Figure 2.4 presents an example of lateral location of three design aircrafts main gears (Boeing 757-300, Lockheed 1011-500 and Boeing 737-800) and the critical sections considered for pavement evaluation (1, 2, 3 and 4).

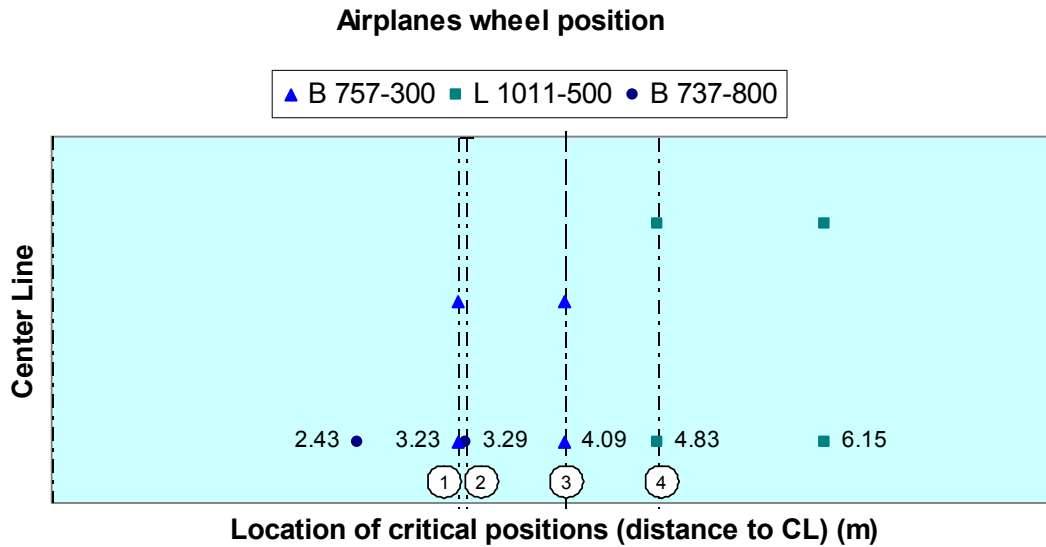


Figure 2.4 – Example of critical positions considered for airport pavement evaluation, for a given group of design aircrafts

2.2 Response models

The response model can be briefly defined as a computing algorithm that supplies the response of the structure to a certain load (P) in terms of the stresses, strains and displacements [AMADEUS, 1999]. The response model is a detailed model of the pavement structure taking into account the pavement geometry (layer thickness (h)) and materials characteristics. It aims at simulating the existing pavement behaviour, as close to reality as possible, in terms of response to a certain load (P), usually modelled as a vertical pressure (p_0) uniformly distributed over a circular area of a radius (a) (see Figure 2.5).

In summary, in order to model the pavement response, the following elements must be defined:

- ✓ The structure geometry (for example layer thickness (h), when the layer is modelled as a multi layer system);
- ✓ The type of materials and their constitutive laws (for example E moduli and Poisson's ratios if the materials are considered as linear elastic);

- ✓ The loads (for example the vertical pressure and the load radius, in case the wheel loads are modelled as uniformly distributed vertical pressure on a circular area).

For the purpose of pavement evaluation, non-destructive load tests (NDT) are performed and the measured deflections are then used to derive a response model of the pavement structure as close as possible to the real situation, when the pavement is loaded by traffic. The definition of a structural model using NDT is usually an iterative process. Within this process, the parameters of the pavement model (geometrical and material properties) are gradually changed, until the calculated response given by the pavement model under the test load will match the response measured in situ.

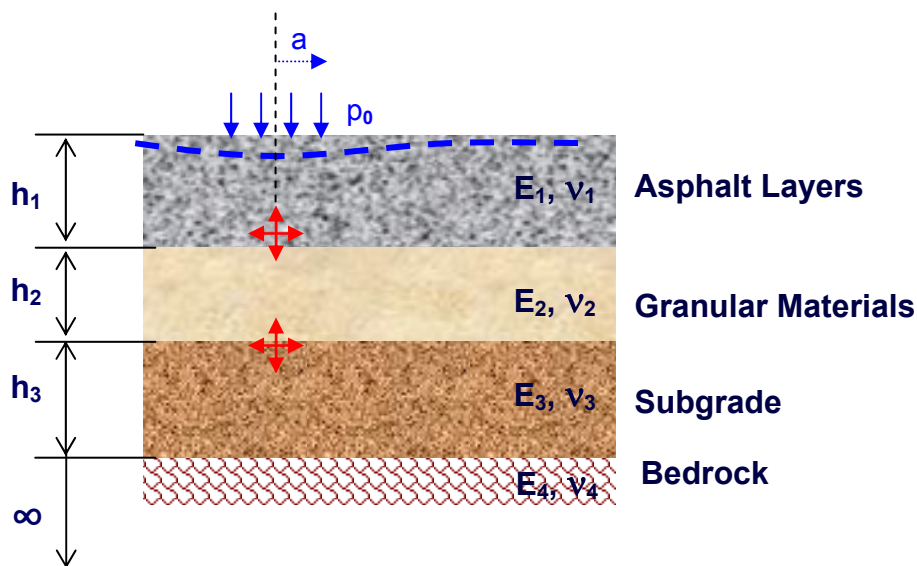


Figure 2.5 – Pavement response model for flexible pavement structure (stresses, strains and deflections)

The main response models used for pavement design are briefly presented herein, as well as their advantages and disadvantages.

2.2.1 Linear elastic approach

2.2.1.1 Boussinesq half space

Modelling of the pavement structure as a system of homogeneous linear elastic horizontal layers is widely used. Several “idealisations” are assumed within this approach, mainly related to the material characteristics and geometric dimensions, in order to provide a simple

method for pavement modelling. More complex aspects such as non-linearity, anisotropy or visco-elasticity of the materials or different geometries are not taken into consideration within this type of model.

The first equations for calculating stresses, strains and displacements in a linear-elastic semi-infinite space were developed by Boussinesq at the end of XIXth century. Initially it applied for the case of a point load (P) acting on the surface (Figure 2.6), and it was later adapted to distributed load (ex. circular load of radius a and pressure p_0) and latter for stiff plate loading.

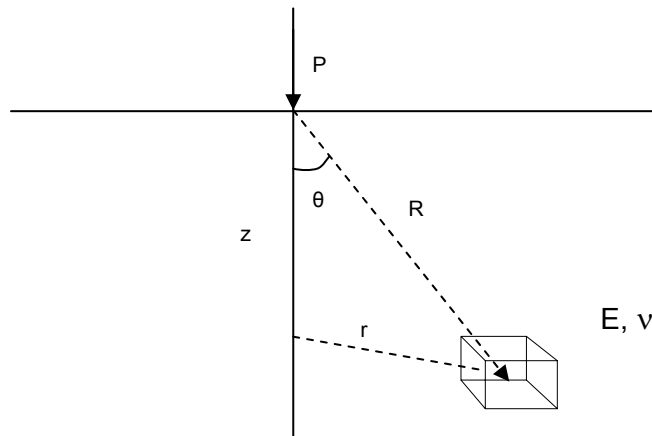


Figure 2.6 – Boussinesq model for a concentrated load

Boussinesq equations [Marchand, J.P. *et al*; 1981; Ullidtz, P.; 1987; Yoder, E.J.; and Witczak, M.W.; 1975]:

Normal stresses:

$$\begin{aligned}\sigma_z &= 3P / (2\pi R^2) * \cos^3 \Theta \\ \sigma_r &= P / (2\pi R^2) * [3 \cos \Theta \sin^2 \Theta - (1 - 2\nu) / (1 + \cos \Theta)] \\ \sigma_t &= P / (2\pi R^2) * (1 - 2\nu) [-\cos \Theta + 1 / (1 + \cos \Theta)] \\ \sigma_1 &= 3P / (2\pi R^2) * \cos \Theta \\ \sigma_v &= 1/3(\sigma_1 + \sigma_2 + \sigma_3) = P / (3\pi R^2) * (1 + \nu) * \cos \Theta\end{aligned}\tag{2.3}$$

Shear stresses:

$$\tau_{rz} = 3P / (2\pi R^2) * \cos^2 \Theta * \sin \Theta$$

$$\tau_{rt} = \tau_{tz} = 0$$

Normal strains:

$$\varepsilon_z = (1+\nu)P / (2\pi R^2 E) * (3 \cos^3 \Theta - 2\nu \cos \Theta)$$

$$\varepsilon_r = (1+\nu)P / (2\pi R^2 E) * [-3 \cos^3 \Theta + (3-2\nu)\cos \Theta - (1-2\nu)/(1+\cos \Theta)]$$

$$\varepsilon_t = (1+\nu)P / (2\pi R^2 E) * [-\cos \Theta + (1-2\nu)/(1+\cos \Theta)]$$

$$\varepsilon_v = \varepsilon_z + \varepsilon_r + \varepsilon_t = (1+\nu)P / (3\pi R^2) * (1+\nu) * \cos \Theta$$

Displacements:

$$d_z = (1+\nu)P / (2\pi R E) * (2(1-\nu) + \cos^2 \Theta)$$

$$d_r = (1+\nu)P / (2\pi R E) * [\cos \Theta \sin \Theta - (1-2\nu)\sin \Theta / (1+\cos \Theta)]$$

$$d_t = 0$$

This model has been used for design purposes, namely to calculate the thickness of the layer above the foundation in order to avoid that the stress at the top of foundation layer exceeds a certain limit. It is also used in the interpretation of plate loading tests.

These equations are widely used in the backcalculation programs. In time, the need for improved pavement models, together with the development of computers, led to the development of multi-layered system models, which allowed for a better simulation of real pavement response.

2.2.1.2 Method of equivalent thickness (Odemark's method)

This method provides a simple and fast algorithm to calculate stresses and strains in layered systems due to a circular load applied at the surface [COST 333; 1999]. Odemark's method is used for transforming a layered system into a semi-infinite elastic half-space on which Boussinesq's equations may be used. Odemark's method is based on the assumption that the stresses and strains below a layer depend on the stiffness of that layer only. [Ullidtz, P.; 1987; Ullidtz, P.; 1998]. If the thickness, elastic modulus and Poisson's ratio of a layer are

changed, but the flexural stiffness (D) remains unchanged, the stresses and strains below the layer should also remain unchanged. In other words, a layer with a given thickness h_1 , a given modulus E_1 and a given Poisson ratio ν_1 can be assimilated as a layer of another material characterised by E_2 and ν_2 , with an equivalent thickness (h_e), which is calculated in order to get the same flexural stiffness (Figure 2.7).



Figure 2.7 – Odemark’s transformation of a two-layered system into a homogeneous half space

Based on this assumption, the equivalent thickness of the layer can be calculated using the following equations:

$$D = \frac{h^3 E}{12(1-\nu^2)} \text{ and } D_1 = D_2 \text{ results:} \quad (2.4)$$

$$\frac{h_1^3 E_1}{1-\nu_1^2} = \frac{h_e^3 E_2}{1-\nu_2^2} \text{ or } h_e = h_1 \cdot \sqrt[3]{\frac{E_1}{E_2} \times \frac{1-\nu_2^2}{1-\nu_1^2}} \quad (2.5)$$

where:

- D is the flexural stiffness (MNm);
- h_e is the “equivalent” thickness(m).

The accuracy of results obtained with this method varies between 89% and 92% of the values obtained from the theory of elasticity [Ullidtz, P.; 1998]. This method represents an attractive solution for network level studies due to its simplicity and efficiency, but at the same time, it may provide less accurate results.

2.2.1.3 Multi-layer linear elastic model

The theory is based on the classical theory of elasticity and its simplicity is given by the following assumptions [Irwin, L.H.; 2002]:

- ✓ all materials are homogeneous, isotropic and linear elastic and no inertia effect is considered;
- ✓ layers are considered to be continuous and infinite horizontally.

- ✓ all layers have a finite thickness except the bottom layer, which is considered to be a semi-infinite half-space.
- ✓ the surface load is uniformly distributed over a circular area;
- ✓ the system is considered axi-symmetric.

The pavement is modelled as a layered system and the materials are characterised by the elastic modulus E and Poisson ratio ν (Figure 2.5).

Some of the misjudges made when applying the linear-elastic theory to pavements are related to the followings:

- ✓ the granular materials have non-linear (stress depending) response;
- ✓ the bituminous materials have a visco-elastic behaviour;
- ✓ the loads are not static but dynamic.

Some more “sophisticated” models are being developed in the attempt to bring the pavement models closer to reality.

2.2.2 Non-linear elastic approach

One of the aspects that are not addressed in the previous models is the materials non-linearity. In reality, the materials present a stress dependent, or “non-linear”, behaviour, which is more important for granular materials and cohesive soils. [Ullidtz, P.; 1998; AMADEUS, 1999; Irwin, L; 2002, Gomes Correia, A.; 1999]]. Depending on aspects such as gradation and moisture content, the modulus can either increase or decrease as the load stress increases. There are two different concepts, depending on material.

For granular materials, the modulus is assumed to be a function of bulk stress, or first stress invariant, ($\theta = \sigma_1 + \sigma_2 + \sigma_3$). The resilient modulus (M_R), which is the deviator stress divided by the reversible strain, is calculated using the “ $k - \theta$ model”:

$$M_R = k_1 \theta^{k_2} \quad (2.6)$$

Where:

- k_1 - constant that depends on material type, ranging from 1600 to 9000;
- k_2 - constant that depends on material type, ranging from 0.4 to 0.7 [Freire, A.C.; 1994].

For cohesive materials, the nonlinearity is generally expressed as follows:

$$M_R = k_1 \sigma_d^{k_2} = k_1 (\sigma_1 - \sigma_3)^{k_2} \quad (2.7)$$

Where:

- σ_d - deviator stress;
- k_2 is negative, which means that the modulus is decreasing with increasing σ_d .

A more realistic model, assuming that the resilient modulus depends both on first stress invariant and the deviator stress was developed by Uzan [Uzan, J. *et al*; 1992],:

$$M_R = k_1 \theta^{k_2} \sigma_d^{k_3} \quad (2.8)$$

or in its non-dimensional form:

$$M_R = k_1 P_a \left(\frac{\theta}{P_a} \right)^{k_2} \left(\frac{\sigma_d}{P_a} \right)^{k_3} \quad (2.9)$$

Where:

- $P_a = 100$ kPa is the atmospheric pressure.

This equation can be used as a “universal materials model” for both granular and fine-grained materials [Uzan, J. *et al*; 1992].

In the tridimensional case, the deviatoric stress is replaced by the octahedral stresses as follows:

$$M_R = k_1 P_a \left(\frac{\theta}{P_a} \right)^{k_2} \left(\frac{\tau_{oct}}{P_a} \right)^{k_3} \quad (2.10)$$

Where:

$$\tau_{oct} = \frac{1}{3} \sqrt{(\sigma_1 - \sigma_2)^2 + (\sigma_2 - \sigma_3)^2 + (\sigma_3 - \sigma_1)^2} \quad (2.11)$$

A non-linear elastic model, taking into consideration the effect of the stress path was proposed by Boyce, as referenced by [Gomes Correia, A.; 1999]. In this model the bulk modulus K, and the shear modulus G are functions of the first stress invariant (θ) and the deviatoric stress (σ_d) [Balay, J.; *et al*; 1997; Akon, Y.; *et al*; 1999; Gomes Correia, A.; 1999]:

$$\begin{aligned} K &= \theta / \varepsilon_v \quad \text{and} \\ G &= \sigma_d / 3 \times \varepsilon_q \end{aligned} \quad (2.12)$$

where:

- ε_v - volumetric strain;
- ε_q - shear strain.

The values of K and G can be related to the stress applied by the following equations:

$$K = \frac{K_a \left(\frac{\theta}{P_a} \right)^{1-n}}{1 - \beta \left(\frac{\sigma_d}{\theta} \right)^2} \quad (2.13)$$

$$G = G_a \left(\frac{\theta}{P_a} \right)^{1-n}$$

$$\beta = (1-n) \frac{K_a}{6 \times G_a}$$

where:

- K_a , G_a and n - constants;
- $P_a = 100$ kPa is the atmospheric pressure.

The Boyce model was subject of improvement, among which the consideration of anisotropy within the model, by multiplying the principal stress σ_1 by a coefficient of anisotropy γ .

Most backcalculation programs treat all layers as being linear elastic, ignoring the stress-dependency [Irwin, L.H.; 2002]. A few programs allow the subgrade layer to be stress-dependent, while MODCOMP allows all layers to be non-linear. A simple way to consider the non-linearity is to substitute the modulus by a non-linear function of the major principal stress. A more fundamental way is to express the volume strain and deviator strain as functions of the hydrostatic and deviator stress. Finite element programs were developed in the 60's, to better accommodate the non-linear characteristics of the materials. Later this type of models was used in backcalculation [Almeida, J.R. de; 1993].

2.2.3 Visco-elastic approach

Bituminous materials, which play a major role in the flexible pavement structures currently adopted, are known to have visco-elasto-plastic behaviour.

In order to model this behaviour a viscous element, which is symbolised by shock absorbers, have to be included in the model together with the elastic component, symbolised by springs. In this way, the visco-elastic pavement behaviour can be modelled either considering those elements in series or in parallel, bringing the results closer to real pavement response to wheel loads.

Figure 2.8 presents the type of visco-elastic material response simulation during stress loading. Several models, such us Kelvin, Maxwell, Burgers [Freire, A.C., 2002] can be used

to simulate the bituminous materials response. One of the models, most widely applied is the Burgers model.

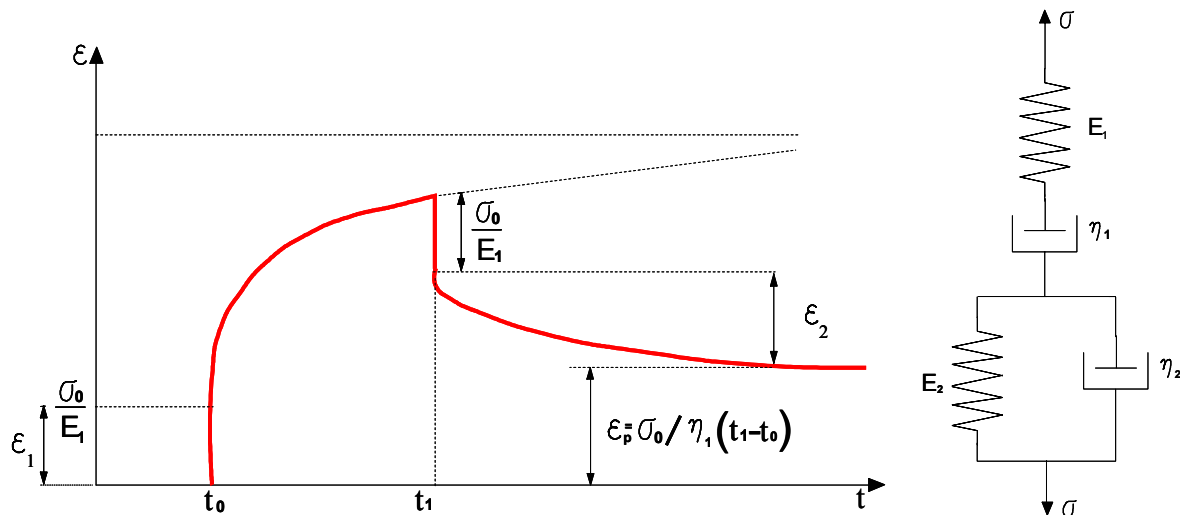


Figure 2.8 – Typical behaviour of asphalt during constant stress loading (left) and Burgers rheological model (right) [Freire, A.C.; 2002]

The Burgers visco-elastic model is considered to be sufficiently accurate to describe the behaviour of bituminous materials, representing a good compromise between accuracy and complexity [Hopman, P.C., *et al*; 1992; Freire, A.C., 2002].

The Burgers model requires four material parameters to characterise the asphalt response [Hopman, P.C.; 1998]:

- ✓ immediate elastic strain ϵ_1 (characterised by E_1);
- ✓ delayed elastic strain ϵ_2 (characterised by E_2 and η_2);
- ✓ permanent strain ϵ_p (characterised by η_1).

The parameters are generally determined based on laboratory test measurements. They are not unique values and are dependent on the type of loading and temperature. Their value is not constant and changes as a result of repeated loading.

Some multi-layer programs, such as *VEROAD* [Hopman, P.C.; 1998], allow for visco-elastic modelling of asphalt materials. The material is characterised by a linear elastic bulk modulus K and a linear visco-elastic shear modulus G .

The main disadvantage of such programs is the number of parameters to be considered and the inherent difficulty of their practical determination or measurement.

2.2.4 Anisotropy

Another aspect of pavement behaviour that is not addressed in the most of the multilayer elastic models is the anisotropy, which may be important mainly in case of unbound materials. The anisotropy is due to the structure of the material itself and to the process of compaction of the material in horizontal layers. As a result, the moduli in different directions may be different.

The equations for anisotropy, in case of uniformly distributed circular load on a semi-infinite half space are presented below:

$$\begin{aligned}\sigma_z &= \sigma_0 / [1-s] * \left\{ 1-s-sz * \left[1/(s^2 z^2 + a^2)^{1/2} - 1/(z^2 + a^2)^{1/2} \right] \right\} \\ \varepsilon_z &= \sigma_0 s / [E(1-s)] * \left\{ (1+\nu) * \left[z/(z^2 + a^2)^{1/2} - 1 \right] - s(n+\nu) * \left[sz/(s^2 z^2 + a^2)^{1/2} - 1 \right] \right\} \quad (2.14) \\ d_z &= \sigma_0 s / [E(1-s)] * \left\{ (n+\nu) * \left[(s^2 z^2 + a^2)^{1/2} - sz \right] - (1+\nu) * \left[z/(z^2 + a^2)^{1/2} - z \right] \right\}\end{aligned}$$

Where:

- $E = E_v$;
- $n = E_v / E_h$;
- $s = \left[(n - \nu^2) / (n^2 - \nu^2) \right]^{1/2}$;
- n - is a constant with a minimum value of 2.25, (usually for granular materials $n = 3$ and for sand $n = 5$),

To be able to model a cross-anisotropic* material, four or even five parameters have to be specified: the vertical elastic modulus, the horizontal elastic modulus, the Poisson's ratios (horizontal and vertical) and the shear modulus, data for all constants is rarely available.

Anisotropic models have been developed and there are even multi-layer programs that accept anisotropic models. [Van Cauwelaert, F; 1977; MINCAD Systems, 1999; Akon, Y. et al; 1999].

Some studies performed within the frame of European project Advanced Models for Analytical Design of European Pavement Systems (AMADEUS) [AMADEUS, 1999] used CIRCLY to study the influence of anisotropy consideration and have concluded that, for the cases studied, the anisotropy influence it was not significant, and the results provided were almost identical to other multi-layered models.

* A material is considered to be cross anisotropic when the E_v and E_h are different, where E_v is the modulus in the vertical direction and E_h is the modulus in the horizontal plane.

2.2.5 Discrete element method (DEM)

All the models presented in the previous sections consider the pavement materials to be continuous and homogeneous. However, this is a simplification of reality, since pavement materials are particulate media, eventually with a binder.

In reality, there are forces between the grains, in soil and granular materials, and displacement of particles occurs. The latter phenomena is the main cause of granular materials deformation, due to rotations and translations that result in sliding grains [Ullidtz, P; 1998]. The distinct element method allows for consideration of these features. The calculation is usually performed in cycles of movement of the individual grains: initially only the external forces and gravity are used to determine the force and moment of each grain, than a movement in a small time increment is calculated, new forces (resulting from the displacement) are determined for the grains and than a new cycle is started.

The development of the discrete (or distinct) element method represents an important step forward in material modelling, especially in the case of unbound materials. By modelling them as particles (see Figure 2.9), elastic and plastic deformation can be considered at the same time.

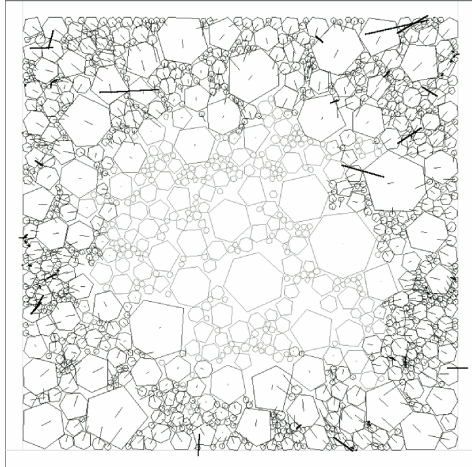


Figure 2.9 – Sample of grains during compaction [Ullidtz, P.; 2002]

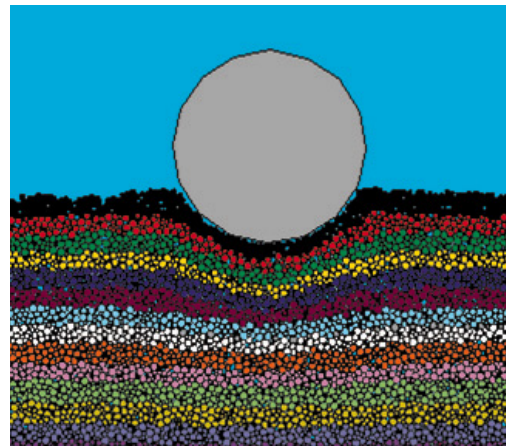


Figure 2.10 – The test simulation with disk in a particulate medium [Ferrez, J.; *et al*; 1996]

Although there are nowadays studies on the soil plasticity [Cheng, Y.P.; *et al*; 2001], on granular material behaviour [Ferrez, J.; *et al*; 1996; Zeghal, M.; 2003] and even on the determination of modulus of asphalt mixtures [You, Z.; Buttlar, W.G.; 2004] based on DEM, the method is still under development being only a research tool for now. It seems to represent a promising tool being able to provide modelling of more complex phenomena, like for example direct prediction of permanent deformation induced by each wheel load [COST

333, 1999]. One disadvantage is that requires high computation efforts and is very time-consuming.

2.2.6 Software for pavement analysis

Computer programs based on multi-layer elastic system were developed in the 60's by the Chevron (CHEV-5) and Shell (BISTRO) companies*. The initial programs were improved in time to allow features such as multiple wheel loads or consideration of partially bond condition between layers.

A list of the programs most commonly used in pavement evaluation and their capabilities is presented in Table 2.1.

Table 2.1 – Capabilities of pavement evaluation software - mechanistic approach

Modelling Capabilities	Available software
Multilayer linear elastic	ELSYM 5, BISAR, NOAH
Multilayer non-linear	KENLAYER
Multilayer visco-elastic	VEROAD, KENLAYER
Multilayer non-linear anisotropic	CIRCLY
Finite element: (non-linear, visco-elastic, dynamic)	FENLAP; CREEPN, AXIDIN etc.

In order to address complex aspects of material behaviour and dynamic response under a moving load, powerful numerical methods can now be used, such as the Finite Element Method (FEM) [Almeida, J.R. de; 1993, Khazanovich, L; 1999; Antunes, M.L.; 1993; Ferreira, P., 2001], the Boundary Element Method [BEM], [Andersen, L. and Nielsen, S.R.K, 2003], or a combination of FME and BEM (hybrid) [Pan, G. and Atluri, S.N.; 1995; Pan, G; *et al*; 1994]. These programs involve a large number of input parameters, some of which are not easily known for pavement materials.

* Michelow, 1963 and Peuz, *et al*; 1968, respectively, as referenced by [Irwin, L.; 2002].

2.3 Performance models

2.3.1 Pavement condition indicators

For the purpose of pavement maintenance planning, the evolution of pavement condition during its service life is usually expressed using performance indicators. The performance indicators most commonly used are:

- ✓ Cracking;
- ✓ Rutting;
- ✓ Other surface defects;
- ✓ Longitudinal unevenness;
- ✓ Deflection;
- ✓ Macro texture;
- ✓ Skid resistance.

These indicators can be divided into two main groups, the ones that are related to the pavement structure (deflection, cracking, rutting) and the ones that influence the user's safety and comfort (rutting, longitudinal unevenness, surface defects, texture, skid resistance etc.) – functional characteristics.

The range of pavement condition indicators considered important for maintenance decision making can differ depending on country specific conditions, not only traffic and climatic but also financial. For example, Nordic countries attach great importance to road unevenness, while other countries consider the surface distress as the most important indicator. Deflection and rutting are also important indicators in many countries.

2.3.2 Pavement design criteria

This study addresses the evaluation of pavement bearing capacity, and consequently its structural deterioration and residual life. Rutting and cracking are considered the main indicators of pavement structural deterioration and they are the ones limited by the design criteria generally adopted. Nevertheless, other deterioration mechanisms (unevenness, ravelling, potholes etc.) can also be in close relation to the pavement structural condition.

Unlike other civil engineering structures that have well defined terminal life criteria, in the case of pavements it is quite difficult to determine the exact moment when the serviceability of a pavement ends. The criteria are different for different countries, depending on the riding or structural conditions considered as tolerable. Generally, there are two main stages considered in pavement design criteria: "failure condition" and "critical condition" (Figure 2.11). For example in U.K. the failure condition corresponds to a 20 mm rut or extensive wheel track cracking while the critical condition is considered for 10 mm rut or the first signs of wheel track cracking.

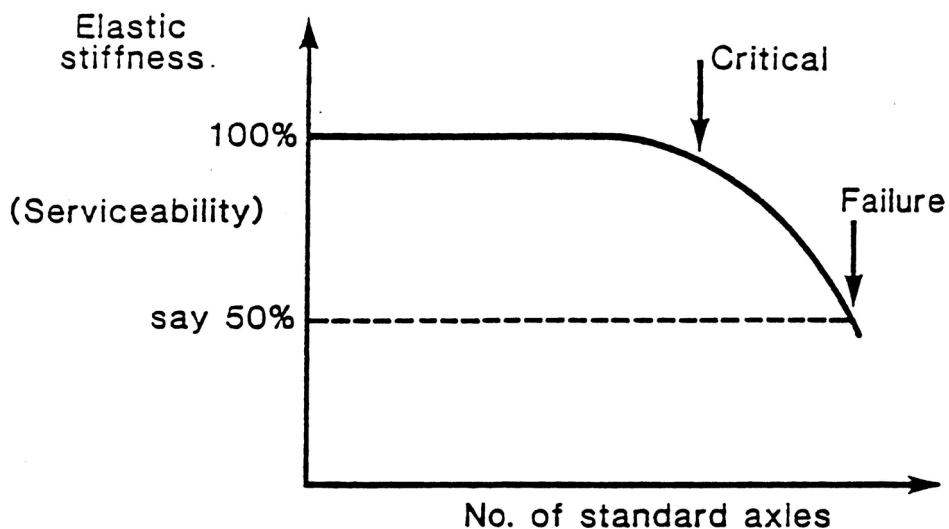


Figure 2.11 – Pavement serviceability evolution in time [Almeida, J. R. de; 1993]

At present, the damage induced in a pavement is still determined mainly using empirical relations.

Rutting is a type of distress that occurs mainly on flexible pavements. It is caused by the sum of permanent (plastic) deformations in the bituminous layers (more evident in case of thick asphalt layers) and permanent deformation in the granular layers and subgrade. Most pavement design methods currently used consider the limitation of the subgrade permanent deformation as a criterion for the limitation of rutting in the pavement's surface. However, with the increase in pavement thickness, the contribution of bituminous layers to rutting has increased. Studies recently developed have shown the importance of this phenomena in the overall pavement performance [White, D.W. *et al*; 2002; Houben, L.J.M. *et al*; 2002; Freire, A.C.; 2002]

The most common types of cracking in the bituminous pavements can be of three different origins:

- ✓ surface cracking “top down”, generally caused by ageing and climatic conditions, sometimes in combination with traffic loads;
- ✓ fatigue cracking “bottom up”, caused by traffic, due to repetitive wheel loading;
- ✓ reflective cracking, which represents a propagation of cracking through the layers that are placed on top of a cracked layer and is more evident in case of composite pavements.

Most pavement design methods in bituminous pavements address the limitation of fatigue cracking in the bound layers. Reflective cracking is taken into account indirectly, and surface cracking is not yet considered in the design methods.

In the mechanistic approach the pavement is usually designed to limit the maximum horizontal tensile stresses or strains at the bottom of asphalt (or concrete) layer and the maximum vertical compressive strain at the top of subgrade in order to take into account fatigue cracking and permanent deformation, respectively [Claessen, A.I.M. *et al*; 1977; Shook, J. *et al*; 1982; Powell, W.D. *et al*; 1984; Zhang, W. and Ullidtz, P.; 2002]. These criteria are generally expressed as relationships between the elastic stresses or strains (ε) induced by wheel loads and the permissible number of load applications (N) [COST 333; 1999]. For fully flexible pavements, these criteria are generally expressed in the form:

$$\varepsilon = aN^b \quad (2.15)$$

Where:

- ε - strain;
- N - number of wheel loads;
- a, b – constants.

The fatigue criterion for cement bound material is usually expressed as a limitation of the ratio between the maximum bending stress induced in the cement bound layer by traffic loads (σ_{\max}) and the maximum flexural strength of the concrete (σ_{fs}).

The most widely used criteria for full flexible pavement are presented in the following sections.

2.3.2.1 Fatigue

The criteria most used for fatigue are presented in Table 2.2.

Table 2.2 – Main criteria used in pavement design – fatigue cracking in bituminous layers

Fatigue	
Shell [Claessen, A.I.M. <i>et al</i> ; 1977]	$\varepsilon_f = (0.856V_b + 1.08)E^{-0.36}N_f^{-0.2}$
Nottingham [Brown, S.F.; Brunton, J.M.; 1990]	$\varepsilon_f = \varepsilon_6 N_f^{-(5.13 \cdot \log(V_b) + 8.63 \cdot \log(RB) - 15.8)^{-1}}$
Asphalt Institute [Shook, J. <i>et al</i> ; 1982]	$\varepsilon_f = 0.0016N_f^{-0.21}$
LCPC [LCPC, 1997]	$\varepsilon_f(T, Fr) = k_r k_c k_s \varepsilon_6 (10^\circ C, 25Hz) \left(\frac{E(10^\circ C)}{E(T)} \right)^{0.5} \left(\frac{N_f}{10^6} \right)^b$
CRR [CRR, 1997]	$\varepsilon_f = G(B') \frac{V_b}{V_b + V_v} \cdot 2.718^{\left(-5 \cdot \frac{V_a}{100} \right)} \cdot \left(\frac{N_f}{10^6} \right)^{-a}$

Where:

- ε_f - maximum tensile strain at the base of asphalt layers;
- N_f - maximum allowable number of wheel loads (fatigue);
- V_b - the binder volume content;
- RB - Ring and Ball softening point;
- E - stiffness modulus;
- T - reference temperature
- ε_6 - the strain corresponding to a fatigue life of 10^6 cycles: $\log(\varepsilon_6) = \left(\frac{14.39 \cdot \log(V_b) + 24.2 \cdot \log(RB) - 46.82}{5.13 \cdot \log(V_b) + 8.63 \cdot \log(RB) - 15.8} \right)$;
- k_r, k_c, k_s - correction factors which multiplied by ε_6 are used to fit the experimental values to real situation;
- V_a - aggregate volume content,
- V_v - void content;
- B' - bitumen penetration susceptibility to loading time;
- G - a coefficient depending on B' ;
- $a = 0.194 \cdot B' + 0.3 \cdot \frac{V_a}{100} - 0.109$.

2.3.2.2 Permanent deformation

Rutting can have different origins within the pavement structure. They can be distinguished based on the shape of the ruts: the asphalt layer permanent deformation is characterised by the existence of “humps” (Figure 2.12 (b)) on the sides of the rutting whereas the permanent deformation originated in the deeper layers corresponds to layer ruts, like the one presented in (Figure 2.12 (a))

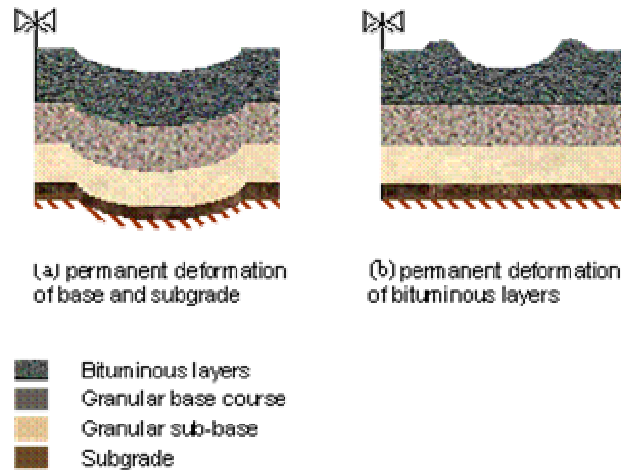


Figure 2.12 – Different types of rutting [Freire, A.C.; 2002]

Generally, the equations for permanent deformation failure criteria express the vertical strain (compression) at the top of subgrade as a function of number of load applications. Some of well-known criteria are briefly presented in Table 2.3 .

Table 2.3 – Main criteria used in pavement design – permanent deformation

Permanent deformation	
Shell [Claessen, A.I.M. <i>et al</i> ; 1977]	$\varepsilon_{pd} = k_1 N_{pd}^{-0.25}$
Nottingham [Brown, S.F.; Brunton, J.M.; 1990]	$\varepsilon_{pd} = 0.0216 N_{pd}^{-0.28}$
Asphalt Institute [Shook, J. <i>et al</i> ; 1982]	$\varepsilon_{pd} = 0.0105 N_{pd}^{-0.223}$
LCPC [LCPC, 1997]	for new roads: $\varepsilon_{pd} = 0.021 N_{pd}^{-0.24}$
	for reinforcements: $\varepsilon_{pd} = 0.028 N_{pd}^{-1/4.1}$
CRR [CRR, 1997]	$\varepsilon_{pd} = 0.011 N_{pd}^{-0.23}$

Where:

- ε_{pd} - maximum vertical compressive strain in the subgrade;
- N_{pd} - maximum allowable number of wheel loads (permanent deformation);
- $k_1 = 1.8 \times 10^{-2}$ for 5% failure probability;
- $k_1 = 2.1 \times 10^{-2}$ for 15% failure probability;
- $k_1 = 2.8 \times 10^{-2}$ for 50% failure probability

The **subgrade failure criteria** generally used are based on the full scale pavement performance studies, which had been used to set-up empirical design methods such as the CBR method [Yoder, E.J.; Wittczak, M.W., 1975] or Road Note 29 [Road Research Laboratory, 1970]. The procedure consists in the calculation of the vertical strains induced by wheel loads at the top of the subgrade and their correlation to the number of loads to failure observed in the full-scale test.

There are also criteria that have been developed based on airfields pavement structure performance evaluation studies [Chou, Y.T., 1982], undertaken by Unites States Army Corps of Engineers. These are more adequate for airfield pavement design as they have been set-up taking into account airfield specific conditions, namely:

- ✓ the pavement structure (with thicker layers)
- ✓ aircraft load application: landing gear configuration, characteristics, and number of passes.

Some design methods take into consideration the contribution of the bituminous layers to the formation of ruts.

2.3.3 Residual life

Each load application (wheel pass) “consumes” an elementary amount of the pavement service life. When the maximum allowable number of load applications is reached the pavement is at the end of its design life, for example the initiation of cracking occurs in case of fatigue.

Depending on the design criteria, the bearing capacity can be calculated as the number of axle loads to the moment of critical condition or failure condition (a certain amount of cracking or a certain rut depth). In this way, taking into account also the effects of former traffic, the residual life of an existing pavement can be determined. The residual life will be given by the minimum of the numbers of allowable axle loads calculated based on each of the design criteria.

The residual life in each moment can be defined as the time or the number of wheel passes until the pavement reaches a critical or a failure condition. Figure 2.13 presents a typical variation of pavement condition in time.

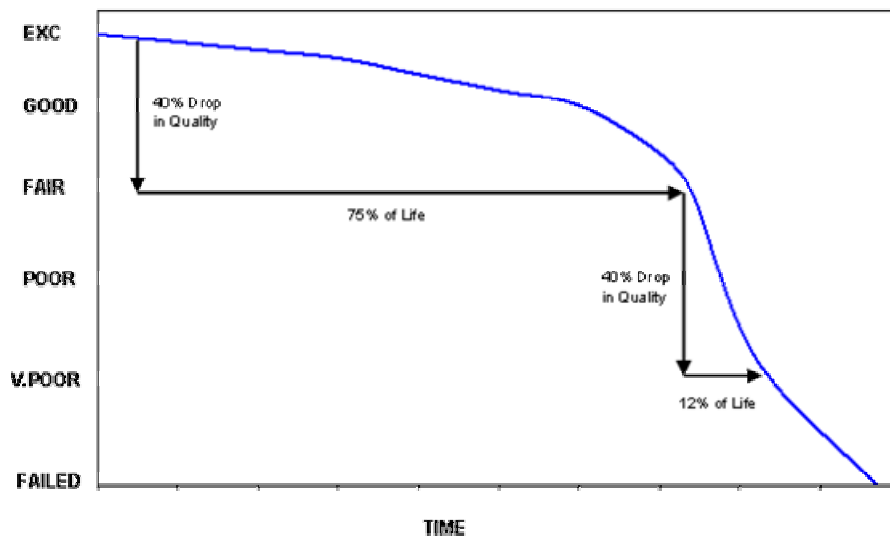


Figure 2.13 – Typical variation of pavement condition in time [Hicks, R. G. *et al*, 1999]

2.3.3.1 Miner calculation of residual life

This is the most common mechanistic approach for residual life estimation. In this method, the damage induced by the former traffic can be added to the damage that will be induced by the future traffic.

The damage is usually defined, for purpose of residual life estimation, as the ratio between the number of wheel loads already applied and the allowable number of loads applications. When this ratio value becomes 1, the pavement service life is considered at its end.

The residual life will be the future number of wheel loads (N_f) corresponding to a total damage equal to 1. In this method, the initial bearing capacity (N_a) is estimated in terms of allowable number of wheel loads applications and the damage induced by the traffic load (N_p) that has already passed is subtracted to arrive at the residual damage that can still be induced by future traffic. This residual bearing capacity can be then estimated in terms of years, if there is a prediction of the number of wheel loads per year.

$$\frac{N_p}{N_a} + \frac{N_f}{N_a} = 1 \quad (2.16)$$

2.3.3.2 Calculation of required overlay thickness

Strengthening of the pavement is necessary if the residual life is shorter than the desired service life. The extension of the residual life may be achieved through overlaying. The stresses and strains will decrease, therefore the allowable equivalent number of standard axle loads to failure will increase to (N'_a). The required overlay thickness depends on the condition of the existing layers, the damage and the desired residual life extension, and is calculated using *Miner's* law as follows:

$$\frac{N_p}{N_a} + \frac{N_f}{N'_a} \leq 1 \quad (2.17)$$

The design of the overlay is made taking into account the followings:

- For the existing bound layers the fatigue damage induced by the past traffic has to be considered when calculating the stresses and strains, using equation (2.17). If the damage induced in the existing layers is too high, it may no longer be interesting to take into account the residual life of these layers. The Miner law is also not applied if the backcalculated stiffness modulus is less than 50 % of a value considered typical for the material. In these situations, the asphalt concrete is assumed to have no

residual bearing capacity and it is treated as a good quality road base, for the calculation of the required overlay thickness.

- For the permanent deformation criteria, since the pavement is overlaid, the damage induced by the past traffic does not have to be considered (the overlay eliminates the former damage) [Antunes, M. L.; 1993]

There are several options to include variances and uncertainties in residual life analysis. They can be taken into account by the following procedures [Dommelen, A. E. van; 2002]:

- ✓ Using characteristic deflection profiles or percentile values for residual life. For example, a 85 % confidence level can be used for selection of the representative deflection bowl (see 3.5.7). A safety factor can be also considered when applying the Miner law;
- ✓ Calculation using percentile values for several design parameters, such as E-moduli or thickness;
- ✓ Full probabilistic calculation. This is more accurate but is time consuming and complex.

Most methods used for residual life analysis only consider the variation in deflection values, while other variations and uncertainties, such as spatial variations of fatigue properties or uncertainties of traffic values, are not taken into account.

To sum up, the result of residual life is usually expressed as a number of load repetitions until failure, and not as the development of structural damage in time.

2.4 Material characteristics

2.4.1 General concepts

The mechanistic approach to pavement evaluation involves the calculation of the stresses, strains and deformations induced by the traffic loads based on a pavement structural model.

Stress-strain models are adopted to characterise the mechanical properties of the various materials which constitute the pavement. Based on stress-strain relationship and taking into

account the loading conditions (short loading time), these materials can be classified into 3 main classes, as follows:

- ✓ Soils and granular materials exhibit a non-linear behaviour, their stiffness depends on the stress state. Their behaviour depends on the material type, (if cohesive), and is sensitive to seasonal variation.
- ✓ Bituminous materials generally exhibit visco-elastic behaviour that depends on the temperature and loading time;
- ✓ Concrete and cement bound layers are considered to present a linear-elastic behaviour under the relatively low level of stresses induced by traffic.

The most important materials parameter that characterise the stress-strain relationship in pavement evaluation is the elastic moduli. This parameter is used together with the Poisson ratio and layer thickness to model the pavement structure. The Poisson's ratio has a very small influence on pavement response, less than 5% deviation in deflection for Poisson's ratios between 0.3 - 0.5, as referenced by Almeida [Almeida, J. R. de; 1993]. Therefore, typical values are usually assumed for Poisson's ratio for each type of material.

Temperatures and moisture condition in the pavement vary over time. Therefore, the stiffness of materials must be converted to design conditions. [Almeida, J. R. de; 1993; Antunes, M.L.; 1993; Van Gorp, C.A.P.M.; 1995]. The main factors that influence the materials stiffness and their consideration in pavement evaluation are presented in the followings sections.

2.4.2 Soil and granular materials

The most important sources of seasonal variation of subgrade stiffness are [Van Gorp, C.A.P.M.; 1995]:

- ✓ stress sensitivity of pavement materials;
- ✓ thermal stress in the subgrade due to soil temperature changes;
- ✓ variation of soil moisture content and suction;
- ✓ pavement surface condition.

In cold countries, the freeze-thaw cycles have an important contribution to changes in subgrade modulus [Zhang, W. and Macdonald, R.; 2000; Djärf, L. *et al*; 1996]. Anyway,

studies performed using FWD have proved that, even without the freeze-thaw action, the subgrade moduli may vary about 15 to 30 % around the annual mean, as referenced by Van Gorp [Van Gorp, C.A.P.M.; 1995].

A study performed at Lisbon airport provided indications about the variability of the subgrade's *in situ* modulus with the variation of the pore water pressure [Antunes, M. L.; 1993; Antunes, M. L. *et al*; 1998a]. The results are presented in Figure 2.14. The study refers to a specific soil type, clayed sand, and it showed that the soil modulus have a reduction of approximately 30% in wet periods, with respect to the maximum value, which takes place in summer.

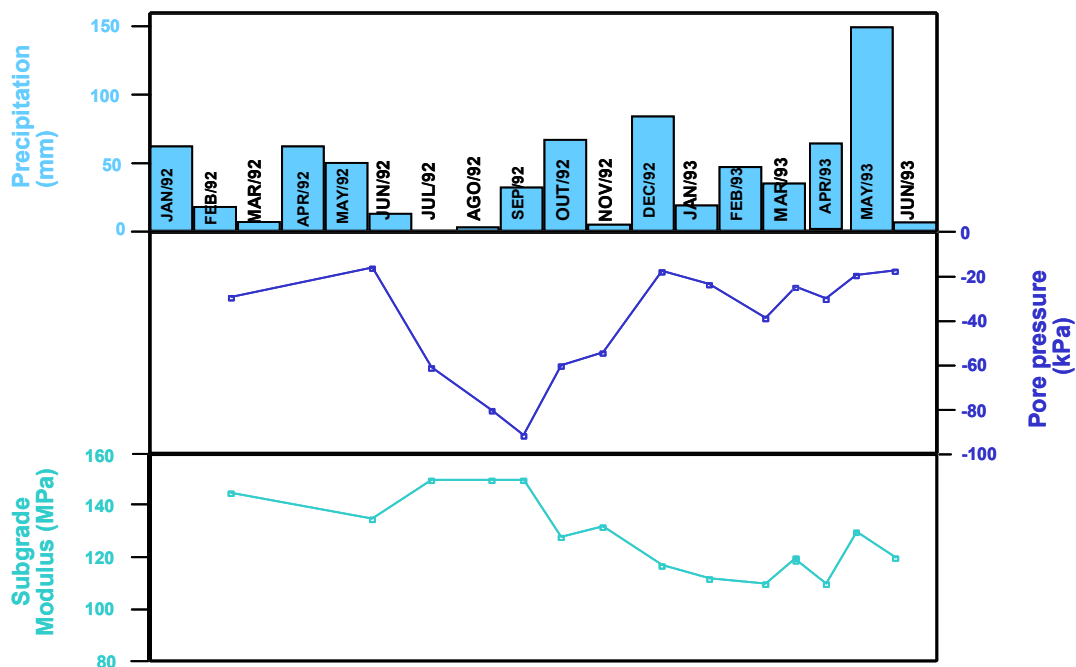


Figure 2.14 – Seasonal variation of subgrade modulus, soil water pressure and precipitation

Usually, in mild climatic zones only the adjustment of the asphalt stiffness to temperature is performed while the seasonal variation in subgrade stiffness is not directly accounted during pavement structural evaluation. At LNEC the results obtained for pavement evaluation are analysed bearing in mind the subgrade condition at the time (of the year) when the FWD tests were performed. This is taken into consideration especially when extreme conditions occur that eventually lead to misinterpretation of the subgrade moduli, by overestimating it during summer or underestimating it on winter.

2.4.3 Bituminous materials

The influence of climatic condition during testing in the pavement's response must be taken into account. The stiffness of the asphalt layers depends on the temperature and the loading imposed. High temperature and long loading time will result in lower asphalt moduli [Claessen, A.I.M. *et al*; 1977; Brown, S.F.; Brunton, J.M.; 1990; Shook, J. *et al*; 1982].

Mechanistic pavement design methods generally use a single asphalt temperature for pavement design calculation. This temperature is known as the equivalent pavement temperature and is generally based on weighted mean annual temperatures of air and pavement [Van Gurp, C.A.P.M.; 1995; Picado Santos, L.; 1994].

This equivalent temperature is defined as the uniform single pavement temperature that can be used to calculate a pavement life that will be the same as the life obtained by summing the damage over the pavement temperatures occurring over the service life of the road. [COST 333; 1999]. This equivalent temperature is a damage and traffic weighted average temperature.

In reality the temperature is not uniformly distributed with depth [Antunes, M:L.; 1993; Picado Santos, L.; 1994; Van Gurp, C.A.P.M.; 1995]. Picado Santos has developed an improved method for modelling of temperature impact on bituminous mixtures, for design purposes [Picado Santos, L.; 1994]. In this methodology it is assumed that the pavement temperature at a certain depth is different in each hour (hourly values) of 24 h considered representative of each month. The study aimed at a better characterisation of the temperature gradients, during the day, the year and, at the same time, with the possibility of generalisation to any pavement case study. This study took into account the specific conditions of different climatic areas in Portugal [Picado Santos, L.; 1994].

There are several design methods for determining the equivalent pavement temperature such as: the SHELL method, the Asphalt Institute method, the UK method, the French method or the Nottingham University, methods that are referenced by [COST 333, 1999]. Usually the equivalent pavement temperature is given as a fixed temperature (e.g. 20°C in the UK method) or as a function of annual air temperature (AAT) either multiplied by a coefficient (e.g. 1.47 for permanent deformation and 1.92 for fatigue, in the Nottingham University method) or as a weighted average air temperature.

2.5 Incremental models for pavement design

The design methods presently used do not take into consideration the changes in pavement structure in time. Most of them consider only the initial material properties for standard climatic condition and under the predicted traffic [COST 333, 1999].

The ideal way to calculate the pavement residual life is to take into account the changes that occur in the pavement structure due to different factors and to be able to estimate the remaining life based on their evolution in time. Due to phenomena complexity and to the difficulty to measure the exact changes in pavement integrity it is almost impossible to model accurately their evolution in time. Developments in this area are expected with the evolution of testing equipment, scientific and computational progress. Meanwhile, pragmatic approaches are recommended in order to take into consideration the degradation in time. [COST 333;1999; FHWA, 2004a] (see also 3.2.4.2).

The methodology proposed by COST 333 is an incremental procedure that takes into account the deterioration in the various elements of pavement structure due to each traffic/climatic cycle during the pavement life. In this incremental method the inputs to the response model and the deterioration laws are updated with the changes in structure and materials properties in time.

There are three different aspects to be considered in the deterioration of pavements in time. First, is the consideration of the changes in materials properties under the traffic action, a second one is the consideration of the climatic effects, in a cyclic way, and a third one accounts for a continuous deterioration due to the time dependent effects (ageing).

The incremental procedure consists in dividing the pavements' life into a number of small time increments (Δt) and to estimate the deterioration that occurs during this period. In addition, within the time increments, the deterioration mechanism can be considered in an incremental way, in other words an incremental damage (Δi). As mentioned above, several factors may cause pavement deterioration. For each of them the calculations are carried out separately, in phase with each other, and with the time being incremented simultaneously [COST 333, 1999]. At the end of each time increment, the pavement model is updated according to the effects of all the deterioration occurred. The damage will be summed until the pavement life reaches the end.

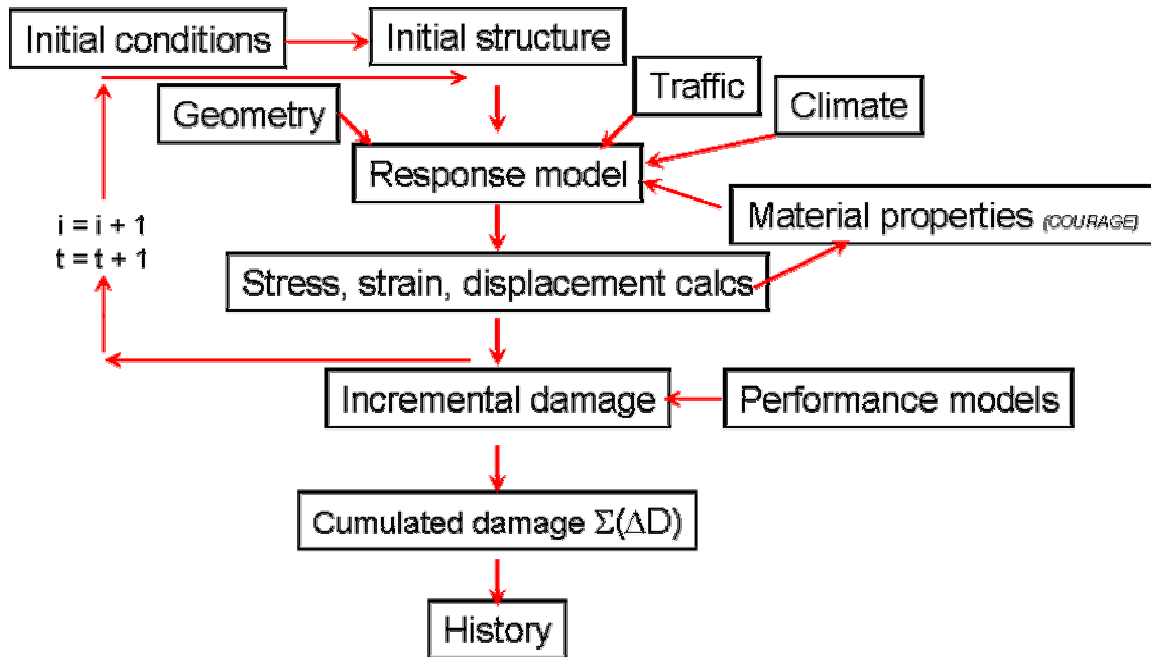


Figure 2.15 – Analytical approach suggested for incremental models [COST 333; 1999]

The problems related with this approach are the absence of suitable models for climatic effects, the difficulties in combining the effects of various deterioration factors such as climatic effects and traffic, as they in reality interact with each other. Therefore, the design criteria method must be modified in order to be used in incremental methods, enabling the consideration of the gradual deterioration of pavement and the effects of time and environment.

2.6 Critical review of pavement design methods

Rutting and cracking are the main indicators of pavement structural deterioration considered in most pavement design methods.

In the mechanistic approach, the pavement structure is generally assessed by using two different types of models combined: response models and performance models. The pavement is usually designed to limit the maximum horizontal stresses or strains at the

bottom of asphalt (or concrete) layer and the maximum vertical strain (compression) at the top of subgrade in order to take into account fatigue cracking and permanent deformation, respectively. These criteria are generally expressed as relationships between the elastic stresses or strains (ε) induced by wheel loads and the permissible number of load applications (N).

Each load application (wheel pass) “consumes” an elementary amount of the pavement service life. When the maximum allowable number of load applications is reached, the pavement reaches the end of its design life, for example the initiation of cracking in case of fatigue of the bound layers.

The residual life is usually expressed as a number of load repetitions until failure and not in terms of the development of structural damage in time.

The design methods presently used do not take into consideration the changes in pavement structure in time. Most of them consider only the initial material properties for standard climatic conditions and under the predicted traffic.

The ideal way to calculate the pavement’s residual life is to take into account the changes that occur in pavement structure due to different factors and to be able to estimate the remaining life based on their evolution in time.

Most pavement design methods currently used consider the subgrade permanent deformation and the fatigue cracking at the bottom of asphalt layers as the only design criteria for residual life estimation. However, with the increase in pavement thickness, the contribution of bituminous layers to rutting has increased. In addition, other deterioration mechanisms (unevenness, ravelling, potholes etc.) can also be in close relation to the pavement structural condition.

An inquiry performed under within the COST 333 (1999) Action has showed that some of the most common forms of deterioration in 22 European Countries (see Figure 2.16) are actually rutting at the surface, followed by loss of skidding resistance and cracking initiated at the surface.

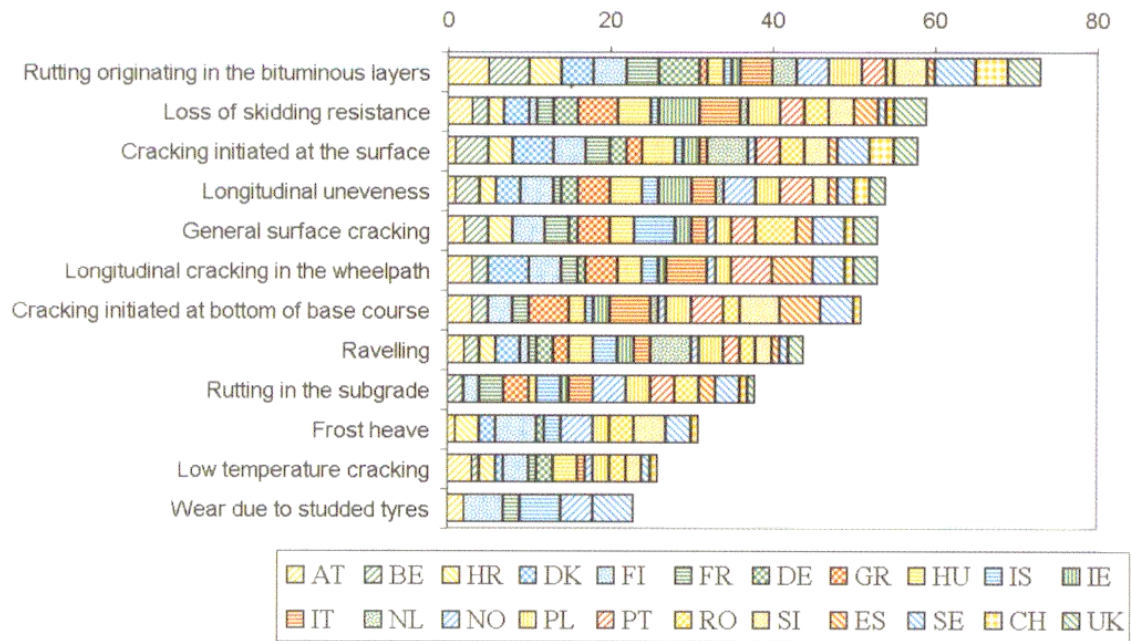


Figure 2.16 – Rating of observed deterioration mechanisms [COST 333; 1999]

In other words, the criteria used in current design methods, which aim at limiting rutting in the subgrade and bottom-up fatigue cracking are not related with the most common forms of pavement deterioration observed in high traffic volume road pavements, which can be a consequence of the conservative design criteria adopted for these phenomena.

Another aspect highlighted by this rating is the fact that important structural deterioration mechanisms, such as permanent deformation of asphalt mixes, cracking initiated at the surface, reflective cracking are not taken into consideration by the pavement deterioration models commonly in use.

3 Methodologies for Pavement Evaluation

3.1 Introduction

In order to evaluate the bearing capacity of a pavement, using a mechanistic approach, a structural model of the pavement is required for the estimation of its residual life.

In the case of an existing pavement, it is essential to evaluate the pavement structural condition in order to set up an adequate model, since the material properties change in time. Furthermore, the existing information on the initial pavement structure is not necessarily available or accurate.

The flowchart presented in Figure 3.1 shows the methodology generally used for structural evaluation of existing pavements. The main steps are the followings:

- ✓ Gathering background information.

The main elements to be taken into consideration when gathering background information are those regarding the subgrade, traffic, maintenance and rehabilitation activities, climatic conditions as well as any other information considered to be relevant for the pavement structural condition. The pavement's surface condition is also an important element included in the "background information".

- ✓ Performing non-destructive load tests (NDT).

In these tests, a vertical load (rolling, steady state vibratory or pulse load) is applied to the pavement's surface and the pavement's response is measured, in terms of vertical displacements (deflections) at the surface. The load should simulate, as close as possible, the effect of heavy vehicle tyres. The deflections are measured and then,

together with the information on layer thickness, they are used for the estimation of "in situ" bearing capacity.

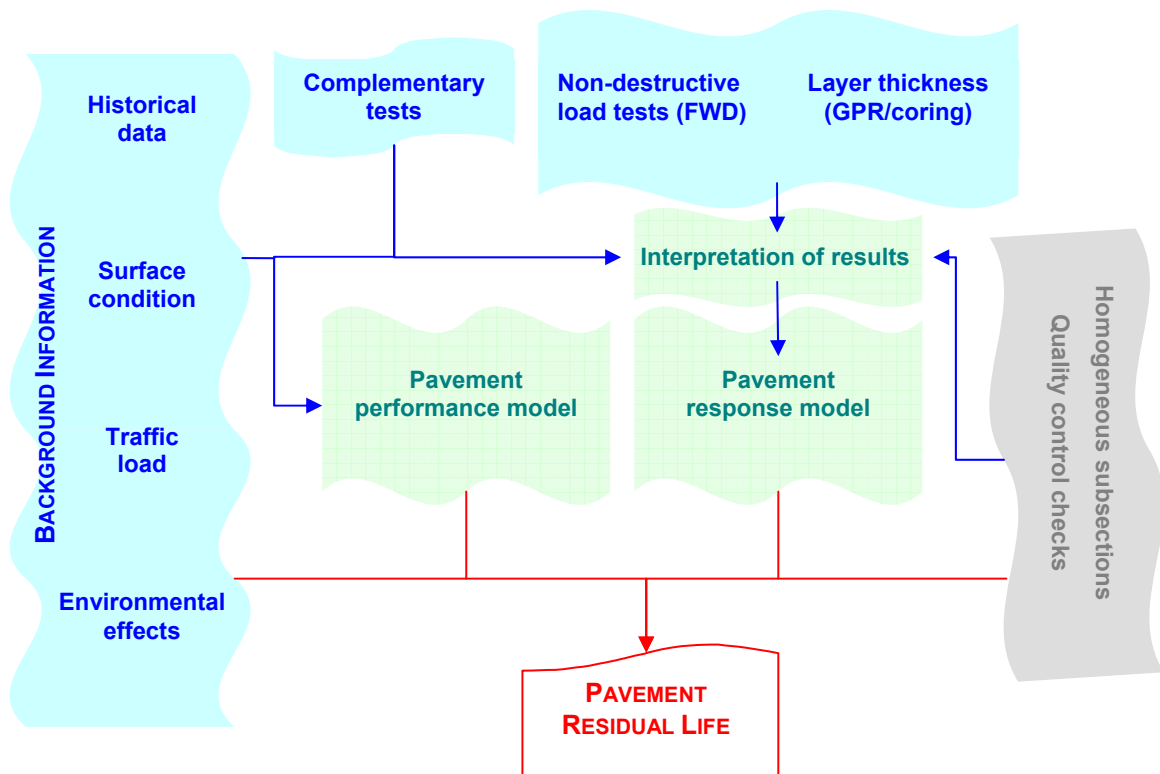


Figure 3.1 – Methodology for structural pavement evaluation

✓ Division into homogeneous subsections.

The pavement is quite heterogeneous, its variability reflects the combination of changes in various parameters that influence its behaviour along the road. Some of those factors are, the type of soil and its condition, earth works (fill or cut), layer thicknesses, construction phases and construction variability, drainage condition, environmental effects, traffic distribution, material properties as well as maintenance and rehabilitation activities performed during its service life.

The identification and division of a pavement into homogeneous subsections is one of the major goals of non-destructive tests in bearing capacity evaluation and can be done in one or several phases of the analysis: before testing (planning purposes), immediately after testing (data post processing), after backcalculation of the pavement layer moduli and/or after the evaluation of pavement residual life. In this way, it is possible to design different rehabilitation solutions for each homogeneous sub-section in order to reach the desired bearing capacity.

✓ Layer thickness.

Information about the existing pavement structure, in terms of type of materials and layer thickness, is important, not only in the backcalculation process, but also in previous stages, namely the preparation of Falling Weight Deflectometer (FWD) measurements or the subsections identification. In general, this type of information can be obtained from historical data, coring and/or trial pits. A continuous measurement of the layer's thicknesses has become possible with the application of Ground Penetrating Radar (GPR) for substructure evaluation and therefore, a more accurate identification of changes in pavement structure. Cores and test pits are also performed for collecting samples of *in situ* materials, which are then tested in the laboratory, in order to get additional information on the material properties – complementary tests.

✓ Interpretation of the results.

From the results obtained in the tests, a response model of the pavement is set up using a backcalculation process. It has to reflect the response of the existing pavement to the test load. In other words, the deflection bowl calculated based on this model should be similar to the one measured "*in situ*".

The tools, such as quality control checks and division into homogeneous subsections, can be applied at any level of information processing, including the final step, namely the residual life estimation.

The traffic load information is important not only as background data but mainly for pavement design and evaluation. It is used to determine the damage already induced in pavement by previous traffic and to evaluate the pavement behaviour under future traffic. Different traffic levels usually require different pavement structures. Accurate traffic predictions enable an economic efficient pavement design.

As already mentioned in Chapter 2, pavement materials are sensitive to temperature and other environmental conditions with seasonal variations. Therefore, environmental effects have to be considered in pavement evaluation and the non-destructive test data have to be converted to design condition [Van Gurp, C.A.P.M.; 1995]. Usually, this is performed through the adjustment of the asphalt stiffness to a design temperature.

Then, performance models (deterioration models) are used to relate the critical stresses and strains under the design load with the pavement residual life. The residual life is defined as the time or number of wheel passes until the pavement reaches a failure condition.

The mechanistic model can be set up using all the information sources mentioned on the flowchart, if available, or only part of them.

The main steps in the methodology are described in more detail in the following sections of this chapter.

3.2 Background information

The background information helps to better understand the behaviour/distresses observed in the pavement under the influence of traffic and environmental conditions. At the same time, it provides additional information to set up the pavement's structural model (for example, if there is information on the type of subgrade soil, it will allow for a better initial estimate of the modulus of the subgrade).

The main elements to be taken into consideration when gathering background information are those regarding surface condition, subgrade, traffic, maintenance and rehabilitation actions, climatic conditions, results from any previous structural evaluation studies as well as any other information considered to be important for the pavement structural condition.

3.2.1 Historical data

All the historical records regarding the pavement structure are important. Information on the initial pavement structure and on all the major maintenance measures performed during its service life should be gathered for a reliable assessment of the residual life of an existing pavement.

The subgrade behaviour has an important influence on the pavement performance in time. Many distresses observed in the pavement can be associated with soil condition. The consideration of subgrade characteristics can improve the pavement structural model, to become more representative of the existing "in situ" condition. [Rohde, G.T.;1990, Uddin, W. *et al*, 1986].

For the subgrade moduli it is important to know the type of existing soil, its sensitivity to water and consequently to seasonal variations [Zhang, W and Ullidtz, P; 2002; Antunes, M.L.; 1993]. Another important factor to be taken into account is the drainage condition [Hall, K

and Correa, C., 2003; Ramos, C.M.; 2004]. Poor drainage conditions can be responsible for a number of important distresses (e.g. local settlements).

The characteristics of pavement layers, adopted in the structural model, depend on the subgrade condition along the pavement. During the backcalculation process using linear elastic models the existence of a "rigid" layer is assumed, as it will be referred later on. One of the issues that relates to this "rigid" layer is the location of the "bedrock" near the surface or the earth works during construction. The distance to the "rigid" layer is different along the road profile and its consideration will result in different subgrade characteristics (thicknesses and moduli).

3.2.2 Surface condition assessment

The road surface distress is an indicator of pavement serviceability in terms of comfort and safety. Therefore, the pavement surface condition should be maintained at a level that, not only ensures the ridding quality and safety for users, but also the pavement integrity preservation (preventing water infiltration) [COST 325, 1997].

The pavement's surface condition also gives important indications about the main problems and the main deterioration mechanisms occurring in the pavement.

The main objectives of surface condition assessment in the context of pavement evaluation are to identify the causes for distress and to provide guidance for the organisation of other pavement evaluation activities. Normally this assessment is performed with more emphasis on the distresses that are more directly related to the pavement's structural behaviour, such as cracking, permanent deformation (rut depth), construction joints condition, etc.

The process consists of identification of the type of distress and evaluation of its extent and severity, and there are several distress identification manuals that provide guidance for this [SHRP, 2003; Austroads, 2002; Austroads, 1987; Antunes, M.L.; 1997; ASTM D 6433–99; 1999; JAE, 1997; Johnson, A.M.; 2000; NPMA, 1999]. The identification of the distress cause is an important issue for a proper rehabilitation policy.

The methods used to perform surface condition assessment are the visual survey or/and optical assessment. A comprehensive inventory of the available equipments was given by PIARC [Wambold, C.J. *et al*; 1995]. More recently, there was further inventory work performed in the frame of the FORMAT European project [FORMAT, 2002b].

Apart from the distresses more directly related to pavement design (cracking and rutting), ravelling may also play a role in the pavement's structural condition. Ravelling is defined as

the loss of aggregate from the surface layer of a pavement. Ravelling can influence negatively the ride quality of the pavement, can cause higher noise levels and increases the occurrence of windscreen damage caused by loose aggregate being projected by tyres. Ravelling will also result in the accumulation of water in the road surface, thus weakening the structural integrity of the upper asphalt layers.

High-speed methods to assess the amount of ravelling are being developed by DWW and CROW in the Netherlands and TRL in the UK [FORMAT, 2004].

3.2.2.1 Visual survey

Presently the most recommended method for a detailed surface condition assessment is to walk along the road site and to record the different type of distresses, the degree of severity and their extent [COST 343, 2002], which should be performed by experienced personnel.

Although detailed, the “visual survey” presents several disadvantages. On one hand, it is a time consuming process and the safety of the personnel during survey can be a problem, especially in roads with high speed traffic. On the other hand, it requires trained personnel and it is subjective, depending on the point of view of the person who performs the survey. In order to improve quality of the survey, the distresses are collected on the basis of distress identification manuals, as mentioned above. Almost every European country has their own distress manuals [COST 343, 2002]. An assessment of different distress identification methods used through Europe was made during the PARIS project [PARIS, 1999], where a team of experts performed a “normalisation” of different classification methods applied by different research laboratories in over 15 countries.

The SHRP Distress Identification Manual [SHRP, 2003] is used by LNEC for visual survey, mainly for Long Term Pavement Performance Studies (LTPP). During the visual survey, the distresses are recorded in quite detail, in order to better reflect their evolution in time. One inspection sheet is filled for 100 m section of road lane [Antunes, M. L., 1997, Antunes, M. L. *et al*; 1999]. The distresses are quantified in terms of extension (length or area). They are also classified in terms of degree of severity as *low*, *medium* or *high*. Any small-scale repairs (as patching, surface treatment, crack sealing etc.) are also recorded in the same sheet. If different severity levels existing within an area cannot be distinguished, the area is rated at the highest severity present.

3.2.2.2 Optical assessment

There are mainly three types of technique used: standard video (analogue or digital); line scan video (analogue or digital) and distance measuring laser cameras (point or line scan).

In Europe a project aiming at assessing and evaluating the existing equipment, proper for measuring at high speed is ongoing [FORMAT, 2004]. In the summer of 2003 TRL Limited (UK) invited interested companies to take part in a comparative study performed on test sections on the TRL site. The devices that took part were TRACS, Babbie TTS, both including versions of PAVUE monitoring system, and HARRIS vehicle provided what is considered, in the UK, a reference device.

The World Road Association has also undertaken a study on the “automated” technologies [PIARC, 2003], that they classified in 2D, for cracking detection and in 3D for roughness and rutting measurements. The main equipment considered within this study were: RoadCrack (CIRO, Australia), LaserVision System (GIE Technologies, Canada), Intelligent Inspection Vehicle (HEPC, Japan), PAVUE (OPQ Systems AB, Sweden), ARIA (MHM Associates Inc., USA), Digital Highway Data Vehicle (Waylink Systems Corporation, USA), ARAN-WiseCrax (Roadware, Canada), Road Assessment Vehicle (OPQ Systems AB, Sweden).

Optical assessment can be either fully automated, if data collection and distress evaluation are both performed by a device, or semi-automated, when data collection is automated but distresses are evaluated manually in the office. The biggest technical problem of this type of equipment is the development of data analysis software for automatic crack detection and characterisation [PIARC, 2003].

The main disadvantages of these systems are the sensitivity to light intensity during the survey and the calibration required before the survey. Cracking is difficult to be automatically assessed, as it is very different in size, shape depth. Therefore, the registration of low severity distresses and the evaluation of distress extents are not so accurate.

Due to the size of the networks, the quality of the data required for pavement evaluation and road maintenance management, as well as for economical and safety reasons, the actual tendency is to develop high speed monitoring devices with improved accuracy. Optical assessment is especially adequate for network level surveys. A video camera installed on a vehicle is used to record the surface distress as well as its exact location.

3.2.2.3 Other indicators

The longitudinal unevenness of a road surface is another important distress that, as transverse unevenness, can be caused by poor subgrade condition, deficient drainage etc. Longitudinal unevenness is not directly caused by a problem in the bearing capacity condition, except in the extreme cases when extensive cracking and potholes occur. Nevertheless, a high longitudinal unevenness may lead to an acceleration of the pavement’s structural deterioration, due to dynamic loads [Sayers, M. and Karamilhas, S.;1998]. The International Roughness Index (IRI) is a widely used pavement condition indicator, which

summarises the roughness qualities that have impact in the vehicle response. An increasing attention is given to IRI prediction models based on initial pavement smoothness [Smith, K. L. *et al.*; 2002].

There is a wide range of testing equipments for measuring the surface longitudinal unevenness [SHRP, 2003; LCPC, 1997; COST 325, 1997]. The measuring capabilities and methods of interpretation currently available in Europe have been recently comprehensively evaluated in the project entitled FEHRL Investigation on Longitudinal and Transverse Evenness of Roads (FILTER) [Descornet, G, 2002].

3.2.3 Complementary tests

The main purpose of complementary tests on pavement materials is to obtain information regarding the materials characteristics and behaviour, in order to support the backanalysis process, and also the adoption of performance models for calculation of the residual life. These tests can be performed either “in situ” or in the laboratory, using samples collected through core drilling and test pits. Some of these tests are briefly mentioned below.

The **Dynamic Cone Penetrometer** (DCP) provides a rapid measurement of in-situ strength of pavement layers and subgrade, being used for estimating the in-situ California Bearing Ratio (CBR) and, more recently, the elastic modulus [Almeida, J. R. de; 1993; George, K.P. *et al.*; 2004]. The DCP consists of a hammer (4 or 8 kg) that falls from a certain height and drives a cone into the soil or granular material base [Saïm, R. and Sousa, J.B.; 2000]. The length of the equipment is modular and can be between 1.0 m, 1.5 m, and recently 2.0 m [Livneh, M *et al.*, 2000]. This represents the penetration depth that the device will reach into the soil (depth of material tested). Another Penetrometer frequently used for in-situ compaction evaluation is the Dynamic Light Penetrometer (DPL). A study aiming at correlation of DPL results with the dry density obtained by volumetric methods was performed at LNEC [Ferreira, H.N. and Nunes, M.M.; 1990].

The **Soil Stiffness Gauge** (SSG) is an instrument for measuring the in-situ stiffness of compacted soil. The changes in the force applied at the surface are given by changes in the vibrations generated by the SSG. Geophones are used to measure both the changes in deflections and force for different frequencies [Siekmeier, J.A. *et al.*, 2000]. The depth of material tested is 100 to 150 mm.

Test pits are performed on the pavement, with the purpose of measuring the thickness of bound, as well as unbound layers (base and sub-base layers), *in situ* characterisation of

materials (density, water content, *in situ* CBR) and collection of samples for laboratory tests [Pinelo, A.M.; 1991] (see 3.4).

There are, within the **laboratory tests** performed on samples, two main types of tests: conventional tests and performance related tests.

Conventional tests performed on pavement materials are generally aiming at their identification (for example, bitumen content on asphalt or grading of granular materials).

There is an increasing tendency to use more performance related tests, such as triaxial tests for granular materials or stiffness, fatigue (Figure 3.2) and permanent deformation tests (Figures 3.3 and 3.4) for bituminous materials [Freire, A.C.; 2002; Capitão, S.; 2003].

In conclusion, results from *in situ* and laboratory tests, complementary tests, will give more information on the material's behaviour and therefore a better initial estimate of their moduli can be used in the interpretation of FWD tests. Furthermore, a better selection of the performance models for residual life estimation can be made, based on results of laboratory performance related tests.

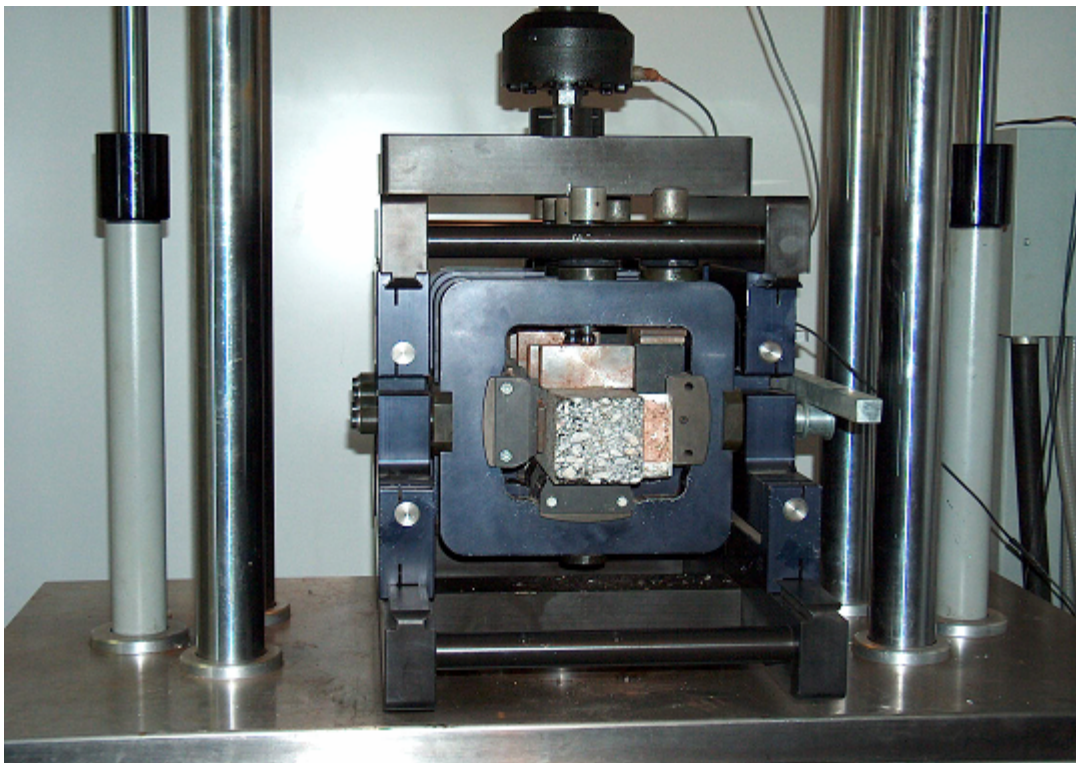


Figure 3.2 – Fatigue equipment LNEC

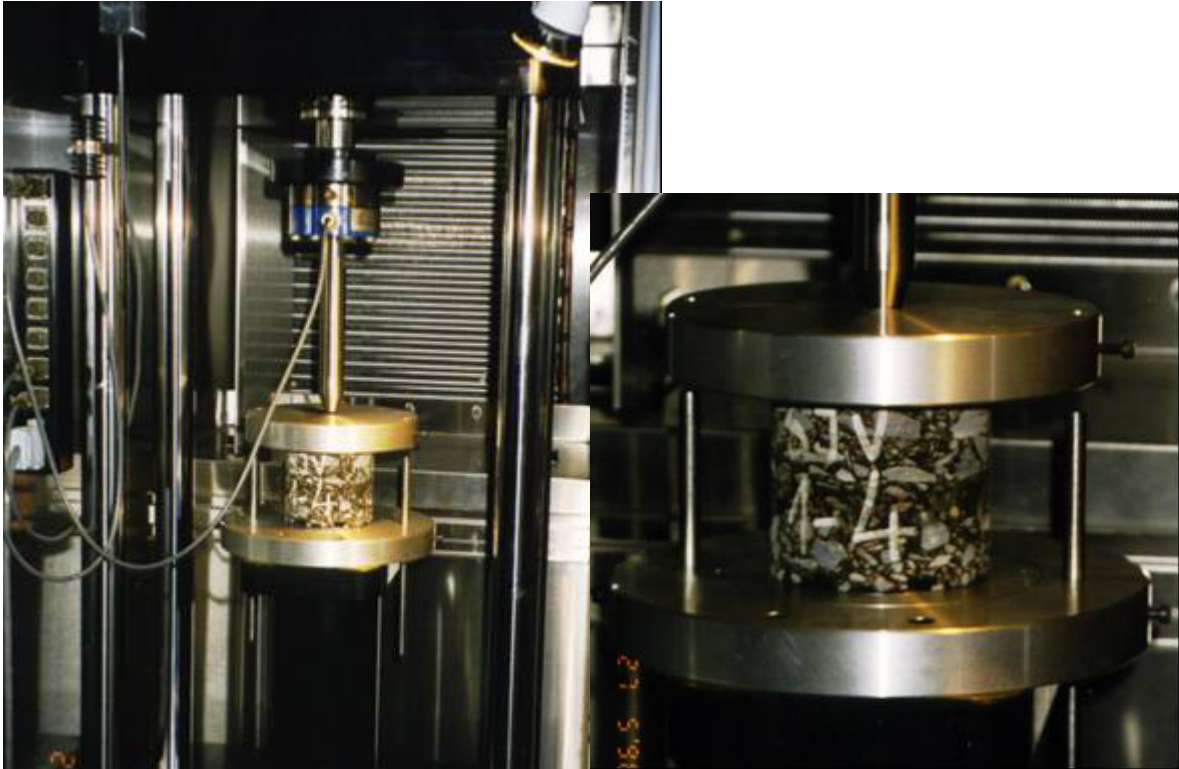


Figure 3.3 - Uniaxial compression testing equipment

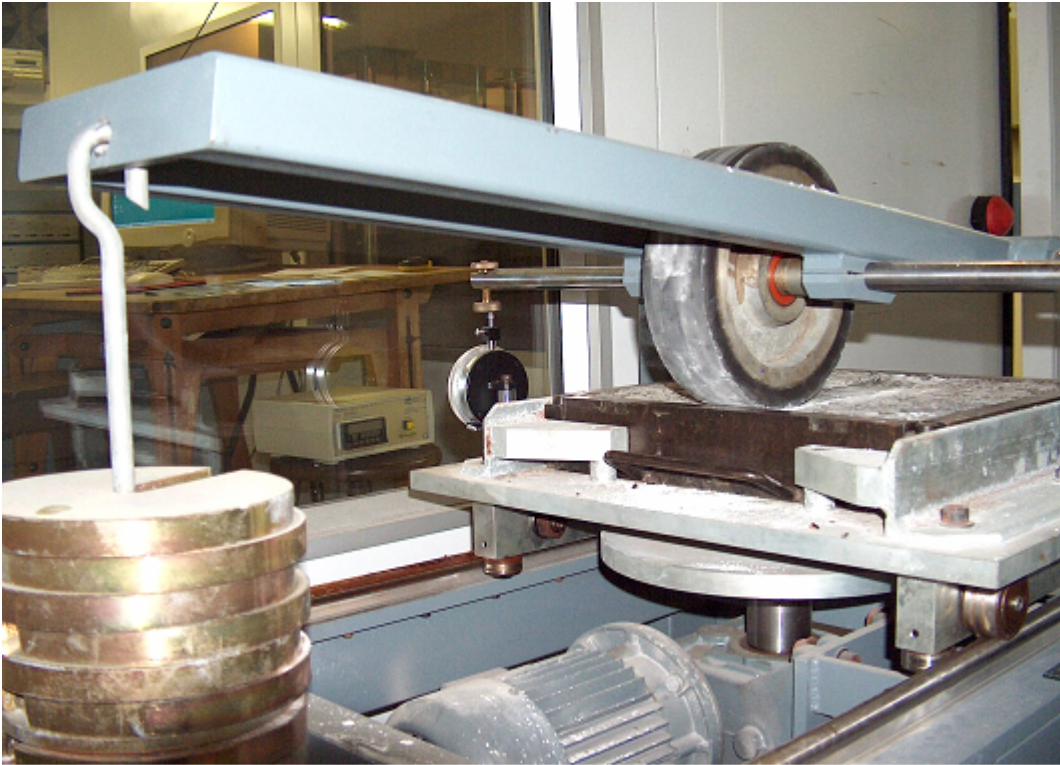


Figure 3.4 – Wheel Tracking equipment LNEC

3.2.4 Traffic and environmental data

3.2.4.1 Traffic information

Pavements are designed for a certain service life. This corresponds to a number of vehicle loads that they bear without reaching the failure condition. Each passage contributes to the accumulation of pavement deterioration. The structural deterioration is mainly induced by heavy vehicle axle loads (see 2.1.3). Therefore, past heavy vehicle traffic information is used for evaluation of the damage induced in the pavement during its service life (see 2.3.3). Information about traffic can also be valuable when performing sub-section identification: different traffic levels can be a reason for different pavement conditions.

The future traffic information is required whenever a new pavement is designed or in case of rehabilitation of existing pavements [JAE, 1995; LCPC, 1997; Asphalt Institute, 1991; Austroads, 2002; MOPU, 1990; Air Force, 1994]. Estimation of the future traffic loads for pavement design and rehabilitation purposes requires specific expertise. The information to be gathered comprises: analysis period, classification and number of vehicles in each class, design period, traffic growth and distribution of traffic in the design lane. On the other hand, based on the traffic distribution along the pavement, different rehabilitation measures can be adopted for areas with different heavy traffic intensities.

The design future traffic may be expressed in terms of number of standard axles, for road pavements, or number of coverages of each design aircraft, for airport pavements (see 2.1.3).

3.2.4.2 Environment

Figure 3.5 presents the cyclic variation in time of materials moduli due to environmental effects.

Basically, throughout the year the asphalt mixture modulus is at minimum in the summer when temperatures are high, the base layer modulus may be at minimum in the spring (when there is thaw or the ground water level is high) and the subgrade modulus is also at its minimum in the spring for the same reasons. The pavement's structural model is derived from a set of test results performed at certain climatic condition. The results obtained should be converted to the corresponding in service condition.

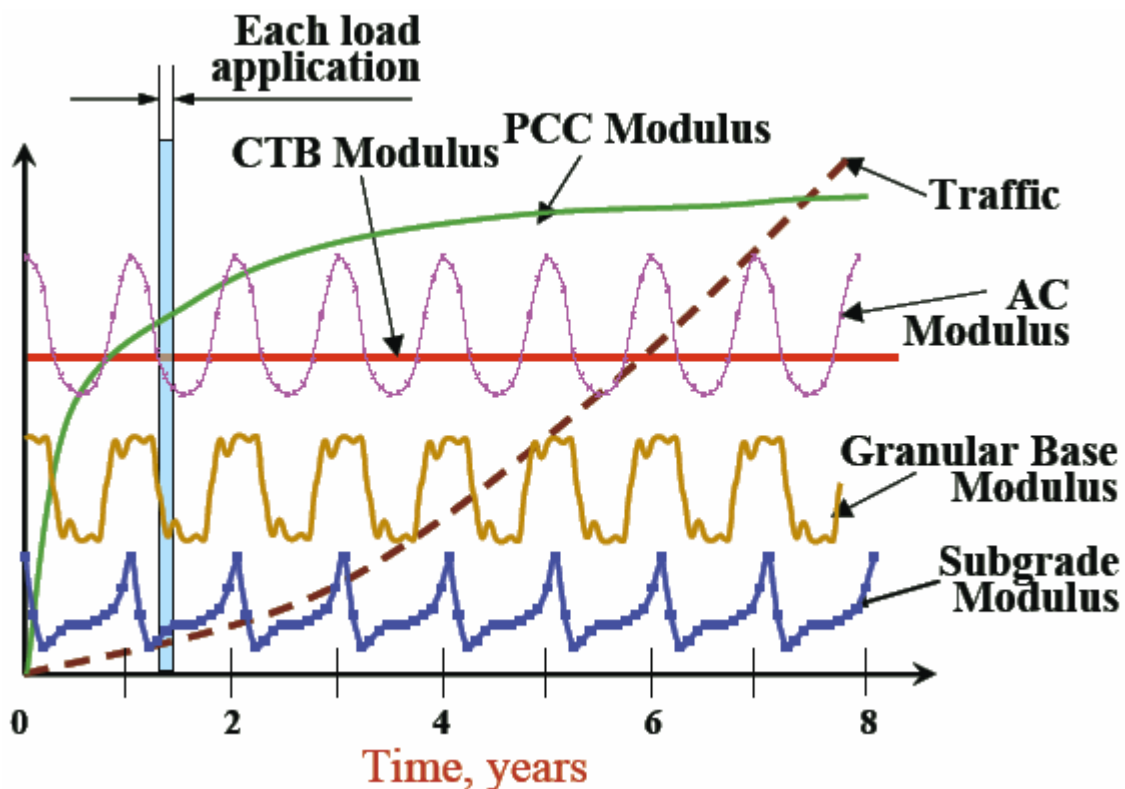


Figure 3.5 – Pavement design variables: material's elastic moduli variation in time [FHWA, 2004a]

Temperature is one of the main factors that influence the pavement's behaviour, which should be taken into account in pavement evaluation studies. The asphalt layers moduli change with temperature and consequently the pavements response to loads will depend on temperature. Therefore, the evaluation should take into account this effect [COST 336, 2002; Van Gurp, C.A.P.M.; 1995; Antunes, M.L.; 1993].

Normally, for pavement design purposes, an “service” (equivalent) temperature is selected for the asphalt layers. This will be a value that is representative of the temperatures that occur in these layers throughout the year [Picado-Santos, L.; 1994].

The hydrologic conditions influence the layer moduli, specially for subgrade soils and granular materials (see section 2.4).

The knowledge about the environmental conditions also helps to explain some of the types of distresses occurring in the pavements.

In countries with cold winters, the brittleness of the bitumen can cause surface cracking. The freeze-thaw process is another distress factor, as well as the surface wear and corrosion caused by the winter maintenance activities, especially the use of de-icing salts [Salt Institute, 2000].

Finally, the choice of a certain type of maintenance or rehabilitation measure should be made taking into account the environmental conditions that the pavement under consideration must withstand.

Also, specific measures should be taken in areas with heavy rain history to prevent the aquaplaning phenomena (grooving or porous asphalt, etc).

Last but not least, in areas with chemical attack susceptibility, special type of materials should be used, or surface protection measures should be adopted.

3.3 Non-destructive load tests

The structural evaluation of a pavement using mechanistic approach is based on non-destructive load tests (NDT). Figure 3.6 presents the deflection distribution within the pavement structure under the influence of a vertical load applied at the surface.

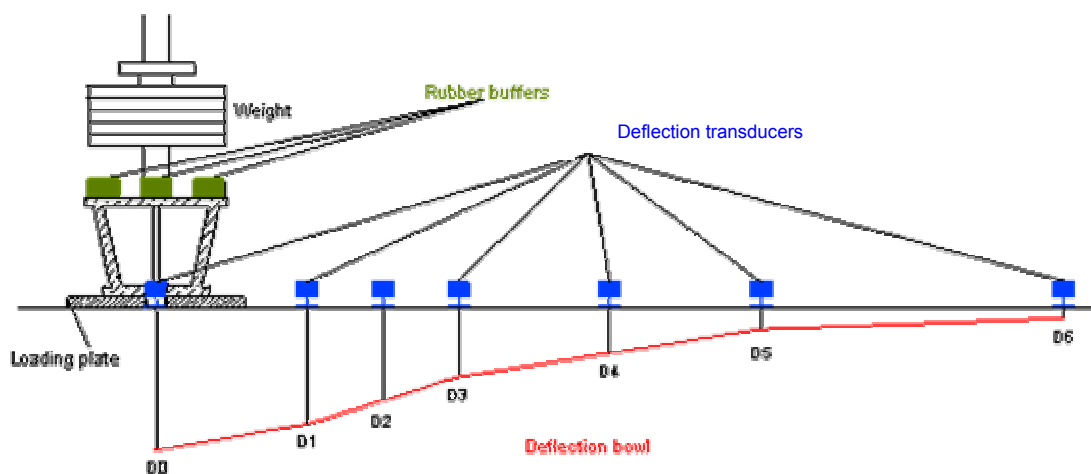


Figure 3.6 – Deflection distribution scheme within the pavement structure under FWD action

The deflections are measured in one or more points, located at different distances from the load (including the centre of the loaded area). Each set of deflections in a testing point represents a “deflection bowl”.

The deflection bowl reflects the influence of the combination of different layers that form the pavement's structure [Irwin, L.H.; 2002]. The measured deflection bowls, together with the information on layer thickness, are used for the estimation of "*in situ*" bearing capacity.

A structural model of the pavement is determined using a “backcalculation process” whereby the layers’ E moduli are estimated once the layers thicknesses are known.

The pavement structural model (layer thickness and materials properties) has to reflect the response of the existing pavement to the test load. In other words, the deflection bowl calculated based on this model should be the same as the one measured "*in situ*".

3.3.1 Summary of deflection testing equipment

Various types of deflection testing equipment are used for structural pavement evaluation. The following sections summarise the main types of deflection testing equipment used in pavement evaluation studies. Taking into account that the models used for interpretation are simple (generally linear elastic) it is important to simulate the traffic loads as close as possible, in order to achieve a representative pavement response.

3.3.1.1 Rolling wheel deflection equipment

Benkelman beam

The Benkelman beam was developed in the 50’s. It may be used for measuring deflections in static plate load tests or for measuring deflections under a rolling wheel of a loaded truck moving at slow speed. Normally, only the maximum surface deflection due to the wheel load is measured with this equipment.

In the 60’s, LNEC developed an equipment for registration of the deflection bowl due to the passing of a rear axle of a loaded truck – “LNEC deflectograph”. This equipment uses a Benkelman beam for deflection measurements, and has a distance transducer connected to the truck wheel. An LVDT is installed on the beam [Antunes, M. L., 1993], in order to get a continuous reading of the surface deflections as the truck moved. (Figure 3.8).

With LNEC’s device, the influence line of deflections due to the moving wheel load was recorded, which means a more complete information about the pavements response, [Pereira, O.A.; 1969] when compared to the standard Benkelman Beam applications where only the maximum deflection was recorded.



Figure 3.7 – “LNEC deflectograph” during tests

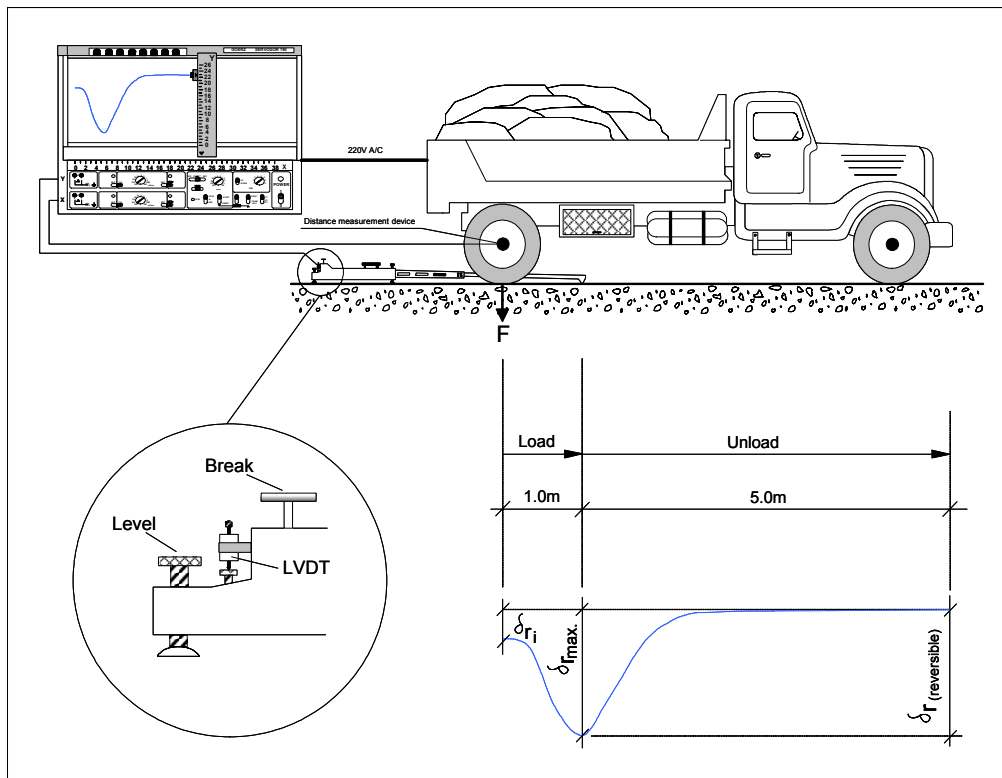


Figure 3.8 – “LNEC deflectograph” functioning scheme

The main disadvantage of this technique is associated with the slow speed of the wheel load, when compared to the normal traffic speed. In fact, due to the nature of pavement materials, especially asphalt, the pavement's response to a wheel load is significantly affected by the speed. Another disadvantage of this technique is the fact that is time consuming, when compared with modern deflection testing devices.

Lacroix deflectograph

The Lacroix deflectograph was developed in France in the 50's in order to be able to carry out Benkelman beam measurements in a more efficient way. The equipment consists of a twin axle, six-wheeled lorry, dragging along a measuring frame beneath the lorry. The measurements are recorded each 3 to 5 m in both wheel tracks at a measuring speed of about 5 km/h [Kenedy, C.K. *et al*, 1978; LCPC; 2004; Saldanha, P.; 2004]. The main disadvantage of the Lacroix deflectograph is the fact that it does not provide the full deflection bowl and it operates at slow speed, when compared to normal traffic speed. Also, the characteristics of the truck can be a problem in places with size and weight restrictions.

The advantage of this technique is that it provides almost continuous results along the tested pavement.



Figure 3.9 The Lacroix deflectograph (<http://www.cedex.es/cec/documenti/survey.htm>)

Curviameter

The measurement with this equipment consists of recording the surface deflection under a rolling wheel with a measuring speed of 18 km/h. The measurements are recorded, by geophones, each 5 m on the right-hand wheel path. Due to the truck weight and size, the Curviameter cannot be used on roads with axle weight restrictions. The advantages of this

technique are that provides the full deflection bowl and is performed at a higher speed than Lacroix, but still slow, when compared to traffic speed.

High speed deflectometers

Efforts have been made in the last decade to develop equipment which are able to perform deflection measurements at traffic speed. The high-speed technique allows large lengths of road to be tested in a relatively short time compared to the FWD technique and with no disturbance to the traffic. Furthermore, it is more representative of actual traffic loads. There are two main research groups involved in the development of this type of equipment:

- ✓ The Rolling Weight Deflectometer [Johnson, R.; 1995; Hall, J.;1999; Bay, J. and Stokoe, K.H., 1998], developed in the USA and the Road Deflection Tester (Figure 3.11) [Lenngren, C.A, 1998], developed in Sweden. These equipments use distance measuring laser sensors to derive pavement surface deflections imparted to the pavement by a loading wheel of a truck travelling at normal traffic speeds (up to 100 km/h). The deflection is calculated as the difference between a loaded and an unloaded profile of the pavement;
- ✓ The High Speed Deflectograph (Figure 3.10) [Hildebrand, G *et al*, 1999] uses a different measuring principle where two laser Doppler sensors mounted in front of the loading wheel measure the vertical velocity of the pavement surface resulting from the applied load from the rear axle of the measuring vehicle. The tests are performed also at normal traffic speed.

All devices are based on trucks or semi trailers and all use laser sensors.



Figure 3.10 - View of the Danish High Speed Deflectograph



Figure 3.11 - The Swedish Road Deflection Tester

None of the devices is yet ready for routine testing. The analysis of the results is quite complex and time consuming and therefore, it is still under development.

The improvement of these devices continues with the aim of producing devices, which on a routine basis, can be used for network monitoring of bearing capacity at high speeds [FORMAT, 2004].

3.3.1.2 Harmonic load deflection equipments

Harmonic load deflection equipments exert a sinusoidal vibration on the road surface by means of a dynamic power generator. “Dynalect”, “WES” and “Road Rater” are some of these equipments, which were developed in the USA, being mostly used there.

The Dynalect (Figure 3.12) [Geo-Log, Inc. 2004] is the best-known instrument in this class. The measurement is stationary while testing. The power is transmitted to the pavement by means of crank operation at a frequency of 8 Hz via two steel wheels. The sinusoidal function, generated in this way, is overlapping with the static load given by the equipment weight. The deflections are measured by five geophones located at different distances from the loading plate. The peak load level is approximately 4.5 kN and cannot be varied.

The disadvantage of the harmonic load deflection systems is that can generate inertia effects that are different from the traffic loads. Apart from the inertia effects, the peak load is very distinct from the loads induced by heavy vehicles axles.

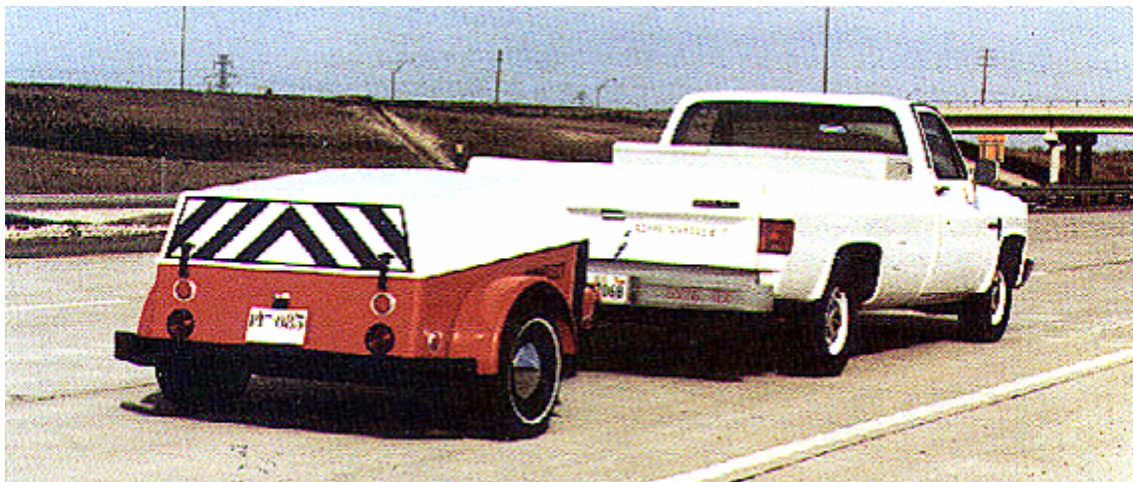


Figure 3.12 – Dynalect [Geo-Log, Inc. 2004]

3.3.1.3 Falling Weight Deflectometer

The Falling Weight Deflectometer (FWD) is presently the device for deflection testing most widely used in Europe, North America and Japan [Irwin, L.H.; 2002]. The test load is obtained by dropping a weight from a certain height on a set of buffers. The deflections are measured by a set of deflection transducers resting on the surface. A more detailed description of the FWD operation is presented in 3.3.2, since this is the equipment used in the present study. This equipment has the advantage that the impact load applied on the pavement can be changed by changing the weight, the height and the loading plate. In this way simulation of various loading is enabled. The equipment measures the pavement response in 6 to 9 points, resulting a deflection bowl that reflects the influence of different layers on pavement response (see Figure 3.17). As disadvantages, the most important are the negative impact on traffic and the time consumption, as it is unable to perform tests at traffic speed and neither in continuum along the pavement. The main advantage of this equipment is that it provides the whole deflection bowl in each test point

A lighter version of FWD is also available. This equipment was developed for tests performed on granular materials and soils, mainly for quality control purposes. On one hand, the light FWD is easy to transport, as it is portable and no car access is required. On the other hand, it can only generate load values up to 14 kN and the deflections are measured in 3 to 4 points, maximum.

3.3.1.4 Wave propagation measurements

Shell Research carried out first wave propagation measurements in the 60's with the Road Vibrator and Goodman's Vibrator [Blaine, J and Burlot, R.; 1970]. The method has not been used for decades, until it started again to be used in the USA with the "Spectrum Analysis of Surface Waves" (SASW), which is still under development. SASW testing is based on the dispersive characteristic of Rayleigh waves when travelling through a layered medium [BAY GEOPHISICAL; 2004]. A dynamic source is used to generate surface waves of different wavelengths (or frequencies) that are monitored by two or more receivers at known offsets.

Recently SHRP upgraded their "Seismic Pavement Analyzer" (SPA). [Wimsatt, A.J *et al*; 1998]. The SPA is a small trailer equipped with two pneumatic hammers, which strike the pavement, producing waves that are picked up by eight transducers. The test is almost fully automated. The data are analyzed by a computer software program, which then generates a report describing the condition, thickness, and stiffness of the pavement; any defects in the pavement subgrade; and other properties that are directly related to pavement performance. SHRP also developed a portable SPA (PSPA), which is a miniature version of SPA used to monitoring the quality and thickness of concrete pavement slabs. Three different seismic

techniques are used: impact echo, ultrasonic body wave and surface wave. Those last two, namely their velocities are used for estimating the Young's modulus and shear moduli [US Army Engineer, 1999], while the first one is used for thickness estimation and recently for compaction control.

As advantages, wave propagation is a global measurement, the resulting profile is representative of the subsurface properties averaged over measured distance and its resolution near the surface is typically greater than with other methods [BAY GEOPHISICAL; 2004]. A disadvantage is given by the fact that greater accuracy requires complex data analysis. Nevertheless, simple empirical analysis can be done to estimate the average shear wave velocity profile.

3.3.1.5 Other methods

The installation of in-depth sensors, able to continuously monitor the structural pavement condition is another possible solution for bearing capacity evaluation, without traffic interference. This method can provide information on pavement deterioration in terms of pavement strain, stress, deflection, temperature, moisture, etc., without any measuring devices causing traffic disturbance on the road [FORMAT, 2004]. However, it will only provide results at one specific spot, which may not be representative of the whole section under study.

3.3.2 Falling Weight Deflectometer (FWD)

3.3.2.1 General presentation and operation

The FWD was first built in France in the early 60's, but its development was interrupted due to difficulties in achieving adequate deflection measurements at that time. Based on the French experiments, prototypes were later built and tested, for example in the Netherlands and in Denmark. The first FWDs were extremely difficult to use. After that, PHØNIX and DYNATEST started to build commercial models of FWDs. In 1969 the method was adopted in Sweden [Tholén, O.; 1980] and in 1976 KUAB started routine operations with FWD. In 1987, Foundation Mechanics, Inc. started to produce JILS-FWD's in the USA. There also are several FWDs produced by Kamatsu (Japan) and several self-built FWDs, especially on the Netherlands and Japan. Presently, the most widely used models are produced by DYNATEST, CARL-BRO (ex PHØNIX) (Denmark) and KUAB (Sweden).

Operation principle

A weight is dropped from a given height on a “spring” system (a set of rubber buffers in present configurations) linked to a loading plate in contact with the pavement’s surface. The response of the pavement is measured through the deflections at several locations in the surface. The weight, the height of fall and the properties of the spring system define the impulse parameters (shape and peak value) [Tholén, O.; 1980].

The load pulse has a variation in time, which simulates the impact of a moving vehicle at 60 to 80 km/h [Ullidtz, P.; 1987, Antunes, M. L.; 1993]. The impact load can range from 20 to 150 kN, in case of LNEC’s FWD, but there are also heavier FWDs, which can generate load pulses of 250 kN. The pulse duration can vary between 25 ms and 60 ms. The response is measured by several transducers (generally 6 to 9) spaced at various offsets from the centre of the plate.

Figure 3.13 presents the FWD operating principles.

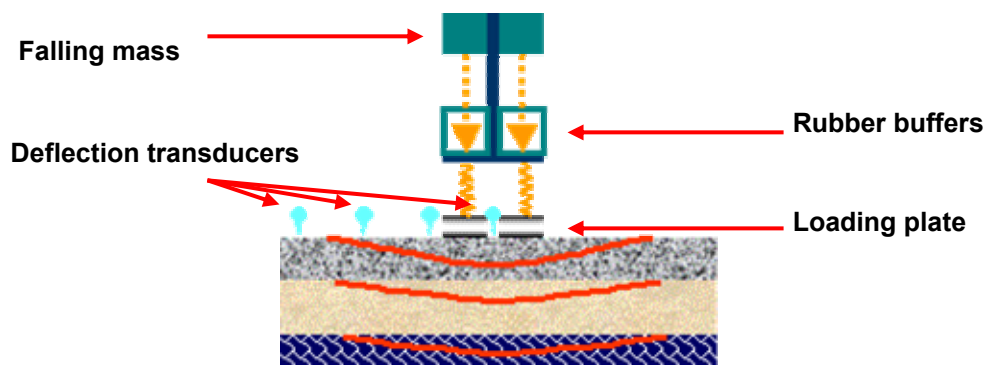


Figure 3.13 – FWD operating principles

The loading-plate is raised hydraulically, as well as the deflection transducers, when moving from one test point to the other.

Several experiments were made, at the beginning of FWD development, aiming at simulating stress/strain pulses induced by the traffic loads in the pavement layers. The following FWD characteristics were studied and improved:

Load pulse

In the earlier versions, the load pulse generation rose difficulties due to the internal oscillation of the spring system and its sensibility to the pavement’s deflection effects. The “spring” systems in the current machines consist of a set of rubber buffers, whose characteristics were designed to minimize these effects. In the KUAB machines, a “spring” system consisting of a mass between two rubber buffer systems was adopted (so called “two mass

system”). This system provides not only a drastic reduction of internal oscillation but also linearity between the peak force and pavement’s deflections [Tholen, O.; 1980].

The load pulse generated by the FWD during testing is different for each drop. The peak load values are not very different from the target value. However, in order to compare the results obtained in different locations, it is necessary to transform, through a simple mathematic operation, the deflections measured into “normalised” deflections corresponding to the target load. This process is called "normalisation". In this way, the results in different test points can be compared and statistically analysed.

Loading plate

An uniform loading area in good contact with the road surface is essential for the accuracy of the test. Good contact is difficult to achieve in weak structures or uneven surfaces using a rigid round plate. Significant differences are obtained in centre deflection values for the same total load, but different stress distributions. A hydraulic load-distributing plate was developed in order to ensure a better contact between the plate and the surface to be tested [Kestler, M.A.; 1997]. The loading plate is generally divided in segments (2 or 4).

Deflection measurement

The main issues taken into account in order to ensure the measurement accuracy are the stability of the signal to environmental effects and to pulse duration. Even more important is to be sure that the maximum value of the deflection is picked and recorded.

In the later versions of FWD, the deflection measuring system is isolated, as much as possible, from the loading system, in order to avoid the influence of the dropping weight in the deflections measured.

There are two main types of deflection transducers used in the current FWD devices [Sorensen, A.; 2004]:

- ✓ *Geophones* (seismic velocity transducers), which measure velocities of the pavement's surface and convert them into deflections, by integrating the signal;
- ✓ *Seismometers* (seismic displacement transducers), which measure directly the deflections of the pavement’s surface.

Testing procedures

The measured values of the load and deflections are automatically recorded for each impact. Initially developed for Dos, nowadays the FWD’s softwares are generally operating in Windows environment. The operator can set the testing parameters on the software (laptop), such as load level, drop sequence, distance between testing points etc. and can also add

information on testing conditions and comments after each test if needed. The output files are generally ASCII and are easy to import to Excel for processing. Although there are FWDs installed in dedicated vehicles, the majority are still mounted on trailers.

More detailed descriptions of the FWD operation principles and characteristics as well as the testing procedures can be found in bibliography [Antunes, M. L., 1993; CROW, 1998; COST 336, 2002].

3.3.2.2 LNEC's FWD

LNEC has a "KUAB 150" FWD since the early 80's. This equipment was later upgraded several times, in order to have the same features as the more recent devices. Figure 3.14 illustrates LNEC's FWD in its present version.



Figure 3.14 – LNEC's Falling Weight Deflectometer

The most recent modification in LNEC's FWD has been modified in order to improve the accuracy of measurements. Therefore, the suspension system of the deflection transducers has been separated from the load generation system. In this way, the sensors become stable in shorter time and the recorded signals suffer less clutter given by the vibrations of the

loading system. At the same time, the deflection transducers' location can be modified, for a better adaptability to the condition of the pavement section under study.

LNEC's KUAB 150 has the following features:

Load pulse

The load generation system is a "two mass system", consisting of an intermediate mass, between two sets of rubber buffers, plus the falling mass.

The variation of load pulse is obtained through the variation of the masses and/or drop height. Also the rubber buffer system can be changed, depending on the intended load pulses.

There are three different heights available in LNEC's FWD. This, together with the variable masses and rubber buffers, allows for a range of variation for the peak load from 20 kN (first height, minimum mass, only two buffers on each side of the intermediate mass) to 150 kN (third height, maximum mass and 6 rubber buffers on each side).

Loading plate

LNEC's FWD has two different loading plate dimensions available. One has 300 mm diameter, aiming at simulating the heavy-lorry tyre contact pressures, which is used for testing road pavements. The other one, with 450 mm diameter, is adequate for airfield pavement tests (as it simulates the airplanes tyre contact area) and for testing pavement layers (base and sub-base) during construction. In this later case, the stress propagation within the pavement depth generates a larger contact area in deeper levels. Therefore, an increasing loading plate diameter will improve the simulation of the stress distribution due to traffic loads in deeper pavement layers.

For both loading plates, the contact surface consists of a rubber disk fixed to a metal plate, which is divided into 4 segments. The load is applied through an oil chamber that ensures equal load distribution for each of the 4 segments. These characteristics give the loading plate a certain "flexibility" and smoothness, providing an improved contact with the pavement's surface.

Deflection measurement

The deflection measurement system used in LNEC's FWD consists of seven seismometers.

After recent equipment upgrades, the measuring system is physically separated from the load generation system therefore, the influence of the last one in the response is negligible and also the transducers become stable faster during measurement.

The seismometers offset can be changed according to the type of pavement under study. The minimum module (distance) between two successive seismometers is fixed to 150 mm, (except for the first two). The maximum distance between the centre of the loaded area and the last seismometer is 2.5 m.

Finally, the deflection and load measurement system allows for recording not only the peak values but also the load and deflection history.

3.3.2.3 FWD survey procedure

It is important to have a sound planning of the tests in terms of location and test configuration according to the pavement to be analysed. The procedure generally used for bearing capacity evaluation using FWD is to measure the deflections in a considerable number of test points. For road pavement studies, these points are generally located along the wheel path or in-between wheel paths. For airfield pavements, the survey alignments are parallel to the pavement runway axle. Nevertheless, there are authors who use different procedures [Stet, M *et al*; 2002], specially for rigid pavements.

For road pavement evaluation, the alignments for deflection measurement can be located either on the outer side-wheel paths or / and in-between the wheel paths. Generally, the tests are performed along the outer side-wheel paths, which are probably more deteriorated than the rest of the pavement. In this case, the deflections are higher and the structural deterioration induced by past traffic can be estimated. The deflection measurement performed between the wheel paths, allows for a better contact between the loading plate and the pavement, than in case of wheel path measurement if there exist permanent deformation, but does not reflect the influence of the past traffic. When the tests are performed in both locations, results can be compared but the process is expensive and time consuming.

In each alignment, the measurements are performed at equal distances, chosen according to the length of the section to be tested (from 10 to 100 m). The target load is chosen in order to better simulate the traffic for the pavement under study. The target load and consequently the height of the drop and the weight to be used, depend on the type of pavement to be studied and the traffic characteristics (airplane main gear, truck axles and their speed). The value of the peak load generally adopted for testing in road pavements is 40 to 70 kN, while for airfield pavements is 150 to 250 kN.

The number of drops to perform per test point has been studied by several authors. Two to three drops per test point are generally recommended since the first drop is used only to improve the contact between the loading plate and the pavement surface.

The seismometers offset can be changed according to the type of pavements under study, in order to better record the deflection bowl. Typical deflections bowls for different types of pavements are presented in Figure 3.15. Therefore, the seismometer location should be optimised in order to measure the deflections at positions that are most sensitive to the elastic parameters in the pavement layers [Almeida, J. R. de; 1993]. As presented, in case of weak pavement the seismometers should be located closer to the loading plate, as the deflection bowl curve changes drastically in loading plate vicinity, while in case of very stiff pavement the distance between seismometers should increase in order to record the entire deflection bowl.

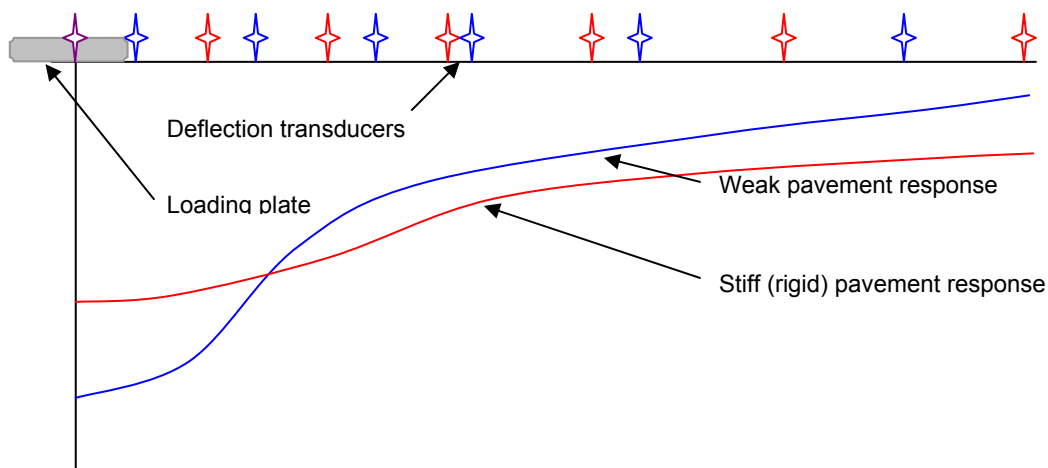


Figure 3.15 – Deflection bowls for different type of pavements

3.3.2.4 Temperature measurements

Due to the dependency of the response of asphalt layers to temperature, deflection test results must always be complemented with information regarding asphalt temperatures at the time of testing. Temperature measurement during testing is always recommended and is used in the analysis to convert the asphalt stiffness moduli, or the deflections, into their equivalent values under a design temperature condition [Antunes, M.L.; 1993; Van Gurp, C.A.P.M.; 1995].

Different approaches can be used for the assessment of asphalt layer temperatures during FWD testing:

- ✓ To measure the air and pavement temperature during testing and estimate the temperature at certain depths inside the asphalt layers;
- ✓ To measure in-depth asphalt temperatures, generally at 3 or more different depths, including the surface, thus obtaining a temperature profile.

Based on the measured or estimated temperature profiles, a “representative” asphalt layer temperature must be assigned to each deflection bowl. The equivalent pavement temperature can be determined using the weighted average of measured temperatures with depth (Figure 3.16).

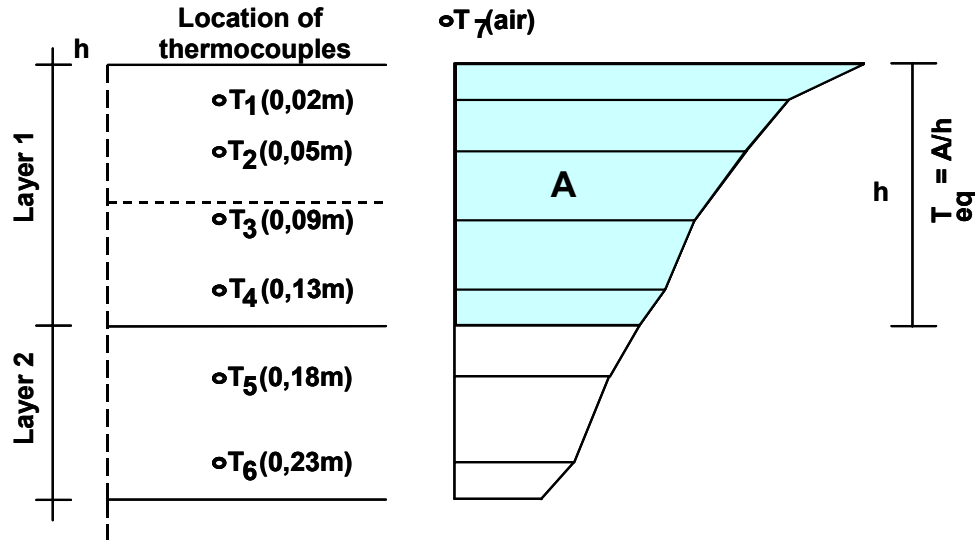


Figure 3.16 – Calculation of “equivalent temperature” [Antunes, M.L.; 1993]

This method has proven to be suitable for representation of the effect of temperature gradients in the deflections [Antunes, M.L.; 1993].

The most commonly used methods for temperature measurements are described below:

Surface temperature measurements

The surface temperature measurement can be performed using either contact thermometers or non-contact infrared sensors mounted on the FWD trailer. Many of the recent FWD's have this type of sensors.

In-depth temperature measurements

In-depth temperature measurements will give a better information regarding the temperature conditions in the asphalt layers. Since it is time consuming to perform these measurements, they are done only on selected test points at one or more depths within the asphalt layers. Holes of 5 mm diameter are drilled in the pavement. It is recommended that the temperature is measured at three depths as follows: 25 mm, half the depth of the asphalt layer and 25 mm above the bottom of the layer. The temperature gradient decreases with depth and becomes almost constant below 250 mm depth [COST 336; 2002]. A drop of contact fluid (usually glycerol) is poured into the hole in order to insure a good thermal contact between the thermometer and the material and not to influence the temperature gradient. In this case,

the asphalt equivalent temperature during tests can be calculated as the arithmetic mean of the available in-depth measured temperatures [COST 336; 2002].

The main disadvantage of measurements of in-depth temperatures is the duration (it is time consuming). Therefore, in order to simplify the process one measurement is often found adequate (usually at a depth of one third of the asphalt layer thickness).

Besides the direct measurements there are alternative methods to estimate the pavement temperature based on the air temperature and on surface temperature.

The most commonly used methods for estimation of asphalt temperatures in depth are mentioned below:

Pavement temperature estimation

BELLS method

One of the more often used methods is BELLS3 regression equation [Stubstad, R.N. *et al*; 1998; Baltzer, S. *et al*; 1994]. The "BELLS" (Baltzer, Ertman-Larsen, Lukanen and Stubstad) method was developed to estimate the pavement temperature using as input 5 day average temperature for the 5 days prior test, the surface temperature, the thickness of the asphalt layer, and the time of the day when the measurement during test is performed. An improved equation (3.1) "BELLS 3" [Stubstad, R.N. *et al*; 1998] has been developed based on the original one. It uses one day, instead of 5 days, average temperature. The method is adequate for routine FWD testing and is useful especially when temperature measurements within the asphalt layer are not available.

The temperature at a certain depth in the pavement is given by the following formula:

$$T_d = 0.95 + 0.892IR + (\log_{10}(d) - 1.25)(-0.45IR + 0.62(1 - day) + 1.83 \sin(hr_{18} - 15.5)) + 0.42IR \sin(hr_{18} - 13.5) \quad (3.1)$$

Where:

- T_d – pavement temperature at desired depth d , °C;
- IR – infrared surface temperature, °C;
- D – depth at which material temperature is to be predicted, mm;
- 1-day – average of the previous day high & low air temperature;
- \sin – sin function over an 18-hour period, and 2π radians equal to one 18-hour cycle;
- hr_{18} – time of the day in the 24-hour system, but calculated using 18-hour Asphalt Concrete (AC) temperature rise and fall time, as explained in the reference.

As limitation of the method the following factors should be taken into account:

- ✓ the method has been developed using *daytime* FWD and Infra Red (IR) temperature data only, thus extrapolation into the night time hours may not be accurate;

- ✓ it should only be used for asphalt pavement thicknesses between 45 and 305 mm;
- ✓ last but not least, the equation is mostly affected by the IR reading, therefore the accuracy and sensor calibration is vital [Stubstad, R.N. *et al*; 1998].

Other methods

There are some other methods available for pavement subsurface temperature estimation, usually developed for certain material characteristics and local conditions.

Park [Park, D *et al*; 2001] developed a temperature prediction model based on experimental data using surface temperature and FWD measurements as input. The equation's coefficients were determined through a numerical optimisation method (quasi-Newton), for correlating the surface temperature with the temperature at a certain depth.

$$T_d = T_{surf} + (-0,3451d - 0,0432d^2 + 0,00196d^3) \sin(-6,3252t_d + 5,0967) \quad (3.2)$$

Where:

- T_d – pavement temperature at desired depth d , °C;
- T_{surf} – surface temperature, °C;
- d – depth at which material temperature is to be predicted, cm;
- \sin – sin function (radians);
- t_d – time when the AC surface temperature was measured. (days; $0 < t_d < 1$; e.g. 1:30 p.m.=13,5/24=0,5625days)

A sinusoidal algorithm was developed by Ovik [Ovik, J. *et al*; 1999] to predict asphalt mixture temperature with depth and time of the year, using surface temperature. Extensive instrumentation, “*in situ*” weather station and deflection testing were used for the development of the method.

$$T_{d,t} = T_{mean} + Ae^{-d} \sqrt{\frac{2\pi}{P\alpha}} \sin\left(\frac{2\pi}{P}(t) - d\sqrt{\frac{2\pi}{P\alpha}}\right) \quad (3.3)$$

Where:

- $T_{d,t}$ – pavement temperature as a function of the desired depth (d) and time (t), °C;
- T_{mean} – average temperature at surface, °C;
- d – depth at which material temperature is to be predicted, m;
- \sin – sin function (radians);
- A – maximum temperature amplitude, $(T_{max} - T_{mean})$, °C;
- P – period of recurrence cycle; $\omega = 2\pi/P = 2\pi/365$;
- α – thermal diffusivity (area/time), gives a measure of the rate at which a material will undergo a change in temperature in response to external change in temperature. For dense graded asphalt concrete was considered $0,121 \text{ m}^2/\text{day}$ based on measurements by [Chadbourn *et al*; 1996].
- t – time measured from when the surface temperature passes through T_{mean} , days.

In the method developed by Freitas [Freitas, E.; 2004] the pavement temperature gradient is estimated in various locations, based on the temperature measured at 5 mm depth along the pavement and using as reference one set of in-depth temperature measurements. The estimation is performed using the Picado-Santos [Picado-Santos; L.; 1994] method for modelling the temperature gradients (see 2.4.3).

3.3.2.5 Pre-processing of measurements

There are several factors that affect deflections during testing. As already mentioned (see 3.3.2.1), in order to compare the results obtained in different test points and different conditions the measured deflections have to be "normalised". Factors, such as peak load or temperature changes during testing affect the measured deflections. The "normalisation" consists of processes that aims at reducing the influence of these factors and, as a result, reproduce the same testing conditions for all measured deflections.

Normalisation for target load

The measured value of the load is automatically recorded for each measurement. The load generated by the FWD for each drop is not constant (has small variations around the target value). Therefore, in order to compare the deflections for different drops, these have to be "normalised". The normalisation consists of calculating the deflection corresponding to the target load value by linear extrapolation. The process is simple and is mathematically expressed as follows:

$$D_n = D_m \frac{L_t}{L_m} \quad (3.4)$$

Where:

- D_n – normalised deflection (μm);
- D_m – measured deflection (μm);
- L_t – target load (kN);
- L_m – measured load (kN).

Deflection bowl evaluation

Once the measured deflection bowl is "normalised" for the target load, deflection plots will give an indicator where structural weakness may be present. The different pavement layers influence different parts of the deflection bowl. Figure 3.17 indicates the parts of the deflection bowl influenced by the different layers [Almeida, J. R. de; 1993] for a typical flexible pavement structure.

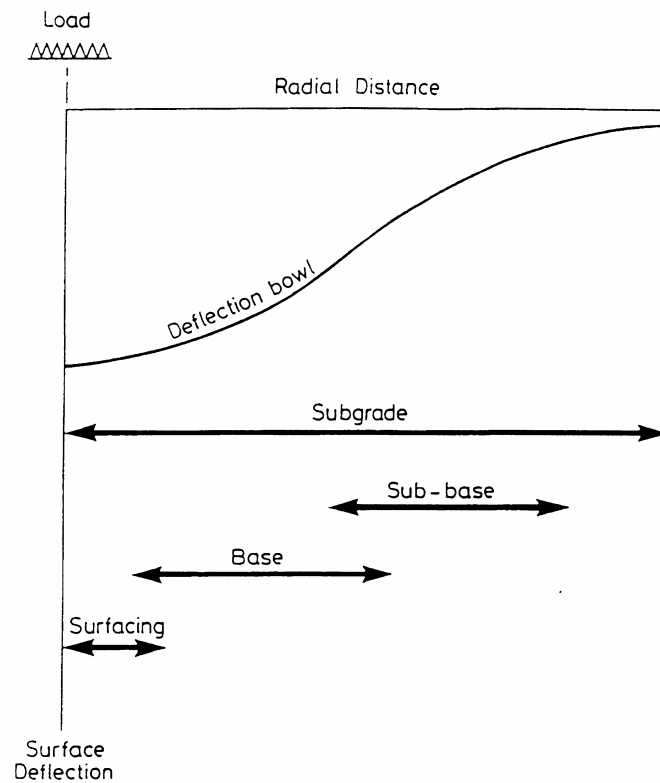


Figure 3.17 – Influence of different layers on deflection bowl [Almeida, J. R. de;1993]

In order to help in the analysis of deflection bowls one or more “deflection bowl parameters” can be analysed. The deflection bowl parameters are the geometric characteristics of the pavement response (shape), as curvature or amplitude. The parameters, represented by deflections and/or relations between them, give us information about the pavement’s structural characteristics: for example, the outer deflection is related with the subgrade condition, whereas a drastic curvature can reflect the existence of a weak layer into the pavement’s structure. A summary of existing deflection bowl parameters adapted from COST 336 [COST 336, 2002] is listed in Table 3.1.

The FWD deflection data, expressed by the selected deflection bowl parameters, can be used for subdivision of the pavement into homogeneous subsections. The method used for subdividing in homogeneous subsections will be described in 3.5.

Table 3.1 – Summary of existing deflection bowl parameters

DEFLECTION BOWL PARAMETER			
Name	Equation	UM	Purpose
Distinct deflections – Centre deflection	D_0	μm	Reflects the overall pavement condition
Distinct deflections	D_r ($r=1$ to n)	μm	Reflects the condition of layer at equivalent depth r
Surface Curvature Index, SCI	D_0-D_r	μm	Reflects the condition of bound layers
Base Curvature Index, BCI	$D_{n-1}-D_n$	μm	Reflects the condition of sub-base layer
Base Damage Index, BDI	D_2-D_r	μm	Reflects the condition of base layer
Curvature Bowl Factor, CBF	$(D_0-D_r)/D_0$	-	Reflects the condition of layer at depth r
Deflection Ratio, DR	D_0/D_r	-	Reflects the condition of layer at depth r

D_0 deflection at the centre of the loaded area;

D_r deflection at distance r from the centre of the loading plate;

D_n deflection at the outmost deflection sensors;

D_{n-1} deflection at the next to outmost deflection sensors;

D_2 deflection at the deflection sensor closest to the edge of the loading plate.

3.4 Layer Thickness

In general, information about the existing pavement structure can be obtained from historical data, coring, trial pits and Ground Penetrating Radar (GPR). Normally, the best approach is to gather as much information as possible, from different sources.

The most common means to determine layer thickness or confirm the available construction records, is by performing cores and/or test pits at selected sites, which will be considered as representative of a certain pavement section.

The **cores** are relatively easy to drill and the impact on the pavement structure is minor (Figure 3.18), as the holes are easy to fill after drilling. On the other hand, they are time consuming and the information obtained from the cores is limited to the bound layers. Sufficient cores should be taken to provide a reliable record of layer thickness data, especially when continuous layer thickness measurements (GPR) are not available.



Figure 3.18 – Core drilling equipment and extracted core

Test pits can give information about the complete structure, but they are even more time-consuming and also more destructive than coring and therefore, they will induce longer road closures at each site. Test pits are performed on the pavement, with the purpose of measuring the thickness of bound, as well as unbound layers (base and sub-base layers, as well as subgrade), *in situ* characterisation of materials and collection of samples for laboratory tests.

Extra care is required for the pit repair afterwards, in order to ensure that the pavement's serviceability remains at the original level. When the materials used for repairing are not adequate, and/or not well placed, it can generate a "weak" point in the pavement structure, which will result in poor surface characteristics or sensitivity to water infiltration into the pavement structure. In many cases, the pits have to be performed on the shoulders, not in the pavement itself, either because of traffic restrictions and/or due to their destructive effects. The results obtained in these cases are not always reflecting the exact condition of the pavement structure. In many projects, it is not even possible to perform test pits, which means that historical data will be the only data available about the unbound layers.

These activities are time-consuming and give only an indication of the pavement structure at localised spots. They are not capable of identifying the exact position of changes in the pavement structure, along the road.

Layer thickness may be quite variable along a pavement structure, therefore continuous information on thickness is needed. Accurate measurements are essential for the analysis of FWD measurements, particularly for the backcalculation process. Incorrect layer thickness can result in erroneous interpretation of the deflections. A continuous measurement of the layer thicknesses has become possible with the application of GPR for substructure evaluations. **GPR** has become an important tool for pavement evaluation, since it allows for continuous measurement of the layer thickness and therefore, a precise identification of changes in pavement structure and, taking into account that historical data are in most of the cases erroneous or incomplete, while the cores give us only local information.

LNEC's GPR equipment has two horn antenna pairs 1000MHz and 1800 MHz. A detailed description of the GPR functioning and survey procedure is presented in Chapter 4.

The information obtained with GPR should be confirmed and completed with additional testing [Fontul, S. and Antunes, M.L.; 2000]. The additional tests consist of core drilling and/or pits. Although destructive tests like the mentioned above are still necessary to complete and calibrate the GPR records, the core drilling can be optimised, as only 2 to 3 cores per GPR file are generally enough to obtain an accurate mapping of the layer's thickness along the pavement. More cores can be needed for deteriorated and very heterogeneous pavements. In this way, the impact on the road users resulting from the traffic restrictions during tests is also reduced.

The continuous information on layer thickness can be also used for the subdivision of the pavement into homogeneous subsections.

3.5 Division in sub-sections

3.5.1 Introduction

Division of a pavement section into homogeneous sub-section should take into account the following parameters [COST 336, 2002; AASHTO, 2001], either individually or combined:

- ✓ construction records,

- ✓ surface distress,
- ✓ subgrade type, earthworks (cut and fill areas),
- ✓ drainage condition,
- ✓ layer thicknesses,
- ✓ traffic volumes,
- ✓ measured deflections and deflection bowl parameters,
- ✓ number of (remaining) measuring points of the (sub)section.

Besides the above factors, other more elaborate parameters may be used for sub-division [COST 336; 2002]:

- ✓ surface modulus plots,
- ✓ layer moduli,
- ✓ residual pavement life,
- ✓ overlay requirement, if the method used calculates the overlay needed at every test point on the road,

The delimitation into homogeneous sub-sections is sensitive to the total number of points considered in the project, in this case the total length of the pavement considered during the division process. Sometimes the main homogeneous sub-sections defined along the pavement (total length) can be also sub-divided into homogeneous "sub-sub-sections".

It should be mentioned that, there is also a risk in dividing a pavement into too many sub-sections. In order to avoid this possibility a statistical method may be applied. This method, is described later in 3.5.4, and allows for validation of the statistical differences between two consecutive sub-sections. If there are no differences, they will be considered as one sub-section. Another factor that must be taken into account when division is performed is the minimum number of parameter values per sub-section in order to be considered statistically significant (generally, a minimum number of 12 values are required).

The division in subsections can be performed, either by engineering judgement using visual assessment of the variation of parameters (designated as "visual assessment") or by statistical methods or by a combination of both.

"Visual assessment" (e.g. division in subsections based on a (expert) subjective analysis of the parameter variation) is used for analysis of construction records, subgrade type, drainage condition and traffic volumes. A "visual assessment" division for other variables such as deflections and layer thickness is very useful even when a statistical method is used, as a complement to this one.

Sometimes the “visual assessment” of the variation of parameters along the section does not easily provide enough information for a proper division. For large databases the visual assessment delineation can become time-consuming and confusing.

There are statistical methods, not very complex and easily adaptable to computer processing and graphic analysis, allowing for a better interpretation of the variability of several parameters along the pavement. The following sections refer to some of these methods.

3.5.2 Cumulative difference method

3.5.2.1 Approach concepts

A relatively straightforward and powerful method is the “cumulative difference” method [AASHTO, 2001; CROW, 1998; COST 336, 2002]. It is widely used for identification and delimitation of statistically homogeneous sub-sections along the pavement, and can be applied for a variety of pavement parameters or response variables such as: deflections, layer thickness, serviceability, surface distresses etc.

Figure 3.19 illustrates the cumulative difference concept, using a basic example with constant parameter values r_1 , r_2 e r_3 within various intervals (0 to x_1 ; x_1 to x_2 and x_2 to x_3) along the pavement length. Part a), of this figure, is an illustration of the parameter values – distance plot. The cumulative area under the values-distance plot can be calculated as illustrated in Figure 3.19 part b). The areas (integrals) are continuous within the respective intervals, the slopes (derivates) of the cumulative area curves are the response values for each interval (r_1 , r_2 e r_3) and the dashed line represents the cumulative area given by the average project response (\bar{A}_x), and its slope is the average parameter value along the pavement.

In this way, at a certain location x , the cumulative area under the value-distance plot, A_x , and the cumulative area corresponding to the plot under \bar{A}_x , of the average parameter value can be calculated using formulas (3.5) to (3.7).

$$A_x = \int_0^x r \, dx \quad (3.5)$$

$$\bar{r} = \frac{\int_0^{x_1} r_1 \, dx + \int_{x_1}^{x_2} r_2 \, dx + \int_{x_2}^{x_3} r_3 \, dx}{L_p} = \frac{A_T}{L_p} \quad (3.6)$$

$$\bar{A}_x = \bar{r} \int_0^x dx \quad (3.7)$$

Where:

- A_x – cumulative area under the value-distance plot at a point x;
- x_i – distance to origin (location);
- r_i – parameter value at distance x_i ;
- \bar{r} - average parameter value;
- \bar{A}_x – cumulative area of the average parameter value at a point x;
- A_T – total area under the value-distance plot;
- L_p – total pavement length;

The cumulative difference variable (Z_x) is calculated for each point as the difference between the cumulative area at that point A_x and the cumulative area of the average parameter value at that point (3.6).

$$Z_x = A_x - \bar{A}_x \quad (3.8)$$

Z_x plotted against distance x is illustrated in Figure 3.19 c). The delimitations into homogeneous subsections are identified from this graph. The border between two sections is given by the change in slope of this plot.

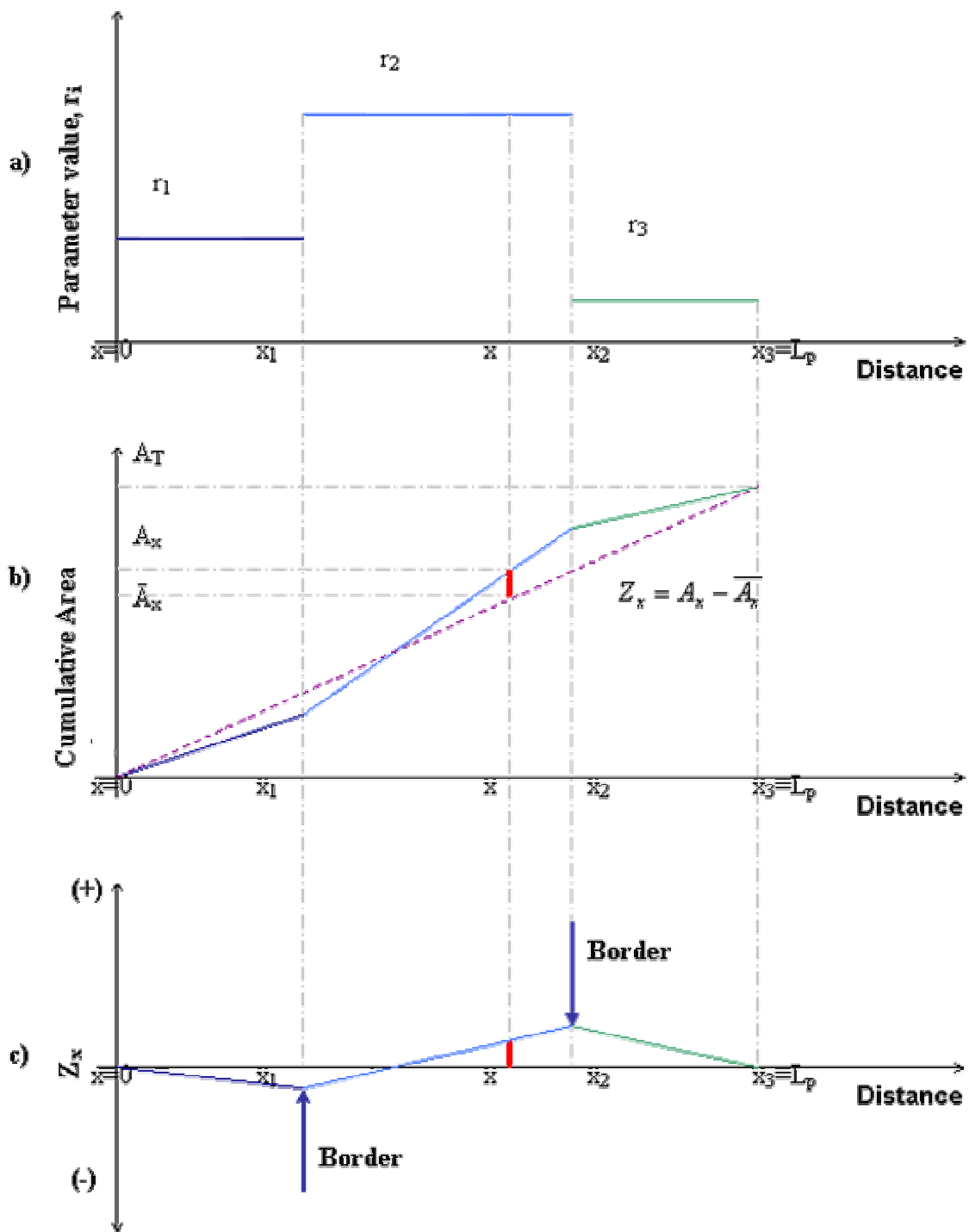


Figure 3.19 – Cumulative Difference Concept [AASHTO, 2001]

3.5.2.2 Application to discontinuous variables

In practice the parameter values are discontinuous (point measurements), and in general the interval between successive measurements is also variable. A numerical difference approach is used [AASHTO, 2001] for the calculation of Z_x , as follows:

$$Z_x = \sum_{i=1}^n a_i - \frac{\sum_{i=1}^n a_i}{L_p} \sum_{i=1}^n x_i \quad (3.9)$$

$$\text{with: } a_i = \frac{(r_{i-1} + r_i) \times x_i}{2} = \bar{r}_i \times x_i \quad (r_0=r_1 \text{ for the first interval}) \quad (3.10)$$

Where:

- n - total number of parameter values taken in project;
- x_i - distance of point i to the origin;
- r_i - parameter value of the i^{th} point;
- \bar{r}_i - average of parameter values between the $(i-1)$ and i^{th} points;
- L_p - total length of the section.

For equal intervals between test points equation (3.9) can be written:

$$Z_x = \sum_{i=1}^n a_i - \frac{n}{n_t} \sum_{i=1}^{n_t} a_i \quad (3.11)$$

An example of the variation of measured FWD deflections with distance is presented in Figure 3.20 while Figure 3.21 presents the plot of the cumulative difference (Z_x) against distance for these deflections.

The division is based on the visual assessment of the graphic obtained for Z_x . The cumulative difference slope changes whenever there is a change in pavement characteristics. Those points are called "borders" between two consecutive subsections.

This method is widely used all over the world in structural pavement evaluation problems, since it is relatively simple, easily adaptable to computer processing and graphic analysis and at the same time allows for analysis of parameters even when the intervals between tests (points) are not equal. Therefore, it can be applied for all the variables taken into consideration during the delimitation of pavements into homogeneous subsections.

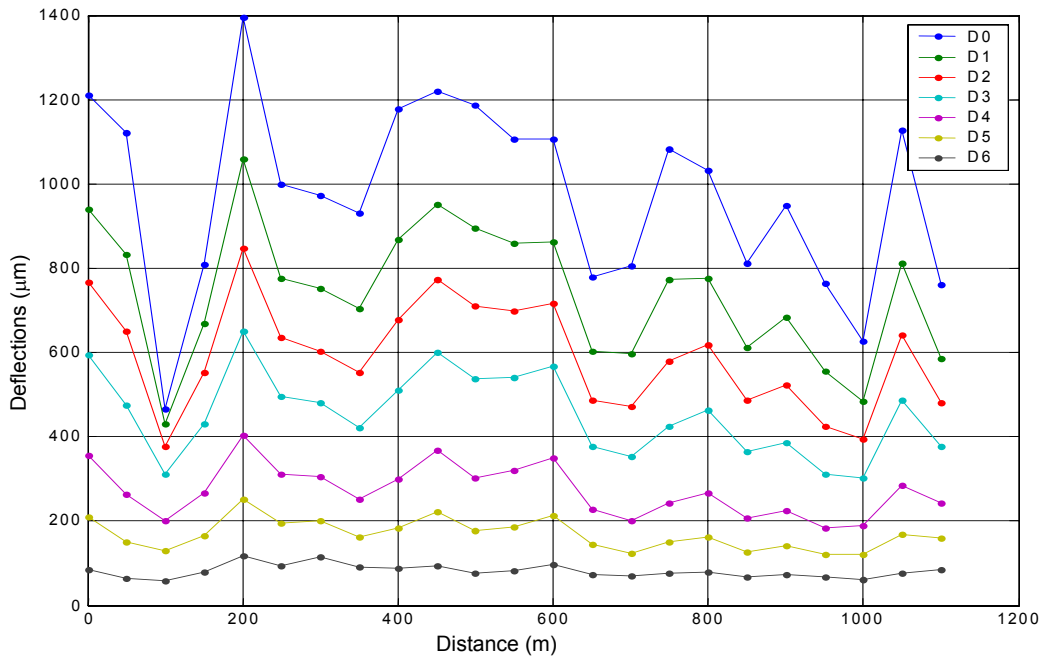


Figure 3.20 – Deflections variation with distance

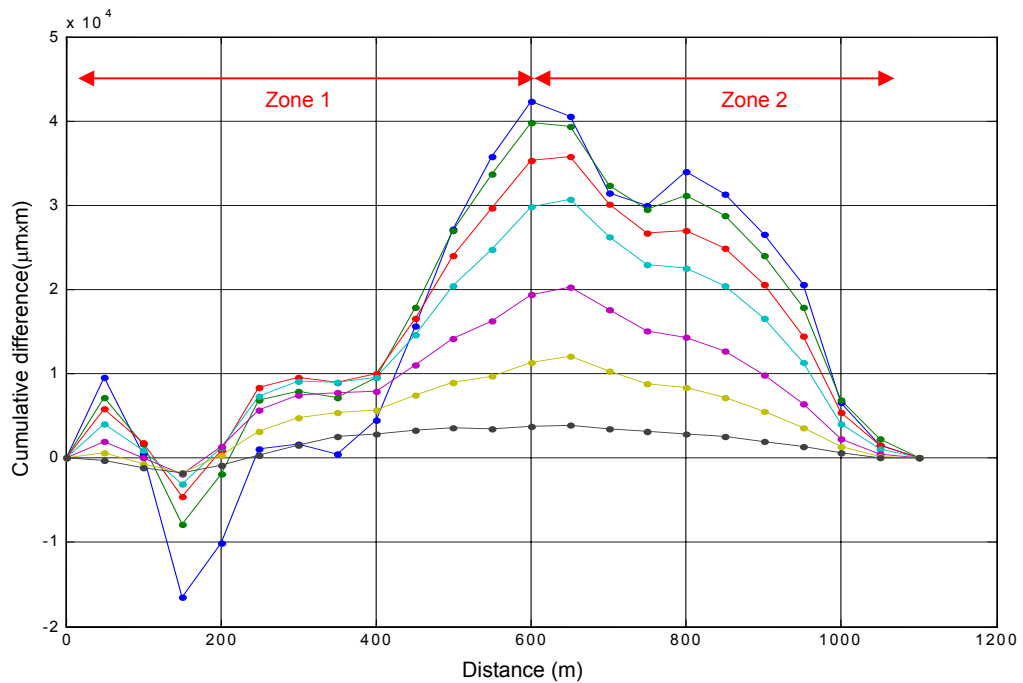


Figure 3.21 - Cumulative difference of deflections variation with distance

3.5.3 Normal distribution criteria

This method is proposed by LPC (*Laboratoires des Ponts et Chaussées*, France) and is used only for parameters measured at constant intervals. The method was initially applied for processing the compaction measurements and then used for deflection analysis [Lebas, M. *et al*; 1981; Mesnil-Adelée, M.; Peybernard, J.; 1984]. Later, a version of it was applied for pavement residual life analysis [Ullidtz, P; 1987].

The method tests the distribution of the parameter values, using statistical criteria, and divides into sub-sections with normal distributions, with a certain confidence level. A brief description of the method presented here. A test (*t-student distribution*) is performed in order to verify the "normality" of the data distribution. A t-student distribution has the particularity that for an infinite number of degrees of freedom it is equivalent to a normal distribution.

For a certain number (n) of parameter values (r_i), taken into consideration in the study, the average is first calculated (\bar{r}).

$$\bar{r} = \frac{1}{n} \sum_{i=1}^n r_i \quad (3.12)$$

Then, a statistic parameter (p) is calculated (3.13) in order to verify if the population follows a normal distribution (p=1). A value of p higher than 1 indicates that data has systematic or periodic variations while a value of p substantially lower indicates rapid fluctuations of data.

$$p = 0.5 \frac{\sum_{i=1}^{n-1} (r_{i+1} - r_i)^2}{\sum_{i=1}^n (r_i - \bar{r})^2} \quad (3.13)$$

The parameter p can be considered random if multiplied by n (the number of values) of a normal population. Therefore, for a certain n (number of elements in a population), the "*t-student distribution*" table gives us the limits p_α and $p_{1-\alpha}$. In other words, the population can be considered as "t-student" distributed, with a confidence level (probability) of $1-\alpha$, if p is between p_α and $p_{1-\alpha}$. Following the same reasoning as before, a value of p lower than p_α indicates rapid fluctuations and a value higher than $p_{1-\alpha}$ indicates systematic or periodic variations, meaning that the section can be divided into homogeneous sub-sections. The coefficient α represents the risk of wrongly considering a section as "t-student" distributed and the number of degrees of freedom is given by the sample size (n - 1). A high confidence level will result in a large number of small subsections, whereas a low confidence level will result in a reduced number of extended subsections.

A reduced normal distribution is applied for large sample sizes, when the number of values (n) is higher than 25. In this case instead of p , another statistic parameter (u) is calculated:

$$u = (1 - p) \sqrt{\frac{n^2 - 1}{n - 2}} \quad (3.14)$$

Then, based on u value and using the "*t-student distribution*" table the test for "t-student" distribution is performed. As in the previous case, if $u_\alpha \leq u \leq u_{1-\alpha}$ then the section is "t-student" distributed, if $u > u_{1-\alpha}$ the section should be divided into sub-sections and if $u < u_\alpha$ the data contains rapid fluctuations, requiring a deeper analysis.

If $u > u_{1-\alpha}$ the delimitation into homogeneous sub-sections is made at the maximum position of function $g(k)$ calculated based on the following equation:

$$g(k) = \frac{n}{k(n-k)} \left(\sum_{i=1}^k y_i \right)^2 \quad (3.15)$$

$$y_j = r_i - \bar{r} \quad (3.16)$$

Where:

- r_i – parameter value of the i^{th} point;
- \bar{r} - average of all parameter values in the subsection.

The calculations are repeated for each of the two sub-sections defined in this way and go on until a "t-student" distribution for each sub-section is achieved.

For some parameters, like moduli and expected residual life, the logarithmic of the parameter may be used instead of the value itself [Ullidtz, P; 1987], [Ullidtz, P; 1998], as they tend to follow logarithmic normal distributions.

3.5.4 Testing statistical significance of sub-sections

After the delimitation into homogeneous sub-sections it is advisable to verify if the sub-sections are statistically different and if they have the minimum number of values (normally 12) required for statistical purposes. Therefore, if there is no statistical difference between the sections, or if they do not have sufficient values, they can be merged. A T-student test can be used to assess if two consecutive sub-sections are statistically different.

Another method is the determination of the "level of homogeneity" by using the Coefficient of Variation (CV). The CV is defined as the ratio of the standard deviation over the mean value.

A possible classification, based on the CV, is recommended by COST 336 [COST 336, 2002]:

- CV < 20%: good homogeneity;

- $20\% \leq CV < 30\%$: moderate homogeneity;
- $30\% \leq CV < 40\%$: poor homogeneity;
- $CV \geq 40\%$: inhomogeneity.

The CV will indicate that a section is not homogeneous but it gives no indication about how to subdivide it.

The criterion presented above is frequently used for verification of the results obtained from “visual assessment” or cumulative difference methods.

3.5.5 Final sub-section identification

The final division should be made based on all the information available concerning the pavement under study. For each of them, the division can be made by engineering judgement or using statistical criteria. Figure 3.22 illustrates an example of a final subdivision based on centre deflection D_0 , layer thicknesses, subgrade and traffic [COST 336, 2002].

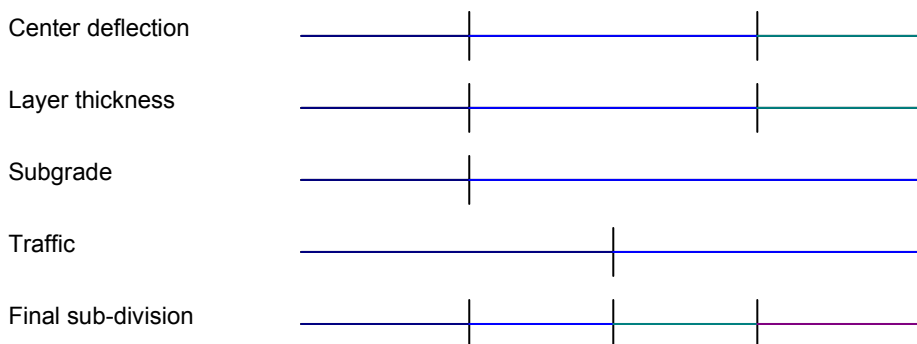


Figure 3.22 – Example of final sub-section identification [COST 336, 2002]

For each homogeneous subsection, the main available information must be stored, since it is essential for the subsequent analysis.

3.5.6 Selection of representative deflection bowl

For a given homogeneous subsection, the pavement structural model can be set up for each test location or for a certain point corresponding to a “representative deflection bowl”. This point will be considered to represent the pavement response observed in the homogeneous subsection.

The representative deflection bowl is the measured bowl, which is the nearest match to a selected “statistical” bowl. The “statistical” bowl is chosen taking into account a given confidence level. The confidence level chosen is usually between 50 % and 97 %. A confidence level of 85% is commonly adopted for bearing capacity evaluation.

For the determination of a “statistical” deflection bowl S_i , the following formula is used for each deflection sensor, i :

$$S_i = \bar{r}_i + b\sigma_i \quad (3.17)$$

Where:

- \bar{r}_i - average of deflections measured by sensor i ;
- σ_i - standard deviation of these deflections;
- b - a factor (depends on the confidence level).

For example, for 85% confidence level, we have:

$$S_i = \bar{r}_i + 1,04\sigma_i \quad (3.18)$$

The representative deflection bowl will be used for the backanalysis of pavement layer moduli. Thus, the structural model set-up for the point where this deflection bowl was measured will be considered as representing the subsection.

Alternatively, the interpretation of deflection measurements can be performed at every test point.

3.6 Interpretation of the results

3.6.1 Introduction

Pavement layer stiffness moduli can be calculated from the FWD deflections using a backcalculation procedure, provided that the layer thickness is known.

Usually the layers thickness are fixed within this process, and assuming typical values for the Poisson's ratios, the deflection bowls are used for backcalculation of E moduli. Assuming a certain pavement structure, the values of the deflections are calculated for the FWD peak load and are compared with the measured deflections. Through an iterative process, the assumed E-moduli values are adjusted in order to reduce the difference between the

deflections bowls, within a certain tolerance. The process is repeated until in order to obtain a "theoretical deflection bowl" as close as possible to the deflection bowl measured *in situ*.

Climatic effects such as temperature and moisture condition in the subgrade and, to some extent, in the granular layers influence the behaviour of the pavement. Therefore, these factors have to be taken into consideration for pavement evaluation.

Once backcalculation is performed and the results are adjusted to "design climatic conditions" the pavement structural model is used to calculate the stresses and strains that are induced by the traffic, which will be related to the pavement's residual life.

3.6.2 Pavement Modelling

3.6.2.1 Pavement structure modelling

In most cases the backcalculation is performed using multilayer linear-elastic models (Chapter 2), which assume that the materials are linear elastic, homogeneous and isotropic. The load is considered static and consists of a vertical pressure, uniformly distributed over a circular area. Full friction is usually assumed at the interfaces between layers.

There are other properties that can be considered when modelling the pavement behaviour such us:

- ✓ Non-linearity of the unbound layers;
- ✓ The dynamic character of the load, instead of simple static; [Antunes, M.L.; 1993; Al-Khoury, R. *et al*; 2001; Uddin, W.; 2002]
- ✓ The friction at the interface layer (none to full); [de Long, D.L. *et al*, 1973].

When setting up a pavement structural model based on FWD results, the following issues must be taken into account:

The existence of thin layers (relatively to the thickness of other layers of the pavement structure) require also special care during modelling. This is due to the fact that changes in elastic moduli of such thin layers will have little influence on the pavement response, therefore these layers should be considered combined with other layers of similar behaviour.

Separate modelling of layers of same material is another issue that has to be considered. This is the case, for example, of granular material layers that are laid in two successive layers for construction reasons, in order to enable a proper compaction. For modelling purposes they must be considered as only one layer, as their elastic moduli is of the same order of magnitude.

If thin or similar material layers are combined for modelling purpose the modulus that is determined is a parameter of the combined layer, not a property of the material. [Irwin, L.; 2002].

3.6.2.2 Subgrade modelling

For modelling purposes, in the interpretation of FWD tests the subgrade is often considered to be divided into two separate layers, a top layer with a limited thickness and a bottom layer. This last one is considered to be semi-infinite in depth and stiffer than the first one and it will be designated as “rigid” layer. This presumption is physically based on the following considerations:

- ✓ The nonlinearity of the soil behaviour that is not addressed when linear elastic analysis is applied.
- ✓ The stratification of the soil and the eventual presence of bedrock at a certain depth not too far away from the surface;
- ✓ The load pulse travel time, which limits the maximum depth that is reached during the measurement window [Antunes, M.L.; 1983].

Several authors have performed studies concerning this issue [Prakas, S.; 1981; Ullidtz, P; 1987; Rohde, G.T. and Scullion, T; 1990; Antunes, M.L.; 1993; Chen, D.H., 2000] and there are several ways in which a depth to rigid layer can be assigned:

1. *In situ* tests such as: test pits, GPR, seismic methods], when there is a bedrock close to the surface. Most of *in situ* tests are destructive, time consuming, expensive and the results are not always relevant.
2. Methods based on the deflection bowl parameters [Ullidtz, P; 1987; Rohde, G.T. and Scullion, T; 1990; Chen, D.H., 2000; CROW, 1998]
3. Criteria based on non-linearity considerations.

Methods based on deflection bowl parameters

A simple tool to compute the distance to the “rigid” layer, based on the surface modulus concept, was developed by Ullidtz [Ullidtz, P; 1987] using Boussinesq’s equation. The surface modulus can be defined as the stiffness modulus that has to be assigned to a linear elastic half space to obtain the same deflection at the given offset as is obtained for the actual layered pavement structure [Van Gurp, C.A.P.M.; 1995] (see Figure 3.23). The “surface modulus” is given by the following equations:

$$E_0(0) = 2 * (1 - \nu^2) * \sigma_0 * a / D_0, \text{ and} \quad (3.19)$$

$$E_0(r) = (1 - \nu^2) * \sigma_0 * a^2 / (r * D_r) \quad (3.20)$$

Where:

- $E_0(r)$ – the surface modulus at distance “r”;
- ν – the Poisson’s ratio;
- σ_0 – contact stress under the loading plate;
- a – the radius of the loading plate;
- D_r – deflection at distance r.

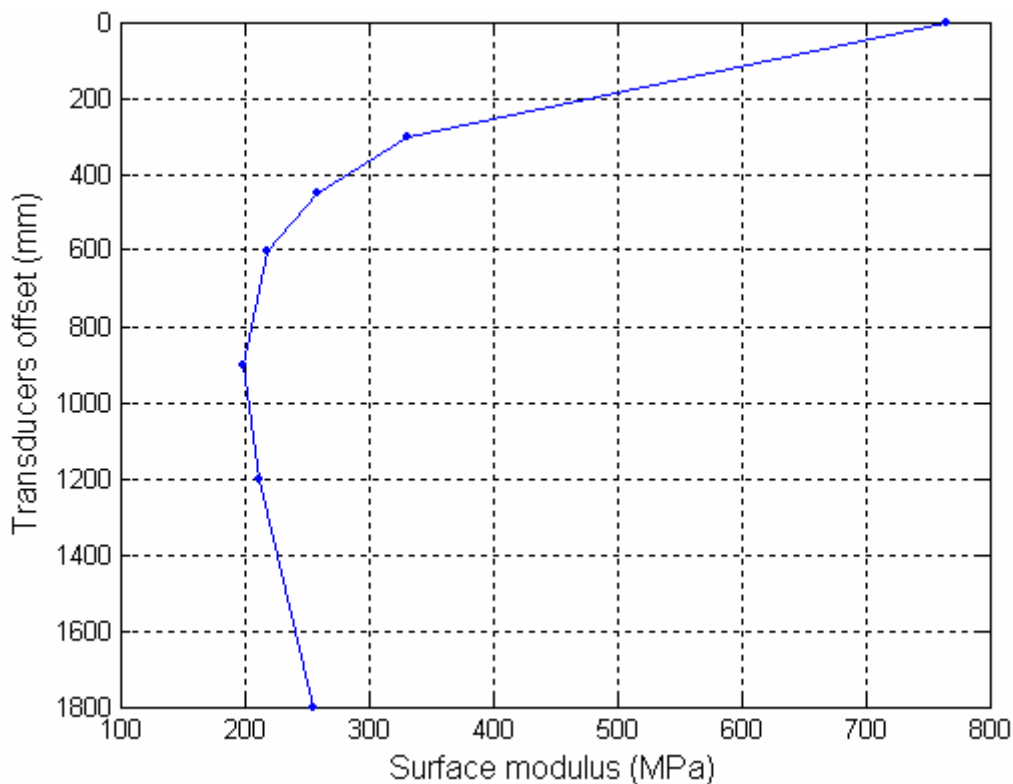


Figure 3.23 – Surface modulus plot for one deflection bowl

The distance to the “rigid” layer can be calculated considering that, if a rigid layer is found at a certain depth, no deflection will occur beyond that offset (the offset were the stress zone intercepts the rigid layer). The depth to the “rigid” layer is obtained from the radial distance from the centre of the loading plate at which the surface deflection reduces to zero.

Rhode and Scullion in 1990 [Rohde, G.T. and Scullion, T; 1990] developed a set of regression expression, based on the Boussinesq’s analysis and Ullitz method, that use the overall deflection bowl for determination of distance to “rigid” layer.

This method use equation (3.20) to determine the inverse of the distance at which a zero deflection is found. Using the plot of the normalised deflection against the inverse of the

transducers offset, the location of the transducer corresponding to a zero deflection is determined by extrapolating the flattest segment of the curve until it intersects the vertical axis (r_0) [CROW, 1998]. The inverse of this value ($1/r_0$) is an indicator of the depth from the pavement surface to the “rigid” layer (B).

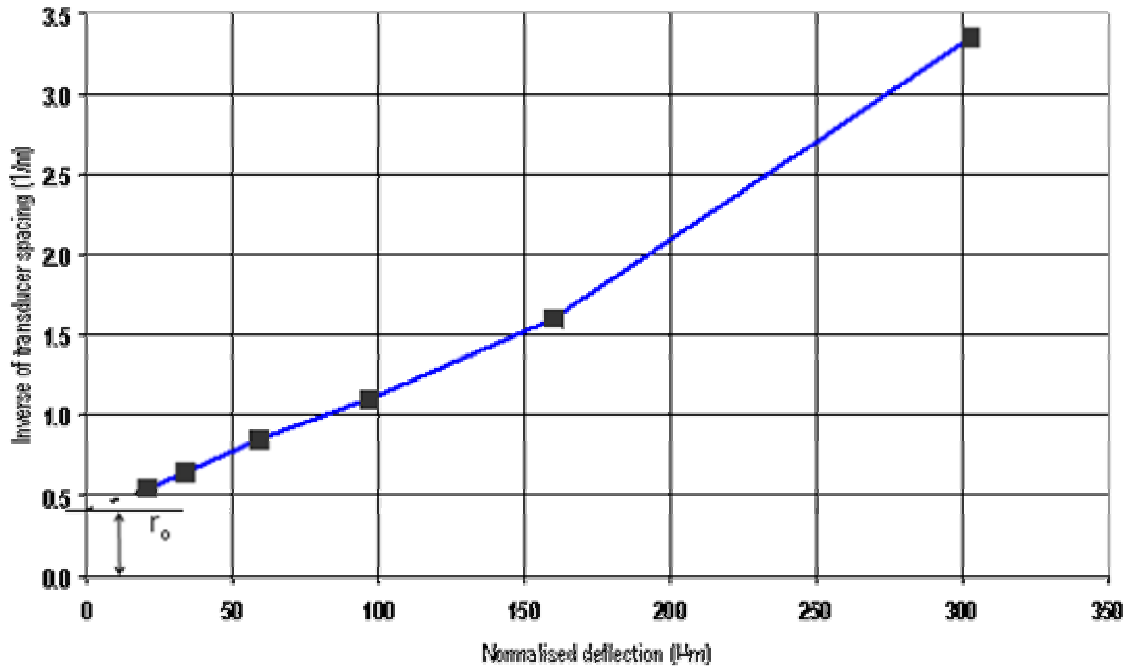


Figure 3.24 – Plot of deflection against the inverse of the geophone offset

For better results, the effect of the thickness and stiffness of the topmost layers, as well as the shape of the deflection basin are taken into consideration. The depth to the “rigid” layer is obtained using the following equations:

- ✓ For asphalt thickness of less than 50 mm:

$$1/B = 0,1188 - 0,3242r_0 + 3,1308r_0^2 - 2,1982r_0^3 - 0,0004BCI \quad (3.21)$$

- ✓ for asphalt thickness of more than 50 mm and less than or equal to 100 mm:

$$1/B = 0,212 + 0,1652r_0 + 1,6548r_0^2 - 1,0222r_0^3 \quad (3.22)$$

- ✓ for asphalt thickness of more than 100 mm and less than or equal to 150 mm:

$$1/B = 0,5188 + 0,9929r_0 - 0,00008SCI300 + 0,00064BDI - 0,2552 \log BCI \quad (3.23)$$

✓ for asphalt thickness of more than 150 mm:

$$1/B = 0,4169 + 0,5669r_0 + 0,9186r_0^2 + 0,00032BDI - 0,2182BCI \quad (3.24)$$

Where:

- B – Depth from pavement surface to “rigid” layer (m);
- r – Geophone offset (m);
- r_0 – Intercept of 1/r-axis, obtained by extrapolating the fattest part of the curve (m^{-1});
- d_r – deflection normalised to 50 kN load measured at distance r (μm);
- SC/300 – d_0 - d_{300} (μm);
- BDI – d_{300} - d_{600} (Base Damage Index) (μm);
- BCI – d_{600} - d_{900} (Base Curvature Index) (μm).

Another reason for considering a “rigid” layer in subgrade modelling is given by the load pulse travel time. The measurement window (e.g. 22 msec in case of LNEC’s FWD) limits the maximum depth reached (recorded) during period. The depth is given by the on the wave propagation speed, which depends on the layers characteristics (moduli, Poisson’s ratio, specific weight). The wave propagation speed v_p can be calculated using the following equation [Prakas, S.; 1981]:

$$v_p = \sqrt{\frac{E(1-\nu)}{\rho(1+\nu)(1-2\nu)}} \quad (3.25)$$

Where:

- E – subgrade modulus (MPa);
- ν – Poisson’s ratio;
- ρ – Specific weight (kg/m^3);
- v_p – wave speed (m/s);

The disadvantage of this method is the fact that the subgrade modulus (generally unknown) enter as input for velocity calculation.

Many studies developed for distance to the “rigid” layer estimation for the past years were usually limited to a certain region or type of foundation, being validated for specific case studies. Therefore, the equations obtained, usually through regression, cannot be extrapolated for other situations without a risk of erroneous application.

3.6.3 Backcalculation of pavement layer moduli

3.6.3.1 “Manual” interpretation

Backcalculation can be done “manually” by trial and error, using one of the computer programs mentioned in Section 2.2. After fixing the layer thickness and Poisson’s ratios, a given combination of layer moduli is assumed. The deflections are calculated and then compared with the deflections measured in situ. If the difference is above a specific tolerance, assumed as acceptable during backcalculation the elastic moduli of various layers are adjusted in order to reduce the error. The process is repeated as many times as necessary to obtain a good correlation between calculated and measured deflections. This is a time-consuming process therefore, computer programs have been developed to automate the interpretation.

3.6.3.2 Automatic interpretation

In the automatic interpretation, the same approach is followed using computer programs that aim at minimising the error functions, in other words the difference between the calculated and measured deflections.

Generally, the range of variation of elastic moduli can be defined and in many cases the user must give an initial estimate of the layer moduli (“seed moduli”).

Most of automatic backcalculation programs rely on a multilayer elastic linear program to calculate the deflection (ELMOD is an exception). Among the most widely used programs for flexible pavements [Irwin, L.H.; 2002; COST 336; 2002] are the following:

- ✓ ELMOD (Dynatest);
- ✓ EVERLAC (Washington State DOT);
- ✓ MODCOMP (Cornell University);
- ✓ MODULUS (Texas A&M University);
- ✓ PADAL (University of Nottingham);
- ✓ WESDEF (U.S. Army, Waterways Experiment Station);
- ✓ PAVERS (KOAC Pavement Consultant);
- ✓ MICHBACK (Michigan State University).

A table with the main features of these and other programs, elaborated by from COST 336, is presented in ANNEX 1.

3.6.3.3 Problems with backanalysis

The main concern during this process is the large number of possible results. As the solution is not unique, several combinations of materials properties and layer's geometry can lead to the same answer, in terms of deflections under a certain load. Not always, the best deflection fitting corresponds to the more realistic pavement model. Therefore, it is essential to use some degree of engineering judgement to evaluate the results. Some of the problems that can arise during backcalculation are presented here.

As the backcalculation programs are generally developed for uncracked pavements, when cracked pavements are evaluated the assumptions that are made have to be realistic and correlated with the *in situ* conditions. For example in case of bound layers (either asphalt or cement treated), when cracked they cannot be considered as having the initial stiffness, as they are not bound any more. In this case, they may be closer to the characteristics of a good unbound granular material.

The additional information collected from complementary tests and historical data can help in overcome the problem of not unique solution.

The experience of the user, in other words to know the type of results that are expected for each material for a given condition is also an important factor in the backcalculation process.

Missing or erroneous thickness data will cause unrealistic results of the backcalculation process. The more information available on pavement structure, the better the backcalculation results.

The application of GPR for pavement evaluation represent an important step forward, as it provides continuous information on layer thickness, for the bound and also unbound layers.

3.6.3.4 Recent developments

Artificial Neural networks

As in other fields of civil engineering, the use of artificial neural networks in pavement analysis has increased during the last years. Artificial Neural Networks (ANN) are biologically inspired. They have the ability to act as functional approximators that can "learn" a functional mapping when repetitively exposed to examples of that mapping [Marcelino, J.; 1996].

The use of ANN in interpretation of FWD test results is a promising approach. An ANN can be "trained" to determine the corresponding pavement layer moduli from deflection basins, based on a database of FWD test results. In order to create a proper database, synthetic deflection basins can complete the experimental data.

Several authors have already proposed the use of ANN for the backcalculation of pavement layer moduli [Meier, R.W.; Rix, G.J.; 1994; Meier, R.W. *et al*; 1997; Meier, R.W.; Tutumluer, E.; 1998; Khazanovich, L.; Roesler, J; 1997; Kim, Y.; Kim R.; 1998].

According to this authors the use of ANN on one hand, it may allow for a drastic reduction in computation time and on the other hand, the values obtained for layer elastic moduli can be more “realistic”, since the answer is derived from the data used in the training. Some authors state that “a network’s response can be, to a degree, insensitive to minor variations in its inputs” [Wasserman, P.D.; 1989].

The applicability of ANN is limited to the test conditions and pavement structure used for training. The feasibility of neural network training decreases as the complexity of the mapping problem increases. So increase the computer resources needed for training [Wasserman, P.D.; 1989; Meier, R.W.; Tutumluer, E.; 1998; Khazanovich, L.; Roesler, J; 1997].

In the frame of this study, a further investigation on the possibilities of using ANN for the interpretation of FWD test results will be made. More details on Artificial Neural Networks and their application in flexible pavements structural evaluation is given in Chapter 5 and 6.

Genetic algorithms

Genetic algorithms are based on Darwin’s theory of natural species selection. A population of individual designs is changed generation-by-generation by applying principles of natural selection. Genetic algorithms generate new feasible solutions from an existing “pool” of feasible solutions (parent pool), and select “fitter” solutions from the new solutions (offspring) to form the next parent pool. It is important to follow an appropriate procedure of offspring generation in order to obtain improved results during this repeated process. Applications of GA in transport engineering have been made in areas such: traffic management [Abu-Lebdeh, G et al, 1999] optimum sensor location of FWD [Kameyama, S et al, 1998], backcalculation [FWA, T.F. et al 1997; Kameyama, S et al, 1998].

The process begins with the identification of the problem parameters and the genetic representation (coding) of these parameters. In this case, the problem parameters are the pavement layer moduli (e.g. A_1 to A_4)(.Figure 3.25) A solution (set of pavement layer moduli) is represented by a string structure similar to the chromosomes in natural evolution. This representation is known as genotype. The value of each gene is called its allele.

No initial values are required for the unknown layer moduli, only a range of possible moduli values must be specified.

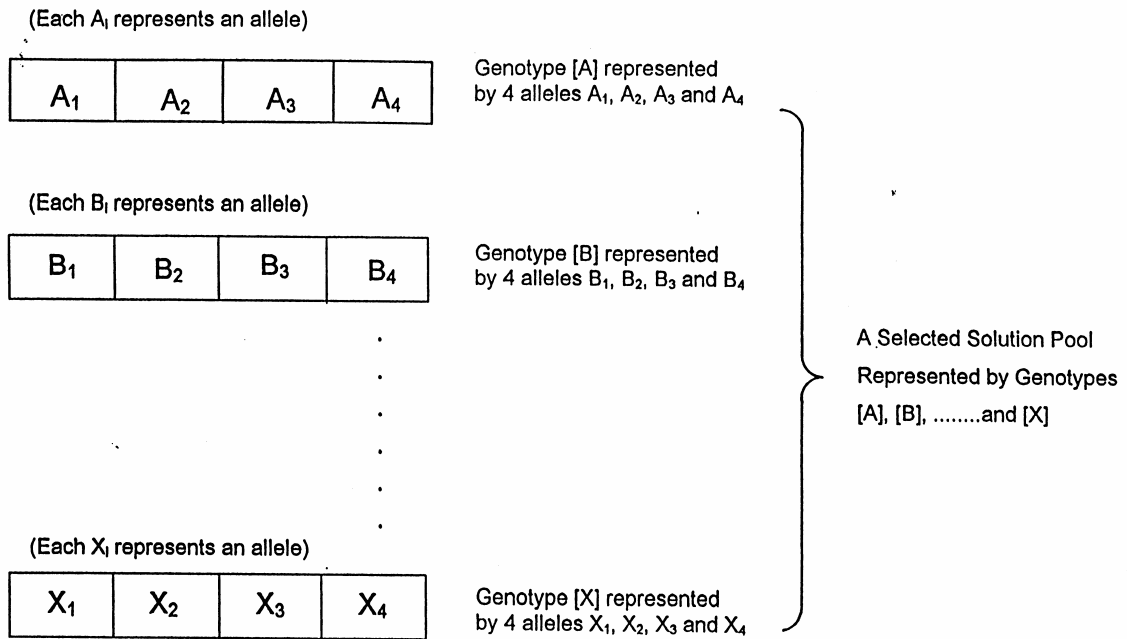


Figure 3.25 – Genetic algorithm representation of information (layer moduli) for a Four-Layer Pavement [Fwa, T.F. et al; 1997]

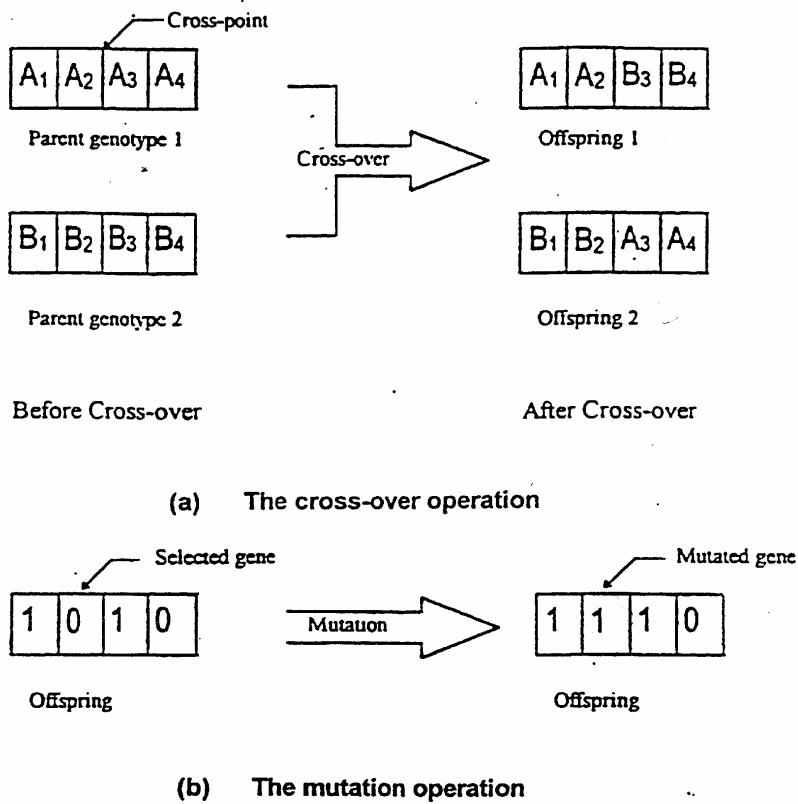


Figure 3.26 – Genetic algorithm operations [Fwa, T.F. et al; 1997]

This process starts by generating an initial random pool of feasible solutions (parent solution pool). Then new solutions are obtained and new parent pools are formed through an iterative process of crossover, inversion and mutation of the genetic representation (see Figure 3.26). The fitness value of each solution is evaluated by means of objective function. This fitness is used to determine its probable contribution in the generation of new solutions. Figure 3.27 presents a flowchart of genetic algorithm process.

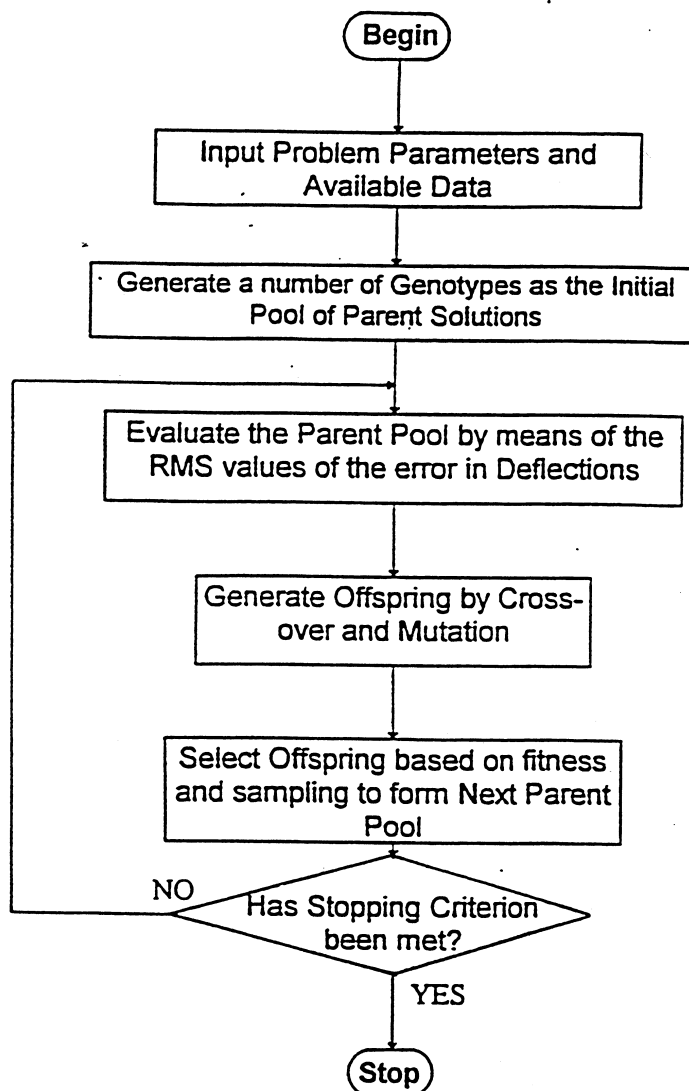


Figure 3.27 – Flowchart of genetic algorithm [Fwa, T.F. *et al*; 1997]

The converge of GA solutions can be assessed by monitoring one of the following:

- ✓ parent pool performance;
- ✓ offspring pool performance;
- ✓ best solution (best genotype in each generation).

Each of these could be use as a performance indicator to terminate the analysis. GA present a solution to overcome the problem of many local minima obtained usually while minimizing an objective function related to the difference between measured and calculated deflections. GA offer repeated perturbation to move out of local optima, perform an effective global search of the solution space, and therefore require a long computation time. Initial moduli values are not required in GA so the dependency of the solution on input values is eliminated. GA are effective methods for inverse problems, in which uniqueness of the solution is not guaranteed [Meier, R.W.; 2002].

3.6.4 Climatic effects

Temperature

There are several methods for prediction of asphalt modulus from mix composition, loading frequency and temperature, such as the ones recommended by Shell and by the Asphalt Institute [AASHTO, 2001]. Nevertheless, the backcalculated asphalt layer moduli are not necessarily the same as the moduli predicted from the above methods, since they will reflect the “*in situ*” material conditions at a given time in the pavements service life.

Several methods have been proposed for correction of backcalculated moduli of asphalt to a reference temperature. Asphalt layer elastic moduli, estimated based on FWD measurements, depend, besides temperature, on various factors such as loading frequency and materials characteristics, mainly bitumen content and type and grading curve. Therefore, in order to simplify the calculation pavement models are generally developed for certain conditions, assuming typical values for bituminous material properties for representative conditions of loading frequency and temperature. Some of these methods are presented below.

As part of a research study performed by Antunes [Antunes, M. L.; 1993; Antunes, M. L. *et al*, 1998] an airport pavement has been instrumented with thermocouples inside the asphalt layers and tensiometers in the subgrade.

The study comprised the monitorisation of pavement behaviour during a period of more than one year, through FWD testing and measurement of temperatures in asphalt layers and pore water pressure in the subgrade. Laboratory tests for determination of the mechanical characteristics of the materials were also performed. The results obtained were later confirmed on test sections, which were monitored at different road sites in the main Portuguese network.

A linear relationship between the E-modulus of asphalt materials and the temperature was adopted. Equation (3.26) expresses the relationship obtained between the FWD back-calculated modulus at temperature t (in °C), and the corresponding modulus at 20°C, E_{20} , for the asphalt concrete (AC).

$$E_t^{AC} = (1,635 - 0,0317t)E_{20}^{AC} \quad (\text{for } t \text{ between } 8^\circ\text{C and } 40^\circ\text{C}) \quad (3.26)$$

There are other methods available for the consideration of the effect of temperature on the asphalt elastic modulus. Some of them are presented below.

University of Minnesota has developed an empirical relationship (3.27) based on laboratory resilient modulus tests conducted at four temperatures [Timm, D. *et al*; 1998].

$$E_t^{AC} = 16693,4 * e^{\left[\frac{(t+26,2)^2}{-1459,7} \right]} \quad (3.27)$$

Where:

- E_t^{AC} - elastic modulus of asphalt mixtures, MPa;
- t - average asphalt temperature, °C.

Ullidtz [Ullidtz, P; 1997] developed a model based on backcalculated moduli from AASHO Road Test deflection data defined by:

$$E_{20}^{AC} = \frac{1}{3,177 - 1,673 \log t} E_t^{AC} \quad (3.28)$$

Where:

- E_{20}^{AC} - elastic modulus of asphalt at 20 °C (normalised modulus);
- E_t^{AC} - back-calculated modulus of asphalt at temperature t (°C).

Another method for asphalt elastic moduli normalisation for a reference temperature was developed by Park [Park, D *et al*; 2001; Park, S.; Kim, R.; 1997].

$$E_{t_r}^{AC} = 10^{a(t_r-t)} E_t^{AC} \quad (3.29)$$

where:

- $E_{t_r}^{AC}$ - elastic modulus of asphalt normalised for a reference temperature t_r (25°C), MPa;
- E_t^{AC} - elastic modulus of asphalt backcalculated at mid depth temperature t , MPa;
- a - regression constant; the slope of the linear fit of temperature versus the log of backcalculation modulus relationship.

In some countries, the backcalculated modulus is normalised also for loading frequency [COST 336, 2002]. For example, in the Dutch method the temperature and frequency normalisation are conducted simultaneously, based on an appropriate asphalt concrete stiffness graph [CROW, 1998].

3.7 Summary

In order to evaluate the bearing capacity of a pavement, using a mechanistic approach, a structural model of the pavement is required for the estimation of its residual life. In the case of an existing pavement, it is essential to evaluate the pavement structural condition in order to set up an adequate model.

For the purpose of pavement evaluation, non-destructive load tests (NDT) are performed and the measured deflections are then used to derive a response model of the pavement structure as close as possible to the real situation. In other words, they aim at obtaining information about the behaviour that the pavement has under traffic loads.

Setting up a structural model using NDT is usually an iterative process. Within this process, the parameters of the pavement models (geometrical and material properties) are gradually changed, until the calculated response of the pavement under the test load matches the response measured *in situ* with the NDT.

This chapter presented the methodology presently used in pavement structural evaluation studies. The main elements highlighted are the collection of background information, the NDT survey, the layer thickness assessment and the data interpretation.

The background information helps to better understand the behaviour/distresses observed in the pavement under the influence of traffic and environmental conditions. At the same time, it provides additional information to set up the pavement's structural model (for example, if there is information on the type of subgrade soil, it will allow for a better initial estimate of the modulus of the subgrade). The main elements to be taken into consideration when gathering background information are those regarding surface condition, pavement construction, subgrade, traffic, maintenance and rehabilitation actions, climatic conditions as well as any other information considered to be related with the pavement structural condition.

Knowledge of the pavement structure (type of materials and layer thickness) is essential for pavement evaluation. Usually, this information is gathered through construction records complemented with site investigations and coring.

The standard procedure for bearing capacity evaluation is to measure the deflections in considerable number of points. Usually the layer thicknesses are fixed within this process, typical values are assumed for the Poisson's ratios and the deflection bowls are used for backcalculation of E moduli. Assuming a certain pavement structure, the values of the deflections are calculated for the FWD peak load and then compared with the measured deflections. Through an iterative process, the assumed E-moduli values are adjusted in order to reduce the difference between the deflections bowls, within a certain tolerance.

The thickness of pavement layers is an important element in this process. The missing or erroneous thickness data will cause unrealistic results of the backcalculation process. The application of GPR for pavement evaluation represents an important step forward, as it provides continuous information on layer thickness, for the bound and also unbound layers.

In most cases, the backcalculation is performed using the multilayer linear-elastic approach. The load is considered static and consisting of a vertical pressure, uniformly distributed over a circular area. Full friction is usually assumed at the interfaces between layers.

The main concern during this process is the large number of possible results. Not always, the best deflection fitting given by some backcalculation software corresponds to a realistic pavement model. Therefore, it is essential to use some degree of engineering judgement to interpret the results. The results from complementary tests, background information and experience of the user may help to overcome the problem of the non-unique solution.

Some alternative approaches to perform the interpretation of FWD test results have been addressed in this chapter. Among these, the use of Artificial Neural Networks was considered a promising approach. On one hand, it may allow for a drastic reduction in computation time and on the other hand, the values obtained for layer elastic moduli can be more “realistic”, since the answer is derived from the data used for training the Network.

4 Use of GPR for structural pavement evaluation

4.1 Introduction

The knowledge of the type of pavement structure and layer thickness is essential for bearing capacity evaluation, both at network and at project level, as a complement to deflection test results.

Construction records are used as input in bearing capacity evaluation studies, providing broad information on the type of pavement structure. However these records are sometimes incomplete or missing and very often it is not possible to have detailed and accurate information about the variations that occur in the pavement structure, originated either during construction or during the pavement's service life, for example due to maintenance activities.

The most common means to determine layer thickness or confirm the available construction records is by performing cores and/or test pits at selected sites, which will be considered as representative of a certain pavement section. These methods have several advantages and disadvantages, as discussed in the previous chapter.

GPR is a non-destructive equipment, performing continuous assessment of pavement structure and giving information about layer thickness and structure changes.

RADAR (Radio Detection and Ranging) is a well-known method to detect objects and determine their position. An energy pulse is transmitted and the time delay of its reflection from an object is used to determine the location of that object. The GPR (Ground Penetrating Radar) is an electromagnetic sounding method, which uses radio frequencies for subsurface investigation.

The GPR was developed in the late 1920's, by the military, for use in detecting subsurface non-metallic mines, although successful measurements applied to earth science problems

were performed only in the late 1950's. Geotechnical applications of ground penetrating radar to rock and soil did not occur until the 1970's [Ulriksen, P.; 1980]. It has become recently available for pavement evaluation [Maser, K.; 1992; Scullion, T.; 1994; Saarenketo, T.; 1992; Van Leest, L.; 1998].

GPR is an interesting tool, both at project and at network level, since it allows for measurements at high speed, and therefore with almost no impact for the road user: It is capable of identifying changes in pavement structure (layer thickness), giving a continuous record along the pavement.

The GPR transmits short duration electromagnetic pulses from a transmit antenna into the material being tested (Figure 4.1). and picks up the reflected energy in the receive antenna. The reflected wave gives information about the pavement's structure. The wave amplitude is related with the difference in dielectric properties (ϵ_i) of two adjacent layers, while the travel time gives the interface location beneath the surface.

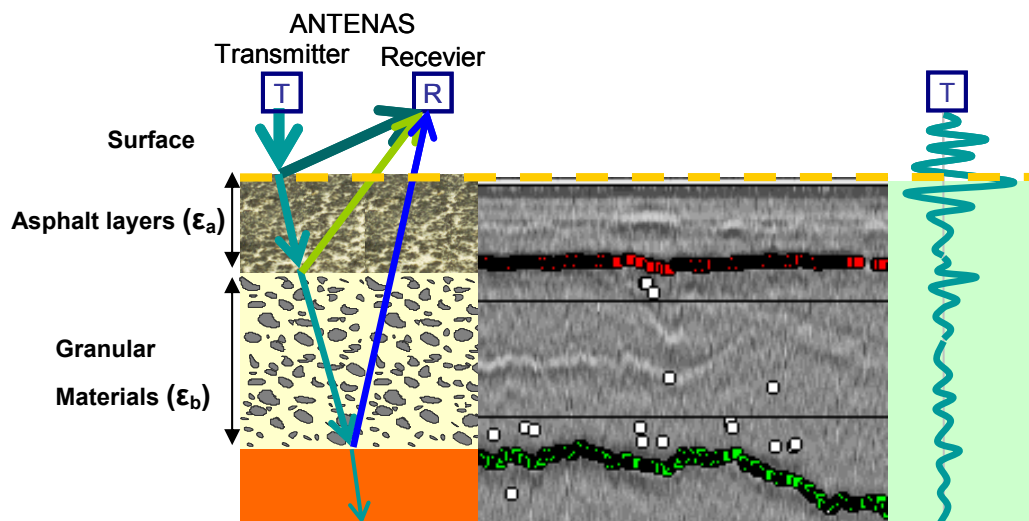


Figure 4.1 – GPR operation

There are several GPR manufacturers, such as Geophysical Survey System Inc (GSSI), Pulse Radar Inc (*Pulse Radar*), Penetradar Corporation (*IRIS*). [U.S.A], Road Radar Inc., Sensor & Software Inc. (*Pulse EKKO*) [Canada], Auscult' (*EURADAR*, *Scanroad*) [France]. Each of these equipments has its own software for data processing and there are also softwares developed by GPR users, such as ROADDOCTOR (Finland).

4.2 GPR Equipment

4.2.1 Available equipment for measurements on road and airfield pavements

Different GPR apparatus will have different capabilities according to the type of antennas and their frequency, which affect the operating speed, the resolution, the penetration and the sampling rate [Highways Agency, 2001; Simonin, J.M., 2002].

GPR antennas are either dipole or horn antennas, with frequencies ranging between 16 MHz and several GHz. They can be ground coupled or air coupled. The size of antennas and their dimensions vary greatly. The frequency and depth of penetration are related, with higher frequency pulses achieving lower penetration, but better resolution.

Dipole antennas can have frequency ranges between 16 MHz and 1500 MHz. They were primarily developed for use in geological survey, normally ground coupled. When used for pavements, dipole ground coupled antennas are suitable for testing at a maximum speed of 8 km/h. Dipole antennas may also be air coupled, allowing for higher test speeds.

Horn antennas, with frequencies between 900 MHz and 2500 Hz, are generally suspended 0.4 m above the surface for operation at traffic speeds, see Figure 4.3 (up to 80 km/h), and therefore they are suitable for pavement evaluation at network level.

Among the existing methods for measurement of layer thickness, the following systems are briefly described within this study:

- ✓ GPR with dipole antennas;
- ✓ GPR with air coupled horn antennas;

The operating principles of these systems are similar, the main difference being the type of antennas used. These types of apparatus are nowadays considered as routine measuring equipment, although the interpretation of the results obtained is still quite complex and requires a lot of experience.

GPR with dipole antennas

Dipole antennas can have a variety of frequencies, ranging from 16 MHz to 1.5 GHz. For pavement applications, the best results are obtained with antenna frequencies in the 400 MHz to 1.5 GHz [TRB, 1998]. In general, the higher the frequency, the lower is the penetration depth and the higher is the resolution. For example, 1.5 GHz dipole antennas will

give a penetration depth of 500 mm and a resolution of 20 mm, while the 400 MHz will give a penetration of 2.00 m and a resolution of 60 mm [CROW, 2000]. The use of multiple antennas, with different frequencies is sometimes adopted in order to optimise the amount of information collected. [The Concrete Society, 1997]

Dipole antennas were mainly developed for use in contact with the surface. In this condition, the radar signal is “ground coupled”. Ground coupling introduces a stronger signal into the pavement, enhancing sensitivity and increasing the depth of penetration [Highways Agency, 2001]. However, GPR with ground coupled antennas are difficult to operate at traffic speed. Normally, this type of equipment is used at speeds no higher than 20 km/h.

Dipole antennas can also operate with air coupling, which makes it more suitable for operation at traffic speed. However, the gap between the antenna and the surface has to be small, in order to provide satisfactory results. In this case, the antenna mounting has to be carefully designed in order to enable surveys to be done at traffic speed. Figure 4.2 shows examples of close air coupled dipole antennas prepared for survey at traffic speeds.



Figure 4.2 - Examples of dipole close air coupled antennas used for survey at traffic speed [FORMAT; 2004]

GPR with horn antennas

This type of GPR was specifically designed for use in pavement evaluation. In the past ten years, this type of equipment has evolved from prototype status to routine use in pavement evaluation studies.

The horn antennas can have frequencies ranging from 1 to 2.5 GHz, corresponding to penetration depths in the order of 0.6 m to 0.4 m, respectively. Their resolution is in the order of 50 mm, for 1 GHz antennas and 25 mm, for the higher frequencies.

The antennas are air coupled, and normally they work suspended at a certain distance from the surface, typically 0.40 m (ranging from 0.4 to 0.6 m). There are several solutions for mounting this type of equipment, either using a trailer or directly from the survey vehicle. Figure 4.3 shows some of the solutions commonly adopted.



Figure 4.3 - Examples of GPR with horn antennas [FORMAT; 2004]

4.2.2 LNEC's equipment

Air-coupled antennas are the most widely used for pavement studies. The antennas are suspended on a van or a trailer and allow for measurements at high speed. They have a better resolution but, at the same time, the penetration depth is restricted to the surface layers.

LNEC's equipment has two pairs of air-launched (horn) antennas (1000 MHz and 1800 MHz). The main elements of the equipment are presented in Figure 4.4. In the same figure (right hand side picture) four air-coupled antennas are seen suspended above the pavement. The two in line antennas behind are separate transmit and receive units 1 GHz (1000 MHz), while those in front are another pair of antennas 2 GHz (1800 MHz).

The main frame provides the transducer interface modules, data collection, and signal processing hardware, data storage devices and connectors to external devices. The

control/display unit is a combination of video monitor and keyboard entry pad that interfaces only to the main frame [Geophysical Survey System, 1994].

The data collected during tests are then transferred to a PC (or lap-top) to be processed.

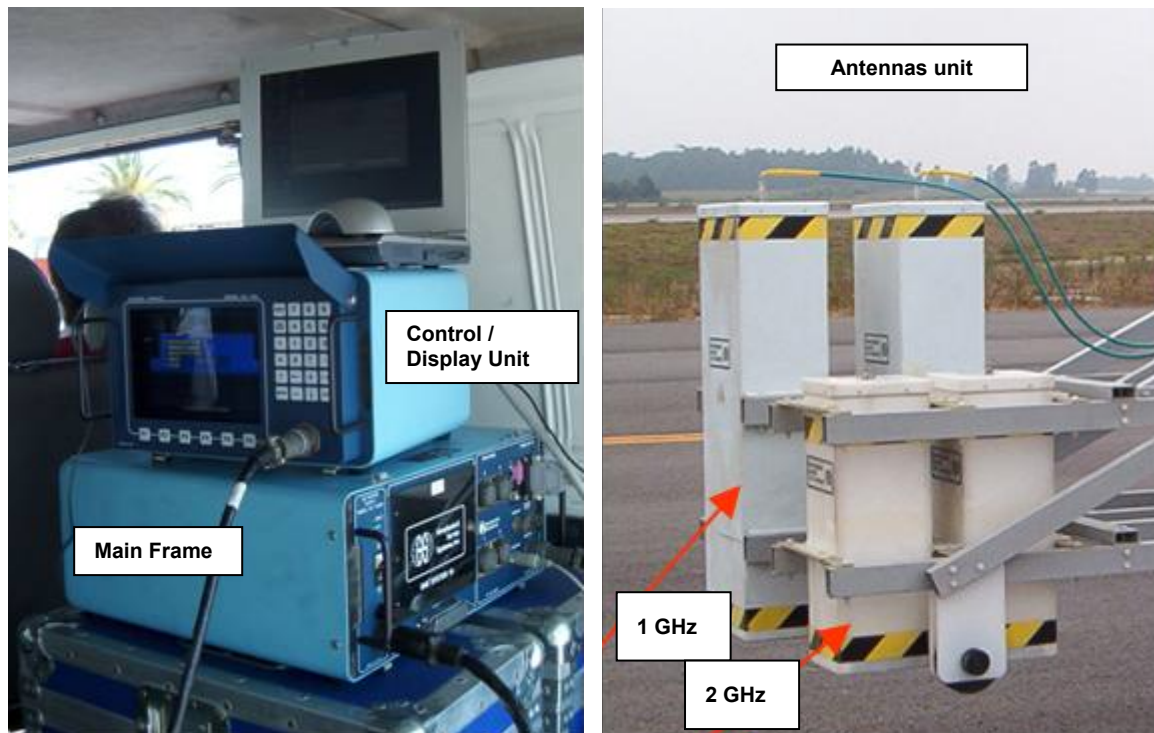


Figure 4.4 – GPR equipment (main elements)

In the original system supplied by GSSI LNEC's GPR antennas were suspended from the vehicle as shown in Figure 4.5. This system was found to be cumbersome and therefore, the initial suspension system of LNEC's antennas has been modified. Figure 4.5 presents the initial structure while the actual structure is presented in Figure 4.6. The changes made aimed to improve several aspects of the equipment installation and functioning, mainly the stability of the antennas during testing.



Figure 4.5 – LNEC’s equipment – initial structure: suspension system



Figure 4.6 – LNEC’s equipment – actual structure: general view in testing position

4.3 Operation principles

4.3.1 General principles

The GPR transmits short duration electromagnetic pulses from a transmitting antenna into the material being tested, and picks up the reflected energy in the receiving antenna. GPR can be used as a non-destructive road diagnostic tool that is analogous to the X-ray in medicine [Berthelot, C. *et al*; 2001]. The operation principles of radar are well documented in literature [Maser, K. *et al*, 1993; Wimsatt, A.J.; *et al*; 1998; Scullion, T. *et al*; 1992; Scullion, T.; *et al*; 1997; The Finish Geotechnical Society, 1992; Ulriksen, P.; 1982; Saarenketo, T.; 1996; Cimadevilla, E.L., 2000; Jaselskis, E.J.; *et al*; 2003].

The propagation speed of the radar wave and its reflection are affected mainly by the dielectric constant of the medium. The travel time (t) and the propagation speed (v) of the pulse within a layer can be used to determine the layer thickness (h):

$$h = v \times (t / 2) \quad (4.1)$$

The wave propagation speed (v) depends on the relative dielectric constant (ϵ_r) of the medium and can be determined as follows:

$$v = c / \sqrt{\epsilon_r} \quad (4.2)$$

Where $c = 3 \times 10^8$ m/s represents the speed of light in vacuum. The vacuum is considered as an ideal medium where the wave does not suffer any changes during propagation. In this way, layer thickness can be estimated if the relative dielectric constant is known.

The amplitude of the reflected signal is related with the difference between the relative dielectric constants at the boundary of two media. The reflection coefficient, expresses the relationship of the relative dielectric constants:

$$\rho = \left(\sqrt{\epsilon_{r1}} - \sqrt{\epsilon_{r2}} \right) / \left(\sqrt{\epsilon_{r1}} + \sqrt{\epsilon_{r2}} \right) \quad (4.3)$$

Where ϵ_{r1} is the relative dielectric constant of the upper medium and ϵ_{r2} is the relative dielectric constant of the lower medium.

The GPR measures the travel time, which is post-processed and converted to layer thickness. The thickness can be estimated if the relative dielectric constant is known.

4.3.2 Air coupled antennas

For air coupled antennas the upper medium is the air. Taking into account that the relative dielectric constant of the air is 1, the dielectric constant at the pavement surface can be calculated using equation (4.3) [Scullion, T.; 1994; Maser, K.; 1994; Berthelot, C. *et al*; 2001].

Figure 4.7 presents a typical air-coupled reflection profile, where A_1 is the GPR reflection from the surface of the asphalt layers, while A_2 and A_3 are the reflections from the top of the granular base and top of the subgrade, respectively.

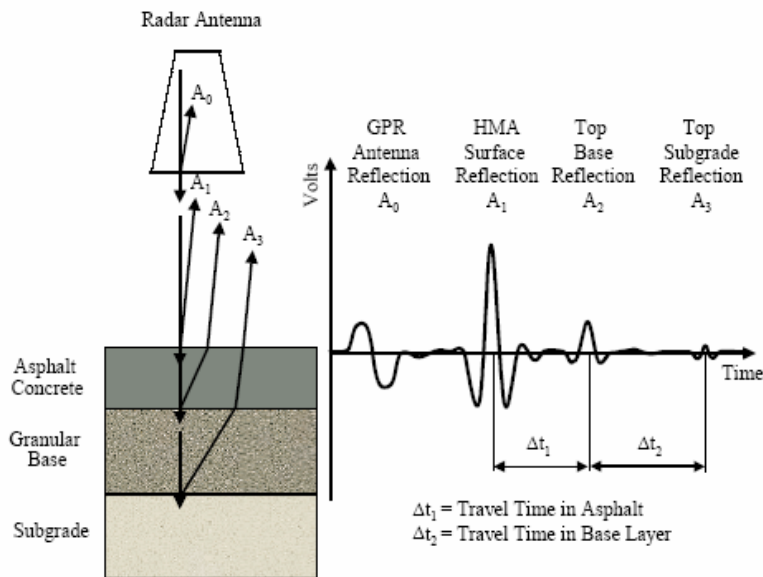


Figure 4.7 – Typical air-coupled GPR profile [Berthelot, C. *et al*; 2001]

The amplitude of the reflected peaks can be used to determine the dielectrical characteristics of the materials as it represents an indicator of the signal absorption and dissipation within the material. For this purpose, in the case of air-coupled antennas the signals reflected from the pavement surface are compared with those obtained from a large metal plate located on the pavement surface, the metal being considered as a perfect reflector. In this way, the dielectric permittivity (constant) of surfacing layers (ϵ_1) and of granular material layers (ϵ_2) can be determined as follows [Wimsatt, A.J.; *et al*; 1998]:

$$\sqrt{\epsilon_1} = (A_m + A_1)/(A_m - A_1) \quad (4.4)$$

Where:

- ϵ_1 – the dielectric constant of surfacing layer;
- A_1 – the amplitude of reflection from surface (volts);
- A_m – the amplitude of reflection from metal plate (negative of incident amplitude) (volts), which represents the 100% reflection case.

In this way the thickness of the surfacing layer is:

$$h_1 = \frac{c\Delta t_1}{\sqrt{\varepsilon_1}} \quad (4.5)$$

Where:

- h_1 - the thickness of the top layer;
- c - the velocity of the radar wave in air as measured by the system;
- Δt_1 - the time delay between peaks A_1 and A_2 (see Figure 4.7).

The dielectric constant (ε_2) of the base material can be obtained in a similar way [Maser, K. *et al*, 1993; Wimsatt, A.J.; *et al*; 1998; Scullion, T. *et al*; 1992]:

$$\sqrt{\varepsilon_2} = \sqrt{\varepsilon_1} \left[\frac{1 - \left(\frac{A_1}{A_m}\right)^2 + \left(\frac{A_2}{A_m}\right)}{1 - \left(\frac{A_1}{A_m}\right)^2 - \left(\frac{A_2}{A_m}\right)} \right] \quad (4.6)$$

Where:

- A_2 - the amplitude of reflection from the top of the base layer (volts);
- ε_b - the dielectric permittivity of the base layer (granular material).

The same process can be repeated iteratively to compute the dielectric constant (ε_n) of the (n)th layer, based on the dielectric constant (ε_{n-1}) of the ($n-1$)th layer [Al-Qadi, I.L. *et al*; 2004].

4.3.3 Electromagnetic characteristics of materials

The electromagnetic properties of materials comprise magnetic permeability, dielectric permittivity and electrical conductivity. The road construction materials are characterised by means of electrical conductivity and dielectric properties only, given that the magnetic permeability of these materials is similar to vacuum [Saarenketo, T.; 1996; Jaselskis, E.J.; *et al*; 2003].

The electrical conductivity, or simply conductivity (σ) is given by the transfer of electrons and ions. All the materials are more or less conductive according to their nature, moisture condition, etc. The vacuum is the only medium considered as a perfect conductor, “transparent” to the electromagnetic wave, as the wave amplitude remains constant during propagation. The air is considered also “transparent” as the wave loss is almost null, when compared with the losses in other materials [Oliveira, M.M.P; Coelho, M.J.; 1994]. On the other hand, most metals are perfect reflectors, “opaque” to wave propagation, due to the high wave reflection at surface associated with strong wave loss. Almost all road construction materials (crushed rock, bitumen) can be considered as electrical insulators [Saarenketo, T.; 1996; Cimadevilla, E.L., 2000].

The dielectric permittivity, or simply permittivity (ϵ) of a material is defined as “a measure of the extent to which the electric charge distribution in the material can be distorted or polarised by application of an electrical field” [The Concrete Society, 1997].

The “relative permittivity” of a medium, known also as the “dielectric constant”, can be defined as follows [King, R.W.P.; Smith, G.S.; 1981, Ulriksen, P.; 1982, Saarenketo, T.; 1996, Bock, R.K.; 1998; Cimadevilla, E.L., 2000, Jaselskis, E.J.; *et al*; 2003]:

$$\epsilon_r = \frac{\epsilon'}{\epsilon_0} \quad (4.7)$$

Where:

- ϵ' - real part of material permittivity;
- ϵ_0 - the permittivity of vacuum : $\epsilon_0 = 8.854 \times 10^{12}$ F/m (Farad/meter).

The dielectric constant, ϵ_r , is the characteristic (dimensionless) used generally to define the electromagnetic properties of a material. The dielectric constants of various materials are presented in Table 4.1. They are ranging from 1 to 81 for most geologic materials, and are influenced by the moisture content and density. The dielectric constant of a material is increasing with moisture and decreasing with the increase in air voids [Scullion, T.; Saarenketo, T.; 2002].

The dielectric constant is different for different materials and, even for the same material, it varies widely with the moisture content [Al-Qadi, I.L. *et al*; 2004]. The dielectric constant of most dry geological materials normally varies between 5 and 10, whereas the dielectric constant of water is around 80. The water content has thus a significant effect on the dielectric properties of materials. Even small changes in the water content may considerably increase the dielectric constant of a material and consequently affect the wave propagation through the material. (see Figure 4.8)

The energy loss has to verify the condition $\sigma/\omega\epsilon_0 \ll 1$ in order to enable the wave propagation in a medium. For GPR application on geological media this is accomplished due to the high frequencies of wave and lower conductivities of these materials. In this situation, the velocity of propagation can be written as:

$$v \approx \frac{1}{(\epsilon'\mu)^{1/2}} \quad (4.8)$$

Where:

- μ - is the magnetic susceptibility of the medium.

Taking into consideration that for non-metallic materials $\mu = \mu_0$ ($\mu_0 = 1.257 \times 10^{-6}$ Henry/m is the magnetic susceptibility of vacuum) and that the wave velocity in vacuum is:

$$c = \frac{1}{(\epsilon_0\mu_0)^{1/2}} = 3 \times 10^8 \text{ m/s} \quad (4.9)$$

the wave velocity can be expressed as in equation (4.2), $v = c / \sqrt{\epsilon_r}$.

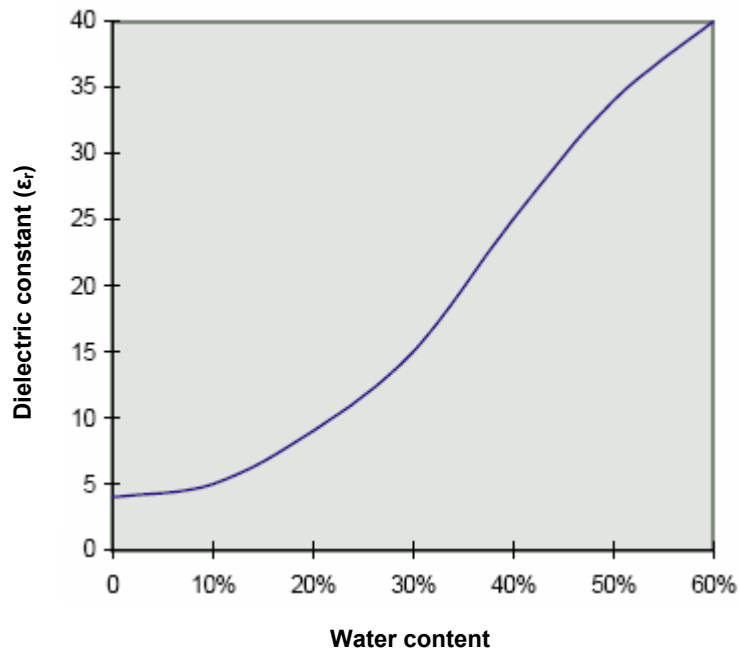


Figure 4.8 - Typical soil dielectric constant variation with water content [King, M.L., 2004]

As already mentioned, a change in the medium moisture content results in significant changes in the dielectric properties and consequently, in modifications of radar signal velocity. For example, if for the dry sand, the dielectric constants range from 4 to 6, for wet sand the values are much higher, ranging from 20 to 30.

It can be noticed that the dielectric constants of water and air have almost the same values in all references while the range of dielectric constant values referred for pavement materials is different from one author to the other. On one hand, this can be explained by the fact that the values are generally related to local materials. On the other hand, materials such asphalt and concrete are a combination of various components (aggregates, air, bitumen or cement). Therefore, the “final” dielectric constant is a result of combined contribution of all these elements.

Table 4.1 – Range of dielectric constant (ϵ_r) for various materials

Material	Cd	R1	R2	R3	R4	R5	R6	R7	R8	R9
Air		1	1		1	1	1	1	1	1
Water		81	81		80	80	80-81	81	81	81
Asphalt	dry	2-4		3-5*						
	wet	6-12	4-10*	4 [#]		3-6*	5-10*		3-6*	3-8*
Concrete	dry	4-10		6-11*						
	wet	10-20	5-9*	9 [#]		6-11*	4-10*		6-11*	6-9*
G.M./Gravel			6-18	5-9 7 [#]						4-6
Sand	dry	4-6		2-6*	3-5	3-5		4-6	3-5	
	wet	20-30		4 [#]	20-30	20-30	4-25	30	20-30	20-30
Silt	dry									
	wet					5-30*	9-23*	10	5-30*	
Clay	dry				5-40*	5-40*	4-16*		5-40*	
	wet	10-40						8-12		
Rock:				6-12* 9 [#]			4-10*			
- granite	dry	5			4-6*			5	4-6*	5-6
	wet	7						7	7-8	7-8
- limestone	dry	7			4-8*			7	4-8*	5-7
	wet	8						8	8	8
- basalt	wet							8		
- shale	wet	6-9								
Cement. treated soil										16
Cement. treat GM										13
Lean concrete			6-9							

key:

- Cd. – material condition;
- R1 to R9 – bibliography reference number, see Table 4.2;
- * – condition not specified;
- # – average value for dielectric constant;
- G.M.– granular material.

Table 4.2 – List of references presented in Table 4.1

Number	Reference
R1	The Concrete Society, 1997
R2	Highways Agency, 2001
R3	ASTM, D 4748–98; 1998
R4	Annan, A.P. and Cosway, S.W., 1991
R5	CROW, 2000
R6	The Finish Geotechnical Society, 1992
R7	Ulriksen, P.; 1982*
R8	Parry, N.S. et al, 1992**
R9	Cimadevilla, E.L, 1996

* - data from Morey, 1974; Keller, 1954 and Von Hippel, 1954, articles not listed;

** - table presented in [TRB, 1998].

The interpretation of GPR test results is complex and involves the calculation of the wave velocity through the pavement structure. The following section presents some of the most widely used methods for calculation of the wave velocity.

4.3.4 Signal velocity calculation

The velocity of the signal is related to the layer's dielectric constant (ϵ_r) by equation (4.2). Different media will have different radar propagation velocities. Several methods are used to calculate the propagation velocity in a medium and to interpret the GPR results. [Ulriksen P, 1982; The Concrete Society, 1997; Highways Agency, 2001;]. The main methods are briefly presented herein:

The most simple, but also less accurate approach, is the **use of “default” values** for the layers dielectric constants. These values are considered typical for different pavement materials (see Table 4.1) and are generally given in the literature, or known from previous experience. As already mentioned, a change in the medium moisture content results in significant changes of dielectric properties and consequently, in modifications of radar signal velocity. Therefore, this method represents rather an indication of possible velocity values

during a preliminary assessment of data and not a consistent calculation of the velocity. For this purpose, adequate calibration should be performed.

The following paragraphs describe some of the methods used for calibration of the GPR data.

1) One of the methods applied for signal velocity calculation is the **common mid-point (CMP)** method [Ulriksen P, 1982; CROW; 2000; Highways Agency, 2001], a method widely used in seismic reflection. This method requires a multi-pole antenna system, in other words, it uses separated single transmitting and receiving antennas [Highways Agency, 2001].

The method is used to obtain an estimate of the radar signal velocity versus depth by varying the antenna spacing (S_i). The antennas are moved apart about a common mid (starting) point in opposite directions as presented in Figure 4.9. Measurements are made at fixed locations, obtaining in this way a number of different ray paths through the material and the travel time for each location (t_i) is measured. With the depth known, the average velocity is calculated using the delay when antenna separation was zero.

$$v = \sqrt{\frac{S_2^2 - S_1^2}{t_2^2 - t_1^2}} \quad (4.10)$$

Where:

- v is the signal velocity in surface layer;
- indices 1 and 2 refer to two different distances between antennas S_1 and S_2 and corresponding signal travel times t_1 (XOY path) and t_2 (WOZ path) both in ns [Highways Agency, 2001].

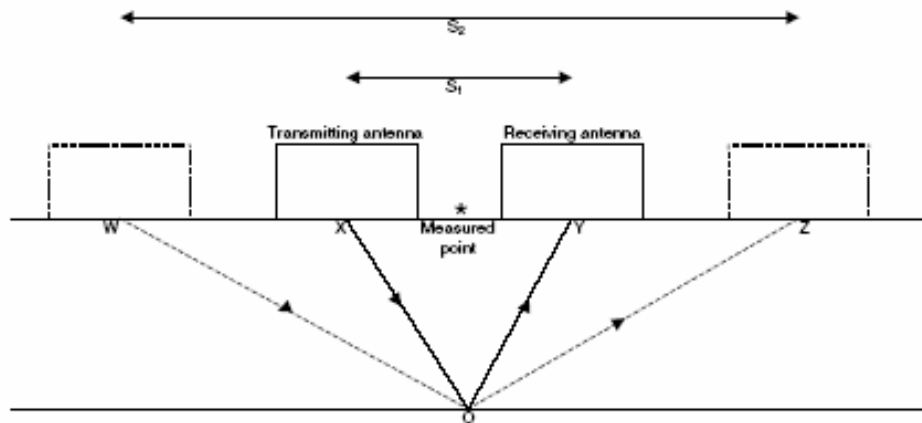


Figure 4.9 – Common mid-point method for signal velocity in surface layer [Highways Agency, 2001]

2) The **wide angle reflection and ranging (WARR)** method is similar to the common mid-point method but the transmitting antenna is kept fixed while the receiving antenna is moved away (see Figure 4.10). The received waves contain information on the several mediums crossed by the wave, such as the airwave (A), the direct wave through the upper medium (G), the refracted wave from the second medium, the reflected waves from the interfaces (R). The average velocity of the wave for each layer is calibrated based on this information.

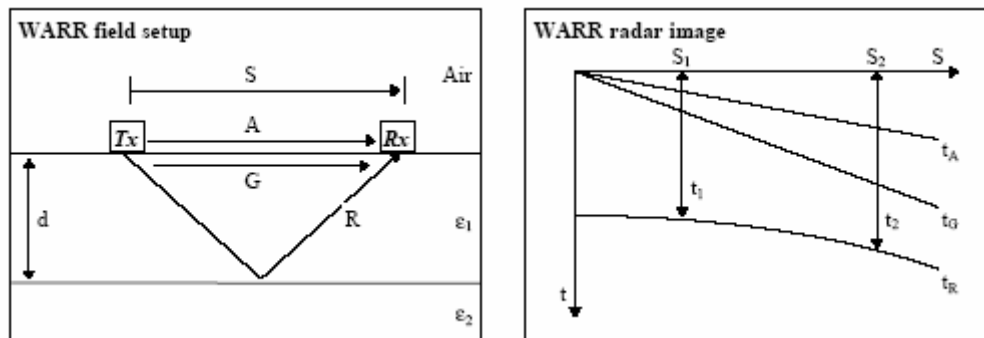


Figure 4.10 – Schematic representation of a WARR survey [Davis, J.L. and Annan, A.P.; 1989.]

3) The **amplitude estimation method** is an automated velocity calibration procedure, is appropriate for air-launched antennas. This is the method used by LNEC.

This method compares the signals reflected from the pavement surface, and underneath layer's interfaces with the reflection obtained from a large metal plate (considered as a perfect reflector), located on the pavement surface at the beginning of the test. References to this calibration principle were made in 4.3.2 and, a schematic representation of it is illustrated in Figure 4.11 .

Using equation (4.2) the signal velocity (v) can be obtained as follows:

$$v = \frac{c}{\left(\frac{A_m + A_1}{A_m - A_1} \right)} \quad (4.11)$$

where:

- v – the signal velocity in the surface layer of the pavement (mm/sec);
- A_1 – the amplitude of reflection from pavement surface;
- A_m – the amplitude of reflection from the metal plate;
- $c = 299 \text{ mm/ns}$ is the signal velocity in air.

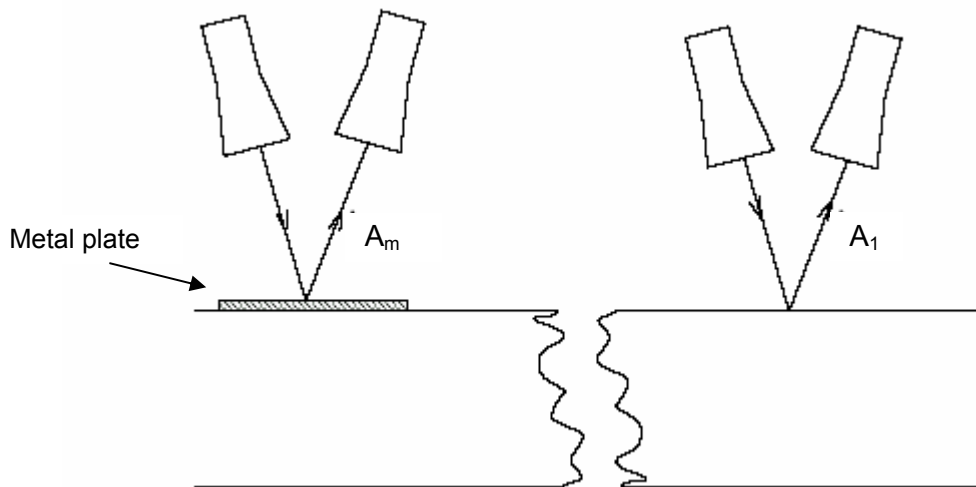


Figure 4.11 – Amplitude estimation method for signal velocity in surface layer of pavement [Highways Agency, 2001]

Besides the calculation of the dielectric constants of pavement layers, this calibration is also used to extract the part of the radar file corresponding to the wave travel through the air. In this way, the pavement surface, representing the 0 (depth) point is clearly identified along the radar file.

This calibration must be performed before each survey. It is advisable to calibrate the system throughout the tests or whenever test conditions change. The height of the antennas must remain constant during testing, and this must be checked periodically.

Another automated calibration procedure, performed in a way which is similar to the common mid point method (CMP) is the **multiple antennas on surface** method. This approach uses for measurements a single transmitting antenna and multiple receiving antennas located close to the pavement surface [The Concrete Society, 1997]. Differences in travel-time for different paths through the layers are measured.

An advantage of these last two methods is the possibility of continuous estimation of signal velocity while in the previous approaches the estimation of velocity is made only at discrete location. The continuity in these last approaches is given by the fact that the reflection of the metal plate is used (for each scan) to calculate the wave velocity in the surface layer. In this way, the changes in layer velocity can be easily identified along the test site.

In order to clear the wave signal an additional operation is required, the **free space signal** measurement. During this process the antenna is directed upwards (so called the

measurement of the sky), in order to avoid any possible reflection (this is considered as a free space echo measurement) and the measurements are performed toward an empty space. In this way, the noise of the signal is eliminated. This operation must be performed periodically, in case of a noisy wave aspect, and whenever the measurement's conditions change, and in this way, influence the answer of all electronics.

4.4 Survey Procedure

The layer thickness data are used during the backcalculation process of FWD test results. Therefore, GPR tests are undertaken along the same longitudinal profiles as FWD tests. Sometimes, depending on the objectives of the study and on the type of structure, GPR tests are also performed along transverse profiles. In this way, a mesh covering the entire area will be available.

Generally, the number of scans per meter used in most studies is 4 (one scan every 25 cm). For tests performed on rigid pavements, due to the GPR wave absorption in concrete, it is advisable to increase the number of scans per meter, in order to get as much information as possible. [FORMAT, 2004; The Concrete Society, 1997].

Using fast scan rates, GPR can collect continuous data, allowing a real time view of the pavement structure. In this way, it is possible to identify the exact location of an event and even to modify the scan rates in order to obtain a better interpretation of the data after testing.

4.4.1 Survey preparation

It is necessary to calibrate the system before each test and whenever the system is turned off. New calibration is required also if the antennas height changes during testing. Improper calibration will result in erroneous data interpretation or even in the impossibility of data processing due to mismatch between calibration and GPR test files.

There are limitations on survey conditions. GPR surveys cannot be performed during rain or on wet pavement surface, as the water will absorb the waves. Also the presence of large metal surfaces (such as: hangar gates, rails or lorries passing near the antennas) induces noise in GPR files due to the strong wave reflection.

One aspect to be taken into consideration is the referencing during tests. This allows for a proper identification of the pavement features in the data file and for a better correlation with

FWD test location. A map of the site should be used to mark the location of FWD and GPR tests, as well as the cores, as accurately as possible. Other features considered important for the study should also be marked.

The distance measurement is generally performed by an electronic distance measuring device which, in most of the GPR systems, is mounted on a survey wheel. The survey wheel is the device that commands the GPR system to perform the scan at fixed distance intervals. This feature is important for the tests, as it enables the user to acquire a fixed number of scans over a unit distance [Geophysical Survey System, 1994; FORMAT; 2004] even at variable survey speed. In this way, a horizontal scale for the survey is provided, marks are placed on the data file at a constant fixed distance, and consequently the location of events in GPR file becomes easier during data processing. The survey wheel has to be calibrated against a known distance and the calibration is checked usually once a year.

Other methods of measuring location can be used, such as global navigation satellite system. [FORMAT, 2004]

4.4.2 Equipment settings

The main parameters that have to be set before every calibration are the following:

- ✓ **Antenna configuration:** the information regarding the type of antennas, where are connected and the transmit rate mode (fast in case of horn antennas) should be specified;
- ✓ **Scan parameters and gain settings.** First of all the vertical and horizontal filters should be set to ensure an appropriate functioning. Then the test parameters are set, namely: the transmission rate, the time window (range), the number of samples per scan, the number of scans per second, the position of the scan and the gain level. These parameters are related with the antenna characteristics and depend on the test conditions and on the dimension of the features that have to be detected. For example, a sampling performed every 250 mm will be unable to detect features with a length smaller than the distance between scans. For a feature to be detected, more than 20 scans are usually required.

4.4.3 Data collection

Some features require a special attention during the data collection, such as:

- ✓ The GPR files should not be larger than 32 767 scans in order to be transferred to the computer. To prevent this situation, a pre-evaluation of the pavement length to test per file has to be performed (depending on the scan rate and antennas performing tests simultaneously).
- ✓ Survey speed over the limit required for proper data collection (e.g., over 80-85 km/h for measuring performed with one horn antenna at a rate of 4 scans/m) will result in missing data. The equipment has a sound alarm for this situation.
- ✓ Any event location (bridges, mileposts, etc.) should be marked on the data file. More information available provides a tool for distance crosschecking and events identification within GPR files.
- ✓ None of the settings of the equipment can be changed during testing without system calibration. Otherwise, data processing cannot be performed.

4.5 Processing and interpretation of data

4.5.1 Automatic interpretation

After the survey, the data files are transferred to a computer and then a preliminary data processing is performed. This first step aims at reducing the noise in order to clean, as much as possible, the reflections obtained.

The basic operation involves identifying the peaks in the data trace. The software automatically locates peaks in a file for every trace and measures amplitudes and time delays [Scullion, T. *et al*; 1992]. From this data, the relative dielectric permittivity and the layer thickness are calculated as described in (4.1).

The interpretation is performed based on the available information regarding the pavement structure, and consists of the following steps [GSSI, 1996; GSSI, 2001; Scullion, T.; Saarenketo, T.; 2002; Cimadevilla, E.L., 2000; Jaselskis, E.J.; *et al*; 2003]:

- ✓ To eliminate unwanted signals (noise, cluttering) from the radar data;
- ✓ To track the reflections between the various layers of the pavement structure;

- ✓ To calculate the two way travel time for each layer;
- ✓ To calculate the dielectric permittivity of the surfacing layer, equation (4.4), then the velocity of the wave equation (4.2), from the reflection amplitude on the road surface (from the data) and the one on metal plate (from the calibration file), as already presented in 4.3.2;
- ✓ To calculate the thickness of the surfacing layer, equation (4.5), then the dielectric permittivities of subsurface layers, equations (4.6) and **Error! Reference source not found.** and finally their thicknesses.

The automatic interpretation with most GPR softwares is performed using default values for the materials dielectric properties and the wave velocity is presumed to decrease with depth.

Data interpretation is performed in two phases: first the “Reflection Picking” and then the “Layer Interpretation”.

The **reflection picking** processing phase has two functions: to eliminate coherent clutter in the data and to locate significant reflection events in each scan.

The clutter represents “*unwanted radar returns or reflections from the surrounding environment, both within the ground or above the ground*” [TRB, 1998]. This can be due to the presence of various elements, such as tree branches, roots, or cars. For example, a constant reflection or noise, consistent along the file, is usually due to the presence of metal parts (e.g. the survey car, rails or other objects), always located at constant distance from the antennas and above the surface. The clutter can influence the data interpretation as can be erroneously identified as a layer interface.

The location of significant reflection within the scan is given by the reflected wave amplitude, which increases with the difference in dielectric properties between two adjacent materials. In other words, in the case of pavement structure studies high amplitude is an indicator of a layer interface. During the process of reflection picking, the user can provide some specific additional data, such as:

- ✓ the expected layer thickness range for up to 3 layers;
- ✓ the polarity criteria, if the significant reflection is expected to be positive or negative.
In other words, if the velocity is expected to decrease or not with depth.

In the **layer interpretation** phase the output from the previous phase (reflection picking) is used to delineate the pavement layer structure.

Like before, the user can also provide specific information, such as:

- ✓ the minimum and the maximum expected depth for each pavement layer, up to seven layers;

- ✓ the polarity criteria (positive or negative) that is presumed to be detected at the layers interfaces (as already mentioned for reflection picking);
- ✓ the wave velocity for each layer, that can be either the one calculated by the program (see 4.3.2) or user-defined. The user-defined velocity is considered constant along the layer.

4.5.2 Limitations and troubleshooting

The experience gathered so far regarding the use of GPR in pavement evaluation [Fontul, S; Antunes, M.L, 2001; Scullion, T., *et al* 1992; Saarenketo,T.; 1996; The Concrete Society, 1997; TRB; 1998 Highways Agency, 2001] has confirmed the advantages in using this equipment, and has also highlighted the difficulties that occur during testing and data interpretation. In order to improve the results some aspects should be taken into account, such as:

- ✓ Interpretation of radar data is complex and should only be carried out by experienced engineers. A special care is required during the filtering process and noise cleaning in order to avoid losing valuable data. All available information about the pavement structure should be gathered and used for the GPR data interpretation.
- ✓ The wave propagation velocity is highly dependent on the material characteristics. It is sensitive to several factors such as compaction degree, cracking, moisture etc. During the automatic interpretation, some “typical” values are assumed for the parameters involved in the process, which may not be applicable to a particular situation.
- ✓ For the reasons presented before, the calibration of GPR results using core data is always recommended (see 4.5.3). To confirm the accuracy of the study, results obtained with GPR can also be compared with additional cores, taken at different locations from those used previously to calibrate the radar system [Antunes, M.L., *et al*; 2004].
- ✓ In general, GPR will not detect interfaces between adjacent layers of the same type of material. Therefore, the consideration of several layers with materials of the same nature should be made with caution.
- ✓ Even for layers with different materials there are difficulties to track the layer delimitation when the boundary between two layers is not clear enough (e.g. granular layers contaminated by soil, penetration macadam over unbound granular layers etc.).

- ✓ There are materials, such as concrete or cement stabilised materials that presents high absorption capacity at GPR wave propagation. The energy losses in concrete are higher than in other construction materials and therefore, the real penetration depth can be reduced to half or more by the influence of defects in concrete as major cracks, voids, presence of water, chemical contamination and poor compaction influence the penetration range. [Antunes, M.L., *et al*; 2004; The Concrete Society, 1997].
- ✓ Some problems may arise with the interpretation of GPR results on specific pavements, like “sandwich” pavements (e.g. pavements with a granular layer between two layers with higher velocity).

4.5.3 Detailed interpretation/ calibration

LNEC’s experience with GPR data analysis highlights the importance of a detailed interpretation of data, once the automatic processing is completed. Taking into account the high sensitivity of the wave to the dielectric characteristics of the materials and the assumptions that are made during the automatic processing, significant errors can be made if one relies only in the automatic interpretation.

In order to improve the reliability of the results it is recommended that the final layer thickness is re-calculated trough a new detailed interpretation process [Fontul, S.; Antunes, M.L.; 2001]. This process is manual and aims at adjusting the wave velocity used in the interpretation for each layer in order to obtain the same thickness as the ones obtained by coring or site investigation at specific locations. (“layer thickness calibration”).

Special care is required in order to ensure that the core location is accurately identified within the radar file, that it has been full depth extracted and that its’ thickness was measured accurately. Usually, this layer thickness calibration is performed in more than one point along the GPR profile, due to the thickness variation along the road. Errors in cores’ thickness or location result in incorrect data interpretation.

The cores are extracted after the GPR survey, in locations where the reflected signal is clear and constant along a certain distance.

The recommended procedure [Fontul, S.; Antunes, M.L.; 2001; Fontul, S. *et al*; 2002a, 2002b.; Antunes, M.L. *et al*; 2004] for layer thickness calibration consists of the following steps:

- ✓ selection of a particular core that may be used as representative for calibration of the GPR results for a certain pavement section;

- ✓ calculation of the average wave velocity and layer thickness, for all the GPR points obtained within 5 m from the core location;
- ✓ adjustment of the average wave velocity in order to get an average layer thickness in this area, which is as close as possible to the thickness measured on the cores.

4.6 Further applications of GPR in pavements

Although the GPR tends to be nowadays routine testing equipment, it may still be considered as a prototype due to the fact that its accuracy and resolution are not yet fully known, and also taking into account the difficulties of interpretation of the results.

GPR is generally used for detection of pavement structure variations and determination of layer thickness. Meanwhile, other applications such as material characterisation, subsurface stripping, cracking, density quality control, thickness of very thin road layers are still under development [Saarenketo, T.; 1996; Rmeili, E.; Scullion T.;1997; Dérobert, 2001; Scullion, T.; Saarenketo,T.; 2002]. Some of the GPR features currently under development are briefly presented herein.

The **moisture content** drastically affects the dielectric properties of materials, and consequently the wave propagation. In order to evaluate the moisture content of unbound pavement layers a method developed by Scullion and Saarenketo [Scullion, T; *et al*; 1992; Saarenketo, T.; 1996] combines the GPR results with surface dielectric measurements in laboratory.

The moisture content of the unbound base is determined from its dielectric constant using a common mixture law called complex refractive index model [Maser, K; Scullion, T.; 1992], which is expressed as:

$$\sqrt{\varepsilon_m} = \sum V_i \sqrt{\varepsilon_i} \quad (4.12)$$

Where:

- ε_m - relative dielectric constant of the mixture;
- V_i - volume fraction of component i . The components of the unbound base material are solid particles, water and air. The dielectric constants of water and air are considered to be 81 and 1, respectively;
- ε_i - relative dielectric constant of component i .

Equation (4.13) [Scullion, T; *et al*; 1992] is used to determine the moisture content based on the bulk density of the material and the dielectric constant of the solids (solid particles*). The material's density is assumed to remain constant.

$$M = \frac{\sqrt{\epsilon_b} - 1 - \gamma(\sqrt{\epsilon_s} - 1)}{\sqrt{\epsilon_b} - 1 - \gamma(\sqrt{\epsilon_s} - 22.2)} \quad (4.13)$$

Where:

- M - moisture content of the unbound base (% of total weight);
- ϵ_b - unbound base dielectric constant, determined from equation (4.6);
- ϵ_s - solid particles (solids) dielectric constant (varies from 4 to 8 depending on source material);
- γ - is the dry density γ_d (lbs/ft³) divided by the density of solids γ_s (~165 lbs/ft³).

For laboratory tests a device, named "Percometer dielectric probe" is used for measuring the surface dielectric constant of materials [Scullion, T and Saarenketo, T; 1997]. Based on measurements performed with the Percometer on several materials, calibration curves were developed, as an additional tool to traditional optimum moisture content determination. Using this calibration curves the unbound base dielectric constant is converted to volumetric unbound base moisture content.

Another feature that was studied by the same researchers was the relation between the surface dielectric and the Hot Mix Asphalt Concrete (HMA) **air voids** of new asphalt layers [Saarenketo, T.; 1996].

The Percometer is used to perform measurements on laboratory moulded and field samples of new HMA layers. The Finnish researchers propose the following exponential relationship [Scullion, T.; Saarenketo, T.; 2002] for air voids evaluation:

$$\% \text{ air voids} = 272.9 \times \exp[-1.3012 * k * \text{surface dielectric}] \quad (4.14)$$

Where:

- k is a calibration constant determined in the laboratory.

The method uses two cores to determine their air void content in the laboratory and to calculate the calibration constant k .

Other features are studied based on the same methodology, such as:

- ✓ performance of the materials under freeze-thaw cycling based on the moisture content and water sensitivity [Scullion, T.; Saarenketo, T.; 1997]
- ✓ moisture trapped within hot mix layers and base layers [Scullion, T.; Saarenketo, T.; 2002].

These approaches are complex and are still under development. At the same time, require specific laboratory measurements. In case of moisture content, the calibration curves were developed for local materials so cannot be adopted for other materials without a proper

research. The assumption made in this approach, that material density remains constant along the road, can affect the results accuracy.

In case of the air void content of HMA new overlays it is assumed that the bitumen content of an asphalt material will remain constant, otherwise the dielectric changes will not reflect the changes in voids content. [Saarenketo, T.; 1996]

Another GPR application under development is the detection of **stripping** in asphalt concrete layers [Rmeili, E. and Scullion T.; 1997]. The methodology is based on the detection of a negative wave reflection between the surface reflection and the bottom of the asphalt layer reflection. This is associated with a lower material density and therefore with stripping. Results were obtained only for moderate or advanced stages of deterioration, that exhibit sufficient contrast in material dielectric.

Recently, the effect of asphalt-binder **ageing** on the dielectric properties of HMA was also investigated. [Al-Qadi, I.L. *et al*; 2004]. It was found that the dielectric constants decrease linearly with time due to changes of materials properties caused mainly by ageing. The asphalt becomes more brittle and its ability to store electric energy decreases, resulting into a decrease of dielectric constant. This method aims to detect degradation of asphalt layers by analysing the linear decreasing in dielectric constant trend. Interferences in this tendency can be considered as indicators of subsurface distresses such as moisture accumulation or stripping.

The detection of **debonding** of asphalt layers is still under development and generally requires the presence of thin air or water in the debonded surface to be detected. [Highways Agency, 1994; Forest, R. *et al*; 2003]

The GPR antennas used routinely are not able to **detect very thin layers** (less than 30 mm). For this purpose, a step frequency radar prototype, capable of operating with very high central-frequency synthetic pulses, is presently being developed in France (LCPC) [Dérobert *et al*, 2002; Simonin, J.M.; 2001; FORMAT; 2004].

GPR can become an interesting tool in the future for quality control with the development of the above-mentioned areas.

4.7 Summary

GPR using close air coupled dipole antennas or horn antennas is a testing equipment, which can operate at traffic speed, for detection of pavement structure variations and determination of layer thickness. This chapter addressed the use of GPR in pavement evaluation studies.

The GPR transmits short duration electromagnetic pulses from a transmit antenna into the material being tested. The signal is like a vertical sinusoidal wave that crosses the pavement structure. During this process, part of the wave is reflected at each layer interface. The reflected energy is picked up by the receive antenna and then is processed. This transmitting-receiving cycle is repeated at short intervals and, in this way, a continuous profile of the pavement's response is obtained during tests.

Although GPR is becoming a routine equipment, the interpretation of radar data is complex and should only be carried out by experienced engineers. A special care is required during filtering process and noise cleaning in order to avoid losing valuable data. All available information about the structure should be gathered for use in the interpretation.

In general, GPR will not detect adjacent layers of similar materials. There are difficulties to track the layer delimitation when the boundary between two layers is not clear enough (e.g. granular layers contaminated by soil, penetration macadam over unbound granular layers etc.)

The energy losses in some materials that exhibit high absorption (concrete, cement stabilised materials) can result in a reduction of the penetration depth in half or even more.

The wave propagation velocity is highly dependent on the material characteristics. It is sensitive to several factors, such as compaction degree, cracking, moisture etc. During the automatic interpretation some "typical" values are assumed for the parameters involved in the process.

The experience gathered so far with GPR testing and interpretation has led to some recommendations to overcome some of the problems associated with this technology.

One of the main recommendations is that a "detailed" interpretation together with layer thickness calibration based on extracted cores, is always required. Additional cores, taken at different location from those used previously to perform the layer thickness calibration, can be used to verify the results obtained with GPR.

Using this methodology will allow for a higher reliability in the use of GPR for pavement evaluation.

5 Artificial Neural Networks

5.1 Introduction

The concept of neural networks is inspired in the brain structure and its functioning. There are two main approaches in the artificial neural network area. One consists in using experimental chips that simulate neurons and interconnect them in a network. The other one is the software approach, which is cheaper and much easier to use and upgrade [Lin, T.; 2002]. This latter approach is presented in this chapter.

The following sections are not intended to give a comprehensive theory on ANNs, which is well covered in bibliography. The purpose of this chapter is to provide a background of the neural networks and their application in structural evaluation.

5.1.1 From biological neuron to artificial neuron

The brain is composed of about 10^{11} neurons that participate in about 10^{15} interconnections. A photo of a biological neurons network is presented in Figure 5.1, while a schematic drawing of a biological neuron is shown in Figure 5.2. Besides the characteristics common to other body cells, a neuron has unique capabilities to receive process and transmit electrochemical signals. It consists of the following elements [Marcelino, J.; 1996; Wasserman, P.D.; 1993; Lin, T.; 2002; Faley, C.; 2003; Intrator, N.; 2004]:

- ✓ *Soma* - the cell body of a neuron, where the *nucleus* is located;
- ✓ *Dendrites* - tree-like network of nerve fibre with chemical receptors (inputs) connected to the soma;
- ✓ *Axon* – a single long fibre with chemical emitters (outputs) at its end;

- ✓ *Synapses* – (or terminal buttons) are interfacing areas, consist of very small gaps that separate the axon of a neuron (outputs) from the dendrites of another neuron (inputs).

Through these synapses the signals are received by dendrites and transmitted to the nucleus where they are summed, resulting in an increase (or decrease) of the electrical potential (excitation) of the cell. When the cumulative excitation (the sum of input from all the cell's neighbouring neurons) exceeds a certain threshold a pulse (signal) is transmitted through the axon to other neurons. This action is called "firing". In reality, this process is much complex, but this is the basic functional outline that most artificial neural networks (ANN) attempt to mimic.

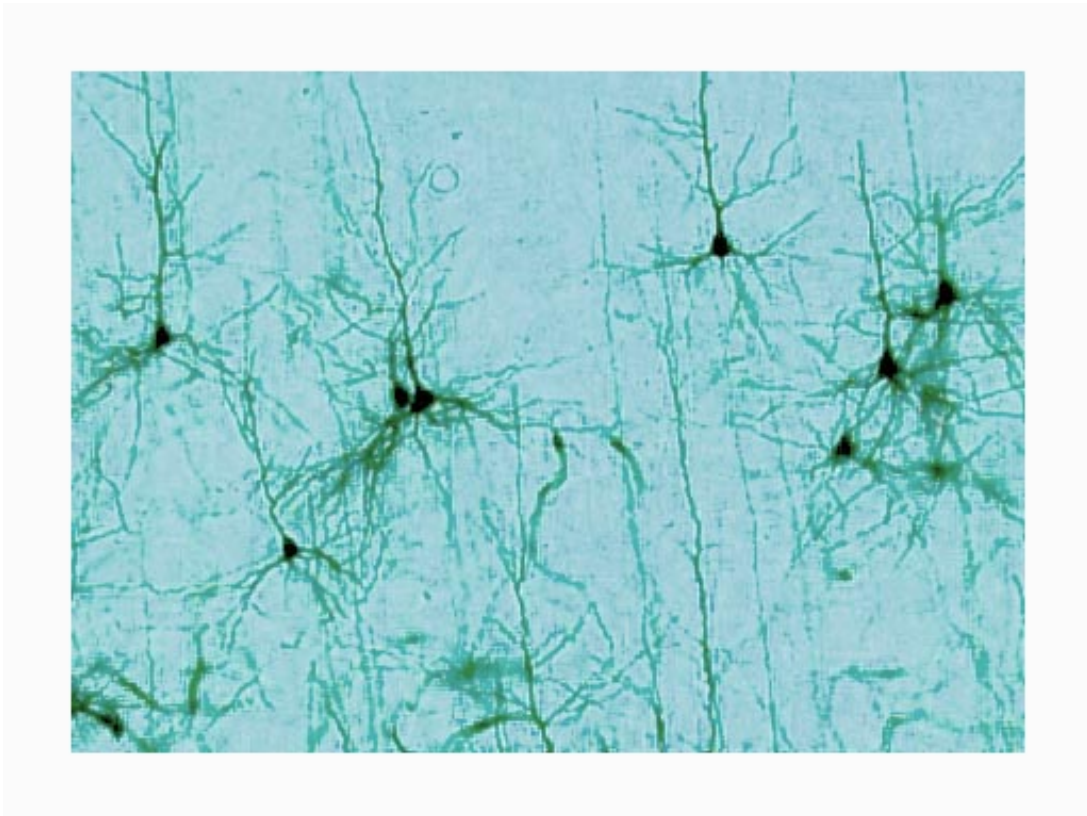


Figure 5.1 – Network of biological neurons [Faley, C.; 2003]

ANNs process information in a similar way that human brain does but their ability is limited and far more inferior than human brain. Even though they cannot think or develop beyond what they are taught [Lin, T.; 2002], they can learn how to do tasks based on the data given for "training" or "initial experience", they can generalise from previous examples to new ones and the computation can be processed in parallel [Wasserman, P.D.; 1989; Lin, T.; 2002; Faley, C.; 2003]. Their use is, for now, limited at tasks as pattern recognition, solving complex problems and feature recognition.

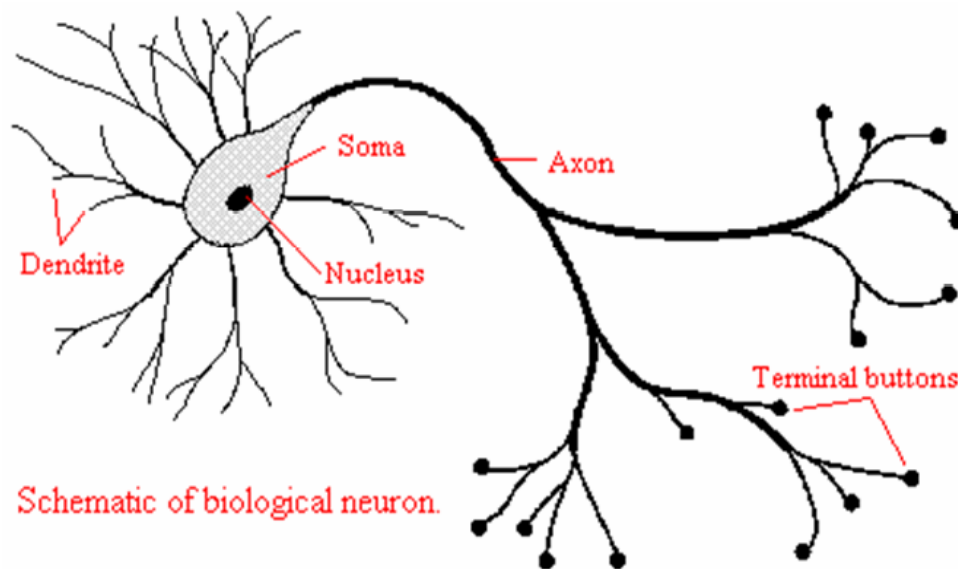


Figure 5.2 – Biological neuron [Intrator, N.; 2004]

As in brain structure, the Artificial Neural Networks (ANN) consist in interconnected “neurons”. ANNs are interconnected assemblages of simple computational elements, patterned after biological processes [Meier, et al, 1998]. An artificial neuron is a device with many inputs and one output (see Figure 5.3). Each neuron receives stimuli from their connections and, performing a rudimentary operation, generates other signals, which are transmitted to the adjacent neurons (see 5.2.1). A weight is associated to each connection between neurons and represents the importance of the connection.

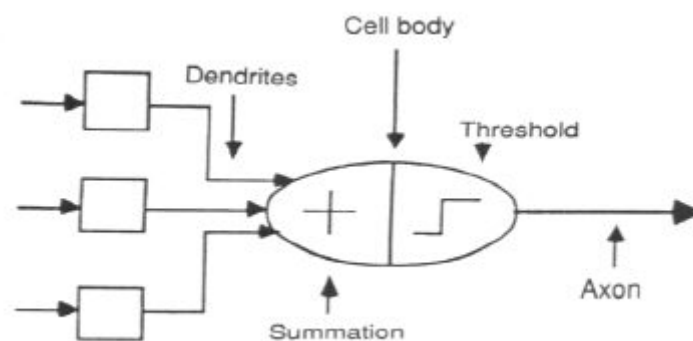


Figure 5.3 – The neuron model [Stergiou, C.; Siganos, D.; 2004]

Like in brain functioning, the input data is currently operated upon by multiple elements. This process is called “parallel distributed processing” and represents an important advantage when compared with traditional computation.

ANNs “learn” to produce a desired output by adjusting the connection weights [Wasserman, 1993; Meier, et al, 1997]. This process is performed by the computational elements themselves, applying learning rules to seek to minimize a given function.

ANNs have the ability to act as functional approximators that can “learn” a functional mapping when repetitively exposed to examples of that mapping. ANNs are able to learn a very complex mapping without previously specifying the functions or rules. However, it is very important to select the correct type of network and the most representative data for the training process in order to properly solve the problem under study.

Although successfully implemented in various areas, neural networks use is still controversial because their functioning is not fully understood just as the brain is not fully understood). Thus, artificial neural networks remain powerful but somewhat mysterious “black boxes” [Pei, J.; Smyth, A.W.; 2003; Stergiou, C.; Siganos, D.; 2004].

5.1.2 Historical evolution

The first attempt in developing neural networks models was made in 1943 by a neurophysiologist, Warren McCulloch, and a mathematician, Walter Pitts, referenced by [Wasserman, P. D.; 1989; Hecht-Nielsen, R.; 1991] that modelled a simple neural network with electrical circuits. In 1949 Donald Hebb proposed a specific learning law for the synapses of neurons and then used it to build qualitative explanation of some experimental results from psychology as referenced by the same authors. It pointed out that the neural paths are strengthened each time they are used. This served to inspire other researchers and the learning law suggested by Hebb became a starting point for ANN training algorithms.

In the 1950's and 1960's, a group of researchers combined these biological and psychological insights to produce the first artificial neural network. Mathematicians, computer engineers, neuroscientists and also psychologists and engineers contributed to the progress of neural network simulations.

The first successful neurocomputer was developed in 1958 by a neuro-biologist Frank Rosenblatt referenced by [Wasserman, P. D.; 1989; Hecht-Nielsen, R.; 1991; Stergiou, C.; Siganos, D.; 2004]. He designed and developed the *Perceptron*, which is a neural network consisting of a single layer of artificial neurons and was built in hardware (in other words by using the motor potentiometers, analogue circuits, wiring) [Hecht-Nielsen, R.; 1991]. It was applied to diverse problems such as weather prediction, electrocardiogram analysis and artificial vision.

In 1959, a different type of neural network processing element, called ADALINE (ADaptive Linear Element) was developed by Bernard Widrow and Marcian Hoff [Hecht-Nielsen, R.; 1991]. This was an analogue electronic device made from simple components, equipped with a powerful new learning law (the least mean squared) which, unlike the perceptron learning rule, is still widely use.

Unfortunately, the earlier successes resulted in overestimation of the potential of neural networks, given the limitation in the electronics available at that time. Network unexpected failures were intensively analysed and in 1969 the book “Perceptrons” written by Minsky and Papert, referenced by [Wasserman, P. D.; 1989; Hecht-Nielsen, R.; 1991; Stergiou, C.; Siganos, D.; 2004, etc.] proved mathematically the inability of single layer networks, in use at that time, to solve many simple problems. With this publication, and given the rigor and prestige of the authors, a decline period of neural network development started and lasted until 1981. Nevertheless, a few dedicated scientists continued their efforts, without neither moral nor financial support.

In 1982, several factors caused a renewed interest in neural network research. The enthusiasm and dedication of an established physicist John Hopfield was one of the main [Hecht-Nielsen, R.; 1991]. With clarity and mathematical analysis, he showed how ANN can work and what they can do. His approach was to create useful devices not only to model the brain.

In the past decades, theory has been translated into applications and the increase of research activities has been explosive. Comprehensive books and conferences provided a forum for people in diverse fields, academic programs appeared and courses were introduced [Stergiou, C.; Siganos, D.; 2004].

Today, artificial neural networks are applied in various fields but they are still at an early stage of development. Advancement beyond current applications appears to be possible, and research is advancing in many fronts. Neural networks have demonstrated performance, potential, but also limitations. Therefore, their use has to be made with caution.

5.1.3 Applications

The use of ANN has increased over the past two decades. They have been successfully used in many areas. They are powerful tools in pattern recognition and trends, being suited for function approximation, optimization, forecasting, data retrieval, automatic control etc. Some applications of ANN are [Lin, T.; 2002; Stergiou, C.; Siganos, D.; 2004]:

- ✓ Data analysis – to predict economic growth;

- ✓ Industrial process control;
- ✓ Data validation;
- ✓ Target marketing;
- ✓ Geographical mapping – to analyse data scanned from satellites;
- ✓ Image processing – to enhance, in combination with other programs, pictures taken from crime scenes;
- ✓ Recognition - use for hand writing, fingerprints and voice recognition.

Besides these general applications, ANNs are used in **medicine** for modelling part of human body and recognising diseases from scans (e.g. cardiograms, ultrasonic scans, etc.) [Sabbatinni, R.M.E.; 2004; Lo, J.Y.; Floyd, C.E.; 2004; Miller, A; *at al*; 1992]. They are well suited for diagnosing and with a proper training, based on large number of medical records including symptoms, diagnoses and treatments, they are able to give the “best” diagnose and treatment for a given medical case.

Other important areas of ANNs application are **business** and **financial analysis**, where they are used at resource allocation, searching for patterns in databases, optimization and scheduling. [Stergiou, C.; Siganos, D.; 2004].

In **civil engineering**, ANNs are applied in various areas such as: modelling material behaviour [Ghaboussi, J.; Wu, X.; 1998; Basheer, P.E.; 2002], detection of structural damage [Masri, S. *et al*; 1999; Sohn, H. *et al*; 2003; Ankireddi, S.; Yang, H.; 1999], collapse of structures [Saraiva, J.M.; Ebecken, N.F.; 1996], prediction of chloride diffusion in concrete [Peng, J. *et al*; 2002] etc.

Over the last decade, significant progress in application of ANNs in **pavement** and **geomechanical systems** has been achieved [Attoh-Okine, N.O.; 1998; TRB; 1999].

In **geotechnical engineering**, ANNs have been successfully applied for site characterisation, foundation engineering, soil liquefaction and constitutive modelling, mainly for subgrade soils and aggregates. Constitutive models have been developed for non-linear behaviour of clay-soils [Penumadu, D. *et al*; 1994], anisotropic stiffness of granular materials from triaxial tests [Tutumluer, E.; Seyhan, U.; 1998], resilient modulus modelling [Tutumluer, E.; Meier, R.W.; 1996], simulation of uniaxial stress-strain constitutive behaviour of fine-grained soils under cycle loading [Basheer, I.A.; Najjar, Y.M.; 1998] as well as simulation of both drained and undrained behaviour of sandy soil subjected to triaxial compression testing [Ghaboussi, J.; Sidarta, D.E.; 1998]. At LNEC ANNs have been applied for simulation of drained triaxial tests [Marcelino, J.; 1998].

The earliest applications in **transport engineering** were on areas such as planning, traffic control, tire/pavement interaction [FWHA, 2001; de Beer, M.; Fisher, C.; 2004], and facilities

management. The last years registered an increasing interest in use of ANN in pavement structural analysis [Meier, R.W.; Tutumluer, E.; 1998] and design as well as in assessment of remaining life of pavements [Ferregut, C *et al*, 1998].

Although ANN may never completely replace the versatility of classical approaches, they can be used to speed the structural analysis task [Meier, R. *et al*; 1997] as surrogates as long as the mapping problem is reasonably constrained [TRB; 1999]. In pavement structural analysis ANN have been used to develop models to compute:

- ✓ lateral and longitudinal tensile stress and deflections at the bottom of joint concrete airfield pavement: as a function of load location, slab thickness, subgrade support and load transfer efficiency at joints [Hausmann, L.D. *et al*, 1997; Ceylan, H. *et al*; 1999];
- ✓ load transfer efficiency of rigid pavement joints from FWD data [Ioannides, A.M. *et al*; 1996].
- ✓ backcalculation of asphalt pavement moduli:
 - from deflection basins measured with FWD for flexible pavements [Meier, R.W.; Rix, G.J.; 1994; Meier, R.W. *et al*; 1997; Meier, R.W.; Tutumluer, E.; 1998];
 - from Surface Waves (SASW) tests [Kim, Y.; Kim R.; 1998];
- ✓ for composite pavement analysis [Khazanovich, L.; Roesler, J; 1997].

There are also applications of ANNs in pavement distress evaluation and prediction:

- ✓ to detect and classify various types of surface cracks by processing images recorded with video [Kaseko, M.S. *et al*; 1994; Chou, J. *et al*; 1994];
- ✓ a neural network computer chip was also developed [Wang, K.C.P. *et al*; 1998] to automatically detect, classify and quantify different type of pavement distress at highway speeds.
- ✓ for pavement roughness prediction [Roberts, C.A.; Attoh-Okine, N.O.; 1998];
- ✓ to assess the relative contribution of input variables on pavement performance prediction [Shekharan, A.R.; 1999];
- ✓ for modelling the durability of aggregate used in concrete pavement construction [Najjar, Y.M.; Basheer, I.A.; 1997].

Recently, a methodology based on ANNs [Ferregut, C. *et al*; 1999] was developed to compute the residual life of flexible pavements subjected to rutting or fatigue cracking, based on deflections measured with FWD and the layers' thicknesses.

5.1.4 Neural networks vs. conventional computer algorithms

Unlike conventional computation, ANNs are not programmed to perform a specific task [Stergiou, C.; Siganos, D.; 2004]. Conventional computer programs use an algorithmic approach in order to solve a problem, in other words only the problems that are already understood can be solved. At the same time, the way the problem is solved must be known and stated in instructions converted into program language.

There are advantages and disadvantages in the two approaches: while the conventional computer program functions in a total predictable way, the neural networks “find out” how to solve the problem by themselves and therefore they are unpredictable. On the other hand, the fact that neural networks can be used to solve problems that are not fully understood can represent an important advantage in some areas.

The neural networks and conventional computer algorithms complement each other. Usually, a combination of the two approaches is used in order to obtain a maximum efficiency.

All ANNs are interconnected assemblages of simple processing elements, that contain limited amount of local memory and perform rudimentary mathematical operations on data passing through them [Marcelino, J.; 1996; Meier, R.W.; Tutumuler, E.; 1998]. The computational program behind this method is rather simple and therefore there are several softwares available, from modules of widely used programs such as: MATLAB or STATISTICA to softwares developed by individuals.

The software behaviour may be improved if numerical tools (see 5.3.4) are used to aid fast training, to reduce problems associated with slow convergence of backpropagation networks, saturation, to help avoiding local minima [Marcelino, J.; 1996; Pei, J.; Smyth, A.W.; 2003; Faley, C.; 2003].

In neural network application, the biggest challenge is the design of the network architecture to better fit the problem under study. There are no guidelines and the physical laws or mathematical formulations of the problem do not give indications on how to set up the network architecture, in terms of number of hidden layers, neurons per layer etc. Therefore, the ANN structure is designed by trial and error, complemented with previous experience [Pei, J.; Smyth, A.W.; 2003].

5.2 General concepts

5.2.1 Artificial neuron

Each processing element in the neural network is called “Artificial Neuron”. It is connected to every processing element in the layer immediately before it and in the layer immediately after it (see Figure 5.4).

Processing elements compute their excitation level as the weighted sum of their inputs:

$$N_j = \sum_{i=1}^n w_{ij} x_i ; \quad (5.1)$$

Where:

- x_i – input arriving from i^{th} processing element in the preceding layer;
- w_{ij} – weight assigned to that connection.

The combined input (N_j) is then modified by an *activation function*.

The output value of the activation function is passed by to another processing element through connection weights. Since each connection has a weight, the signals on the input are modified by these weights before being summed.

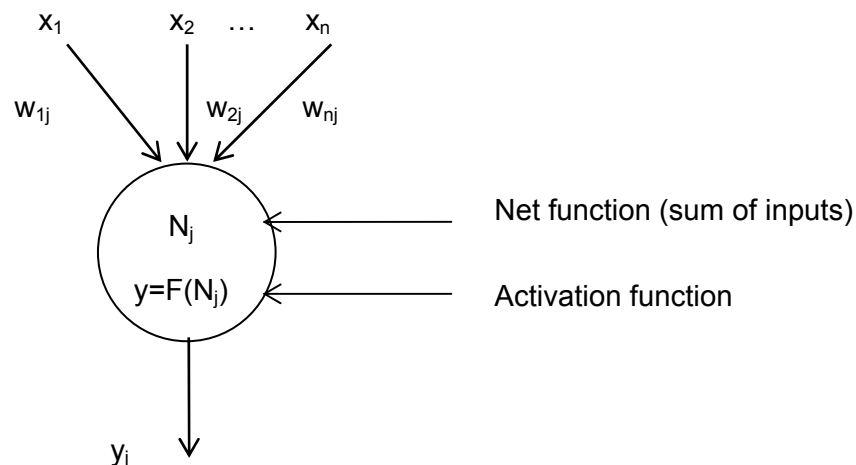


Figure 5.4 – Artificial neuron

5.2.2 Activation functions

The activation function, sometimes called transfer function, accepts a value that is the weighted sum of neuron inputs and returns a value that represents the output of the neuron. This determines if the neuron should “fire” (see 5.1.1). Similarly to biological neurons, whose output is restricted due to electrochemistry to the [-30, 70] mV range, the activation function output is limited to a specific range such as [0, 1] or [-1, 1] [Faley, C.; 2003].

The activation function usually assumes one of the forms presented below [Wasserman, P. D.; 1989; Marcelino, J.;1996; Meier, R.W. *et al*, 1997; Bishop, C.W.; 1999; Faley, C.; 2003; Stergiou, C.; Siganos, D.; 2004].

- 1) A simple **linear** function (or ramp):

$$F(N) = k(N) \quad (5.2)$$

where k is a constant and the output activity is proportional to the total weighted input.

- 2) A **threshold** function, which only passes information, if the activity level reaches a threshold, which can be a constant value or a continuous function of a combined input:

$$F(N) = \begin{cases} 1 & N > k \\ 0 & \text{otherwise} \end{cases} \quad (5.3)$$

where k is a threshold value or a function, which defines the intended response for the neuron.

- 3) A **sigmoidal** type function (S-shaped):

$$F(N) = \frac{1}{1 + e^{-N}} \quad (5.4)$$

The activation function can be seen as giving a nonlinear gain for the artificial neuron. This gain corresponds to the ratio of the change in function when a small change in N occurs.

The graphic shape of a sigmoidal function is presented in Figure 5.5.

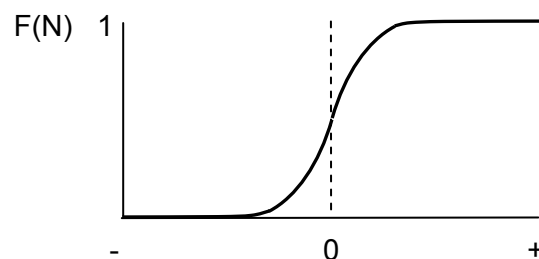


Figure 5.5 – Sigmoidal function

The gain shape varies from very low values at large negative or positive excitations to a high value near zero excitation. This function accepts input over a range $(-\infty, +\infty)$ and uniquely maps it into the range $[0, 1]$. The high gain of the central region provides the processing of small input signals, while the regions of decreasing gain at positive and negative extremes are appropriate for large input signals. This prevents the output from excessive growing as they are repeatedly summed and passed on, and at the same time, introduces nonlinearity into network calculations [Meier, R.W. *et al*, 1997]. This non-linear gain solves the *noise saturation problem* and without it, the output would represent only linear combinations of input and the ANN mapping ability would be severely limited.

The noise saturation problem, as explained by Grossberg [Grossberg, 1973] can be briefly described as follows:

The network has to handle both small and large signals. The small inputs require high gain and their amplified noise together with high-gain of the high inputs can saturate the network. Due to its sigmoidal function shape, the neuron performs with appropriate gain over a wide range of input levels [Wasserman, P. D.; 1989].

4) **Hyperbolic tangent function:**

$$F(N) = \frac{e^N - e^{-N}}{e^N + e^{-N}} \quad (5.5)$$

The graphic shape is presented in Figure 5.6.

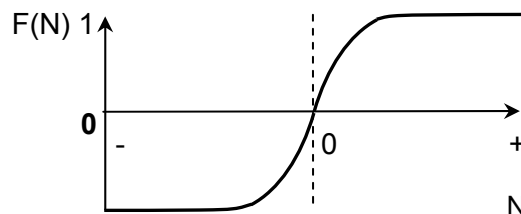


Figure 5.6 – Hyperbolic tangent function

The hyperbolic tangent function is similar in shape to the sigmoidal function, but the output is symmetrical around the origin. It accepts input over a range $(-\infty, +\infty)$ and uniquely maps it into the range $[-1, 1]$.

5.2.3 Neural network types

The “Artificial Neural Network” is a collection of connected neurons, arranged by layers.

There are several types of neural networks. They differ in the architecture, in the degree of connectivity, in the types of calculations performed within each element, the degree of supervision during learning, the determinism of the learning process, etc. [Wasserman, P. D.; 1989; Hecht-Nielsen, R.; 1991; Meier, R.W.;Tutumuler, E.; 1998; TRB, 1999]. Some of the more frequently used ANN are briefly presented below:

- 1) **Hopfield networks** store a set of patterns in such a way that the network, when presented with a new pattern, responds with the stored pattern that most closely resembles the new pattern. They implement an energy function in which each stored pattern is a local minimum. Any new pattern will follow the surface of that energy function to the nearest local minimum.

They can be used for pattern recognition, completion, and classification and as a content addressable memory. Hopfields networks have been successfully used for finding near-optimal solutions to combinatorial optimisation problems, as the “Travelling Salesman Problem” (TSP)* [Hopfield, J.J.; Tank, D.W.; 1985].

- 2) **Adaptive Resonance Theory (ART) networks** [Carpenter, G.A.; Grossberg, S.; 1988] have the ability to learn new patterns and, at the same time, maintain the patterns that have been learn previously. They store a set of patterns in such a way that the network, when presented with a new pattern, either matches it to a previously stored pattern or, if it is not sufficiently similar to any of the existing ones, stores it as a new pattern prototype to which future patterns can be matched. This process is called “unsupervised learning” because the network adapts to its environment without interference from the user.

ART networks can be used in the same areas as Hopfield networks. They can also be used for knowledge processing, to detect anomalies in data, as the creation of a new pattern prototype indicates an anomalous feature vector.

* In the “Travelling Salesman Problem” the goal is to find the shortest distance between N different cities: The path that the salesman follow is called tour. Testing every possibility of an N city tour would be N! math additions.

- 5) The **Kohonen maps** [Kohonen, T.; 1982] (also called Self-Organised Feature Maps) self-organise to produce consistent outputs for similar inputs. The process is called topology-preservation and consists of taking data from one space and projecting them into a lower-ordered data-space in a way that similar features project onto points in close proximity to one another.

This type of networks can be used for pattern recognition and classification and for data compression, in other words data are mapped in a space with fewer dimensions, preserving as much information as possible. For example, a Kohonen map can take 3-dimensional colour inputs and project them onto 2-dimensional plane with a finite number of “pixels”.

- 6) The **counterpropagation networks**, developed by Robert Hecht-Nielsen in 1986 [Hecht-Nielsen, R.; 1991] while seeking a way to use the self-organising map to learn explicit functions. These hybrid **networks** combine supervised and unsupervised learning to create a self-organising *look-up table* capable of generalization. This can be used for function approximation and classification. Vectors from a training set are presented to the network (inputs), unsupervised learning is used to create a topology-preserving (Kohonen) map of the input data while supervised learning is used to associate an appropriate output feature vector with each point on the map. The output is the average output of all the feature vectors that map to that point.

Once trained, each new vector presented to the network will trigger a response that is the average for those feature vectors closest to it in the input data space. This is a function of *look-up table*. The advantage compared with conventional look-up table is that the Kohonen map provides statistically optimal coverage of the input space even if the mathematical form of the underlying function is completely unknown. These networks train much faster than the backpropagation networks but are not so versatile and are slower at producing outputs.

- 7) The **Radial Basis Function (RBF) networks** [Moody, J.; Darken, C.; 1989] are also hybrid networks. The concept used is the fact that summing a series of Gaussian functions can approximate any continuous function. In three dimensions, the Gaussian functions appear as “bumps” with radial symmetry.

The RBF network has a mapping layer in which each neuron represents one “Gaussian bump”. As with the counterpropagation network, unsupervised learning is used to determine how best to partition the data space given a limited number of neurons. Each neuron is assigned to a cluster of input vectors and affects a Gaussian bump

located at the centre of the cluster. Once the data space has been partitioned, supervised learning is used to adjust the heights of the bumps to produce the best approximation of the function. The response to a new input vector is the sum of the outputs from every Gaussian bump in the network weighted according to the distance from the input vector to the centres of the bumps.

This type of networks also train much faster than the backpropagation networks but they are not so versatile and they are slower in use, as each output requires that hundreds of Gaussian functions are evaluated.

- 8) **Generalized Regression Neural Networks (GRNN)** [Specht, D.F.; 1991] are closely related to radial basis function networks. In a GRNN, each neuron in the mapping layer represents a Gaussian bump that coincides with one of the inputs from the training set. The weights are set by hand using the input and the output feature vectors, for each example. Therefore, the training time is almost zero but many neurons are wasted, as the training examples do not optimally cover the input space. More neurons are needed to achieve the same error level as a Radial Basis Function network. They are even slower at producing an output.

- 9) In the **Backpropagation Neural Networks (BNN)** [Wasserman, P. D.; 1989; Hecht-Nielsen, R.; 1991] the inputs are propagated initially through each layer to emerge as output. The errors of those outputs with respect to the correct answers are then propagated backwards and so the connection weights are individually adjusted to reduce the error. After several data propagations the mapping function is “learned” within some tolerance.

The back-propagation algorithms are faster than other approximation networks but much harder to train. They are multi-layered, *feed-forward* neural networks and are trained using an error-backpropagation algorithm (see 5.6.2). In *feed-forward* neural networks each unit during computation gets input independent on its output [Intrator, N.; 2004].

The BNN are powerful and versatile networks that can be “taught” a mapping from one data space to another, using examples of the mapping to be learned [Meier, R.W.; Tutumluer, E.; 1998]. This process is called “supervised learning”. This type of training enables a certain control of ANN response, as the answer will be within the range of values used for training. The back-propagation neural networks are excellent at data modelling and classification.

For the reasons presented above, the back-propagation neural networks are considered well suited for pavement structure modelling they will be used in this study. For simplicity, whenever neural networks are mentioned from this point onwards it will be the back-propagation type of networks (ANN). Other types will be addressed by their name.

5.3 Backpropagation Neural Networks

5.3.1 Structure of ANN

A backpropagation neural network, that for simplicity reasons will be referred as ANN instead of BNN in this study consists of several layers of neurons:

- ✓ The first layer, representing the input layer;
- ✓ One or more intermediate layers, defined as “hidden” layers;
- ✓ The last layer, representing the output layer.

Figure 5.7 presents an example of a NN structure with two intermediate layers.

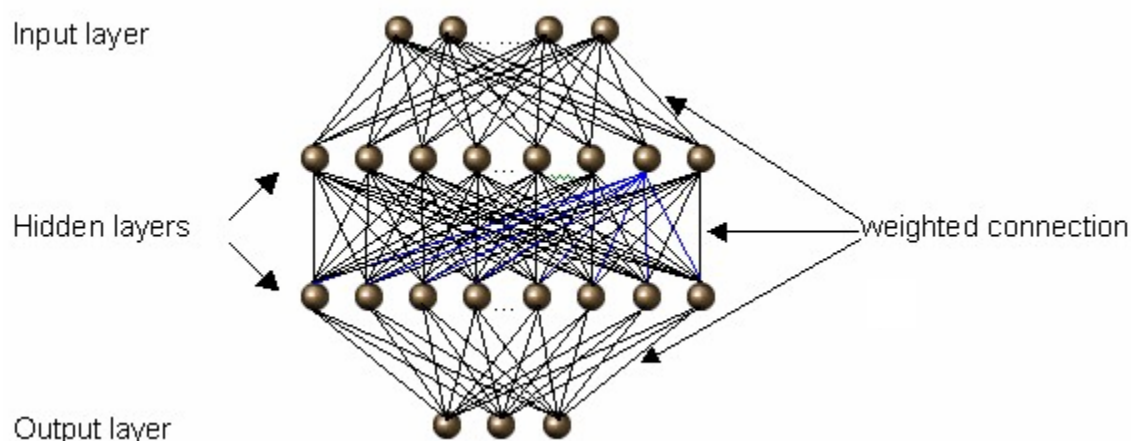


Figure 5.7 – Neural network structure

The number of neurons in the first and the last layer is equal to the number of input and output parameters, respectively. On the contrary, there are no well-established rules for choosing the number of neurons in each hidden layer. Therefore, trials must be used to

determine the optimum network architecture, which has to be the best combination between accuracy and training speed.

There are, however some considerations to be taken into account:

- ✓ The increase in the number of neurons increases the memory capacity of the network, but at the same time reduces the capacity of reasoning. In other words, the network will be incapable of performing mappings from datasets that were not memorised (not used during training);
- ✓ It is possible to approximate any functional mapping with a network with only one hidden layer. However, two hidden layers often allow the same functional mapping to be learned with fewer neurons [Meyer, R.W. and Rix, G.J.; 1994].

5.3.2 Training of ANN

The process by which a neural network adapts to the intended environment is called “training” and consists of the modification of the weight of the connections between the neurons. The description of this process in case of multi-layer backpropagation neural network is presented here. A multi-layer neural network consists of one input layer, one output layer and at least one hidden layer.

Before training, it is necessary to establish initial values for the weights of all the connections. To ensure rapid convergence it is important that the initial weights are “small” random numbers (between -0.1 and 0.1) [Marcelino, J.; 1998].

The training process consists of three distinct phases:

- ✓ In the first phase (forward propagation) of training, the input signals are propagated through the hidden layers until they reach the output neurons, resulting in a collection of values.
- ✓ In the second phase, the “errors” are calculated*. They are given by the difference between the “expected” outputs and the values calculated in the first phase (forward propagation). Once the errors for each neuron are known, they are back-propagated during the third phase.

* The error can be calculated either as the simple difference between the desired and the actual output or as the square of the difference between them [Stergiou, C.; Siganos, D.; 2004]

- ✓ In the third phase (backward propagation) the weights of the connection are corrected in order to achieve an improvement of the network response.
- ✓ This process is repeated as many times as necessary to obtain a satisfactory ANN response.

The network architecture has to be the best combination between accuracy and training speed. The computer resources needed to training an ANN are proportional to the size of the training database. After the training process is finished, it is convenient to test the ANN, through a process called validation.

5.3.3 Learning rule

The learning process occurs in the human brain when the properties of dendrites change at a synapse in order to become more or less receptive to signals. Similar to this process the artificial neural networks are taught through a learning process. In general, there are three types of learning [Intrator, N.; 2004]: supervised, unsupervised and reinforcement learning. In this study, the first one is addressed.

In supervised training, there is a “teacher” that presents input patterns to the network, compares the resulting outputs with those desired, and then adjusts the network weights in such a way as to reduce the error [Wasserman, P. D.; 1989].

The most common learning algorithm used in backpropagation networks is the “delta” rule [Wasserman, P. D.; 1989; Hecht-Nielsen, R.; 1991; Marcelino, J.; 1996]. The references are made for the training of an artificial isolated neuron (see Figure 5.4). This rule allows for calculation of the corrections Δ applied to each weight in the following way.

- a) An input is applied and the output y is calculated;
- b) The difference between the target answer T and the actual answer y of the neuron is calculated:

$$\delta = (T - y) \quad (5.6)$$

- b.1) if the target answer is correct ($\delta = \text{zero}$), then go to first step (a);
- b.2) if the target output differs from the one obtained ($\delta \neq 0$), then each input (x_i) is multiplied by a value Δ_i , which is calculated using the following equation:

$$\Delta_i = \eta \delta x_i \quad (5.7)$$

Where:

- η - a coefficient called “learning rate”;
- δ - the difference calculated before (5.6);
- x_i - the i^{th} input.

c) In this way, the weight of the input i in the next iteration, $w_i(n+1)$, can be written as follows:

$$w_i(n+1) = w_i(n) + \Delta_i \quad (5.8)$$

Where:

- $w_i(n)$ - is the weight before the adjustment;
- Δ_i - the correction calculated in 5.7.

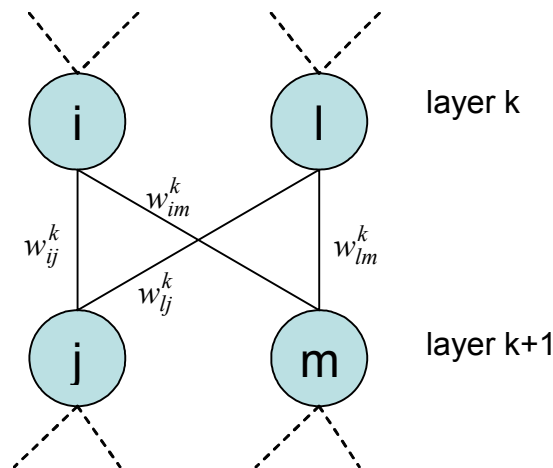


Figure 5.8 – Matricial notation for the neural network

To enable the systematisation of the formulation a vectorial notation describing the various elements in the networks is introduced [Marcelino, J.; 1996]. The weight matrix is W , where w_{ij}^k represents the weight of the connection between neuron i of layer k to neuron j of layer $k+1$ (Figure 5.8). The inputs that a layer receives form the matrix X and the outputs of a layer form the matrix Y . The target results matrix is the vector $\{T\}$.

For each layer the impulses for each neuron can be written in the following form:

$$\{N\} = \{X\}^T [W] \quad (5.9)$$

The output of the layer will be a function of the input impulse:

$$\{Y\} = F(\{N\}) = F(\{X\}^T [W]) \quad (5.10)$$

where F is the activation function.

The training consists of three distinct phases, as already described in 5.7.1:

In the first phase, the input is propagated through the successive layers and the answer of each layer is calculated using equation (5.10). This last one represents the input impulse for the following layer, and so on until the last layer (the output layer).

In the second phase, the error is calculated at the output layer level by the difference between the vectors of the target answer and the ones obtained from the propagation of the impulses through the neural network.

$$\{E\} = \{T\} - \{Y\} \quad (5.11)$$

Finally, this error is back propagated (propagated from the output layer to the input layer) and the weights of each connection are corrected in order to improve the answer of the network and to minimise the error.

To back propagate the error, its value is multiplied by the derivative of the activation function. In this way, by reducing the importance of the elevated signals and increasing the reduced signals, the gain of the neuron is adjusted (Figure 5.9). Therefore, it is very important to use activation functions that can be easy to derivate.

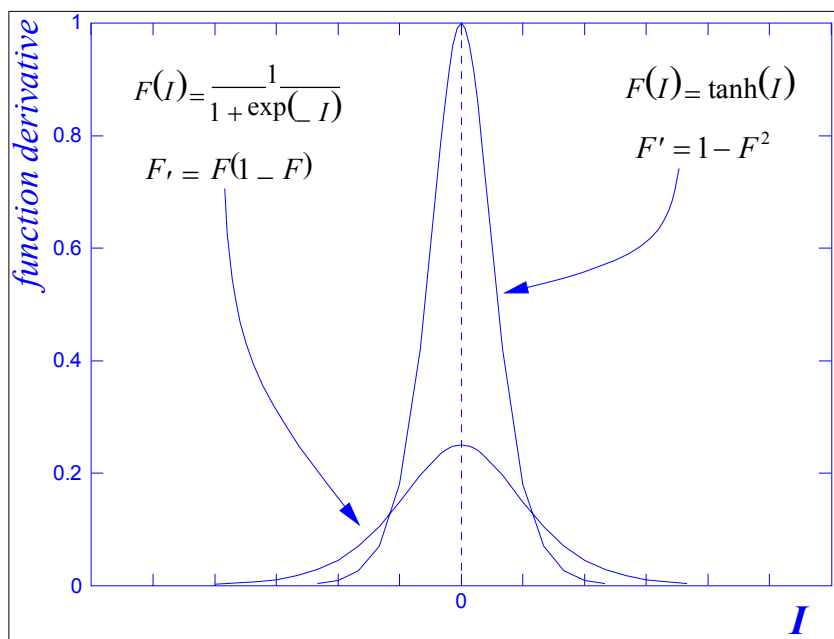


Figure 5.9 – Derivate of the activation function [Marcelino, J.; 1996]

In the hidden layers, the value of the error cannot be calculated directly, as the outputs have no known target value for comparison. Therefore, it is necessary first to correct the weights that connect to the output layer. As in the case of the isolated neuron, the corrective term of the weight will be:

$$\Delta w_{ij}^k = \eta \delta_j^k y_i^{k-1} \quad (5.12)$$

Where:

- Δw_{ij}^k - the corrective term of the weight of connection between neuron i (of layer k-1) and neuron j of layer k;
- η - the learning rate (typically between 0 and 1);
- δ_j^k - the difference between the target result and the output of the network for neuron j of layer k, calculated using equation 5.6;
- y_i^{k-1} - the output of neuron i of layer k-1.

The corrected weights for iteration n+1 will be:

$$w_{ij}^k(n+1) = w_{ij}^k(n) + \Delta w_{ij}^k \quad (5.13)$$

The vector δ for the previous layer is calculated using equation 5.13 and reflects the contribution of each neuron in layer k-1 for the error calculated in layer k.

$$\delta_i^{k-1} = F'(N_i^{k-1}) \left[\sum_j \delta_j^k w_{ij}^k \right] \quad (5.14)$$

Based on the values of δ calculated in this way for each layer, it is possible to adjust the weights of the connections until the input layer.

The training stops when the error $\{E\}$ is close (or equal) to zero. Usually a small value (e.g. 0.001) is assumed (in the program) for the error, and when this value is reached, the training ends. Anyway, this value it is not always easy to be achieved, as depends on the data used for training and on the network architecture. Another approach is to set-up a certain number of iterations for training, and to analyse the error obtained at the end of this process. The general idea is to follow the network training evolution and if the error stabilise the training can be considered ended. The training can be improved (if the error is still high) by either changing the ANN architecture (increasing the number of neurons in hidden layers) or by using some of the techniques described below.

5.3.4 Training troubleshooting

5.3.4.1 Problems

During training, the main problems that can occur are that the network can paralyse or be “trapped” in a local minima instead of the absolute minima.

Network paralysis

This phenomenon, also called saturation, is caused by high values of connection weights. Saturation occurs if, during training, the weights are adjusted to large values and the output is close to the extremes [Craven, M.P., 1997]. In this case, the derivative is too small to make further significant weight changes, and the network paralyses (see Figure 5.10). The main causes of saturation are: large values of initial weights, high learning rate, overtraining.

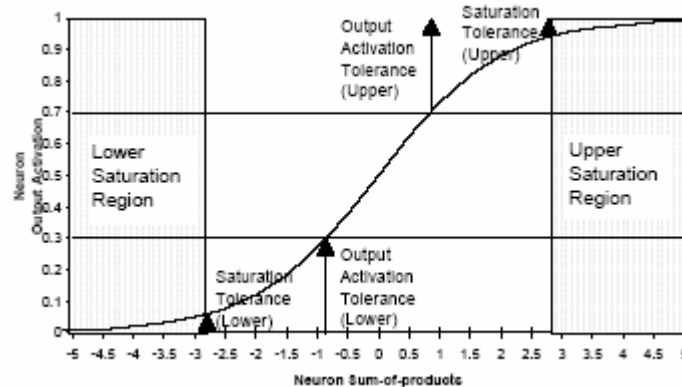


Figure 5.10 – Typical saturation limits for a neuron output [Craven, M.P., 1997]

Local minima

Back propagation employs a type of descendent gradient, in other words, it follows the slope of the error surface downward, constantly adjusting the weights to a minimum. [Wasserman, P.D.; 1989]. The problem is that nonlinear transfer functions in multilayer networks introduce many local minima in the error surface that for a complex network can be full of hills, valleys, folds in high dimensional space (Figure 5.11).

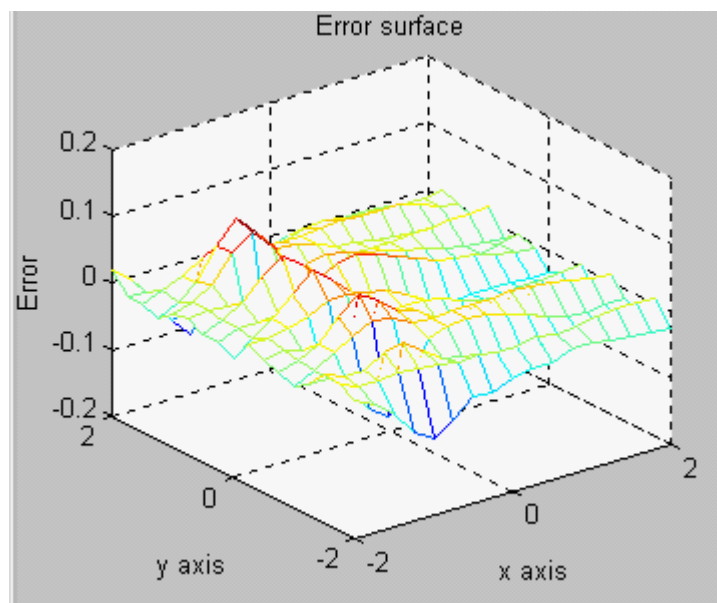


Figure 5.11 – Aspect of an error surface [Koivo, H.N; 2000]

As gradient descent is performed on the error surface it is possible for the network solution to become trapped in one of these local minima instead of the global minimum (Figure 5.12).

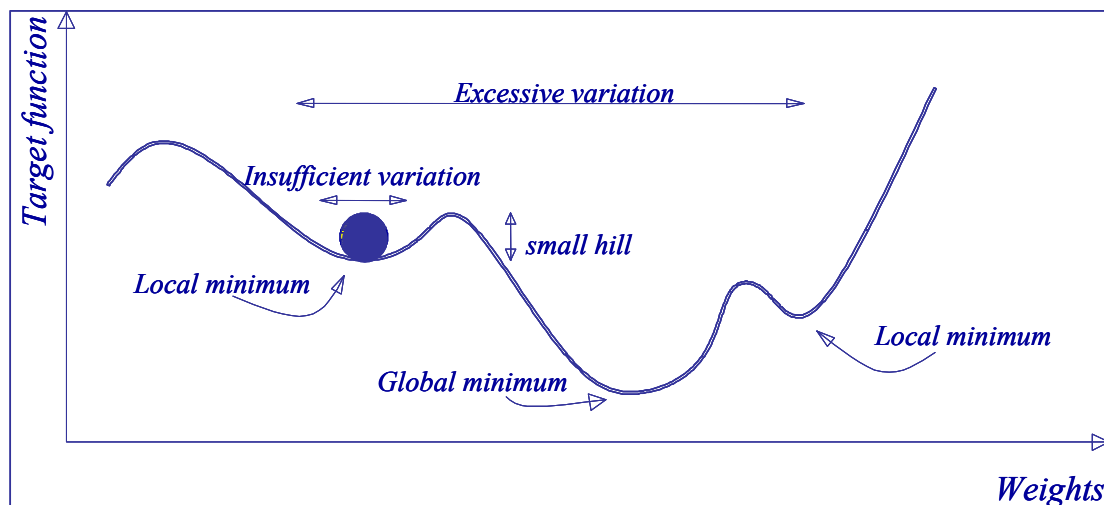


Figure 5.12 – Example of error surface, local and global minima [Marcelino, J.; 1989]

This may happen depending on the initial conditions. Some of the techniques used to avoid this occurrence are presented below.

5.3.4.2 Solutions

The efficiency of training algorithms may be improved through the introduction of small “tricks” or special learning techniques [Marcelino, J.; 1996].

1. A simple way to avoid saturation and local minima is to initialise the weights to small random numbers. Local minima can be also avoided by inducing random shaking in order to help the network to jump the local minima (Figure 5.12).
2. Mixed learning rules can be also very useful in preventing the pathologies described above. The mixed rule consists of combining backpropagation with statistical methods [Wasserman, P.D.; 1989; Marcelino, J.; 1998] and recently even genetic algorithms and annealing are used to improve the training [Borenstein, E.; 2004].
3. One of the methods, generally used consists of adding an extra neuron to each neuron layer, called “**bias neuron**”. The output of this neuron is a constant and equal to +1, and the connections to this neuron are trainable weights. This allows for changing the position of the “origin” of the activation function whenever necessary, in a way that enables this function to work in the maximum gain range to optimize its answer. The current practice (adopted here, too) normalises the inputs and the

outputs to a range of [-3; 3] and [0,+1], respectively [Marcelino, J.; 1998]. This is considered the optimal range to avoid saturation (see Figure 5.10) and enable an efficient training.

4. Another method, called “**momentum**” [Rumelhart, D.E. *et al*, 1986] consists of adding a term to the weight correction that is proportional to the amount of the previous weights change. This method improves the training time while enhancing the stability of the process. The adjustment can be mathematically expressed by the modification of the equation (5.12) as follows:

$$\Delta w_{ij}^k(n+1) = \eta \delta_j^k y_i^{k-1} + \alpha [\Delta w_{ij}^k(n)] \quad (5.15)$$

where the coefficient α (momentum) normally assumes values of less than 0.9 [Marcelino, J.; 1998].

There are other techniques more complex or still under development such as the application of second order derivatives of the transfer function (also called *second order backpropagation*), the exponential smoothing of the weights, the application of a backward pass during training [Craven, M.P.; 1997] etc. Although their use is not justified in the actual development stage, they may prove to be fundamental in the future.

Sometimes, the only way to guarantee that the best solution has been achieved is to reinitialize the network and retrain several times.

5.3.5 Computer program Redes 3

The computer program “Redes 3” has been used for the automatic calculation of the backpropagation multilayer neural network, developed at LNEC [Marcelino, J.; 1996]. The program was developed using two programming languages, *Fortran 77* for the numerical calculation routines and *Visual Basic* for the interface [Marcelino, J.; 1998]. Figure 5.13 presents the flow chart of the main module of the program.

This program allows for selecting the characteristics of the neural network, such as:

- ✓ the training parameters: normalisation values for inputs and outputs, number of iterations, the desired error value;
- ✓ the type of transfer function: sigmoidal, hyperbolic tangent or linear;
- ✓ the training technique to be used: backpropagation or statistics (training is performed separately for every one input parameter).

It also incorporates methods for training improvement, such as bias neuron, momentum, random shaking [Marcelino, J.; 1998].

This program was modified for use in backcalculation of pavements deflection data by increasing the maximum number of data sets used during training from 1 000 to 10 000.

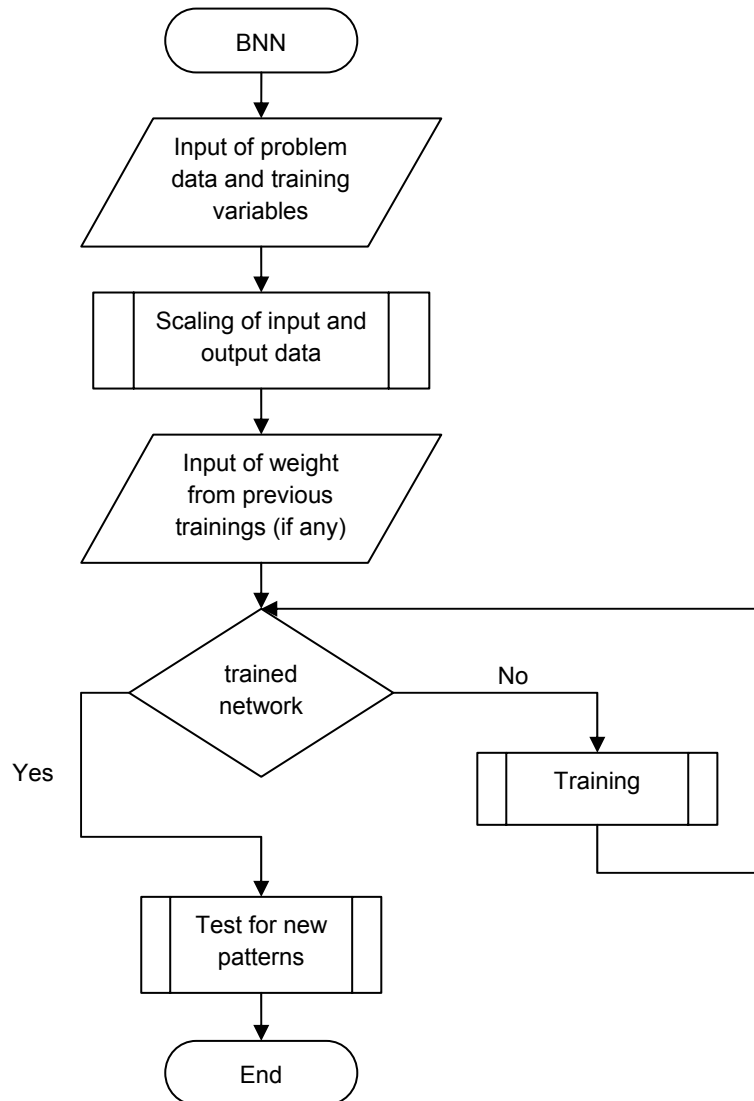


Figure 5.13 – Backpropagation Neural Networks program flowchart [Marcelino, J.; 1998]

5.4 Summary

The use of artificial neural network (ANN) for solving engineering problems has increased during the last years, and is considered a promising tool for NDT interpretation. This chapter introduces ANN, with a view of their use in pavement evaluation.

All ANNs are interconnected assemblages of simple processing elements, that contain limited amount of local memory and perform rudimentary mathematical operations on data passing through them. The neural networks and conventional computer algorithms complement each other. Usually, a combination of the two approaches is used in order to obtain a maximum efficiency.

Among the different types of ANNs the backpropagation neural networks (BNN) are considered well suited for pavement structure modelling because they are powerful and versatile networks that can be “taught” a mapping from one data space to another, using examples of the mapping to be learned. This type of training, called “supervised learning”, enables a certain control of NN response, as the answer will be within the range of values used for training.

Backpropagation ANNs can be “trained” to determine the corresponding pavement layer moduli from deflection basins, based on a database of FWD results. A computer program, REDES 3, which has been developed at LNEC for geotechnical applications, has been adapted for this purpose.

In neural network application, the biggest challenge is the design of the network architecture to better fit the problem in study. It is very important to select the correct type of network and the most representative data for the training process in order to properly solve a given problem under study.

There are no guidelines and the physical laws or mathematical formulations of the problem under study do not give indications on how to set up the network architecture, in terms of number of hidden layers, neurons per layer etc. Therefore, the NN structure is designed by trial and error, complemented with previous experience.

6 Improved method for pavement evaluation

6.1 Introduction

In order to evaluate the bearing capacity of a pavement, using a mechanistic approach, a structural model of the pavement is required for the estimation of residual life.

This Chapter presents the methodology developed for structural pavement evaluation based on both Falling Weight Deflectometer (FWD) and Ground Penetrating Radar (GPR) results, using artificial neural networks (ANN). The main contributions of the proposed method with respect to the methods currently used (see Chapter 3) method are highlighted in the flowchart presented in Figure 6.1.

The particularities of the non-destructive tests (NDT) data selection and pre-processing are presented and the method proposed for NDT results interpretation, using ANN, is described. Specific aspects related with its application in pavement structural evaluation are discussed.

The proposed method aims at combining the FWD and GPR data and at processing the results in an efficient way. The main objective is to perform the interpretation of all FWD test results and consequently to evaluate the pavement structure in all FWD test points. For this purpose, the GPR results are used as an average value of layer thickness over a 5 m interval around each FWD test point. For an efficient backcalculation an artificial neural network is trained (using synthetic deflections) and then used for layer moduli estimation based on measured deflections and layer thickness.

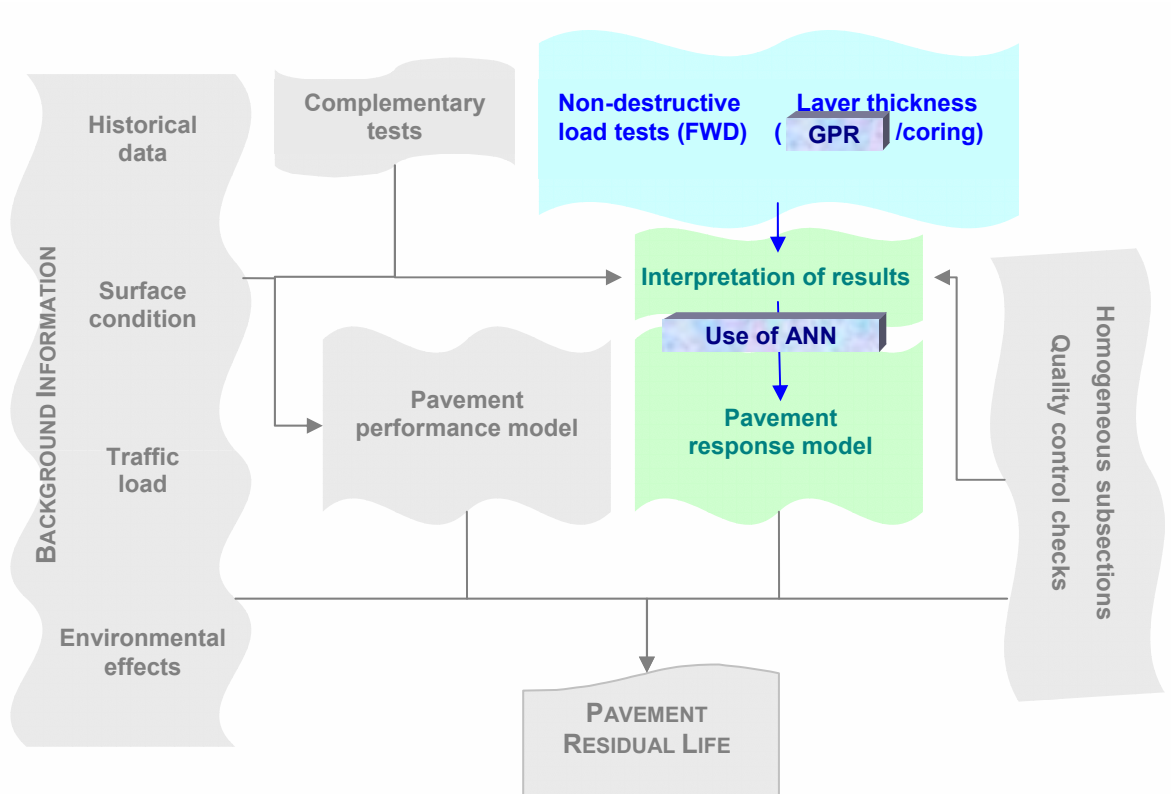


Figure 6.1 – Flowchart for pavement structural evaluation – main contributions

A study of ANN performance is also presented: the main aspects analysed are the influence of ANN training database type in the results obtained and the effect of input variation on ANN response.

6.2 Selection of data for analysis

The number of testing points and their location have to be chosen in order to properly cover and characterise, as well as possible, the pavement under study, while performing only a minimum number of tests. The selection of FWD test points must be performed taking into account the costs, the time required to perform the tests and the consequent traffic disruptions, as well as the need to provide a good characterisation of the pavement under evaluation. Therefore, the engineering judgment and experience are very important in

organising a testing plan, based on the available information about the pavement condition and experience from previous studies.

Generally, after normalisation of the measured deflections, the area under study is divided in statistically homogeneous sub-sections. For a given subsection, the pavement structure is modelled in order to match a representative deflection bowl (see 3.7), for a given set of layer thickness preferably, given by coring and/or test pits performed at the location where this deflection bowl was measured.

The continuous measurement of layer thickness provided by the use of GPR allows a quite accurate interpretation of all the FWD test points, as the pavement structure is known in all of them.

Ground Penetrating Radar is used for continuous layer thickness measurement. The information obtained with GPR should be confirmed and completed with additional testing (see Chapter 4). The additional tests consist of core drilling and/or test pits.

The GPR results can be also used for the subdivision of the pavement into homogeneous subsections, based on layer thickness information. Like in the deflection case, the division may be performed using the cumulative difference method, already described in 3.5.2. This method is used as it is considered to represent a good compromise between simplicity of calculation and accuracy of results. To process the subdivision a rather simple computer program is required. Even more important is the fact that this method has no restriction regarding the distance between testing points (while normal distribution criteria method require equidistance). Especially in the case of GPR tests, the equidistance is difficult to be achieved in all points along the test profile, due to factors such as wave absorption, localised changes in pavement structure etc.

The density of data obtained during GPR surveys is very high. For example, LNEC's equipment usually performs four measurements per meter. Due to the high amount of information, a pre-processing of the data obtained during tests is necessary. In order to make this process more efficient the following procedure is recommended. The distribution of GPR results obtained after the automatic interpretation (see 4.5.1) performed with the software supplied by the manufacturer is statistically analysed. This evaluation enable a sound feedback on the layer thicknesses distribution (histograms), helps to clear the noise and inconsistent measurements and provide information on the number of layers that may be considered within each subsection. Figure 6.2 presents a layer thickness distribution before cleaning of noise and inconsistent reflections while Figure 6.3 presents an example of a data file histogram where two layers have been detected and consequently will be taken into consideration (instead of one) for the detailed interpretation. Although this type of information

is easy to identify on GPR files, the use of statistics gives an overall information on layer thickness distribution and improves the detailed interpretation by enabling a more accurate choice of layer thickness range.

The data regarding the layer thickness distribution is also used to produce the database for the pavement structural model (see 6.4). In fact, the need to clear data and to define thickness ranges for ANN training is one of the reasons for developing this procedure for thickness distribution analysis. The database used for the ANN training should include the range of layer thickness variation (the lower and the upper values of each layer).

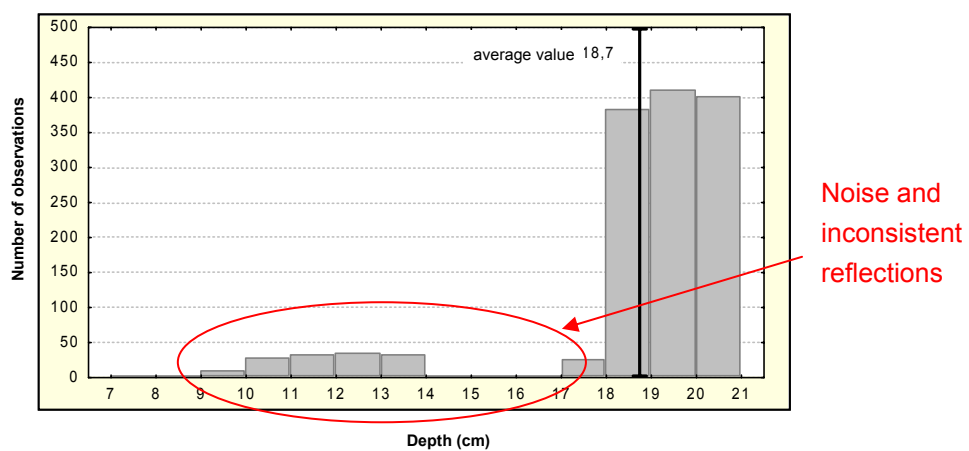


Figure 6.2– Layer thickness distribution histograms before the statistical analysis

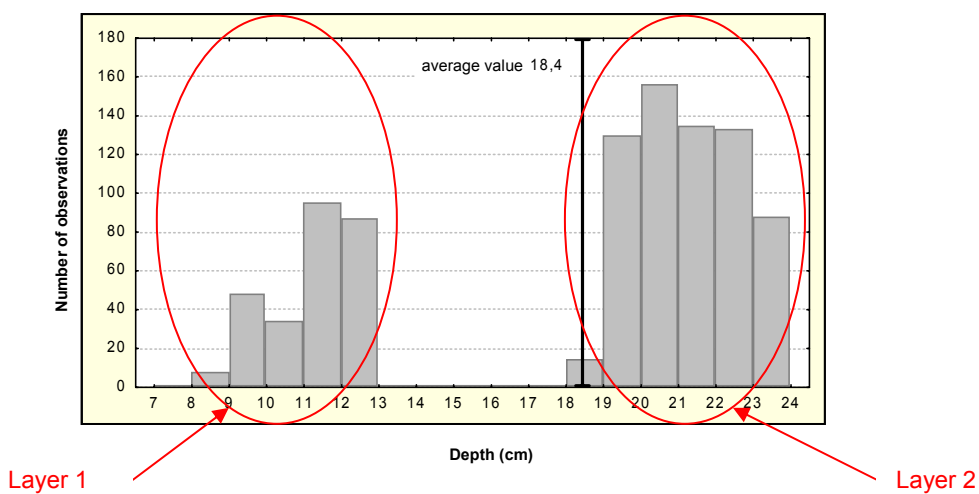


Figure 6.3 – Layer thickness distribution histogram (existence of two layers)

6.3 Pre-processing of FWD and GPR data

Due to the large number of measurements with GPR it is necessary to compile this information with the FWD results. During the interpretation of FWD measurements for pavement evaluation only the layer thickness around the FWD test point is required.

For this purpose a computer program “FWD_GPR” has been developed using “*Matlab*” software. The processing consists in combining the FWD and GPR test results.

The information in the resulting file will have for each FWD test point the corresponding pavement structure (layer thickness). This last value is represented for each layer by the average of the GPR measurements located at 5 m around the FWD test point (2.5 m ahead and behind it). This file is then used together with the corresponding deflections measured “in situ” as inputs to the artificial neural network (already trained) for pavement structural evaluation.

A problem that may arise is the lack of layer thickness information at some locations, sometimes even along the 5 m used. This is more probable to occur in case of rigid pavements or deeper layer in poor condition (contaminated granular layer and soils). In this situation, the following options can be considered:

- ✓ The thickness average can be extended, for example from 5 to 10 m around the FWD test point. This method is suitable for the upper layer of rigid pavements, as the absorption of the radar wave is higher in this type of material and, at the same time the layer thickness of the concrete slabs has generally lower variability along the road;
- ✓ A “design” thickness can be assumed based on background information. This approach is suitable for deeper layers, such as base and subbase, due to the reduced influence of their thickness variation in the pavement structural model (see 6.5.3);
- ✓ Interpolation between adjacent points can be performed. The software supplied by manufactures (in case of GSSI) is not prepared to consider a continuity of a layer if the distance between 2 consecutive points is more than 10 m. Therefore, sometimes the interface between layers is visible in the GPR record but is not detected by the program. In this case, reliable results are obtained by interpolation between adjacent points.

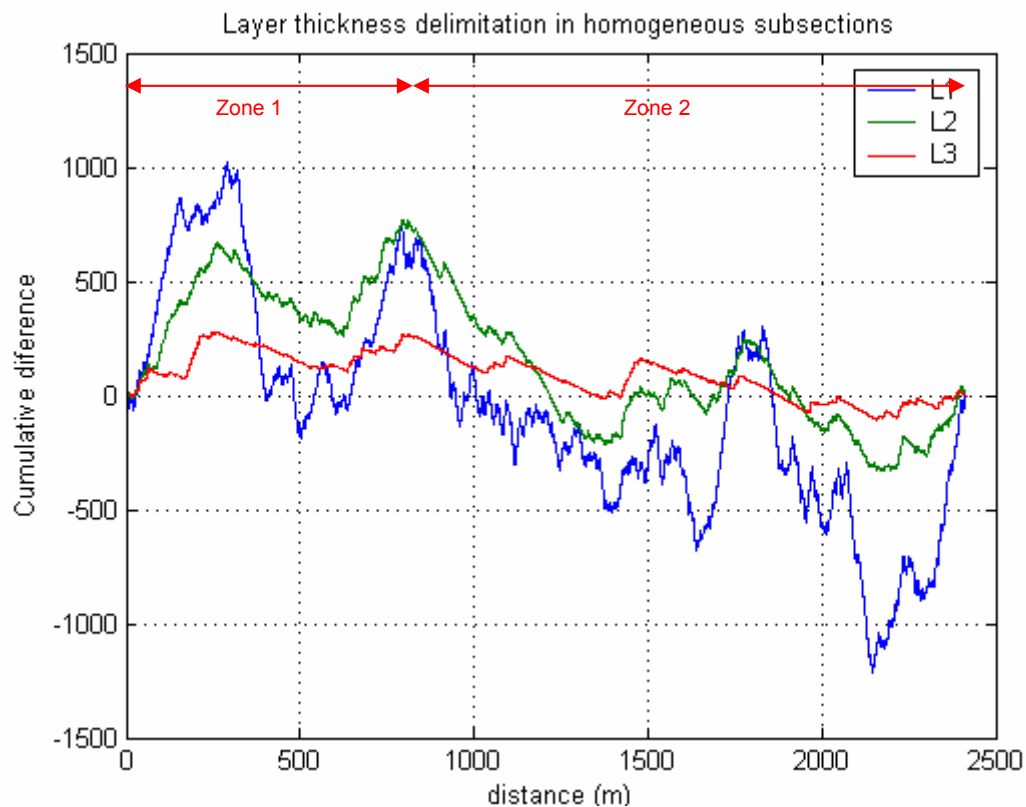
Even if these points are not used for pavement evaluation it is always advisable to analyse them. Peculiar data or lack of information in GPR files usually represents an indicator of local problems, such as layer contamination, excessive moisture content etc. Taking this into

account, the program for pre-processing was developed to provide a list of GRP locations with missing layer thickness information.

The “FWD_GPR” computer program mentioned above has a module that allows for automatic calculation of the cumulative difference, for **division into homogeneous subsections**. Figure 6.4 presents an example of this division applied for layer thickness obtained with GPR.

The program allows for choosing the pavement length to be considered for the division (entire length or only parts) and enables also the testing of statistically difference between consecutive subsections (see 3.5.4).

The program allows for a quick processing and graphic representation for both GPR data and all FWD deflections. (see Figure 6.5)



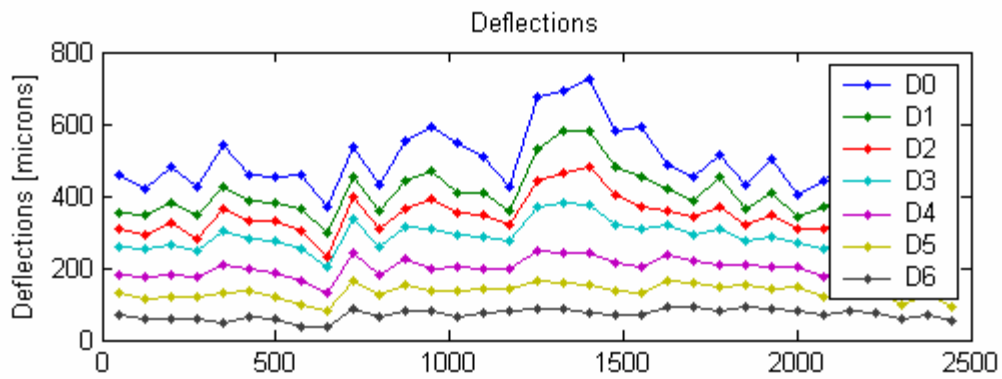
were:

L1 – Layer n° 1 (asphalt layers);

L2 – Layer n° 2 (granular base- 1st layer);

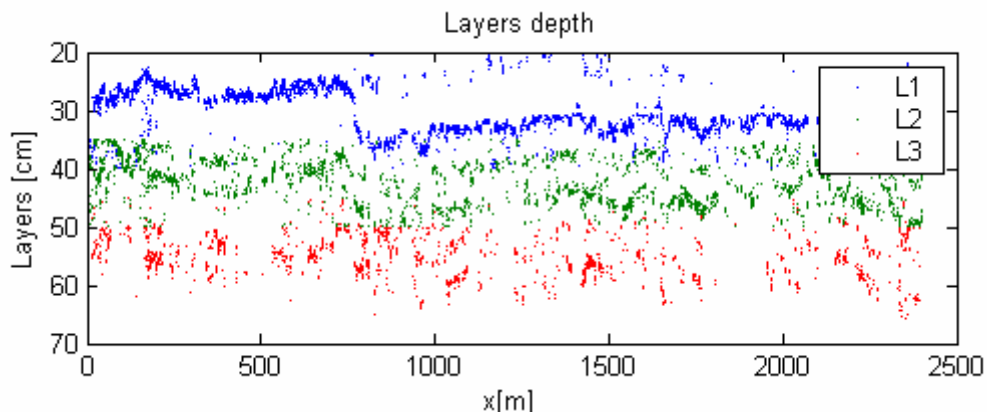
L3 – Layer n° 3 (granular base- 2nd layer);

Figure 6.4 – Cumulative difference of the layer thickness with distance



were:

- D0 to D6 – Deflections at 0 to 1.80 m from the centre of the loaded area.



were:

- L1 – Layer nr°1 bottom (Layer 1/Layer 2 interface depth);
- L2 – Layer n° 2 bottom (Layer 2/Layer 3 interface depth);
- L3 – Layer n° 3 bottom (Layer 3/subgrade interface depth).

Figure 6.5 – Example of FWD and GPR results plot

6.4 Development of an ANN for interpretation of NDT results

6.4.1 Introduction

The main problem related with the backcalculation process is the multi-solution. The solution for a pavement model is not unique, unrealistic values for stiffness moduli can be obtained. The engineering judgement it is always required for analysis the solution obtained.

In order to improve this process, a methodology, which uses neural network algorithms, was developed. In this way, it is possible to include in the interpretation method the engineering judgment contribution by restricting the range of pavement structure parameters. As presented in Chapter 5, when using ANN algorithms a previous training of the network (for the case under study) is required. The response of the ANN depends on the training data, so the results will be within the range considered for training (see 5.7).

The application of ANN algorithm for layer moduli calculation from deflection basins is presented below.

6.4.2 Designing and training an ANN for pavement evaluation

An artificial neural network can be “trained” to determine the corresponding pavement layer moduli from deflection basins, based on a database of FWD test results. The applicability is limited to the range of testing conditions and pavement structures used for training.

For a better comprehension of the ANN application for backanalysis of FWD test results, an example of a training process is presented below (see Figure 6.6). This example refers to structural assessment of three-layered flexible pavement structure on a “rigid” layer.

The first task in neural network training process is to analyse the parameters that interfere in the training database by establishing the following:

- ✓ the variables that can be fixed within the calculation;
- ✓ the types of pavement sections to be considered;
- ✓ the range of pavement layer properties to be included in the training.

The variables considered fixed in this example are: the size of loading plate, the FWD peak load, the layer materials Poisson's ratios and the distance between the deflection sensors in this case at 0, 300, 450, 600, 900, 1200 and 1800 mm.

Figure 6.6 shows the flowchart of the neural network training for backanalysis of FWD test results. The main steps of the training process are the following:

Using the response model selected for the pavement under consideration (generally multi-layer linear elastic model) synthetic deflections (D_i) are calculated for the pavement structure (h_i ; E_i) under study. In this way, data sets of deflections, layer thickness and elastic moduli are obtained. From this database, during training, deflections and layer thicknesses are considered as inputs, while the corresponding elastic moduli represent the target outputs.

As already mentioned, before training all the connections are assigned arbitrary weights (w_i^0), which are "small" random numbers.

In the first phase (*forward propagation*) of training the input signals (D_i and h_i) are propagated through the hidden layer(s) until the output neurons, resulting in a collection of values (E_i^{NN}).

In the second phase the "error" (e_r) is calculated. The error is given by the difference between the "target" outputs (E_i used in the generation of the data sets) and the values calculated in the first phase (E_i^{NN}).

Once the error is known, it is back-propagated during the third phase (*backward propagation*). In this phase, the weights of the connection (w_i) are corrected in order to achieve an improvement of the network response.

This process is repeated as many times as necessary to obtain a satisfactory ANN response.

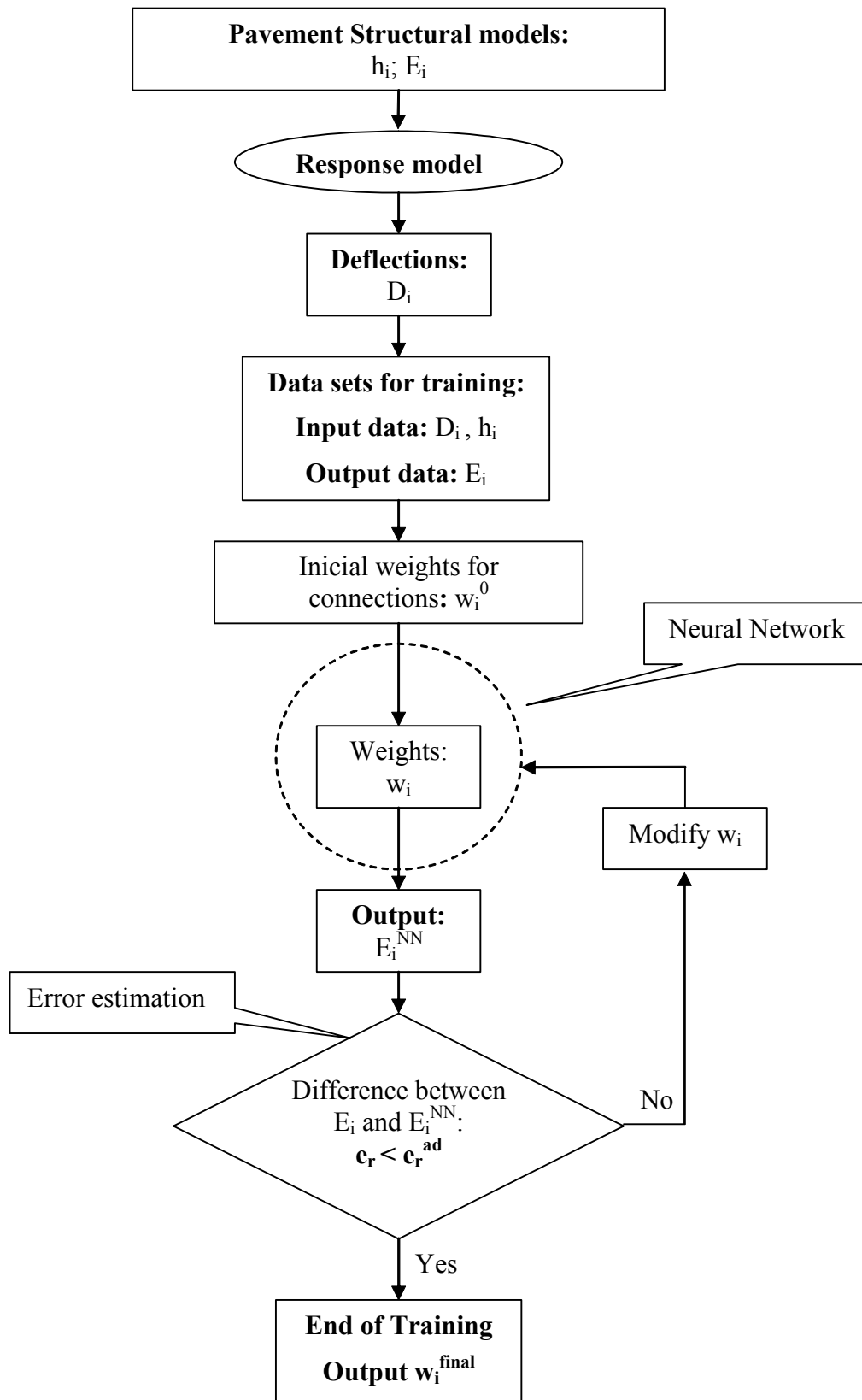


Figure 6.6 – Flowchart of ANN training for backcalculation of FWD test results
[Fontul, S. et al; 2003]

As already mentioned, after the training process is finished, it is convenient to test the ANN, through a process called **validation**. This training validation is generally performed using data within the same range as the training data, but not used during training. Thus, input data (D_i and h_i) from the datasets are used to obtain the E moduli (E_i^{NN}), based on the already trained neural network. Then, these E moduli are compared with those from the datasets ("target moduli"), providing an idea of the network's performance when exposed to new data.

The main aspects that have to be considered when designing an ANN for pavement evaluation, are the following:

- ✓ The parameters that may be fixed within the calculation and the ones that are variable;
- ✓ The type of pavement sections to consider;
- ✓ The type of activation function;
- ✓ The number of cases needed for training;
- ✓ The type and size of ANN structure in order to achieve the optimal balance between the training speed and the "reasoning" of the network;
- ✓ The range of parameters and their increments for the training.

Once trained, the ANN can be used for subsequent evaluations of the same pavement as long as the pavement structure does not change. For example, if the pavement is overlaid it is necessary to perform another ANN training, suitable for the new condition.

A program "Tr_Data" has been developed to generate the synthetic databases needed for training. It was developed in Visual Basic programming language and uses ELSYM 5 as subroutine. This can be adapted for use with any other response model.

The program allows for selecting the limits and the increment for different parameters. The variation of pavement structure parameters has to be made in order to uniformly cover the range of values in use.

The parameters that are variable during this process are the thickness and the stiffness of the pavement layers. The results are the deflections obtained for all these combinations of pavement structures parameters. The deflections database obtained must cover the measured deflections variation.

The range of the parameters must be chosen in accordance to the condition of the pavement in study.

- ✓ For the layer thickness, the distribution obtained during the GPR surveys give the (minimum required) range of variation (see 6.2);
- ✓ The variation of the layer stiffness has to correspond to the type of material and its condition. The information collected in other tests, either in situ or in laboratory and the experience of the engineer should be taken into account when the range of variation is chosen.

It is advisable to widen all the ranges of values for each parameter in order to prevent extrapolations.

A good spreading of the training samples over the problem under study provides better results of the ANN training [Tong, F. and Liu, X.L.; 2004]. Therefore is important to have training data set with small increments (see 6.5.1). This leads to a very large data base to be generated for training, usually over 30 000 data sets for a case study. [Fontul, S. *et al*; 2002a, 2002b, 2003; Antunes, M.L.; *et al*; 2004].

Only part of the database is used (maximum 10 000 datasets in case of Redes 3) in order to avoid the saturation during training. The combinations used for training are randomly chosen within the data obtained previously and they must include the upper and lower limits of the database. This approach has proven to be efficient, enabling a proper training and good ANN results (see 6.5.1).

6.4.3 Use of Redes 3 for backanalysis of FWD test results

The “Redes 3” computer program, developed at LNEC [Marcelino, J.; 1996], is used for training of the backpropagation multilayer neural networks. The main features of the program are described in 5.8.

The training is performed using the database, obtained as described above. During this process, the inputs are the deflections and the corresponding pavement layers thickness. The outputs are the layer elastic moduli.

For the training, the input and the output (sets of data) are both known. During this process the ANN modifies its structure in order to mach as well as possible the target values. Among the options available a “sigmoidal” activation function was chosen for training.

For each case, several neural network architectures have to be studied. The difference between ANNs are either in terms of number of hidden layers and/or in terms of the number of neurons per hidden layers. The purpose is to find the best combination between accuracy and training speed. As already mentioned, the increase in the number of neurons in the hidden layers increases the memory capacity of the network, reducing the training time, but at the same time reduces the capacity to “reasoning” i.e. the capacity to react to data which do not form part of the learning. [Marcelino, J.; 1998].

The training process can be more or less time consuming, depending on issues such as the complexity of the data or the type of the network. During training, “Redes 3” allows for applying of additional techniques to avoid saturation, like, for example “shaking” of structure to ensure that global minima is reached (see 5.8.4).

6.5 Study of ANN performance

6.5.1 Introduction

The ANN performance when applied to structural pavement evaluation was studied. The first task was to study the ANN behaviour to various training databases. From bibliography it is known that a uniform coverage of the data range variation has to be ensured by the datasets used for training. The issue that arose was related with the response of ANN to training, namely if its performance is better when a database uniformly distributed over the range is used or when only a part of a larger data base, randomly selected over the data variation range is used.

A three layered flexible airport pavement structure (asphalt layers + granular layers + subgrade) resting on a “rigid” layer was studied. Synthetic databases were generated for the two situations mentioned above, one with large increments and the other one with small increments for the parameters variation. The ANN structures were identical (9x15x15x3), with two hidden layers of 15 neurons each. The parameters considered fixed were the loading plate diameter, the load and the distance between deflection transducers. The ratio between the elastic moduli of the “rigid” layer (E_4) and the subgrade layer (E_3) was fixed to

$E_4=5x E_3$. The variable parameters were the layer's thickness and moduli. The difference between the two databases is given by the increment of elastic moduli variation, which in the large increment case is 1.5 to 2.5 times more than in small increments case. More details as well as the results obtained are presented in the subchapter 6.5.2.

Once established the better training technique the next task was to study the ANN performance in case of a general application as well as its sensitivity to changes in input, in order to see the influence of having an "erroneous" measurement. For this purpose, two pavement structures were studied: one is a typical road pavement structure and the other one is an airport pavement structure. Both structures are three layered flexible pavements (asphalt layers + granular layers + subgrade) resting on a "rigid" layer. For the airport pavement, a four layered pavement structure was also studied.

In both cases the parameters considered fixed during training are: the loading plate diameter (300 mm for the road case and 450 mm for the airport case), the load (50 kN for the road case and 150 kN for the airport case) and the distance between deflection transducers. Also, the ratio between the elastic moduli of the "rigid" layer (E_4) and the subgrade layer (E_3) was fixed to $E_4=5x E_3$. This relation is usually adopted in LNEC's studies, unless the information available contradicts this hypothesis.

Besides these parameters, two different situations were analysed for both case studies: the consideration of the distance to the "rigid" layer as variable or fixed. In this latter case, two distances to the "rigid" layer were studied.

All ANN trained have the same architecture in terms of hidden layers, 2 hidden layers of 15 neurons each, while the number of inputs and outputs is as follows:

- ✓ for the three layered pavement structure (3L) with fixed distance to the "rigid" layer there are 9 inputs (7 deflections, h_1 , h_2), and 3 outputs (E_1 , E_2 , E_3). The ANN architecture is $9x15x15x3$;
- ✓ for the three layered pavement structure with variable distance to the "rigid" layer there are 9 inputs (7 deflections, h_1 , h_2), and 4 outputs (E_1 , E_2 , E_3 and h_3). The ANN architecture is $9x15x15x4$;
- ✓ for the four layered pavement structure (4L) with fixed distance to the "rigid" layer there are 10 inputs (7 deflections, h_1 , h_2 , h_3), and 4 outputs (E_1 , E_2 , E_3 and E_4). The ANN architecture is $10x15x15x4$:

The parameters considered variable during this study are layer thicknesses h_1 , h_2 , h_3 and layer moduli E_1 , E_2 , E_3 and E_4 (4L). The parameters range of variation considered for each case study is presented below.

In order to study the ANN sensitivity to input variations, the inputs were changed as follows:

- ✓ $\pm 2\%$ - the deflections D_0 , D_3 and D_6 ;
- ✓ $\pm 5\%$ - the thicknesses h_1 , h_2 and $h_3(4L)$.

These variations (2%; 5%) correspond to the manufacturers' specification limits, respectively for deflections measured by the FWD and for thickness given by the GPR.

Variations of $\pm 10\%$ in all inputs were also studied for some of the ANNs in order to see the influence of having an "erroneous" measurement.

More details and the results obtained are presented in 6.5.3.

6.5.2 Sensitivity to training database type

In order to verify the neural network response at different training conditions (small and large increments of each parameter) two different databases were used. These databases have the same range of variation, but the data sets structures were obtained in different ways, as follows:

1. In the first case the variation increment for each parameters is larger, consequently a reduced number of datasets are obtained. The **entire** data base is then used for ANN training;
2. In the second case the variation increment is smaller and consequently the data base obtained is larger. Therefore, due to the limitation related with the maximum number of data sets for training (see 6.4.3), only **part** of this data base is used. The training file includes the limits of range variation of parameters together with other datasets (up to 10 000) randomly chosen within the database previously obtained.

Table 6.1 presents the variable parameter range and the increments considered for both cases presented above.

Table 6.1 – Variable parameters of pavement structure

Parameter	h_1 (m)	E_1 (MPa)	h_2 (m)	E_2 (MPa)	h_3 (m)	E_3 (MPa)
Minimum value	0.25	1000	0.28	200	2.00	80
Maximum value	0.38	6000	0.32	500	3.50	240
Large increments	0.01	2500	0.01	150	0.50	80
Small increments	0.01	1000	0.01	100	0.50	40

In this study, only the increments for elastic moduli were modified (blue shaded cells) while those for thickness variation were maintained.

The two ANN networks trained have the same architecture. The verification of ANN response is made for each of them using data sets within the same range of variation, but different from those used for training. The case studied and their characteristics are presented in Table 6.2,

Table 6.2 – Case studies - characteristics of data used for ANN training

Case	Variations of data in the database	Data sets used for training
1	Large increments	Entire database
2	Small increments	Part of the database (randomly selected)

The results obtained for these three situations are presented in Figure 6.7 charts, where the red line represents the target values, the yellow dots represent the results obtained when the small increment database is used for training and the blue dots represent ANN results when the large increment data base is used for training.

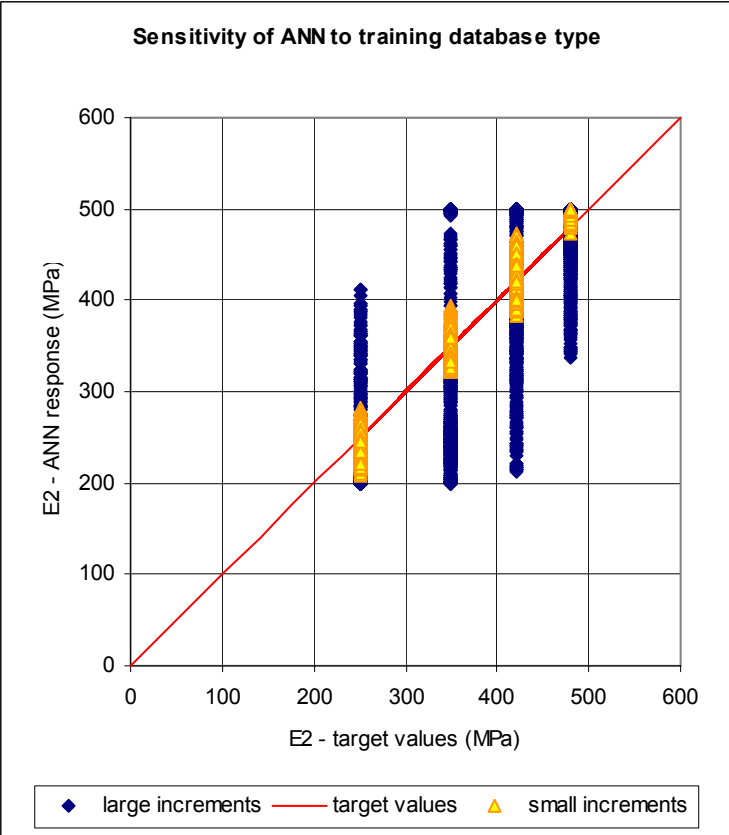
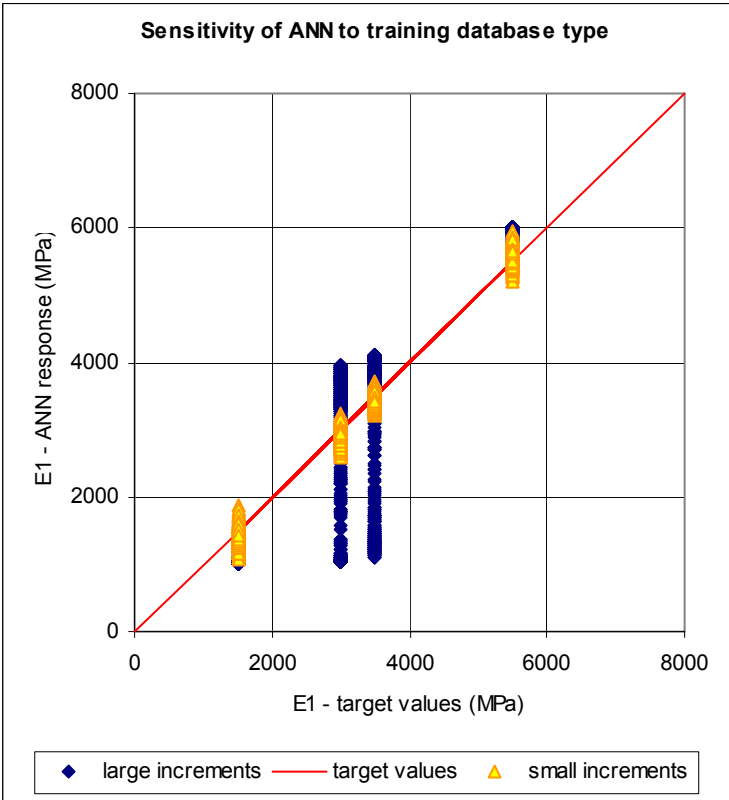


Figure 6.5 a) – ANN sensitivity to training conditions

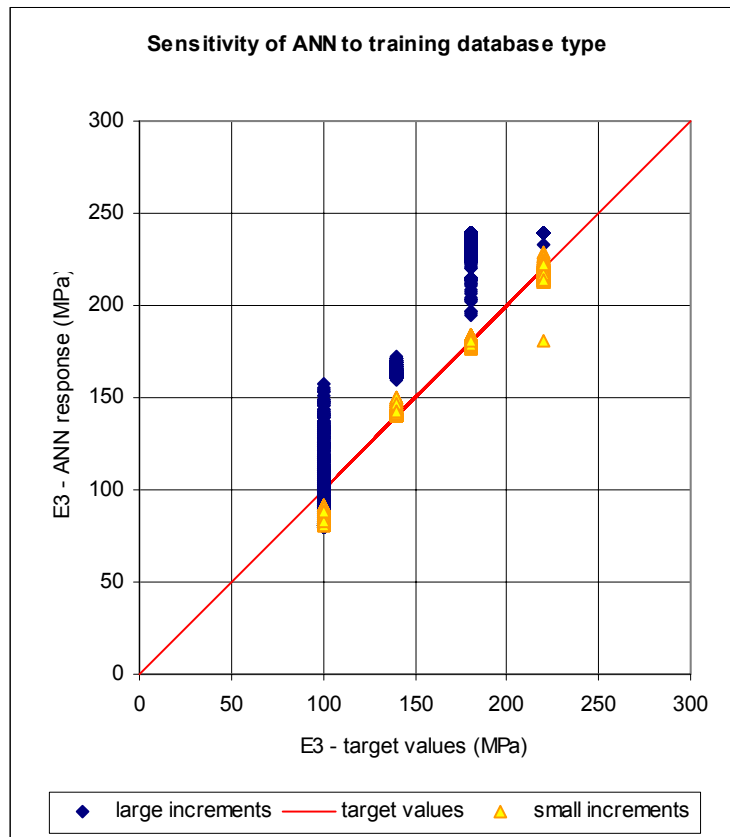


Figure 6.7 b) – ANN sensitivity to training conditions – continuation

As a conclusion from the graphs presented in Figure 6.7, the response of the ANN is much better in case of smaller steps of parameter variation, even though only part of the data base is used for training. This is related with the “reasoning” properties of the neural networks, as they are “taught” with data uniformly spread over the range of answers will develop the ability to better interpolate the results when exposed to data that were not used during training as long as they are within the same range of variation.

The only situation when the reduced data base has good results is when validated with data corresponding to its data base. This raises a recommendation for ANN validation: it is advisable to validate with data different from the database initially produced. In this way, a realistic behaviour of the ANN when exposed to new data is obtained.

A good uniformity (spreading) of training samples is really helpful to enhance the ANNs' generalisation performance. Techniques to better choose the data in order to be representative of the range of parameters to be used for training, are under development nowadays. [Tong, F. and Liu, X.L.; 2004].

6.5.3 Sensitivity to input variation

6.5.3.1 Road pavement

The ranges of variables considered for the road pavement structure (Case A) are presented in Table 6.3, while Table 6.4 presents the range of variation of the deflections obtained using the pavement structures resulting from various combinations of these variables. 22 680 datasets were produced using “Tr_Data” programme from which 8000 were used for training (randomly chosen data together with data corresponding to the range limits) and another 1000 were used for testing the ANN. The ANNs were trained and tested using synthetic data.

Table 6.3 – Variable parameters of pavement structure – range of variation (case A)

Parameter	h_1 (m)	E_1 (MPa)	h_2 (m)	E_2 (MPa)	h_3 (m)	E_3 (MPa)
Minimum value	0.10	1000	0.17	100	0.50	40
Maximum value	0.15	6000	0.23	500	2.00	240
Increment	0.01	1000	0.01	100	0.75	40

Table 6.4 – Deflections obtained – range of variation (case A)

Deflections (μm)	D_0	D_1	D_2	D_3	D_4	D_5	D_6
Minimum value	164	95	63	28	10	6	4
Maximum value	1540	889	621	455	276	182	93

Three ANNs were trained: in the first one (A1) the distance to the “rigid” layer was considered variable (h_3 between 0.50 and 2.00 m); in the other two ANNs (A2 and A3) the distance to the “rigid” layer was fixed to 1.25 m, 2.00 m respectively.

All three ANNs were then tested using data from the database with variable depth to “rigid” layer for response to two situations:

- correct input (D_0 , D_1 , D_2 , D_3 , D_4 , D_5 and D_6 and h_1 , h_2);
- variation in inputs.

The main characteristics of the ANNs and the combinations considered for the sensitivity study in case of road pavement structure are presented in the table below.

Table 6.5 – Road pavement structure – ANNs used in sensitivity study to input variation

Artificial neural network identification	ANN A1	ANN A2	ANN A3
ANN structure	9/15/15/4	9/15/15/3	9/15/15/3
Pavement structure	3L	3L	3L
Trained with datasets that have the distance to the “rigid” layer	variable*	1.25 m	2.00 m
Tested with data sets that have the distance to the “rigid” layer	variable	variable	variable
Variations in inputs			
D_0 ; D_3 and D_6	$\pm 2\%$; $\pm 10\%$	$\pm 2\%$	$\pm 2\%$
h_1 and h_2	$\pm 5\%$; $\pm 10\%$	$\pm 5\%$	$\pm 5\%$

Where:

3L – three layered flexible pavement structure;

4L – four layered flexible pavement structure;

* distance to the “rigid” layer variation range 0.5 m – 2.0 m.

In the graphs below an example of the deviations obtained for output (E1) resulting from the correct input and from variation in inputs of $\pm 2\%$ (D_0 ; D_3 and D_6) and $\pm 5\%$ (h_1 and h_2) for ANN A1 is presented. The analysis of results obtained for all the situations tested is presented in section 6.5.3.3.

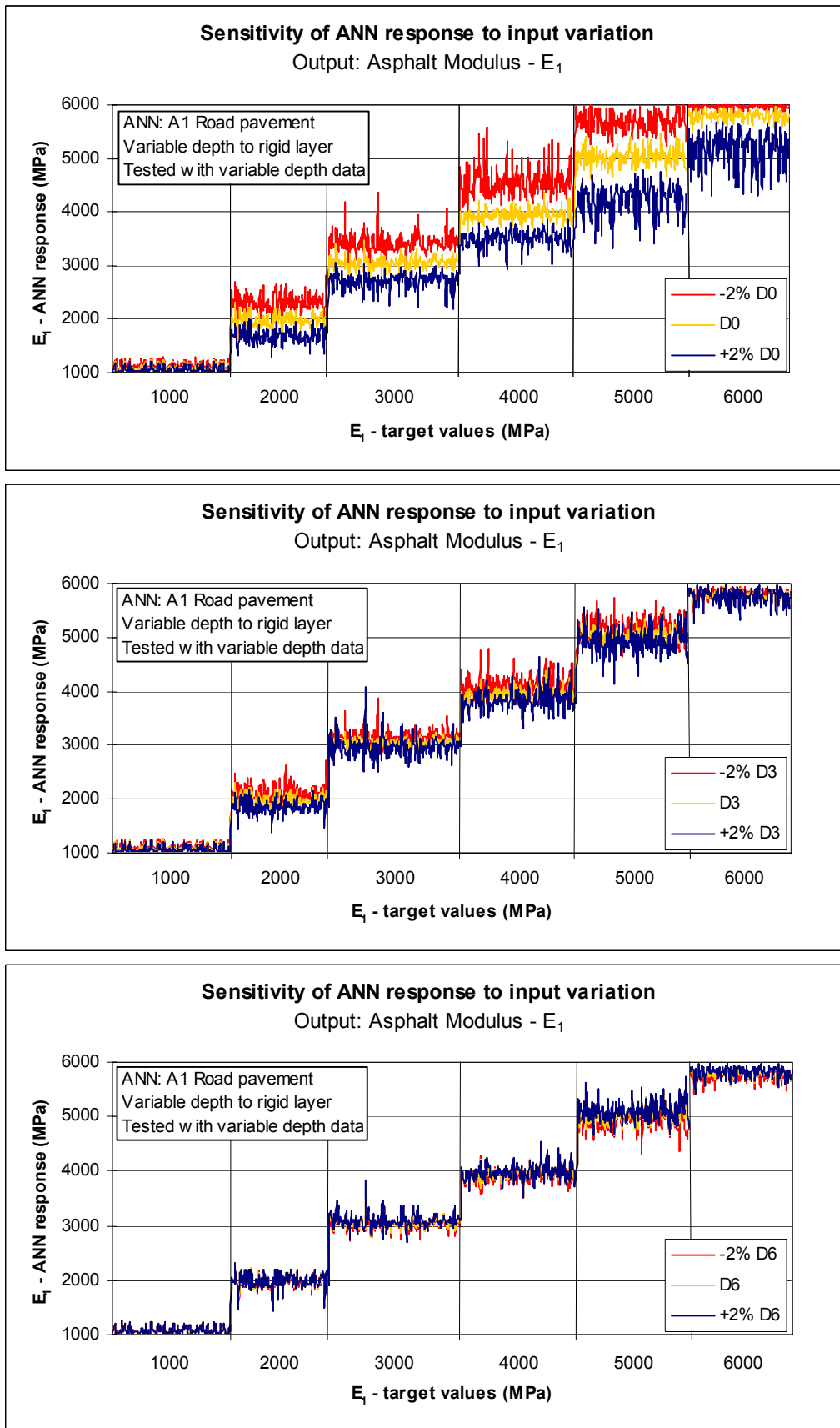


Figure 6.8 a) – Deviation in E_1 – ANN A1: training and testing with variable distance to the “rigid” layer datasets

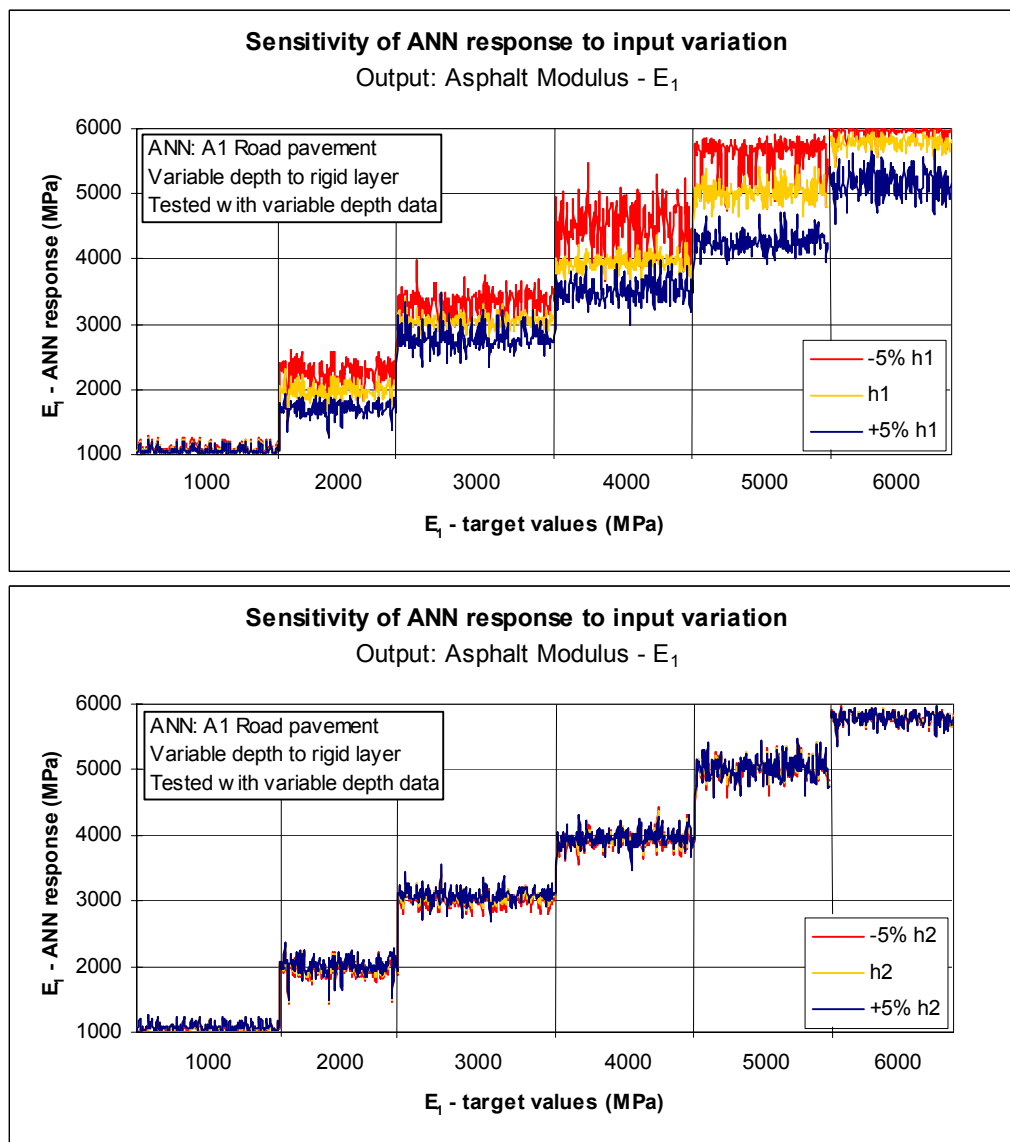


Figure 6.9 b) – Deviation in E_1 – ANN A1: training and testing with variable distance to the “rigid” layer datasets – continuation

6.5.3.2 Airport pavement

Similarly to the road pavement case, the range of variation of parameters and the deflections obtained for Case B, airport pavement structure (3L), are presented in Table 6.6 and Table 6.7, respectively. 80 640 datasets were produced and, like in case A, 8000 of those were used for training and another 1000 datasets were used for testing the ANNs response. In the first one (B1) the distance to the “rigid” layer was considered variable (h_3 between 0.80 and

2.00 m), in the second and third ANNs (B2 and B3) the distance to the “rigid” layer was fixed to 1.20 m and 2.00 m, respectively.

Table 6.6 – Variable parameters of pavement structure (3L) – range of variation (case B)

Parameter	h_1 (m)	E_1 (MPa)	h_2 (m)	E_2 (MPa)	h_3 (m)	E_3 (MPa)
Minimum value	0.22	2000	0.26	100	0.80	40
Maximum value	0.37	8000	0.36	500	2.00	240
Increment	0.01	1000	0.02	100	0.40	40

Table 6.7 – Deflections obtained (3L) – range of variation (case B)

Deflections (μm)	D_0	D_1	D_2	D_3	D_4	D_5	D_6
Minimum value	196	156	134	116	85	43	16
Maximum value	1700	1380	1160	961	646	438	243

Besides these ANNs, a fourth case (B_4) was trained for a four layered airport pavement structure on a “rigid” layer. The second layer from the surface is a bituminous macadam layer, of approximately 100 mm thick, with very low binder content. This type of material was used in airport pavement construction until the 70’s. Its characteristics are very different, when compared with asphalt or granular material layers, and therefore it was considered as a separate layer in the pavement model. In this case, the distance to the “rigid” layer was fixed (1.20 m). The parameters range and the deflections obtained for four layered airport pavement structure (4L) are presented in Table 6.8 and, Table 6.9, respectively. 270 000 datasets were produced, 8000 of those were used for ANN training and another 1000 for ANN testing.

Table 6.8 – Variable parameters of pavement structure (4L) – range of variation (case B)

Parameter	h_1 (m)	E_1 (MPa)	h_2 (m)	E_2 (MPa)	h_3 (m)	E_3 (MPa)	h_4 (m)	E_4 (MPa)
Minimum value	0.14	3000	0.08	500	0.26	100	0.80	40
Maximum value	0.25	8000	0.12	2500	0.34	500	2.00	240
Increment	0.01	1000	0.01	500	0.02	100	0.40	40

Table 6.9 – Deflections obtained (4L) – range of variation (case B)

Deflections (μm)	D ₀	D ₁	D ₂	D ₃	D ₄	D ₅	D ₆
Minimum value	244	197	167	142	101	50	18
Maximum value	1880	1500	1220	991	646	437	243

Similarly to the previous cases, ANN characteristics and various combinations used in the sensitivity study are presented in Table 6.10.

Table 6.10 – Airport pavement structure – ANNs used in sensitivity study to input variation

Artificial neural network identification	ANN B1	ANN B2	ANN B3	ANN B4
ANN structure	9/15/15/4	9/15/15/3	9/15/15/3	10/15/15/3
Pavement structure	3L	3L	3L	4L
Trained with datasets that have the distance to the “rigid” layer	variable*	1.20 m	2.00 m	1.20 m
Tested with data sets that have the distance to the “rigid” layer	variable	variable or fixed at 1.20m	variable	1.20 m
Variations in inputs				
D ₀ ;D ₃ and D ₆	±2%; ±10%	±2%; ±10%	±2%	±2%
h ₁ ;h ₂ and h ₃ (4L)	±5%; ±10%	±5%; ±10%	±5%	±5%

Where:

3L – three layered flexible pavement structure;

4L – four layered flexible pavement structure;

* distance to the “rigid” layer variation range 0.8 m – 2.0 m.

An example of the results obtained for E1 in case of ANN B2 is presented in Figure 6.9. The ANN B2 was trained and tested with fixed distance to the “rigid” layer datasets, aiming at studying the network performance when the distance to the “rigid” layer is known.

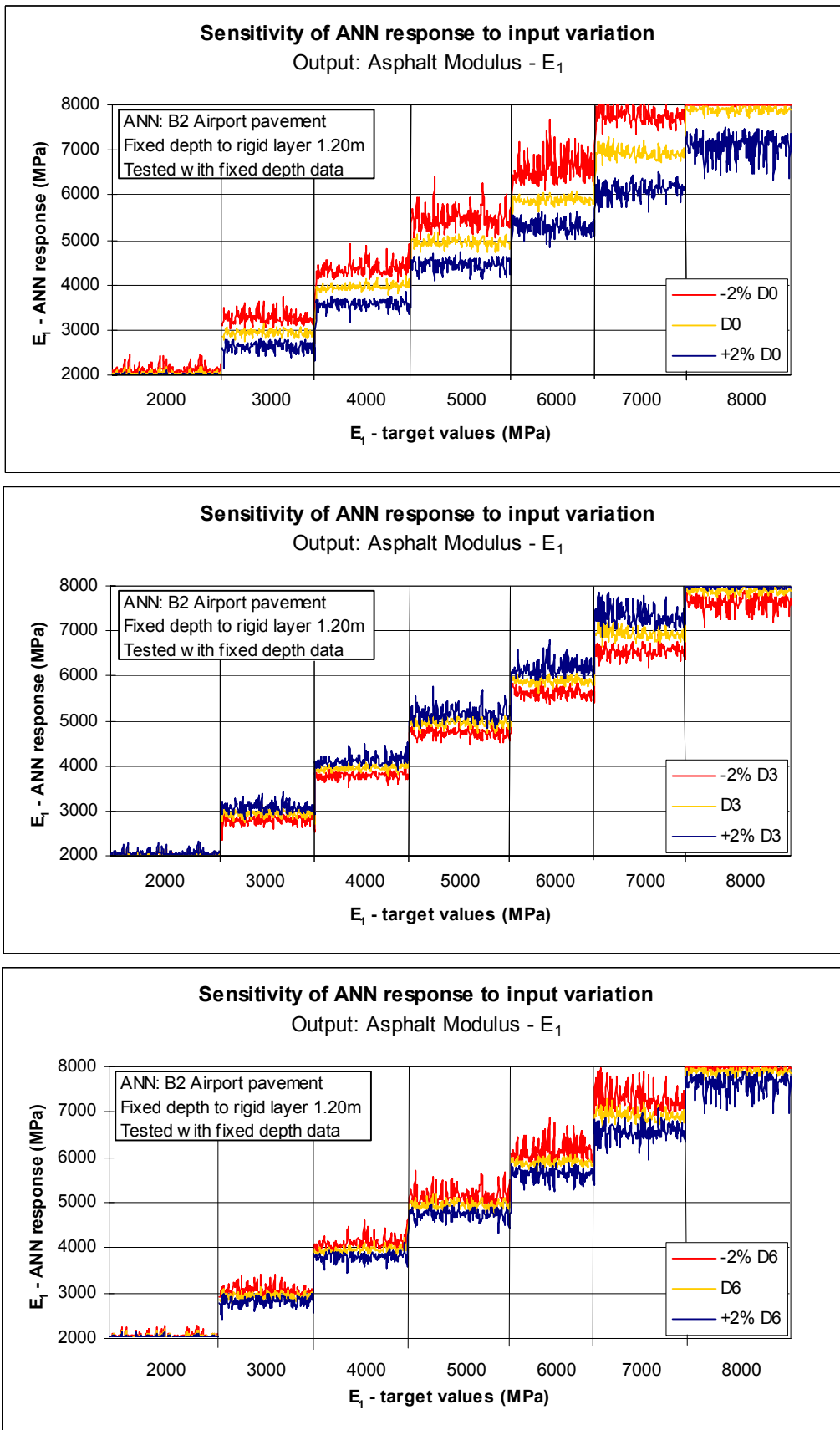


Figure 6.9 a) – Deviation in E_1 – ANN B2: training and testing with fixed distance to the “rigid” layer datasets

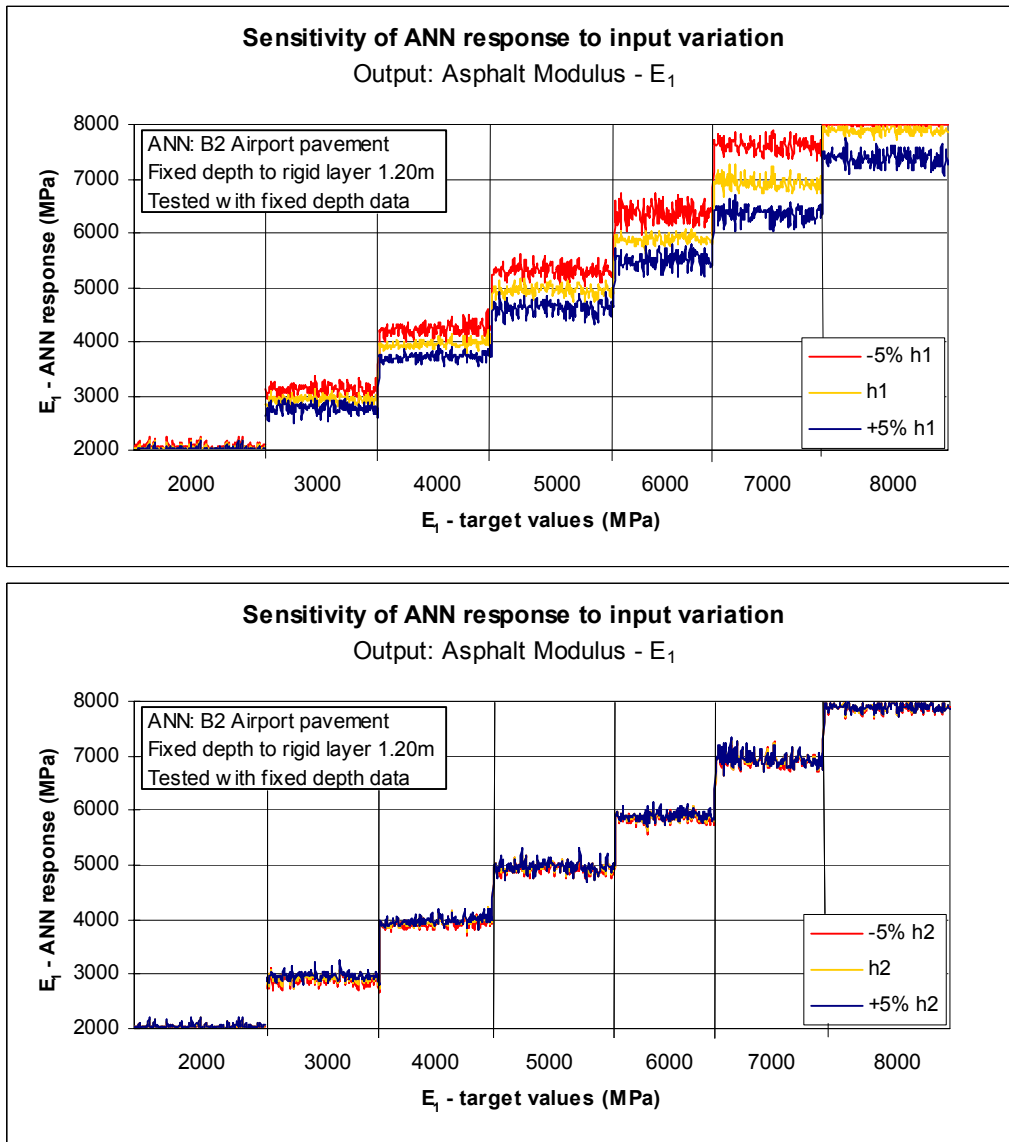


Figure 6.7 b) – Deviation in E₁ – ANN B2: training and testing with fixed distance to the “rigid” layer datasets – continuation

6.5.3.3 Analysis of results

In order to evaluate the ANN performance the average difference (E_r) between the target values (v_t) and the ANN response (v_{ANN}) was calculated using the following equation:

$$E_r = \frac{1}{n} \sum_{i=1}^n \left(\frac{|v_t - v_{ANN}|}{v_t} \right) \quad (6.1)$$

The results obtained for all cases (no variation and variation in inputs) are presented in Annex 1.

Tables 6.11 to 6.14 present a summary of the results obtained for the average differences between target values and ANN response, which are classified in low ($E_r \leq 10\%$), medium ($10\% < E_r < 25\%$) and high ($E_r \geq 25\%$). Deviations in moduli below 10% are considered to be acceptable for pavement structural evaluation purposes. [Antunes, M.L.; 1993].

Table 6.11 – Road pavement structure – ANN sensitivity to input variation

Output		E ₁	E ₁	E ₁	E ₂	E ₂	E ₂	E ₃	E ₃	E ₃
ANN		A1	A2	A3	A1	A2	A3	A1	A2	A3
all	0%	L	M	M	L	M	M	L	M	H
D ₀	±2%	M	M	M	L	M	H	L	M	H
D ₃	±2%	L	M	M	L	M	H	L	M	H
D ₆	±2%	L	M	M	L	M	H	L	M	H
h ₁	±5%	M	M	H	L	M	H	L	M	H
h ₂	±5%	L	M	M	L	M	H	L	M	H
D ₀	±10%	H			H			M		
D ₃	±10%	M			H			H		
D ₆	±10%	L			L			M		
h ₁	±10%	M			L			L		
h ₂	±10%	L			L			L		

Where:

A1, A2, A3 – ANN identification see Table 6.5;

L, M and H – average difference between the target value and the ANN response:

L $E_r \leq 10\%$,
 M $10\% < E_r < 25\%$ and
 H $E_r \geq 25\%$.

Table 6.12 – Airport pavement structure 3L – ANN sensitivity to input variation

Output		E ₁	E ₁	E ₁	E ₂	E ₂	E ₂	E ₃	E ₃	E ₃
ANN		B1	B2	B3	B1	B2	B3	B1	B2	B3
all	0%	L	L	L	L	M	M	L	M	M
D ₀	±2%	M	L	L	M	M	M	L	M	M
D ₃	±2%	L	L	L	M	M	M	L	M	M
D ₆	±2%	L	L	L	L	M	M	L	M	M
h ₁	±5%	L	L	L	M	M	M	L	M	M
h ₂	±5%	L	L	L	L	M	M	L	M	M
D ₀	±10%	H			H			H		
D ₃	±10%	M			H			H		
D ₆	±10%	M			M			M		
h ₁	±10%	L			H			L		
h ₂	±10%	L			L			L		

B1, B2, B3 – ANN identification see Table 6.10;

L, M and H – average difference between the target value and the ANN response:

L $E_r \leq 10\%$, M $10\% < E_r < 25\%$ and H $E_r \geq 25\%$.

Table 6.13 – Airport pavement structure 4L, fixed distance to the “rigid” layer – ANN sensitivity to input variation

Output		E ₁	E ₂	E ₃	E ₄
ANN		B4	B4	B4	B4
all	0%	L	L	L	L
D ₀	±2%	H	H	L	L
D ₃	±2%	L	M	M	L
D ₆	±2%	L	H	L	L
h ₁	±5%	L	M	L	L
h ₂	±5%	L	L	L	L
h ₃	±5%	L	L	L	L

Same key as in Table 6.12.

Table 6.14 – Airport pavement structure 3L, fixed distance to the “rigid” layer – ANN sensitivity to input variation-results

Output		E ₁	E ₂	E ₃
ANN		B2	B2	B2
all	0%	L	L	L
D ₀	±2%	L	M	L
D ₃	±2%	L	M	L
D ₆	±2%	L	M	L
h ₁	±5%	L	M	L
h ₂	±5%	L	L	L
D ₀	±10%	H	H	L
D ₃	±10%	M	H	M
D ₆	±10%	M	H	L
h ₁	±10%	M	M	L
h ₂	±10%	L	M	L

Same key as in Table 6.12.

From the studies performed, the following considerations can be drawn:

ANN performance in case of general application, no variation in inputs (yellow line in graphs):

1. Whenever the distance to the “rigid” layer is known it should be used, as its use improves the ANN response (see Table 6.14). The errors in outputs E1 and E3 were reduced from 4% to 2% in case of training and testing with fixed distance to the “rigid” layer data. Errors in E2 remained the same, as the pavement response is less sensitive to granular layer characteristics (see also 3).
2. If the distance to the “rigid” layer is unknown, the ANN should be trained with variable distance to the “rigid” layer, as it has a better performance (e.g. see results of A1 compared with A2 or A3 in Table 6.11). The cases when the ANN behaved worse (errors above 10%) was when a ANN trained with fixed distance was tested with variable distance data.
3. Variations in granular layer moduli (E2) are higher in the case of airport pavement, due to the fact that in a pavement structure with thick bituminous layers the influence

of the granular layer in the pavement's response is lower, so the same deflection bowl can be obtained for a wider range of granular layer moduli (see Figure 6.10).

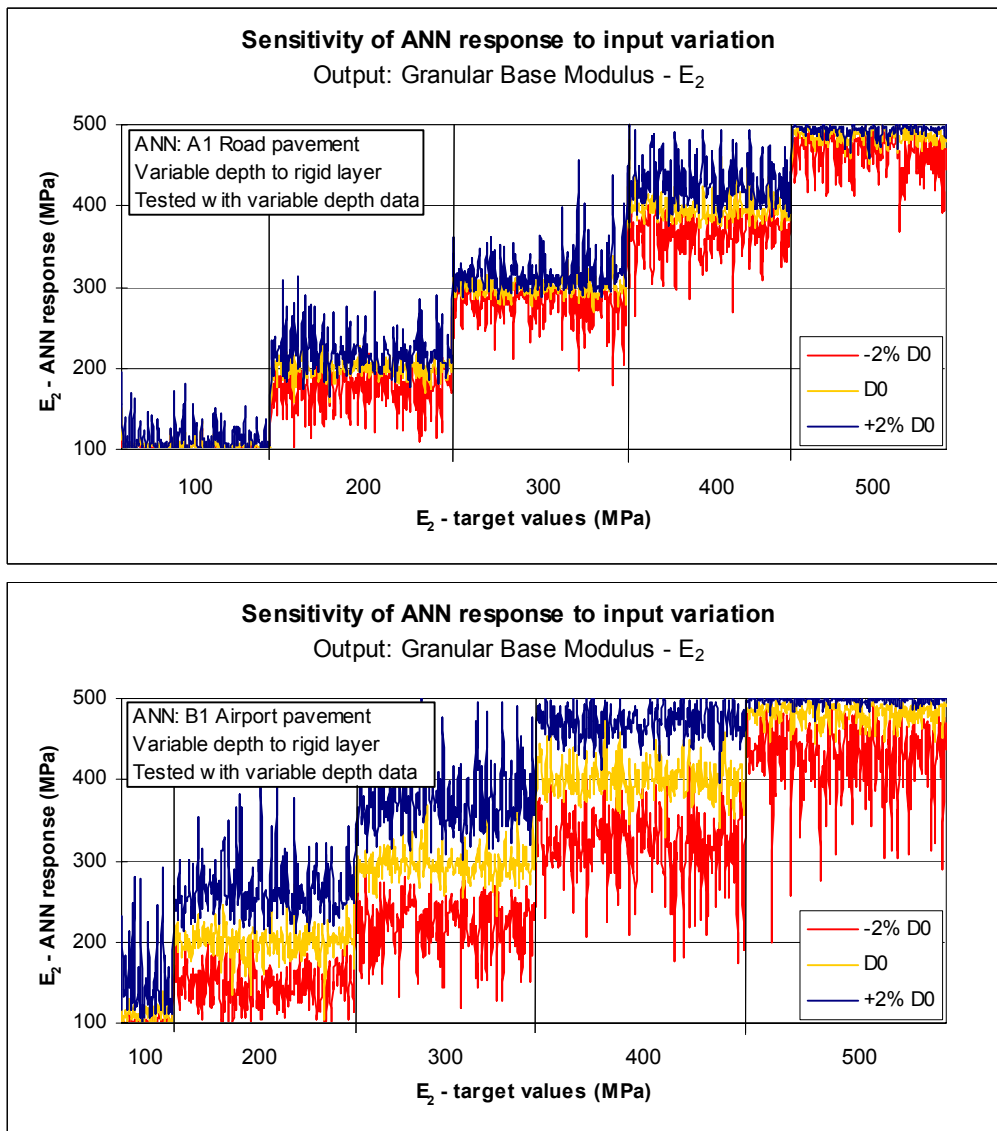


Figure 6.10 – E₂ deviation in road pavement case (above) and airport pavement (below)

- Deviations on E₃, are very low (below 4%) and ignorable (2%) in case of fixed distance to the “rigid” layer testing (see Figure 6.11).

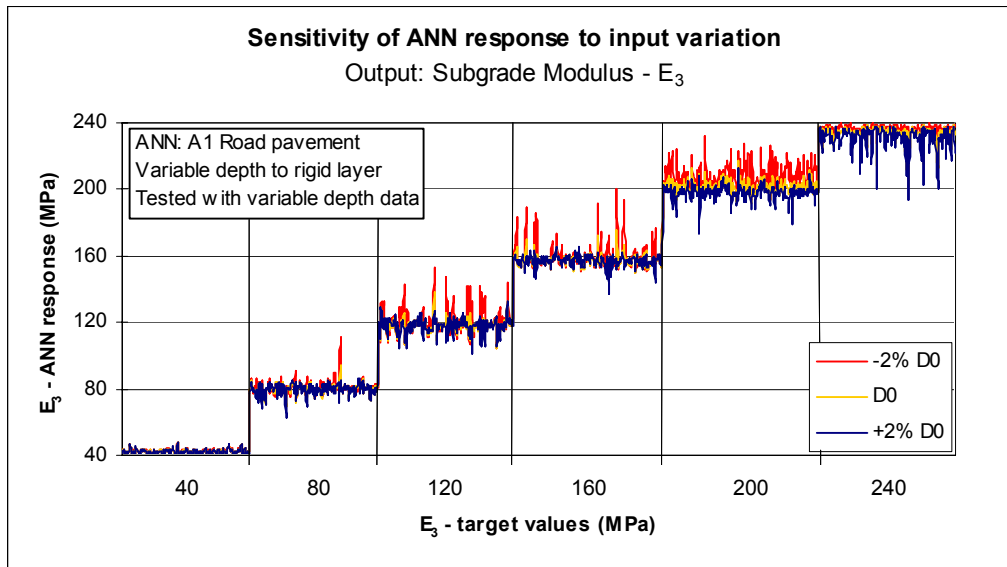


Figure 6.11 – Example of deviation in E3 – A1

5. In case of four layered airport pavement structure (B4), due to the large number of datasets obtained through the combinations of pavement structures (270 000 datasets) and taking into account that only 2% of them were used for training, the ANN convergence is more difficult. Consequently, the training error is higher and therefore localised peaks of erroneous results appear in ANN response (mainly in E3 and E4). Figure 6.12 presents an example of this phenomenon. These peaks are easy to identify and eliminate in pavement structural evaluation process. The engineering judgement is called once more to improve the analysis of results and filter the “unnatural” data.

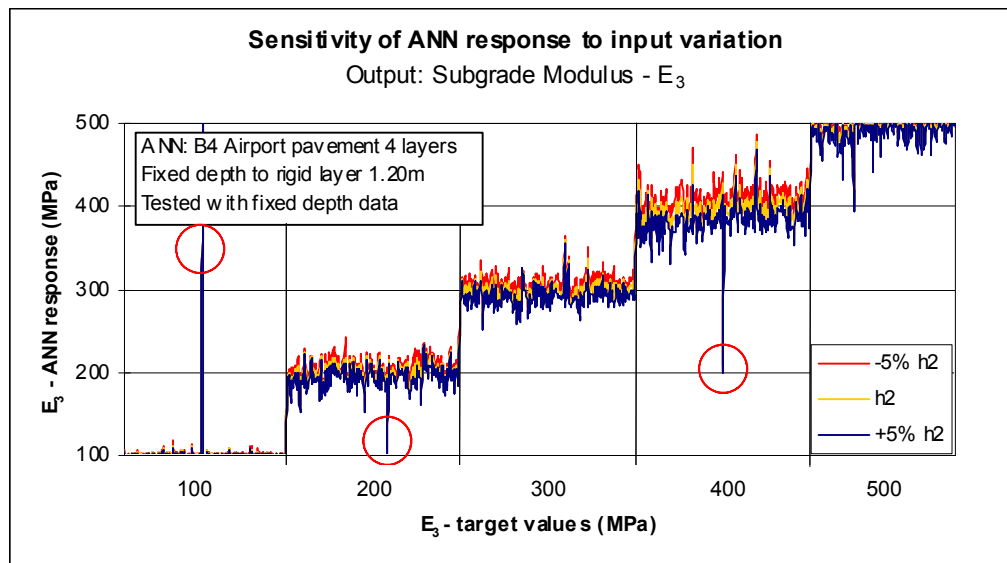


Figure 6.12 – Example of localised erroneous ANN B4 response

ANN performance in case of erroneous inputs:

- Sometimes, the deviation in outputs is distributed over the same range for negative and positive variation in inputs (see Figure 6.13). This aspect occurs mainly in case of ANN trained with fixed distance to the “rigid” layer and tested with variable distance data and in general for all ANNs in case of small deviations in outputs.

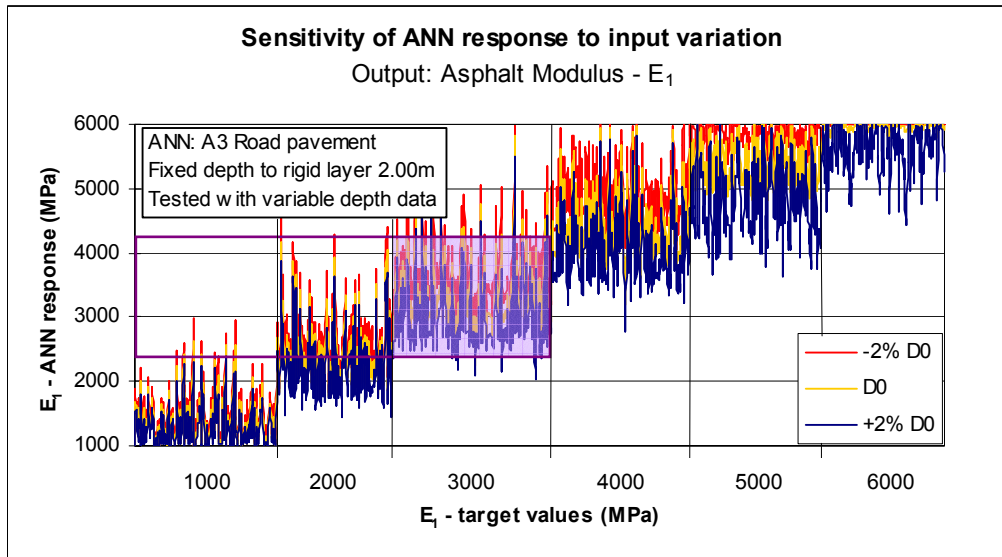


Figure 6.13 – Example of ANN response distributed over the same range for negative and positive variation of inputs

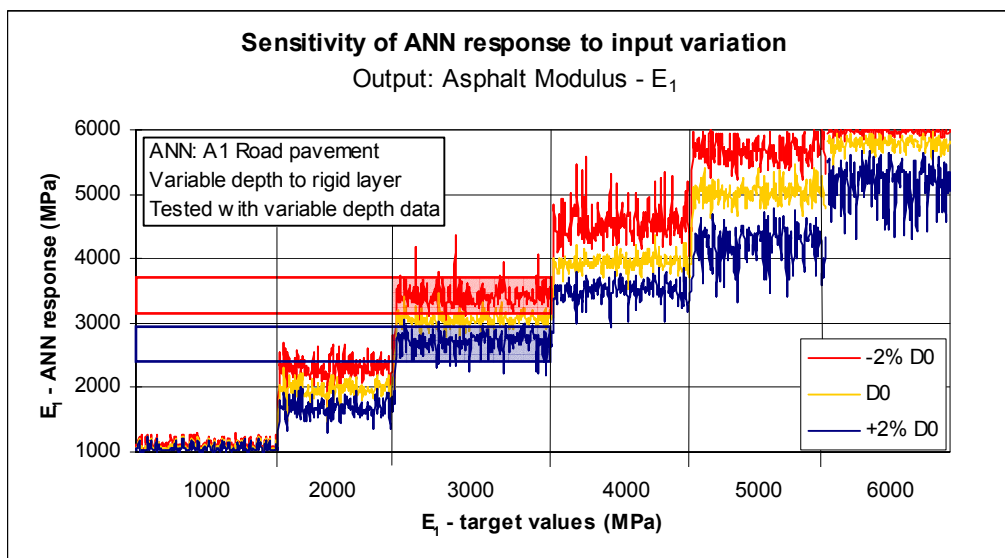


Figure 6.14 – Example of ANN response distributed over distinct ranges for negative and positive variation of inputs

7. For variations of 2% in deflections, within the manufacturers specified limits, the deviation in the outputs are acceptable (generally below 12%, the only exception is once again E2 with a maximum error of 21%). Variations of 10% in deflections may have a significant impact (sometimes over 50%) on the outputs (see Figure 6.15). The results obtained in this study have shown that the ANN response is not insensitive to variations in one of the inputs, thus contradicting some authors that stat that “a network’s response can be, to a degree, insensitive to minor variations in its inputs” [Wasserman, P.D.; 1989].

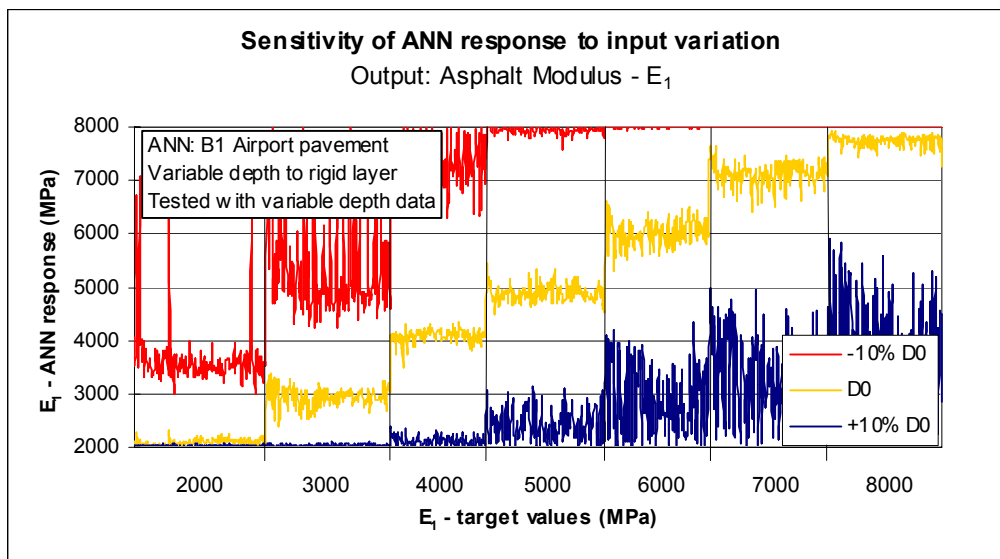


Figure 6.15 – Example of deviation in E1 with 10% variation in D0 – ANN B1

8. Changes in asphalt layer thickness of 5 to 10% have small to moderate influence while changes of 10% in granular layer thickness have almost no influence in the ANN response (see Figure 6.16). Therefore, errors in layer thickness of GPR equipment (which in case of horn antennas are below 5%) can be considered insignificant, as they do not have a big impact on the ANN behaviour.

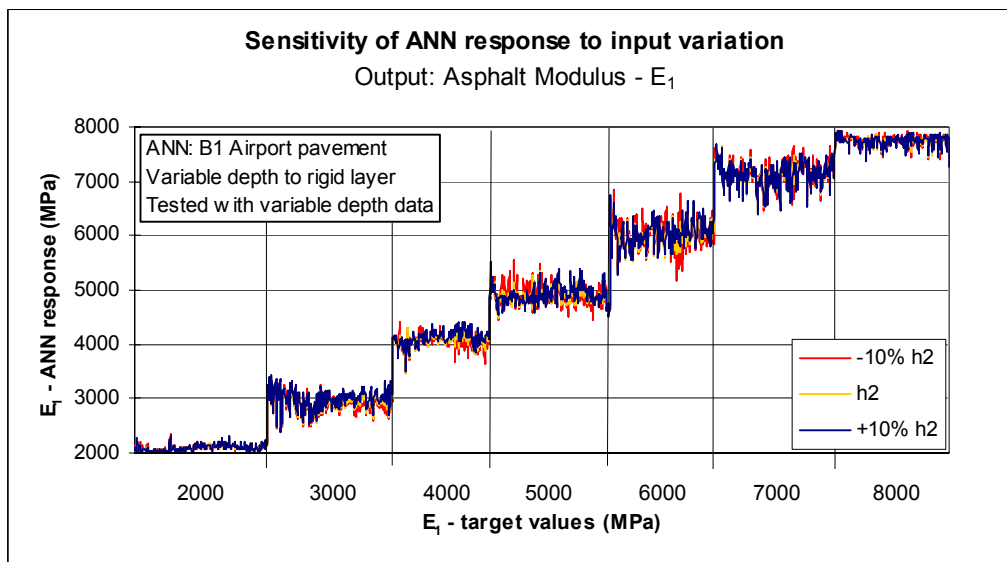
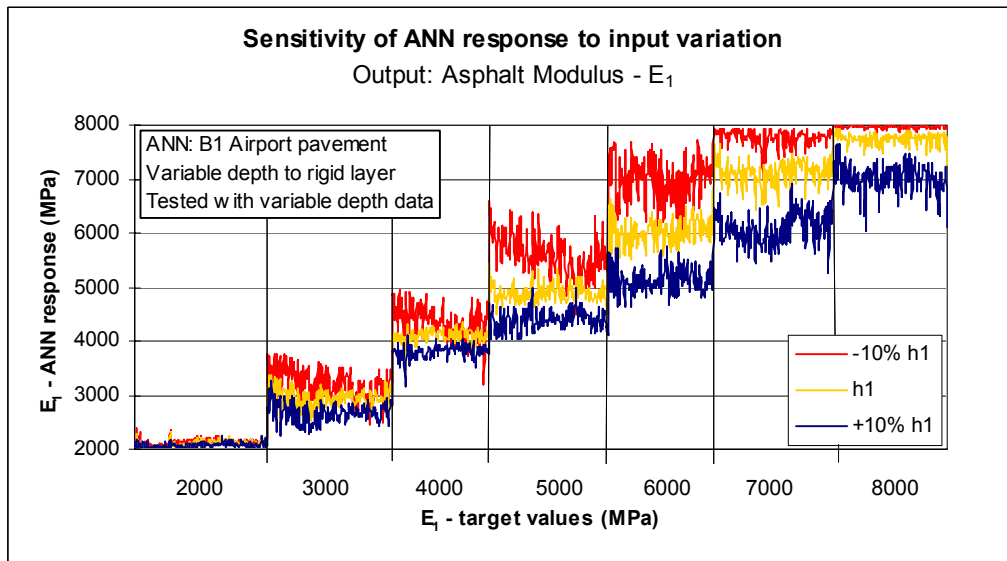


Figure 6.16 – Example of deviation in E_1 with 10% variation in thickness – ANN B1

6.6 Summary

This chapter presents a method for structural pavement evaluation, which makes use of GPR data combined with FWD test results. The interpretation of FWD test results is performed in each test point using Artificial Neural Networks (ANNs). The average layer thickness determined with GPR around the FWD test point (5 m) is used for the interpretation. A computer program “FWD_GPR” has been developed for the purpose of processing GPR data and combine it with FWD test results.

An ANN is designed to determine the corresponding pavement layer moduli from deflection basins, based on a database of FWD tests and GPR layer thickness results. The computer program “Redes 3” has been used for the ANN calculation.

Before using the ANN for pavement evaluation, it must be “trained”. Synthetic data are used during this process. A program “Tr_Data” has been developed to generate the entire database needed for training an ANN for solving backcalculation problems. It was developed in Visual Basic and uses ELSYM 5 as subroutine. This program allows for selecting the limits and the increment for different parameters. The variation of pavement structure parameters has to be made in order to uniformly cover the range of values in use.

Generally, the limits chosen for the database used during training of neural network are wider than those expected for the pavement section or obtained from GPR tests in order to avoid any extrapolation of the ANN. The same neural network can be later used for data interpretation of future tests, as long as the pavement structure does not suffer any modifications.

A good spreading of training samples over the full range of variation is really helpful to enhance the ANNs' generalization performance. The response of ANN is much better in case of smaller steps of parameter variation (used to create the training database), even though only part of the data are used for training.

The ANN performance is improved by the use of a fixed distance to the “rigid” layer, if this information is available. If the distance to the “rigid” layer is unknown, the ANN should be trained with variable distance to the “rigid” layer, as it has a better performance.

The sensitivity of the proposed method to variations in the pavement thickness or to variation in deflections was addressed. The ANN was tested for two types of pavement structures: one which is a typical road pavement structure and the other one an airport pavement structure.

From this study it can be concluded that for variation of inputs within the manufacturers specified limits (2% for deflections and 5% for thickness), the deviations in outputs are acceptable. On the other hand, 10% variations of inputs may have a significant impact on the outputs. Changes in thickness have limited influence in the ANN response.

The use of artificial neural networks in backanalysis of FWD test results presents important advantages. Although training of an ANN is somewhat time consuming, once this is done for a specific pavement structure, it allows for a drastic reduction in computation time and an efficient interpretation of all FWD test results, using thickness obtained with GPR. Since the answer is derived from the data used in the training, it is possible to include some engineering judgment in the processing by limiting the range of pavement structure parameters. However, the applicability of ANN is restricted to the range of testing conditions and pavement structures used for training.

7 Application of the proposed methodology to an airport pavement

7.1 Introduction

For a better understanding of the application of the proposed methodology to pavement evaluation, a case study of a runway pavement evaluation is presented.

The runway pavement was built in 1965 and is 2400 m long and 45 m wide. Since construction the initial structure has suffered two major rehabilitations in 1980 and 1990 as well as several local repairs.

The actual pavement has the following structure (Figure 7.1) above the subgrade:

- ✓ 0.30 m – unbound aggregate;
- ✓ 0.10 m – bituminous macadam;
- ✓ 0.05 m – asphalt layer (the initial surface layer);
- ✓ 0.06 m – asphalt layer, (overlaid in 1980);
- ✓ 0.07 m – asphalt layer between 0 and 700 m^{*}, (overlaid in 1990);
- ✓ 0.12 m – asphalt layer between 700 and 2400 m^{*}, (overlaid in 1990).

^{*} All the references are made taking into account the direction 10-28



Figure 7.1 – Pavement structure sketch

The field tests analysed here were performed in December 1999. The testing programme for structural evaluation of the pavement consisted of the following:

1. Visual survey ;
2. FWD tests;
3. Layer thickness assessment (GPR tests and core extraction);

The work performed by LNEC also included the collection of background information, the interpretation of results and the ACN/PCN classification and rehabilitation design.

7.2 Background information

7.2.1 Historical information

Since 1965, when it was built, the runway pavement was the subject of two main rehabilitations, as already mentioned above. Several studies for pavement structural evaluation and surface characterisation have been performed by LNEC since 1985. [Mogas; J. and Pinelo, A.; 1986; Antunes, M.L.; 1989, 1992, 1999; Antunes, M.L. and Fontul, S.;2000, 2002].

These studies provide, together with the construction records, valuable information on pavement geometry, maintenance actions already undertaken on the runway, material characteristics (soils, granular and bituminous materials).

The information regarding the pavement foundation taken from the construction records, was the following:

Table 7.1 – Pavement foundation characteristics

Distance to the runway end 10	Foundation	Type of subgrade soil*
0 – 700 m	Cut	Sandy soil (0.5 to 2.0 m thick) Sandy clay (0.5 to 1.5 m thick)
700 – 2400 m	Fill (small heights)	Clayey soil (red clays and sand)

* top to bottom

During the previous studies, besides the FWD tests and visual surveys, complementary and laboratory tests were also performed on the materials extracted *in situ* (cores and test pits). A summary of these data is presented in section 7.2.3.

7.2.2 Pavement condition assessment

During this study, a detailed visual survey was undertaken for the assessment of the pavement condition. The pavement had longitudinal cracks in almost all its extension, with some areas of alligator cracking and potholes. The construction joints were also in bad condition. There were also some localised areas on the runway that had been already repaired. Some of the surface defects are shown in Figure 7.2.

It should be stressed that the deterioration observed in the pavement was restricted to the surface layer. This conclusion was made after coring of the asphalt layers. The pavement condition had to be considered during the structural evaluation, due to the existence of cracks, that can affect the radar records. The moduli assumed for the asphalt layers during backcalculation can also reflect this surface condition. On the other hand, if rehabilitation is required, milling of the pavement surface must be considered.



Figure 7.2 – Pavement surface condition: longitudinal joint (left) and pothole (right)

7.2.3 Complementary tests

The complementary tests presented in this section were performed in previous studies [Antunes, M.L.; 1989, 1992]. The test pits excavated and the cores extracted provided, besides the information on layer thickness, the material samples to be characterised in the laboratory. The tests performed and the main results are presented herein:

Subgrade:

- ✓ *in situ* density $\gamma_d = 2.05 \text{ g/cm}^3$;
- ✓ *in situ* water content $\omega_o = 5.8\%$;
- ✓ soil type: A-2-7; plasticity limits: LL=43%, IP=23%;

Bituminous mixtures

- ✓ composition, aggregate grading and recovered bitumen characterisation (see Table 7.2 and Table 7.3).

Table 7.2 – Aggregate grading of bituminous mixtures

	D_{max}	% passed on n°200 sieve
	mm	%
AC (1980)	19.1	4.5-5
AC (1965)	25.4	4-5
BM (1965)	38.1	1-2

Where:

- AC – asphalt layers;
- BM – bituminous macadam;
- D_{max} – maximum aggregate size.

Table 7.3 – Bituminous mix composition and recovered bitumen characteristics

	Y_{ap}	T_b	V_b^*	V_v^*	V_a^*	Pen(25°)	Softening point
	g/cm ³	%	%	%	%		°C
AC (1990)	2.32-2.34	4.7-5.2	-	-	-	24	-
AC (1980)	2.28-2.36	5.4-5.9	13	6	81	17	71.4
AC (1965)	2.31-2.43	4.2-4.8	10	5	85	25	64.1
BM (1965)	2.31-2.39	2.8-3.1	6	7	87	20	66.5

* average values.

Where:

- Y_{ap} - bulk density ;
- T_b – binder content percent by mass of dry aggregate;
- V_b – volume of binder;
- V_v – volume of air voids;
- V_a – volume of aggregate;
- Pen(25°) – bitumen penetration at 25°C;
- AC – asphalt layers;
- BM – bituminous macadam.

The values presented in Table 7.3 show low penetrations values and high softening points, which indicate some bitumen hardening due to ageing, taking into account that the bitumen used was a 60/70 penetration grade [Antunes, M.L.; 1989].

As a particularity of this pavement structure it should be mentioned that the bituminous macadam presents a very low bitumen content (see Table 7.2). This type of material is not used anymore in pavement construction.

7.2.4 Traffic information

Table 7.4 presents the main aircraft movements that were performed on the runway since the last rehabilitation. The traffic data is given per airplane type, together with the main characteristics of the airplanes.

Table 7.4 – Traffic information (1990 – 1999)

Aircraft	Max take-off weight (kN)	Wheel arrangement	Load on each tire (kN)	Tire pressure (MPa)	Total number of movements (1990-1999)
B727	243	D	178	1,15	2173
B737	769	D	183	1,47	113349
A320	735	D	173	1,28	41851
A319	627	D	149	1,38	1500
E145	201	D	45	0,96	1270
M80	622	D	148	1,17	23573
F100	447	D	107	0,98	17783
BA 146-100	406	D	96	0,88	2234
MD-DC9	658	D	157	1,24	1909
F28	295	D	68	0,69	1881
B757	1205	DT	139	1,35	41273
A300	1539	DT	179	1,08	7062
B767	1387	DT	155	1,26	6025
A310	1500	DT	176	1,42	7370
L-1011	2214	DT	256	1,27	6627
MD-DC10	2690	COM	255	1,24	4381
A330	2254	COM	214	1,42	1442
Others	-	-	-	-	7636

Were:

- D - dual;
- DT – dual tandem;
- COM – complex.

Then these aircrafts are grouped in main categories with similar characteristics and a “design” aircraft (the shaded in the table) is then selected for each group. Based on this traffic data the damage already induced in pavement by the passed traffic can be evaluated.

7.3 Survey procedure

7.3.1 Deflections

FWD tests were performed along 7 longitudinal profiles parallel to the center line (CL), one along the CL and the others located at 3, 10 and 20 m on each side. The distance between the test points was of 75 m for the 3 central longitudinal profiles and 100 m for the other 4 longitudinal profiles.

In each test point three drops were performed from the third height in order to obtain a peak load of 150 kN. The last two drops were recorded. The loading plate of 45 mm diameter was used. The deflections at pavement surface were measured in the following locations: 0 m (D_0); 0.30 m (D_1); 0.45 m (D_2); 0.60 m (D_3); 0.90 m (D_4); 1.20 m (D_5) and 1.80 m (D_6) from the center of the loaded area.

Air and pavement temperatures were measured during testing. The pavement temperature was measured at 25 mm depth. Given the fact that the tests were performed during night, the temperature measured above was considered representative for the whole asphalt layer, as no significant temperature gradient in depth occur after mid-night [Van Gorp, C.A.P.M.; 1995].

The deflections were then normalised for 150 kN load. Figure 7.3 presents an example of these deflections for a testing profile. A division in homogeneous sub-sections was performed using the normalised deflections.

FWD results - testing profile located at 3m right of CL

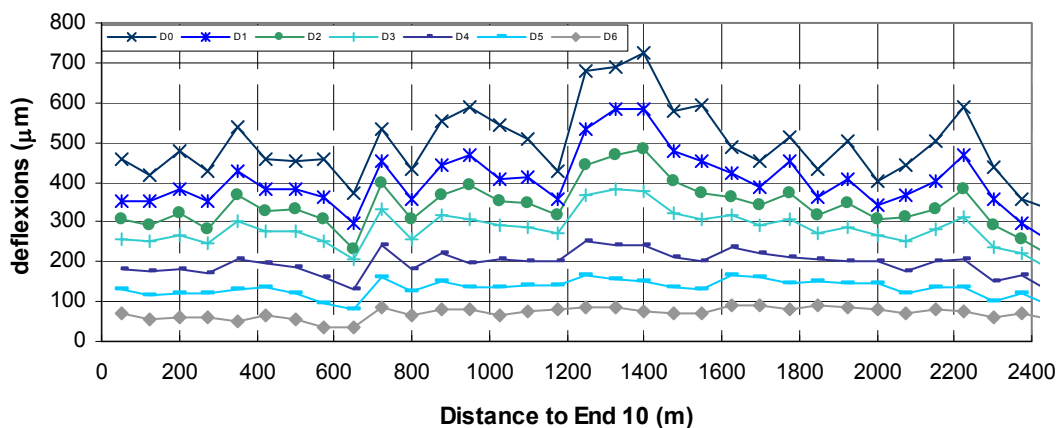


Figure 7.3 – Example of FWD results file – deflections normalised for 150 kN

7.3.2 Layer thickness

GPR tests were undertaken along 6 longitudinal profiles, the same as FWD tests except the CL (due to the presence of metal parts that affect the results). The measurements were performed with both horn antennas pairs (1 GHz and 2 GHz) and the number of scans per meter used was 4 (one scan every 25 cm), like in most studies conducted by LNEC. Figure 7.4 presents an example of a raw GPR file. The delimitation between the two different structures of the runway pavement (around 770 m from End 10) is evident in this file.

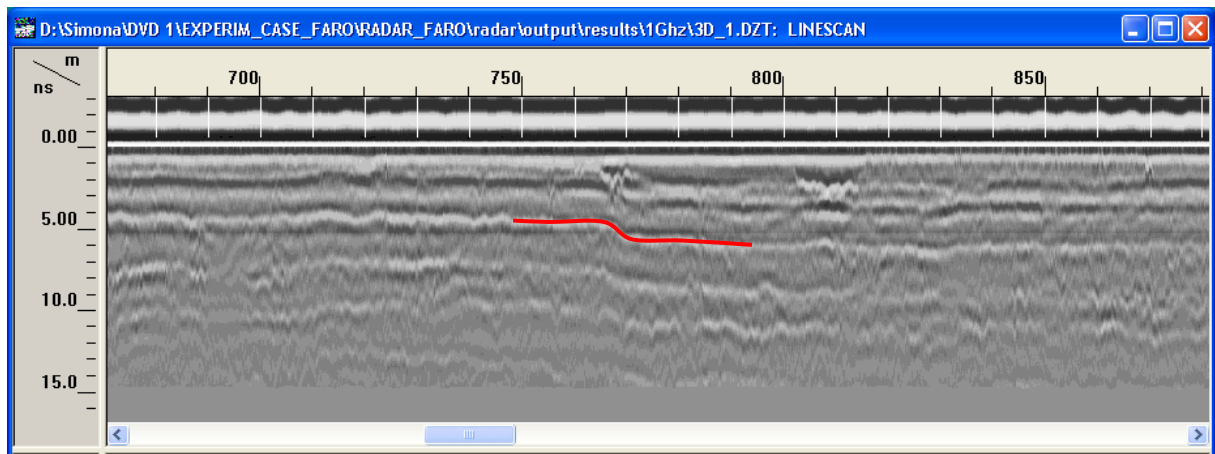


Figure 7.4 – Example of raw GPR file – delimitation between the two different structures

Cores were extracted to complete the layer thickness information during detailed GPR data interpretation. In each homogeneous sub-section (see 7.4.1) several cores were extracted, thus uniformly covering the runway length. Figure 7.5 shows a photo of these cores.

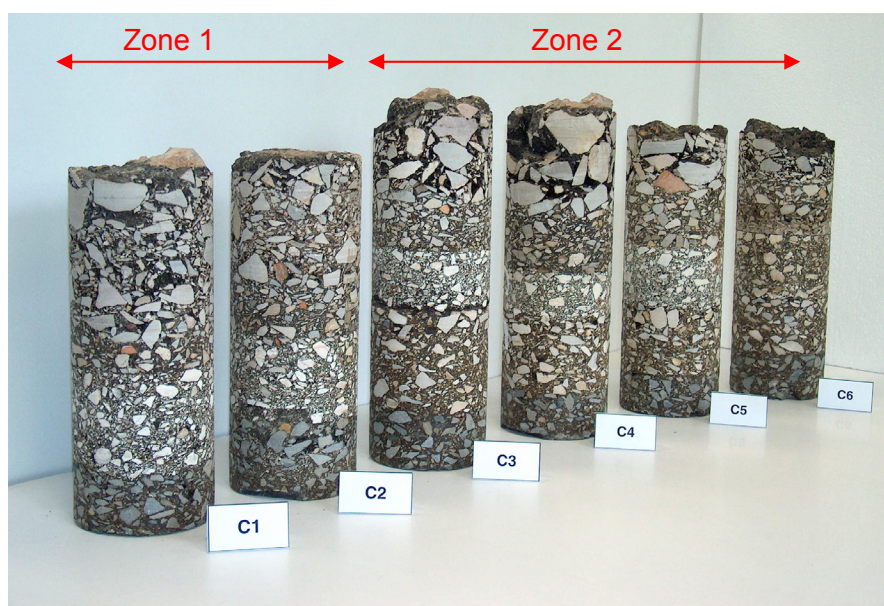


Figure 7.5 – Cores extracted – general view

Table 7.5 presents the core thickness as well as the GPR results in the same locations.

Table 7.5 – Layer thickness information

Core n°	Location		Asphalt layers thickness (mm)					Granular base thickness (mm)		
	End 10	CL	Cores				GPR average value ⁽⁴⁾	Design data	GPR average value	
			h _{AC} ⁽¹⁾			h _{BM}				Total
	(m)	(m)	1992	1980	1965					
C1	200	3mR	45	70	45	95	255	254	300	322
C2	600	3mL	60	65	45	100	270	265		321
C3	1400	3mL	50+85	50 ⁽²⁾	40	80	305	308		299
C4	1900	3mR	40+70	45	55	95	305	309		317
C5	2100	3mL	40+70	60	50	>70	>290 ⁽³⁾	288		271
C6	2300	3mR	50+60	70	55	>60	>295 ⁽³⁾	296		307

⁽¹⁾ – thickness of various layers of bituminous layers from top to bottom;

⁽²⁾ - debonding between the 2nd and 3rd asphalt layer;

⁽³⁾ - desegregation of bituminous macadam layer during core extraction;

⁽⁴⁾ – thickness average of 5 m around the core location after detailed interpretation.

7.4 Data processing

7.4.1 Division in homogeneous subsections

The division in homogeneous subsections was performed based on normalised FWD deflections, using the cumulative difference method, already described in 3.5.2. Two distinct sub-sections were identified, and they are similar to those obtained in previous studies.

Table 7.6 – Deflections per homogeneous sub-sections (mean and standard deviation)

Zone	Distance to		Deflections (μm)													
	End 10	CL	D ₀		D ₁		D ₂		D ₃		D ₄		D ₅		D ₆	
			A	σ	A	σ	A	σ	A	σ	A	σ	A	σ	A	σ
1	0 – 750 m	20mL	387	74	286	64	237	56	186	45	120	30	78	20	42	12
		10mL	341	87	262	69	218	59	176	50	116	35	76	24	40	12
		3mL	487	55	382	42	322	37	261	33	173	28	11	23	52	15
		0	568	132	452	11	376	96	304	80	206	59	137	41	66	20
		3mR	459	51	374	43	316	45	266	35	183	28	121	22	57	15
		10mR	327	78	248	61	201	56	160	44	103	31	67	20	36	9
		20mR	348	33	247	26	196	25	154	22	97	21	64	16	37	11
2	750 – 2400 m	20mL	391	53	303	43	256	38	210	32	148	25	106	19	64	13
		10mL	349	46	284	39	242	35	211	30	156	25	114	20	68	12
		3mL	479	104	389	82	334	63	281	48	200	32	140	24	79	16
		0	458	81	389	70	344	63	295	55	219	44	158	32	90	19
		3mR	512	103	417	81	351	62	292	47	202	29	139	19	77	10
		10mR	369	62	297	51	256	43	215	36	157	26	115	19	69	11
		20mR	405	46	312	34	259	28	214	23	148	18	105	13	62	8

Where:

- A – mean value of deflections;
- σ – standard deviation of deflections
- L – left side of the CL considering the direction End 10 to End 28;
- R – right side of the CL considering the direction End 10 to End 28.

The three central FWD testing profiles have a similar division and therefore they may be grouped. Figure 7.6 presents the graphic of the cumulative differences method for the central FWD testing profiles

The case presented herein corresponds to the testing profile located at 3 m on the right side of the runway (3mR).

The structure studied is a three layered flexible pavements (asphalt layers + granular layers + subgrade) resting on a “rigid” layer consists of asphalt layers, a base layer and a subgrade and a “rigid” layer as shown in Figure 7.7.

Figure 7.8 presents the cumulative difference chart for the FWD profile located at 3m right from CL, while Figure 7.9 presents the processed GPR results for same profile (3mR). It can be observed that the division into homogeneous sub-sections is easily detected in the GPR file as the change in layer thickness is evident.

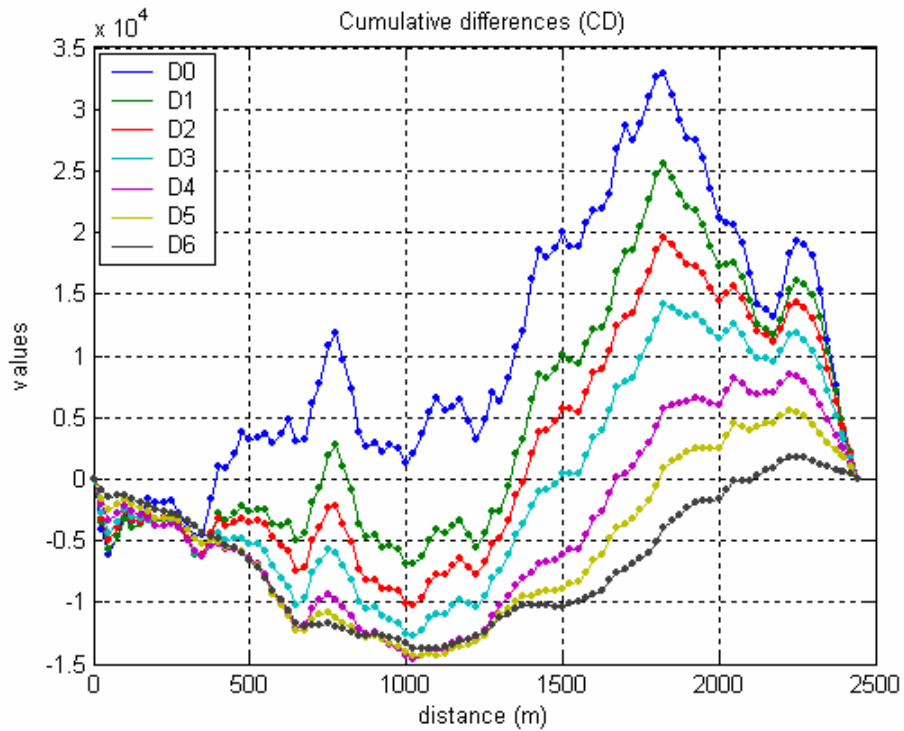
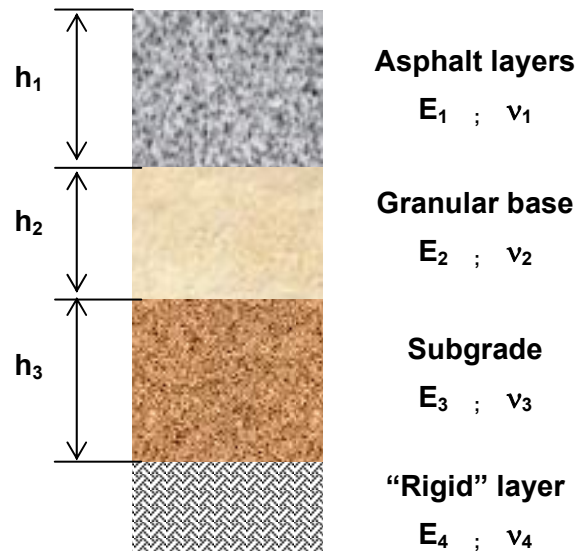


Figure 7.6 – Cumulative difference for the three central FWD testing profiles (CL, 3mLand R)



where:

- E_1, E_2, E_3, E_4 - Modulus of asphalt layer, granular base, subgrade and "rigid" layer;
- h_1, h_2, h_3 - Layer thickness of asphalt layer, granular base and subgrade layer;
- $\nu_1, \nu_2, \nu_3, \nu_4$ - Poisson's ratio of asphalt layer, granular base, subgrade and "rigid" layer.

Figure 7.7 – Pavement structural model

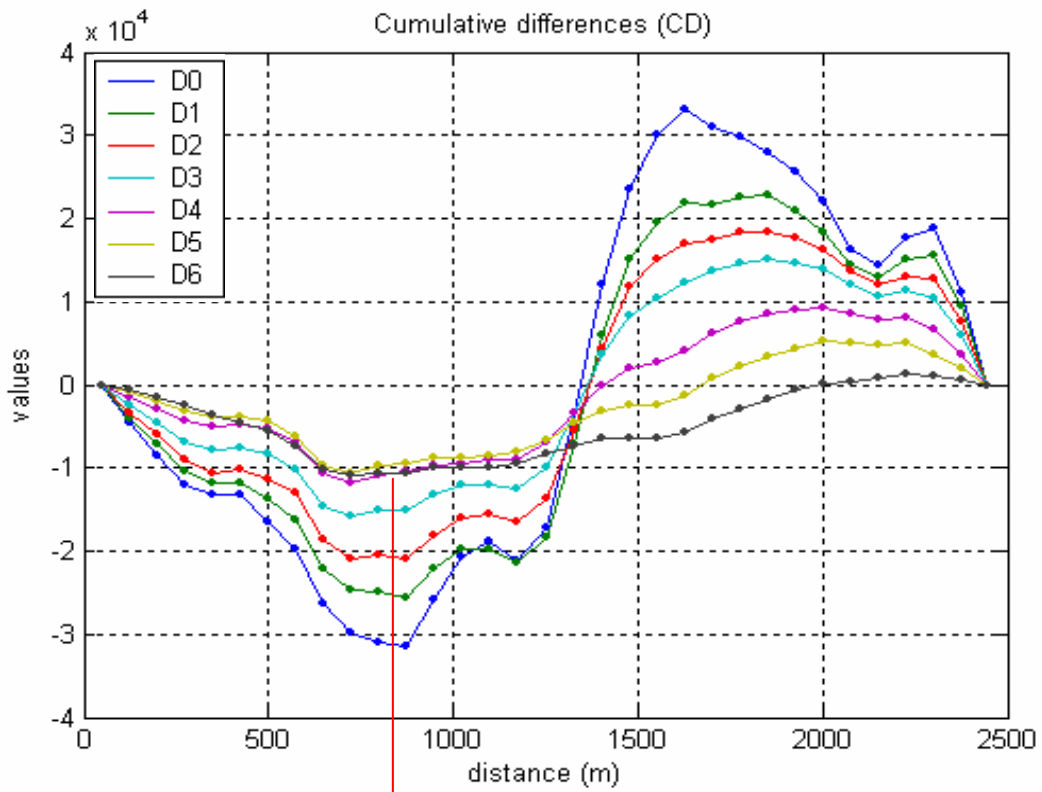


Figure 7.8 - Cumulative difference for FWD testing profile – 3mR

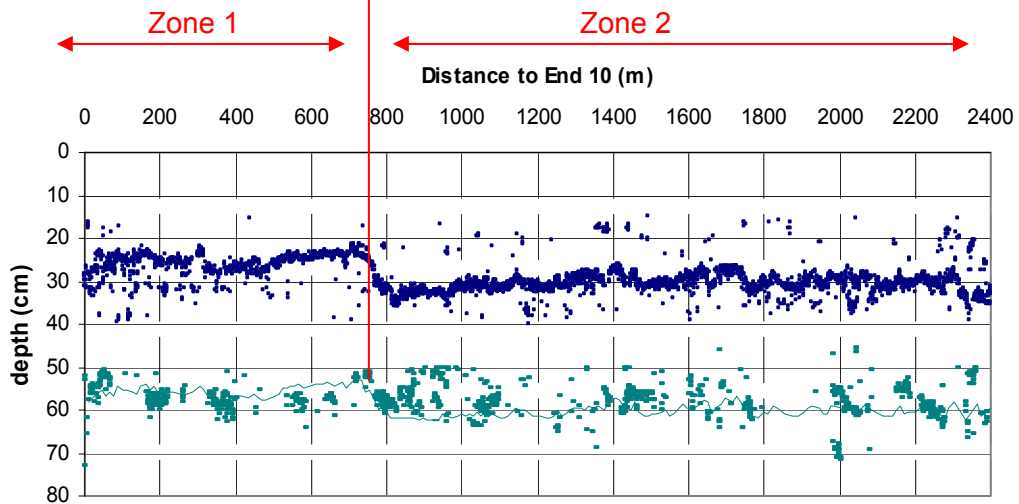


Figure 7.9 – Layer thickness - GPR results for testing profile 3mR

7.4.2 Detailed GPR interpretation

GPR detailed interpretation is always required for the reasons already presented in Chapter 4. Figure 7.10 presents a GPR file after automatic interpretation, while Figure 7.11 presents a file after detailed interpretation.

The detailed interpretation of GPR results consists in wave velocity “calibration” which is made based on cores (see Table 7.5).

The existence of two distinct zones in terms of thickness, as already known from the background information, was clearly identified in the GPR files (see Figure 7.9). Due to differences in thickness range these two zones were processed separately, for a better interpretation. The sub sections considered are as presented in Table 7.6.

For each of these subsections the detailed interpretation was performed. The main steps and the reasoning behind this procedure are presented below.

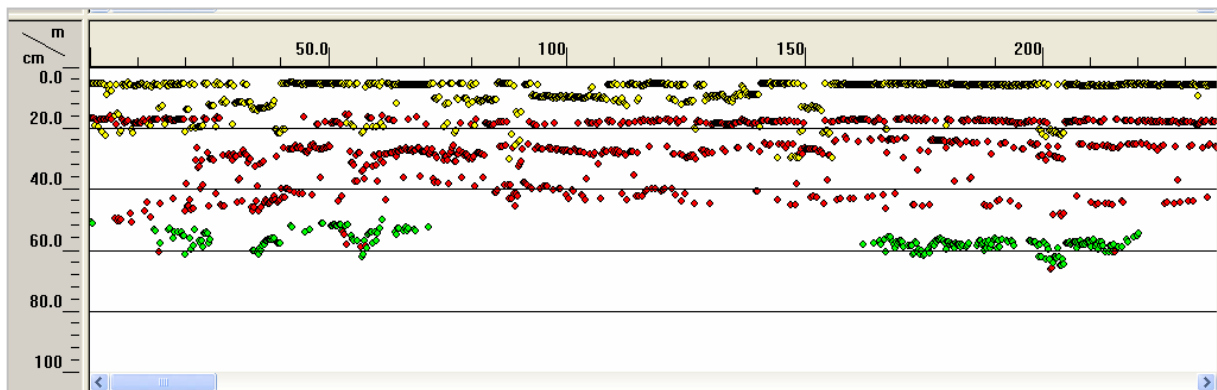


Figure 7.10 – Aspect of GPR file after automatic interpretation

Although with the GPR it is possible to identify 5 distinct layers in this study case (see Figure 7.10), the consideration of these layers for the pavement structure evaluation makes no sense. Therefore, the engineering judgment is used once again. Here is presented the reasoning behind the selection of layers for pavement structure evaluation:

1. Thin layers, such as the surface layer (yellow) which is about 50 mm thick, have to be modeled together with similar layers. This is due to the fact that changes in elastic moduli of such thin layers will not influence the pavement response. In this study this layer will be modeled together with the other asphalt layers.
2. Layers of same material, like the granular material layers, have to be considered as only one layer for the modelling purpose, as their elastic moduli is almost the same.

They are identified as separated layers in the GPR file (blue and brown) because of their construction process: to ensure a better compaction, two different layers of about 150 mm each were placed.

3. The bituminous macadam layer, although clearly identified in the GPR file (red), it is modelled together with the others asphalt layers, like in similar studies. From this moment on, all bituminous materials layers are addressed as asphalt layer.

Consequently, from five layers initially identified in the GPR file, only two layers are considered for pavement structure modelling: the asphalt layer (including the bituminous macadam) and the granular base layer (Figure 7.11).

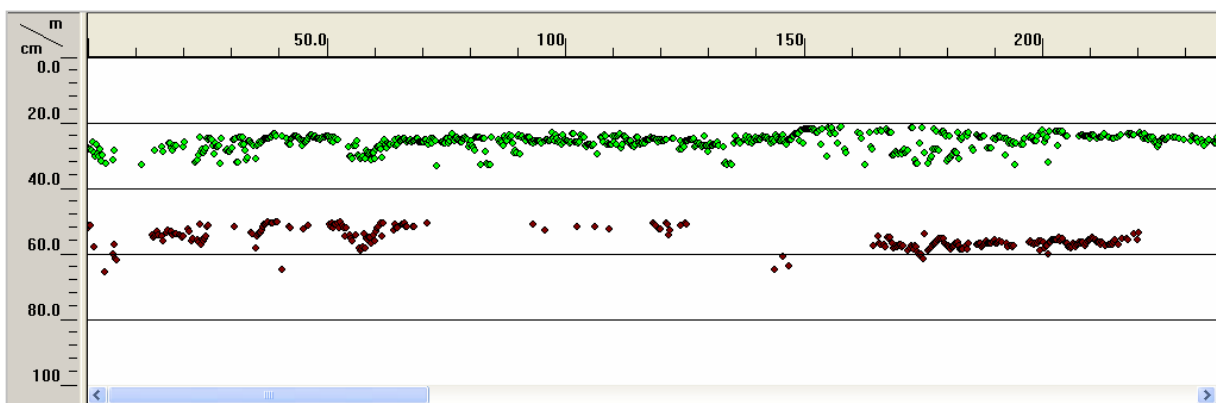


Figure 7.11 – Aspect of final GPR file used for calibration based on core data

The detailed interpretation was performed, for these two layers, using the core information together with historical and construction records. The data obtained for layer thickness distribution is also used to establish the database limits, in terms of thickness range, for the pavement structure modelling based on Artificial Neural Network (ANN).

7.4.3 Pre-processing of FWD and GPR data

The information in the file resulting from application of the “FWD_GPR” programme (see 6.3) will have for each FWD test point the corresponding pavement structure (layer thickness). This last value is represented for each layer by the average of the GPR measurements located at 5 m around the FWD test point as already presented in 6.3. This file is then used together with the corresponding deflections measured “in situ” as inputs to the artificial neural network (already trained) for pavement structural evaluation.

7.5 Application of ANN for interpretation of NDT results

7.5.1 Pavement structure modelling using ANN

The first task in neural network training process is to analyse the parameters that interfere in the training database by establishing the following:

- ✓ the variables that can be fixed within the calculation;
- ✓ the types of pavement sections to be considered;
- ✓ the range of parameters and their increments for the training.

The parameters considered fixed in this case study were: the size of loading plate (450 mm), the loading force (150 kN), the Poisson's ratios (0.40 for bituminous materials, and 0.35 for the others materials), the distance between the deflection sensors location at 0, 300, 450, 600, 900, 1200, 1500 and 1800 mm. Another parameter considered fixed in this study was the ratio between the "rigid" layer modulus and subgrade modulus ($E_4 = 5 E_3$). This ratio had been already used in previous studies and it was considered to represent the nonlinear response of the subgrade soil. This assumption will improve the ANN performance by reducing the number of variables. Studies were performed with E_3 and E_4 independent and unknown but the results obtained led to difficulties of network training and bad ANN performance. A three-layered flexible pavement structure overlaying "rigid" layer was analysed.

7.5.2 ANN training

7.5.2.1 Database for training

Synthetic data were used for training the ANN for pavement evaluation. The "Train_Data" programme, which uses ELSYM 5 as subroutine, was used to produce the database. The variation of pavement structure parameters was made in order to uniformly cover the range of values in use.

The range of the parameters was chosen related to the condition of the pavement in study.

- ✓ For the layer thickness, the distribution obtained during the GPR survey gave the (minimum required) range of the variation (see 6.2.2);
- ✓ There was no precise information on the subgrade thickness therefore it was considered variable during this study (see 6.5.3);
- ✓ The variation of the layer moduli corresponds to the type and the condition of the material that constitutes each layer. The values obtained in previous tests were taken into account, also some “manual interpretations” (for representative deflection bowl, 85%) were performed in order to have an idea of the moduli expected for this study.

The ranges of pavement layer properties included in the training are presented in Table 7.7.

Table 7.7 – Variable parameters of pavement structure – range of variation

Parameter	h_1 (m)	E_1 (MPa)	h_2 (m)	E_2 (MPa)	h_3 (m)	E_3 (MPa)
Minimum value	0.22	1000	0.26	100	0.80	40
Maximum value	0.38	8000	0.36	600	2.40	240
Increment	0.01	1000	0.02	100	0.40	40

The maximum subgrade thickness generally adopted in LNEC’s studies is of 2.50 m. The study developed by Antunes [Antunes, M.L.; 1993] showed that above this value the maximum vertical stresses induced by FWD represent less than 5% of the vertical and horizontal stresses given by the structure’s own weight. Based on this assumption the upper limit of the subgrade thickness variation range adopted in this study was 2.40 m. Additionally a verification was made with an ANN trained with subgrade variable thickness up to 3.50 m. The results obtained (Figure 7.12) showed that a significant percentage of these values are below 2.40 m.

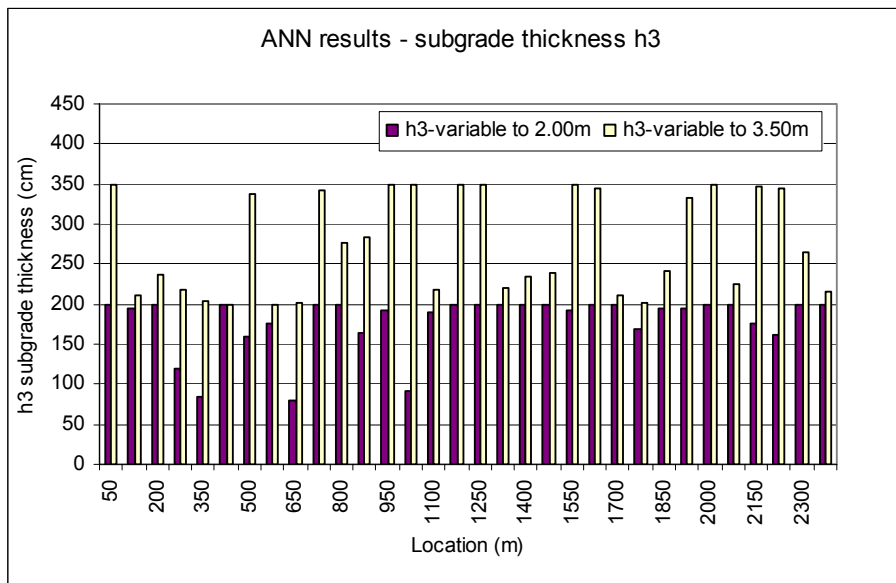


Figure 7.12 – Results obtained for subgrade thickness h_3

Synthetic deflections were obtained based on various pavement structures, resulting from combinations of layers thickness and moduli. Table 7.8 presents their range of variation.

Table 7.8 – Deflections obtained – range of variation

Deflections (μm)	D_0	D_1	D_2	D_3	D_4	D_5	D_6
Minimum value	196	156	134	116	85	43	16
Maximum value	1890	1590	1370	1170	829	588	333

$D_0, D_1, D_2, D_3, D_4, D_5$ e D_6 are deflections measured at 0, 300, 450, 600, 900, 1200, and 1800 mm.

7.5.2.2 ANN architecture

A four-layer, feed forward network was used. The network consists of an input layer and an output layer separated by two hidden layers, each of them with 15 neurons (9/15/15/4). During training, the inputs were the deflections (D_0 to D_6) and the pavement layer thickness (h_1 and h_2) and the outputs were the layer moduli ($E_1, E_2,$ and E_3) and the subgrade thickness (h_3).

7.5.2.3 ANN training

The number of datasets obtained in this process is usually very large and only part of them are used during training, in this case 9000 data randomly chosen from 106572 produced.

Figure 7.13 presents an example of the convergence of the ANN response (green) during the training process for the target layer moduli (blue).

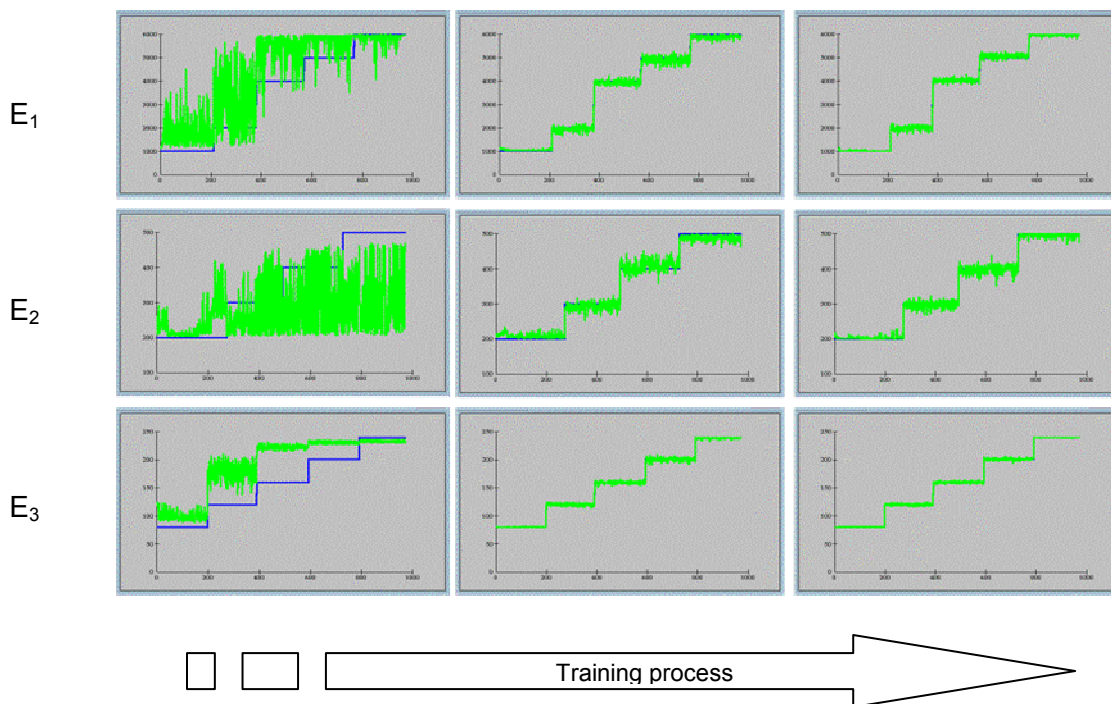


Figure 7.13 – ANN convergence during training

The verification of ANN training has been made using 1000 data from the datasets initially produced and not used during training. Figure 7.14 shows the results obtained.

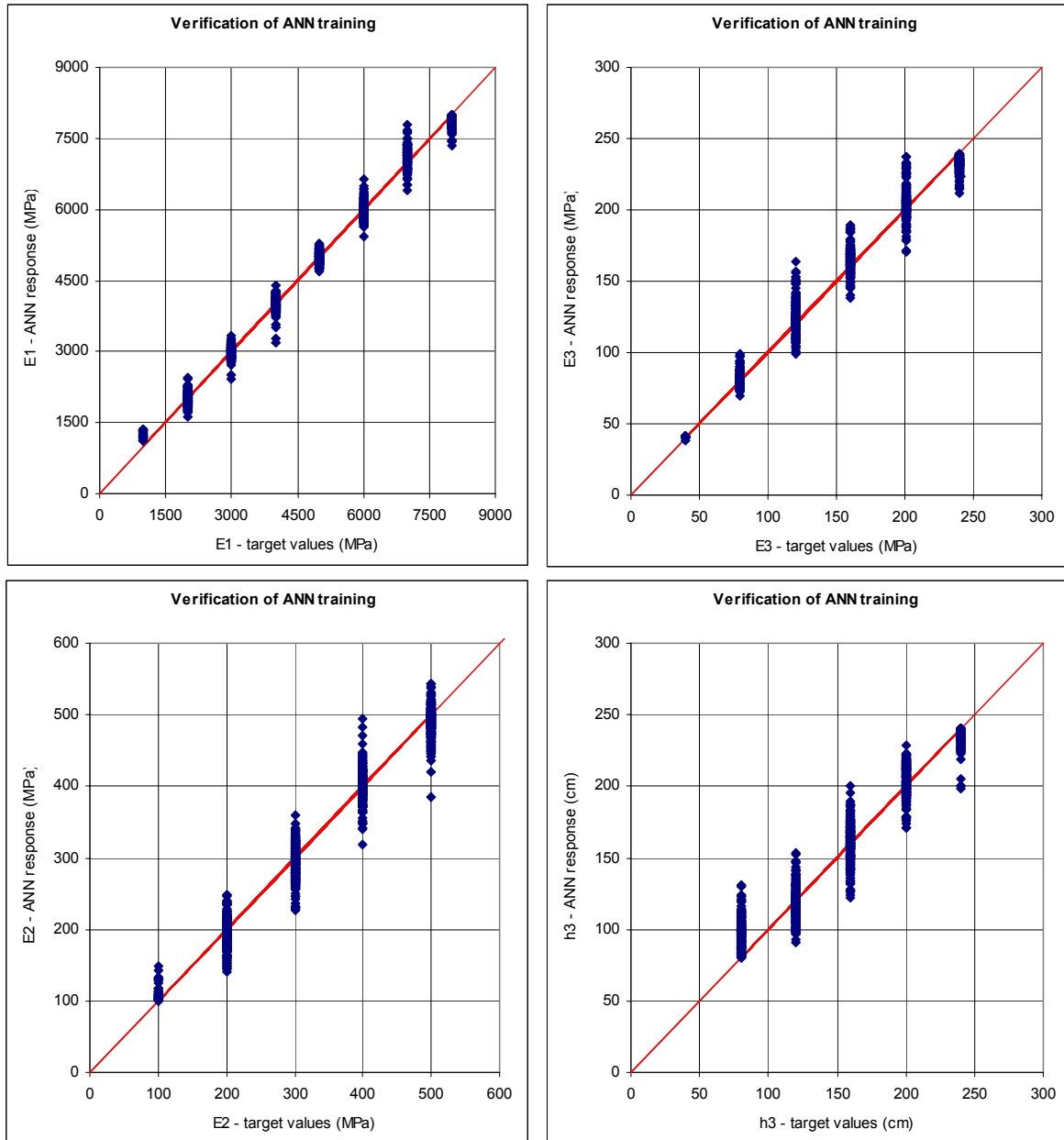


Figure 7.14 – Verification of ANN training

7.5.3 Results

This ANN has been used to estimate the structural pavement model of the runway, based on FWD and GPR tests performed *in situ*. The ANN inputs used (deflections and layer thickness) and the results obtained (moduli and subgrade thickness) are presented in Figure 7.15 .

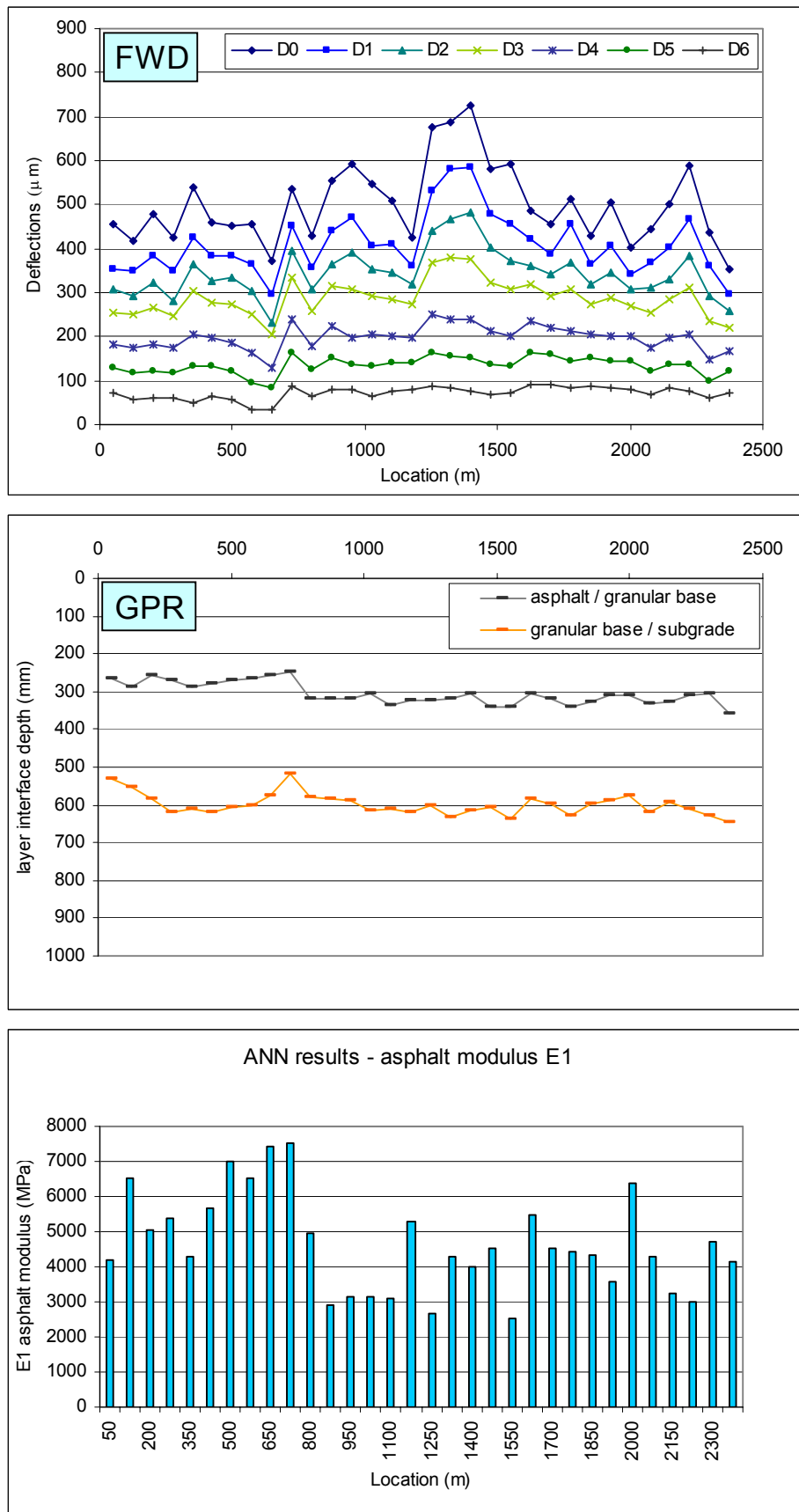


Figure 7.15 a) – ANN inputs (D_0 to D_6 and h_1 , h_2) and outputs (E_1 , E_2 , E_3 and h_3)

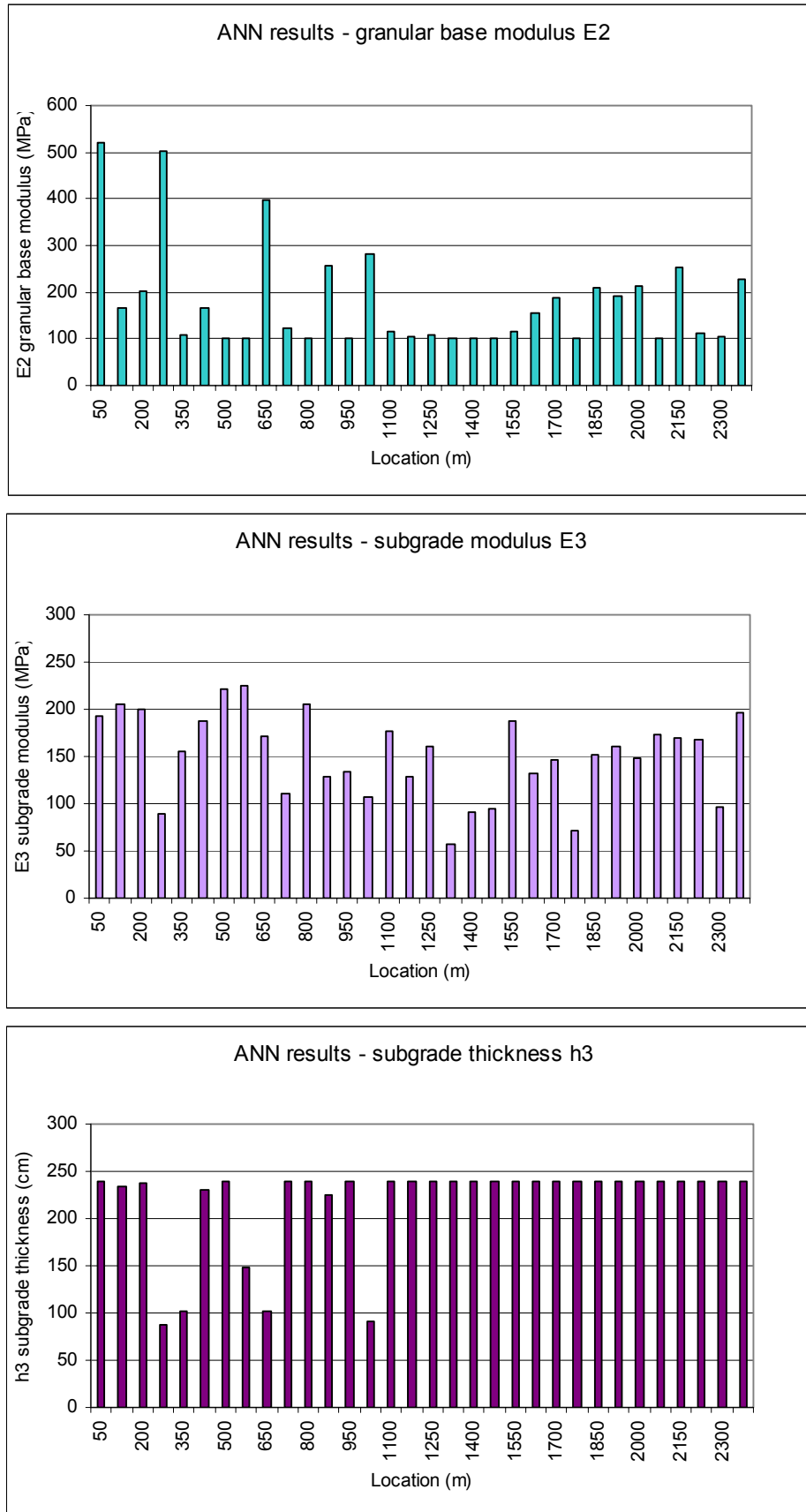


Figure 7.15 b) – ANN inputs (D_0 to D_6 and h_1, h_2) and outputs (E_1, E_2, E_3 and h_3) - continuation

The pavement response (deflections) was calculated for the structures obtained using ANN, then these deflections were compared with those measured *in situ* (see Figure 7.16).

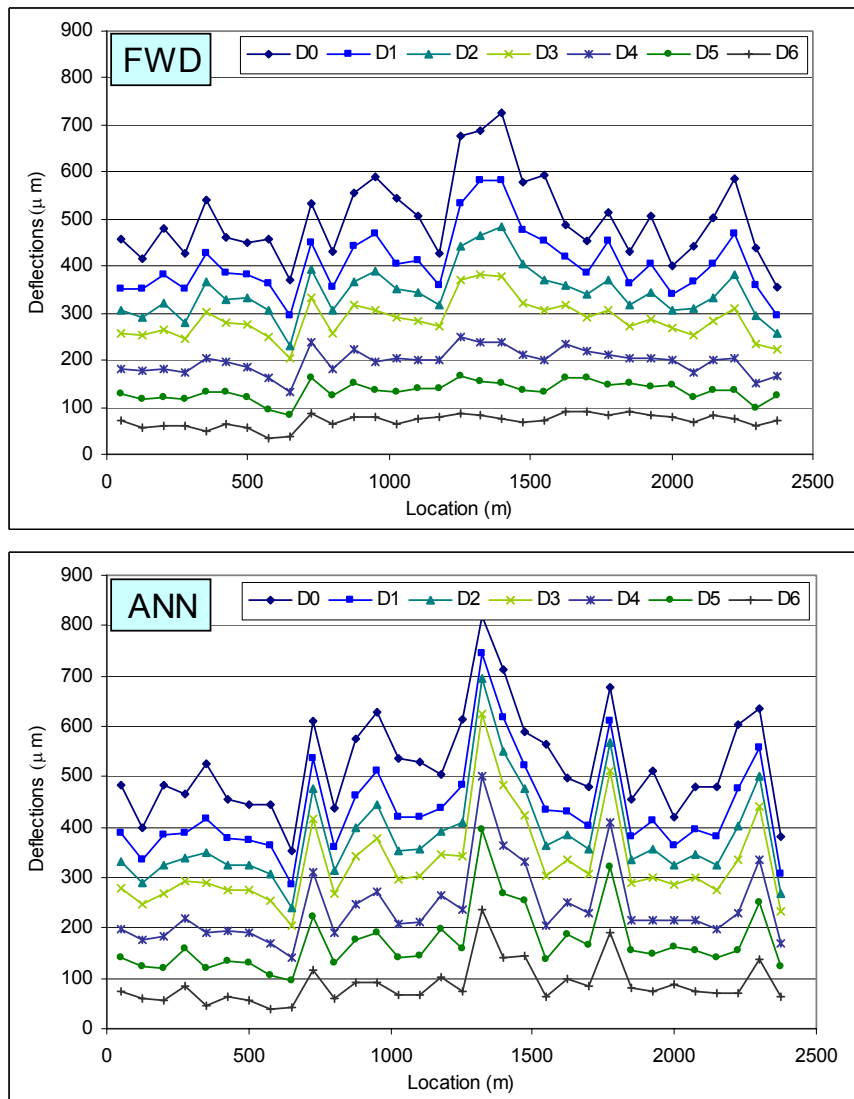


Figure 7.16 – Deflections measured *in situ* and calculated using ANN pavement structure

A relative error between the measured deflections (D_i^m) and those calculated based on ANN pavement structure (D_i^c) was calculated. Figure 7.17 presents the results obtained for each deflection and the corresponding average error E_r , per deflection, calculated using the following equation:

$$Er = \frac{1}{n} \sum_{i=1}^n \left(\frac{|D_i^m - D_i^c|}{D_i^c} \right) \quad (7.1)$$

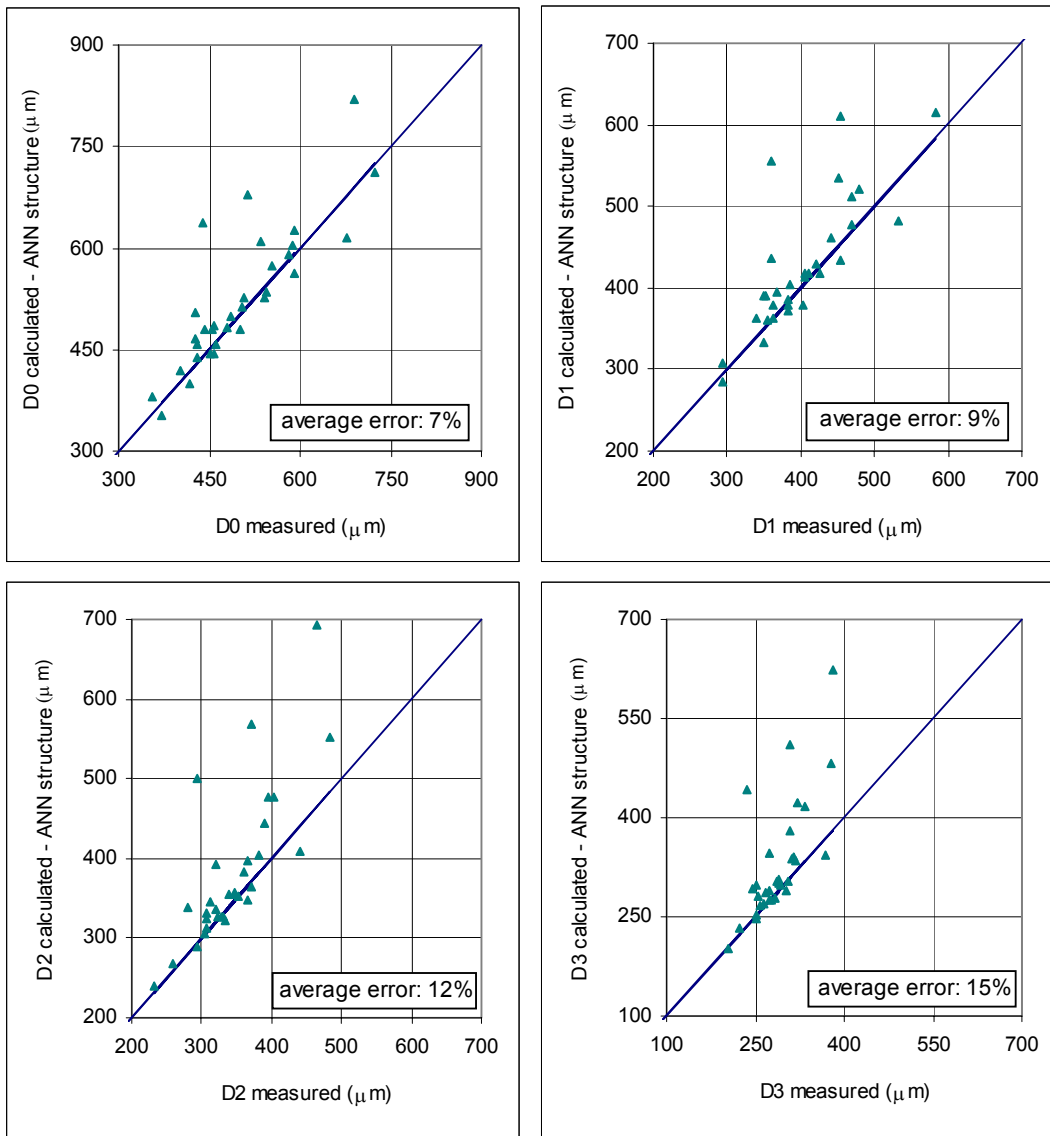


Figure 7.17 a) – Deflections comparison and average error per deflection

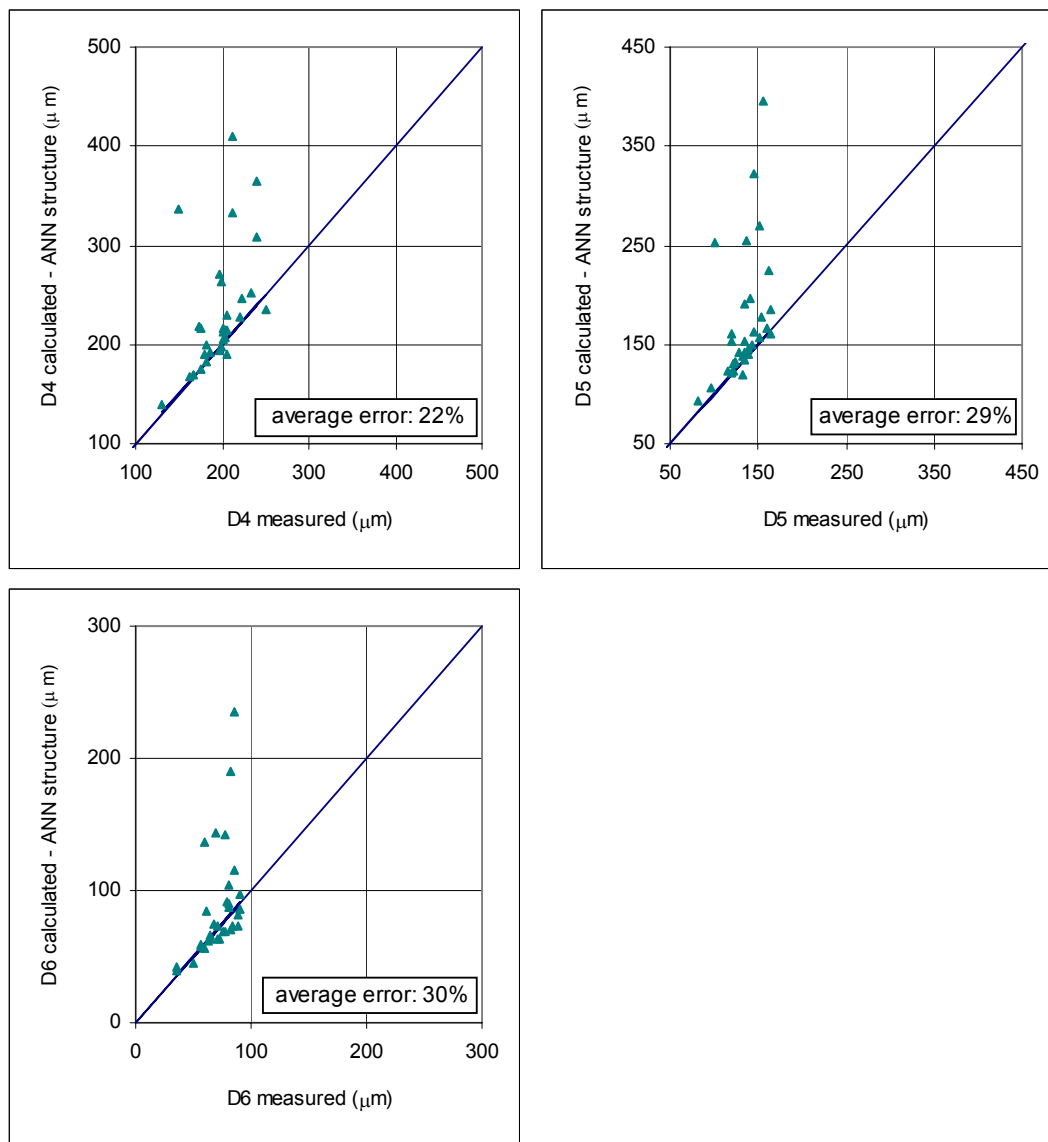


Figure 7.17 b) – Deflections comparison and average error per deflection – continuation

As results from the graphs presented above the average error is growing from D_0 to D_6 deflection.

The major error is given by the test points where the ANN had difficulty to find a solution within the trained range. Therefore, attention has to be paid to the test points which interpretation leads to elastic moduli situated on the training range limits. In this case, they can be either ignored (if they are on the safe side or very few) or the training is repeated with extended variation range. The engineering judgement should be used for the analysis of results and to evaluate their “realism”.

The results obtained are not very different of the obtained using classic approach interpretation of a representative deflection bowl (see Figures 7.18 and 7.19).

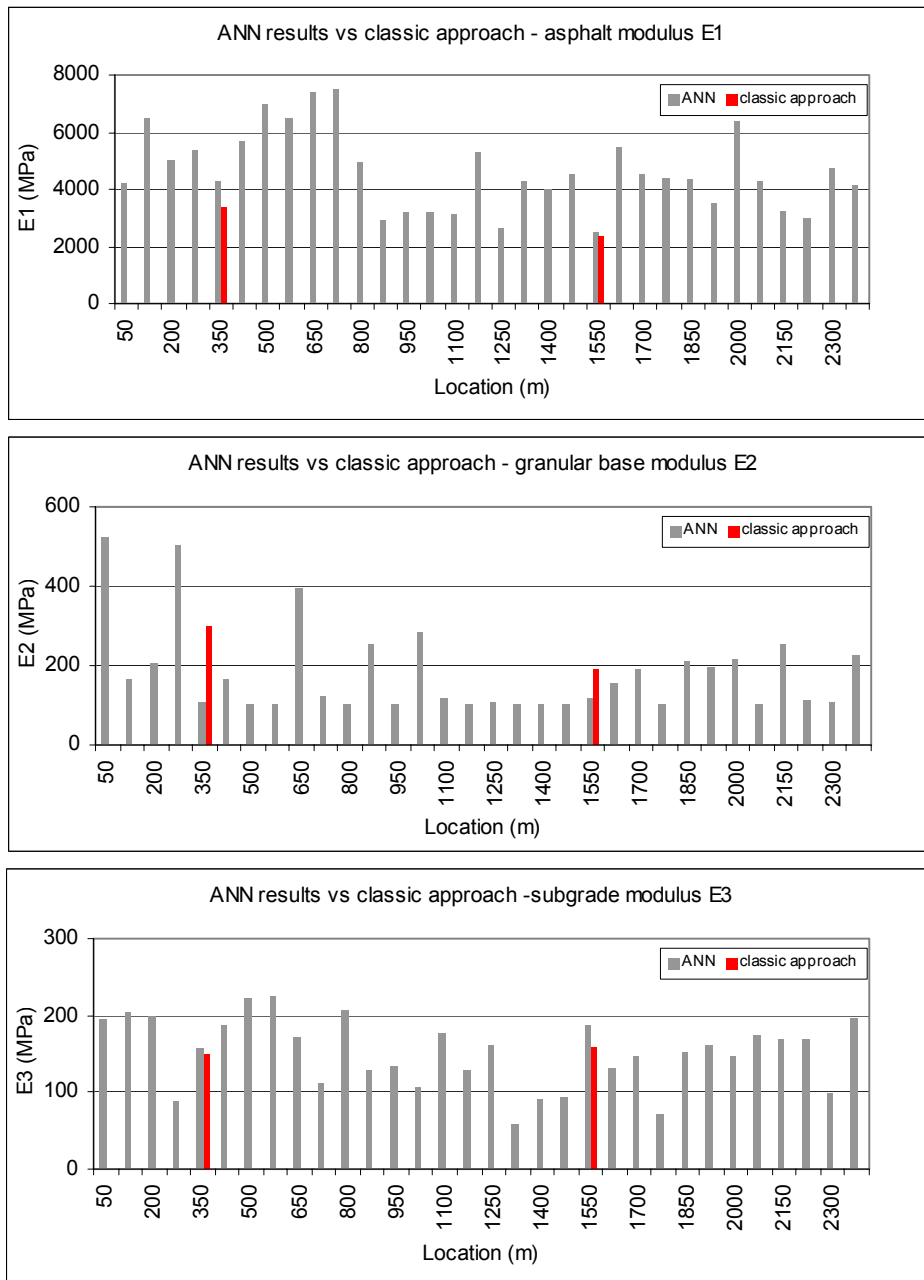


Figure 7.18 – Comparison between ANN results and classic approach

The proposed methodology represents also a useful tool for the detection of reduced subgrade thickness (for example the presence of bedrock near surface) in order to be considered in the backcalculation process, as it has an important effect on the pavement response.

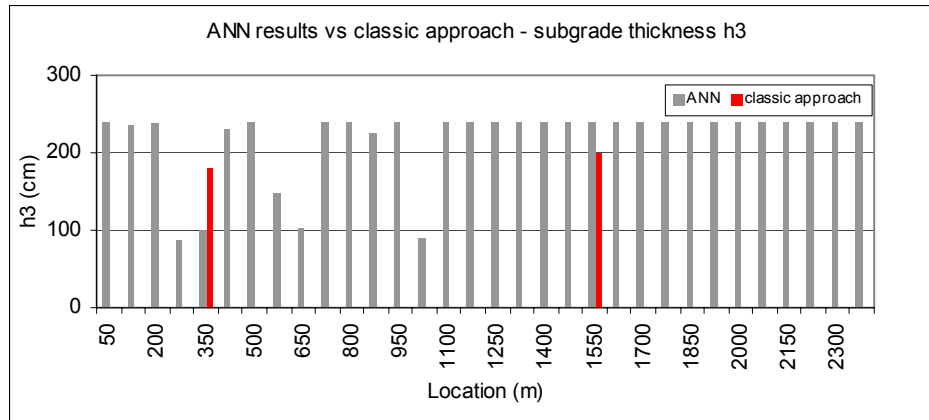


Figure 7.19 – Subgrade thickness results

It is important to perform the interpretation of few FWD tests (using classic approach) before training the ANN in order to obtain feedback on the expected moduli, information needed to set-up the variation range. Taking into account the temperature during testing, the range for the asphalt modulus may differ from the values expected for the design temperature.

7.6 Summary

An application of the proposed methodology to an airport pavement evaluation was addressed in this chapter.

The application aimed at analysing the reliability of the developed methodology when applied to real case studies and to establish the procedure to be followed.

Based on the results obtained, it can be observed that the values obtained for layer elastic moduli are “realistic” as they are within the data used in the training and that the results obtained with neural network and conventional backcalculation program (using layered elastic model) are not significantly different.

The proposed methodology represents an appealing alternative to the classic approach as it reflects the pavement structural condition along its extension

This study has proven the reliability of the use of artificial neural networks in backanalysis of FWD test results.

8 Conclusions and Future Developments

8.1 Conclusions

For the purpose of pavement evaluation, non-destructive load tests (NDT) are performed and the measured deflections are then used to derive a response model of the pavement structure as close as possible to the real situation under traffic loads.

Knowledge of the pavement structure (type of materials and layer thickness) is essential for pavement evaluation. Usually, this information is gathered through construction records complemented with site investigations and coring. The missing or erroneous thickness data will cause unrealistic results of the backcalculation process. The application of GPR for pavement evaluation represents an important step forward, as it provides continuous information on layer thickness, for the bound and also the unbound layers.

GPR using is a testing equipment, which can operate at traffic speed, for detection of pavement structure variations and determination of layer thickness. Although GPR is becoming a routine equipment, the interpretation of radar data is complex and should only be carried out by experienced engineers. The experience gathered so far with GPR testing and interpretation has led to recommendations to overcome some of the problems associated with this technology.

One of the main recommendations is that a “detailed” interpretation together with layer thickness calibration based on extracted cores, is always required. Additional cores, taken at different location from those used previously to perform the layer thickness calibration, can be used to verify the methodology used for GPR interpretation.

Other aspects that have to be taken into account when using GPR to pavement evaluation are the following:

- ✓ In general, GPR will not detect adjacent layers of similar materials. Therefore, the consideration of several layers within the same material should be made with caution.
- ✓ There are difficulties to track the layer delimitation when the boundary between two layers is not clear enough (e.g. granular layers contaminated by soil, penetration macadam over unbound granular layers etc.)
- ✓ The energy losses in some materials that exhibit high absorption (concrete, cement stabilised materials) can result in a reduction of the penetration depth in half or even more.

The consideration of these recommendations can contribute to a higher reliability in the use of GPR for pavement evaluation.

The next step in pavement evaluation is the establishment of a structural model based on NDT results. This is usually an iterative process in which the parameters of the pavement models (geometrical and material properties) are gradually changed, until the calculated response of the pavement model under the load will match the response measured *in situ* (backcalculation). In most cases, the backcalculation is performed using the multi-linear elastic approach, which assumes that the materials are linear elastic, homogeneous and isotropic.

The main concern during this process is the large number of possible results. As the solution is not unique, several combinations of materials properties and layer's geometry can lead to the same answer, in terms of deflections under a certain load. Not always, the best deflection fitting given by some backcalculation software corresponds to the more realistic pavement model. Therefore, it is essential to use all available information, as well as some degree of engineering judgement to evaluate the results and select a realistic solution.

Some alternative approaches to perform the interpretation of FWD test results have been mentioned in this work. Among these, the use of Artificial Neural Networks (ANNs) was considered a promising tool and therefore its applicability was studied in this study.

ANNs are interconnected assemblages of simple processing elements that contain limited amount of local memory and perform rudimentary mathematical operations on data passing through them. They have the ability to act as functional approximators that can "learn" a functional mapping when repetitively exposed to examples of that mapping. ANNs are able to learn a very complex mapping without previously specifying the functions or rules. However,

it is very important to select the correct type of network and the most representative data for the training process in order to properly solve a given problem under study.

Among the different types of ANNs, backpropagation neural networks are considered well suited for pavement structure modelling due to the fact that their training, called “supervised learning”, enables a certain control of ANN response and at the same time they are powerful and versatile networks. This type of ANN can be “taught” a mapping from one data space to another, using examples of the mapping to be learned, and therefore the answer will be within the range of values used for training.

Backpropagation ANNs can be “trained” to determine the corresponding pavement layer moduli from deflection basins, based on a database of FWD results.

In neural network application, the biggest challenge is the design of the network architecture to better fit the problem in study. There are no guidelines and the physical laws or mathematical formulations of the problem under study do not give indications on how to set up the network architecture, in terms of number of hidden layers or neurons per layer for example. Therefore, the ANN structure is designed by trial and error, complemented with previous experience.

This study presents a method for structural pavement evaluation, which makes use of GPR data combined with FWD test results. The interpretation of FWD test results is performed in each test point using ANN.

Synthetic data are used during the training process. A program “Train_Data” has been developed to generate the entire database needed for training an ANN for solving backcalculation problems.

A good uniformity of training samples helps to enhance the ANNs' generalization performance. The response of ANN is much better in case of smaller steps of parameter variation, even if the train is performed with only a part of the database generated in this way. The use of ANN for structural evaluation of two typical pavement structures (road and airport) was studied. The ANN behaviour to variable and “fixed” distance to the “rigid” layer was also analysed. The results obtained have shown a good behaviour of the ANN and the errors in moduli obtained were generally less than 4%. The use of distance to the “rigid” layer, when known, will result in an improved ANN behaviour.

The sensitivity of the proposed method to variations in the pavement thickness or to variation in deflections was also analysed. This analysis has shown that variations in individual deflections in the order of 10%, for example due to problem with one of the deflection sensors, may have some impact on the ANN response. On the other hand, variations within

the accuracy range specified by manufacturers, which are, in case of GPR horn antennas below 5% and, in case of FWD equipment below 2%, will not significantly affect the ANN response.

For a better understanding of the application of the proposed methodology to pavement evaluation, a case study of a runway pavement evaluation was presented. The GPR tests were used to obtain continuous, reliable information on layer thickness. Based on this information, all the FWD test points were used for backcalculation, using ANN.

The application of the proposed methodology to a real case study has proven that the use of artificial neural networks in backanalysis of FWD test results presents important advantages. It was possible to include some engineering judgment in the process by limiting the range of pavement structure parameters used in the training process.

8.2 Future developments

As future developments, the following issues can be identified:

GPR is a promising tool for pavement evaluation, but further research is needed in the field of data pre-processing and analysis in order to obtain reliable results and to reduce the time required for interpretation, bringing its use closer to routine level.

Besides pavement evaluation for maintenance planning purposes, other interesting applications of GPR can be envisaged in the future, once this is achieved, such as acceptance of pavement construction works, for example.

The application of GPR for pavement condition estimation, other than thickness, for example crack detection and moisture content is also interesting. However, further developments in the GPR technology are needed in order to reach this stage.

The methodology for pavement evaluation proposed in this study focuses on flexible pavements, since this is the main type of pavement structure used in Portugal and in most European countries.

The cases analysed in this work, which are typical road and airfield flexible pavement structures, have shown that the use of ANN in backanalysis of pavement layer moduli is a

promising approach. On one hand, it allows for a drastic reduction in computation time and on the other hand, the values obtained for layer moduli can be “realistic”.

However, the type of structure model and the ANN architecture must be carefully chosen for each case under study. Therefore, the applicability of the proposed method to other type of pavements such as rigid or composite pavements is not straightforward. The extension of the method to other type of pavements is needed.

The work presented herein addressed the use of a multilayer linear elastic programme for training the ANN. It is acknowledged that this type of response model is a simplification of the pavement's behaviour. However the proposed methodology can be applied using more sophisticated pavement models, in order to take into account the viscoelastic behaviour of asphalt materials or the non-linear response of soils and granular materials.

The use of ANN could also be an interesting approach to derive pavement's residual life directly from measured deflection basins, specially for studies at network level.

The use of ANN in other fields associated with pavement modelling is also a topic for future development. An example is to use ANN for the prediction of development of pavement deterioration in time.

The application of ANN on the interpretation of results from GPR and other testing equipments is also a topic for future research.

References

AASHTO - "AASHTO Guide for design of pavement structures"- American Association of State Highway and Transportation Officials, Washington, D.C. 2001. [AASHTO, 2001]

Air Force, - "Pavement Design for Roads, Streets, and Open Storage Areas, Elastic Layered Method"- Air Force AFJMAN 32-1018, Army TM 5-822-13, Department of the Army and the Air Force, Washington, D.C. , 1994. [Air Force, 1994].

Akon, Y.; Heck, J.V.; Hornych, P.; Azai, A.; Odeon, H. and Piau, J.M. – "Modelling of Flexible Pavements Using the Finite Element Method and a Simplified Approach". COST 337, Workshop on *Modelling and Advanced Testing for Unbound Granular Materials*, Lisbon, January. 1999. [Akon, Y.; *et al*; 1999]

Al-Khoury, R.; Scarpas, A.; Kasbergen, C.; Blaauwendraad, J. and Van Gorp, C. – "Forward and Inverse Models for Parameter Identification of Layered Media". 1st European FWD User's Group Meeting", Delft, 2001. [Al-Khoury, R. *et al*; 2001]

Almeida, J. R. de – "Analytical techniques for the structural evaluation of pavements", Ph.D. Thesis, University of Nottingham, 1993. [Almeida, J. R. de; 1993]

Al-Qadi,I.L.; Lahouar, S.; Jiang, K. and Freeman, T.E. – "Effects of asphalt aging on hot-mix asphalt dielectric constant" Transportation Research Board 83rd Annual Meeting, Washington, D.C., U.S.A., 2004. [Al-Qadi,I.L *et al*; 2004]

AMADEUS – "Guidelines on the Use of Models for Pavement Design and Assessment". Project AMADEUS – Advanced Models for Analytical Design of European Pavement Systems, Report, 1999. [AMADEUS, 1999]

Andersen, L. and Nielsen, S.R.K. "Boundary element analysis of steady-state response of elastic half-space to a moving force on its surface". Engineering Analysis Bound Elements 2003. (www.sciencedirect.com) [Andersen, L. and Nielsen, S.R.K; 2003]

Ankireddi, S. and Yang, H. – “Neural Networks for sensor fault correction in structural control”. Journal of Structural Engineering, September, 1999. [Ankireddi, S. and Yang, H; 1999].

Annan, A.P. and Cosway, S.W. – “ Ground penetrating radar survey design”. 53rd Annual Meeting of the European Associations of Exploration Geophysicists. Florence, Italy, 1991. [Annan, A.P. and Cosway, S.W, 1991]

Antunes, M. L. – “Desenvolvimento de modelos de degradação de pavimentos”, Colóquio sobre conservação, JAE, Lisbon, 1997 (in Portuguese). [Antunes, M. L.; 1997]

Antunes, M. L.; Fontul, S.; Campos, A. and Barros, R. ; –“*Estudo de Técnicas a Aplicar no Reforço de Pavimentos Flexíveis Fendilhados*”, 1^o Relatório LNEC – Report Proc 92/1/10726, Lisbon, 1998. (in Portuguese). [Antunes, M. L. *et al*, 1998b]

Antunes, M. L.; Fontul, S.; Pinelo, A.; Prates, M.; Campos, A; –“*Estudos relativos a técnicas de reforço de pavimentos flexíveis fendilhados*”, 10^o Congreso Ibero-Latinoamericano del Asfalto, Sevilla 1999. (in Portuguese). [Antunes, M. L. *et al*, 1999]

Antunes, M. L.; Pinelo, A.; Correia, A. G. – “Seasonal variation of pavements response to falling weight deflectometer”, 5th International Conference on the Bearing Capacity of Roads and Airfields, Trondheim, July 1998. [Antunes, M. L. *et al*, 1998a].

Antunes, M.L. – “Overlay Design for Faro Airport’s Flexible Pavements” – LNEC – Report Proc 92/1/9154, Lisbon, 1989. (in Portuguese) [Antunes, M.L.; 1989]

Antunes, M.L. – “Pavement Bearing Capacity of Faro Airport” – LNEC – Report Proc 92/1/10400, Lisbon, 1992. (in Portuguese) [Antunes, M.L.; 1992]

Antunes, M.L. – “*Avaliação da capacidade de carga de pavimentos utilizando ensaios dinâmicos*” - Ph.D. thesis, Lisbon 1993. (in Portuguese) [Antunes, M.L.; 1993]

Antunes, M.L., Fontul S.; “Bearing capacity of pavements close to runway 03-21 at Lisbon Airport” – LNEC – Report Proc 92/1/13677, Lisbon, 1999. (in Portuguese) [Antunes, M.L., Fontul S.; 1999]

Antunes, M.L., Fontul S.; “Bearing capacity runway 10-28 at Faro Airport” – LNEC – Report Proc 92/1/13835, Lisbon, 2000. (in Portuguese) [Antunes, M.L., Fontul S.; 2000]

Antunes, M.L.; Domingos, P.; “Caracterização Final dos Pavimentos do IC1 – Nó de Viana / Nó da Meadela (1ª Fase) e do IP9” Rel. Proc nº 0702/1/14578, LNEC, 2003 [Antunes, M.L.; Domingos, P.; 2003]

Antunes, M.L., Fontul, S. and Domingos, P. – “Layer Thickness Trials in Valencia, Spain 2004”. FORMAT, D12, 2004. [Antunes, M.L., *et al*; 2004]

Asphalt Institute – “Thickness Design – Asphalt pavements for Highways and Streets”, Manual series nº1, Lexington, 1991. [Asphalt Institute, 1991]

ASTM, D 4748–98 – “Standard test method for Determining the thickness of bound pavement layers using short-pulse radar”.1998 [ASTM, D 4748–98; 1998]

ASTM, D 6433–99 – “Standard Practice for Roads and Parking Lots Pavement Condition Index Surveys”.1999 [ASTM, D 6433–99; 1999]

Attoh-Okine, N.O. – “Artificial Intelligence and Mathematical Methods in Pavement and Geomechanical Systems”. Proceedings of the International Workshop on Artificial Intelligence and Mathematical Methods in Pavement and Geomechanical Systems, Florida, USA, 1998. [Attoh-Okine, N.O.; 1998]

Austrroads – “2002 Austroroads Pavement Rehabilitation Guide “- Final Draft AP-T15, Sydney,2002.[Austrroads, 2002]

Austrroads – “A Guide to the Visual Assessment of Pavement Condition”, Austrroads, Sydney, 1987. [Austrroads, 1987]

Balay, J.; Gomes Correia, A.; Jouve, P. Hornych, P. and Paute, J.L. – “Mechanical Behaviour of Soils and Unbouns Granular Materials, Modelling of Flexible Pavements – Recent Advances” 8th International Conference on Asphalt Pavements, Seattle, 1997. [Balay, J.; *et al*; 1997]

Baltzer, S., Ertman-Larsen, H.J., Lukanen, E.O. and Stubstad R.N. – "Prediction of AC Mat Temperatures for routine Load/Deflection Measurements". 4th International Conference on the Bearing Capacity of Roads and Airfields, Minneapolis 1994. [Baltzer, S. *et al*; 1994]

Basheer, I.A.; Najjar, Y.M. – “Modeling Cyclic Constitutive Behaviour by Neural Networks Theoretical and Real Data”. Proceeding of the 12th Engineering Mechanics Conference, La Jolla, California, 1998. [Basheer, I.A.; Najjar, Y.M.; 1998]

Basheer, P.E. – “Stress-strain behaviour of geomaterials in loading reversal simulated by time-delay neural networks”. Journal of Materials in Civil Engineering, May/June, 2002. [Basheer, P.E.; 2002]

BAY GEOPHISICAL – “Spectral Analysis of Surface Waves (SASW) Method” (<http://www.baygeo.com/html/sasw.html>) downloaded in 2004. [BAY GEOPHISICAL; 2004]

Bay, J and Stokoe, K.H. – “Development of a Rolling Dynamic Deflectometer for Continuous Deflection Testing of Pavements” Project Summary Report 1422-3F, Centre for Transportation Research, Texas, 1998. [Bay, J. and Stokoe, K.H., 1998]

Berthelot, C.; Scullion, T; Gerbrand, R. and Safronetz, L. – “Application of Ground Penetration Radar for Cold in-place Recycled Road Systems” – Journal of Transportation Engineering – American Society for Civil Engineers. Jul/Aug 2001, Vol.127 No. 4, 2001. [Berthelot, C. *et al*; dtd 2001]

Bishop,C.W. – “Neural Networks for Pattern Recognition”. Oxford University Press, U.K., 1999. [Bishop,C.W.; 1999];

Blaine, J and Burlot, R. – “Non-destructive Testing of Asphaltic Concrete using the Light Goodman Vibrator – Study of the influence of temperature on the viscoelastic properties of Material”- Journal of the Association of Asphalt Paving Technologist, Vol. 39, 1970 [Blaine, J and Burlot, R.; 1970]

Bock, R.K. – “Maxwell’s equations” 1998
(<http://rd11.web.cern.ch/RD11/rkb/PH14pp/node108.html>) [Bock, R.K.; 1998]

Borenstein, E. – “Neural Networks”. (<http://www.cs.tau.ac.il/~borens/courses/alw-04b>), 2004. [Borenstein, E.; 2004]

Brown, S.F. and Brunton, J.M. – “An Introduction to the Analytical Design of Bituminous Pavements”. 3rd Edition, Nottingham, 1990. [Brown, S.F.and Brunton, J.M.; 1990]

Burmister, D.M –“The general theory of stresses and displacements in layered soil systems”, Journal of Applied Physics, Vol. 6, No. 2, pp. 89-96, No. 3, pp. 126-127; No. 5, pp. 296-302, 1945 [Burmister, 1945]

Burmister, D.M -“The theory of stresses and displacements in layered systems and applications to the design of airport runways”, Proceedings of Highway Research Board, pp. 126-148, 1943. [Burmister, 1943]

Capitão, S. – “Caracterização mecânica de Misturas Betuminosas de Alto Modulo de Deformabilidade”. Ph.D. thesis, Coimbra, 2003. (in Portuguese) [Capitão, S. 2003]

Carpenter, G.A. and Grossberg, S. – “The ART of Adaptive Pattern Recognition by self-Organizing Neural Network”. Computer, 1988.[Carpenter, G.A.; Grossberg, S.;1988]

Cement and Concrete Association of Australia – “Thickness Design for Concrete Roads pavement - Cement and Concrete Association of Australia, 1982. [CCAA; 1982]

Centre de Recherches Routières – “Code de Bonne Practiquepour la Formulation des Enrobés Bitumineux”, Recommandation C.R.R.-R 69/97, Bruxelles, 1997. [CRR, 1997]

Ceylan, H.; Tutumluer, E. and Barenberg, E.J. – “Artificial Neural Network Analysis of Concrete Airfield Pavements Serving the Boeing B-777 Aircraft”. Transportation Research Record 1684, Washington, D.C., U.S.A., 1999. [Ceylan, H. *et al*; 1999]

Chadbourn, B.A., Luoma, J.A., Newcomb D.E. and Voller, V.R. – "Consideration of Hot Mix Asphalt Thermal Properties During Compaction" – Quality Management of Hot Mix Asphalt, ASTM STP 1299, 1996. [Chadbourn, B.A. *et al*; 1996]

Chen, D.H. – “Determination of bedrock depth from FWD data” Texas Department of Transportation, Texas, 2000. [Chen, D.H., 2000]

Cheng, Y.P., Bolton, M.D. and Nakata, Y. – “Micromechanical modelling of soil plasticity using Distinct Element Method (DEM)” – University of Cambridge, 2001 [http://www-civ.eng.cam.ac.uk/geotech_new/posters/helen.pdf] [Cheng, Y.P., *et al*, 2001]

Chou, J., O'Neill, W.A. and Cheng, H.D. – “Pavement Distress Classification Using Neural Networks”. Proceedings IEEE International Conference on Systems, Man, and Cybernetics, Vol.1, 1994. [Chou, J. *et al*; 1994].

Chou, Y.T – “Structural Behaviour of Flexible Airfield Pavements Pavements”. Proceeding of Bearing Capacity of Roads and Airfields, Trondheim, 1982. [Chou, Y.T.; 1982]

Cimadevilla, E.L. – “Prospección Geofísica de Alta Resolución mediante Geo-Radar Aplicación a Obras Civiles” CEDEX, Madrid, Spain, 1996. (in Spanish) [Cimadevilla, E.L., 2000]

Claessen, A.I.M.; Edwards, J.M.; Sommer, P. and Ugé, P. – “Asphalt Pavement Design. The Shell Method”. Fourth International Conference on Structural Design of Asphalt Pavements , 1977. [Claessen, A.I.M. *et al*; 1977]

Concrete Society, The – “Guidance on Radar Testing of Concrete Structures” Technical Report N° 48. Slough, 1997. [The Concrete Society, 1997]

COST 325 – “New road monitoring equipment and methods” – Final report of the Action 1997. [COST 325, 1997]

COST 333 – “Development of new bituminous pavement design method”, Final report of the Action, 1999. [COST 333, 1999]

COST 336 – “Falling Weight Deflectometer”, Final report of the Action, Final Draft, 2002. [COST 336, 2002]

COST 343 – “Reduction of road closures by improved pavement maintenance procedures”, Lisbon, 2002. [COST 343, 2002].

Craven, M.P. – “A Faster Learning Neural Network Classifier Using Selective Backpropagation”. Proceedings of the Fourth IEEE International Conference on Electronics, Circuits and Systems, Cairo, Egypt, December 15-18, 1997. (<http://www.crg.cs.nott.ac.uk/people/Mike.Craven/icecs97backprop.pdf>) [Craven, M.P., 1997]

CROW – “Deflection profile – not a pitfall anymore” Record 17, Ede, 1998. [CROW, 1998]

CROW – “Toepassing Radartechniek in de Wegenbouw”; CROW Publicatie 149, Ede, 2000. [CROW, 2000]

CROW – “Uniformering Evaluatiemethodiek Cementbetonverhardingen” Record 136, Ede, 1999. [CROW, 1999]

Davis, J.L. and Annan, A.P. – “Ground-penetrating radar for high resolution mapping of soil and rock stratigraphy”, *Geophysical Prospecting* 37, 1989. [Davis, J.L.; Annan, A.P.; 1989]

de Beer, M.; Fisher, C. – “Evaluation of Non-Uniform Tyre Contact Stresses on Thin Asphalt Pavements”. *Response Models*, dd2004. [de Beer, M.; Fisher, C.; dd2004]

de Jong, D.L.; Peutz, M.G.F and Korswagen, A.R.; - “Computer program BISAR” – External Report AMSR.0006.73, Shell-Laboratorium, Amsterdam, 1973. [de Long, D.L. *et al*, 1973].

Dérobot, X. Dérobot, C. Fauchard, PH. Côte, E. Guillaumont – “The performance of pavement testing radars at test sites”, *Bulletin des Laboratoires des Ponts et Chaussées* - 230 - January February, 2001. <http://www.lcpc.fr/fr/sources/blpc/index230uk.dml> [Dérobot, X *et al*; 2001]

Descornet, G. – “The HERMES Project” Additional session 39, XXIInd World Road Congress, Durban, 2003. [Descornet, G, 2003].

Descornet,G; - “Inventory of High-Speed Longitudinal and Transverse Road evenness Measuring Equipment in Europe, Filter Project Forum of European National Highway Research Laboratories Technical Note 199/01, Brussels, 2002. [Descornet, 2002].

Djärf, L. Wiman, L.G. and Carlson, H.; - “A new flexible pavement design method” VTI meddelande N° 778A, Linköping, 1996. [Djärf, L. *et al*; 1996].

Dommelen, A. E. van – “Residual life concepts”, FWD/Backcalculation workshop, 6th International Conference on the Bearing Capacity of Roads, Railways and Airfields (BCRA), Lisbon, 2002. [Dommelen, A. E. van; 2002]

FAA – “Airport Pavement Design and Evaluation”. Federal Aviation Administration, Washington, D.C., 1978. [FAA; 1978].

Faley, C. – “Artificial Neural Networks” – Colin Fahey’s Guide. [<http://www.colinfahey.com>], 2003. [Faley, C.; 2003]

Ferregut, C.; Abdallah, I. Melchor-Lucero, O. and Nazarian, S. – “Artificial Neural Networks-Based Methodologies for Rational Assesment of Remaining Life of Existing Pavements”. Report TX-99 1711-1, Texax Department of Transportation, Austin, U.S.A., 1999. [Ferregut, C. *et al*; 1999]

Ferreira, H.N. and Nunes, M.M. – “Possibilidade de Controlar a Compactação de Aterros pelo Penetrómetro Dinâmico Ligeiro”, Informação Técnica LNEC, Lisboa, 1990. [Ferreira, H.N. and Nunes, M.M.; 1990]. (in Portuguese)

Ferreira, P. – “Prediction of Permanent Deformation in Bituminous Layers of Pavements”- Master of science thesis, Lisbon, Portugal, 2001 [Ferreira, P., 2001]

Ferrez, J.A.; Müller, D. and Liebling, Th. M. – “Parallel Implementation of a Distinct Element Method for Granular Media Simulation on the Cray T3D” Internal Report RO960718, Lausanne, 1996. (<http://dmawww.epfl.ch/roso.mosaic/papers/paracundall/paracundall.html>) [Ferrez, J.; *et al*; 1996]

FHWA – “Development of a Tire/Pavement Contact-Stress Model Based on Artificial Neural Networks”. Federal Highway Administration, FHWA-RD-99-041, U.S.A., 2001. [FHWA, 2001]

FHWA – “Ground Penetrating Radar for Measuring Pavement Layer Thickness”. Federal Highway Administration FHWA-HIF-00-015. U.S.A., downloaded in 2004. (<http://www.fhwa.dot.gov/infrastructure/asstmgmt/gprbroc.pdf>) [FHWA, 2004b]

FHWA – “Guide for Mechanistic-Empirical Design, New and Rehabilitated Pavement Structures 2004” Federal Highway Administration, NCHRP 1-37A Guide. U.S.A, downloaded in 2004. (<http://www.fhwa.dot.gov/pavement/>) [FHWA, 2004a]

FINDLAY IRVINE – “The Grip Tester. Summary of design and use: Airports”, August 2000. [Findlay Irvine, 2000]

Finish Geotechnical Society, The, “Ground penetrating radar – Geophysical research methods” Tampere, 1992. [The Finish Geotechnical Society, 1997]

Fontul, S; Antunes, M.L and Marcelino, J. “Aplicação das Redes Neurais na Caracterização Estrutural de Pavimentos” 2º Congresso Rodoviário Português, Lisbon, 2002. (in Portuguese) [Fontul, S. *et al*; 2002b]

Fontul, S; Antunes, M.L and Marcelino, J. “Structural evaluation of Pavements Using Neural Networks”. Proc. “2nd European FWD User’s Group Meeting”, Cascais, Portugal, 2002a.[Fontul, S. *et al*; 2002a].

Fontul, S; Antunes, M.L and Marcelino, J. “Structural evaluation of Pavements Using Neural Networks”. Proc. of 3rd International Conference on Maintenance and rehabilitation of Pavements and Technological Control (ed. Pereira, P.& Branco, F.), Guimarães, Portugal, 2003.[Fontul, S. *et al*; 2003]

Fontul, S; Antunes, M.L; “Application of ground penetrating radar and falling weight deflectometer to pavement evaluation (case studies in Portugal)” Proc. “1st European FWD User’s Group Meeting”, Delft, 2001.[Fontul, S.; Antunes, M.L.; 2001]

Fontul, S; Antunes, M.L; “Utilização do Equipamento Radar na Caracterização Estrutural de Pavimentos” 1º Congresso Rodoviário Português, Lisbon, 2000. (in Portuguese) [Fontul, S; Antunes, M.L.;2000]

Forest, R. Pynn, J.; Alani, A. and Ferne B. – “The use of Ground Penetrating Radar for the monitoring of road properties” Transport Research Laboratory, Annual research review 2003, U.K; 2003. [Forest, R. *et al*; 2003]

FORMAT – “Assessment of high speed monitoring prototype equipment”, Fully Optimised Road Maintenance report D12, 2004. [FORMAT, 2004]

FORMAT – “Inception Report”, Fully Optimised Road Maintenance, 2002. [FORMAT, 2002a].

FORMAT – “Selection of Maintenance Techniques and Procedures for Implementation”, Fully Optimised Road Maintenance report D2, 2002. [FORMAT, 2002b]

Freire, A.C. – “Deformações Permanentes de Misturas Betuminosas em Pavimentos Rodoviários”. Ph. D. Thesis, Lisbon, Portugal, 2002. (in Portuguese) [Freire, A.C.; 2002]

Freire, A.C. – “Estudos Relativos a Camadas de Pavimentos Constituídas por Matérias Granulares”, Master of Science Thesis, Lisbon, 1994. (in Portuguese) [Freire, A.C.; 1994].

Freitas, E. – “Contribuição para o Desenvolvimento de Modelos de Comportamento dos Pavimentos Rodoviários Flexíveis – Fendilhamento com origem a superfície”; Ph. D. Thesis, Guimarães, 2004. (in Portuguese) [Freitas, E.; 2004]

Fwa, T.F.; Tan, C.Y. and Chan, W.T. – “Genetic-Algorithm Based Approach for Backcalculation Analysis of Pavement”. Transportation Research Board 76th Annual Meeting, Washington, D.C., 1997. [Fwa, T.F. *et al* 1997]

Geo-Log, Inc. 2004 – “DYNAFLECT - Dynamic Deflection Determination System” Texas, 2004 (<http://www.dynaflect.com/>). [Geo-Log, Inc. 2004]

Geophysical Survey System, Inc. – “SIR SYSTEM-10H User’s Manual”, North Salem, 1994. [GSSI, 1994]

George, K.P., Bajracharya, M. and Stubstad, R – “Subgrade Characterization Employing the Falling Weight Deflectometer”; 83rd Annual Meeting of the Transportation Research Board, Washington, D.C., U.S.A., 2004. [George, K.P. *et al*; 2004]

Ghaboussi, J. and Wu, X. – “Soft computing with neural networks for engineering applications: fundamental issues and adaptive approaches”. Structural Engineering Mechanics – 1998.[Ghaboussi, J. and Wu, X.; 1998]

Ghaboussi, J.; Sidarta, D.E. – “New Nested Adaptive Networks (NANN) for Constitutive Modeling”. Computer and Geotechnics, Vol. 22, n^o 1, 1998. [Ghaboussi, J.; Sidarta, D.E.; 1998].

Gomes Correia, A. – “Review of Models and Modelling of Unbound Granular Materials”. COST 337, Workshop on *Modelling and Advanced Testing for Unbound Granular Materials*, Lisbon, January. 1999. [Gomes Correia, A.; 1999]

Groenendijk, J. and Molenaar, A.A.A. – “Pavement Design Methods” Delft University of Technology Report 7-93-209-31, The Netherlands, 1993

GSSI - “Advanced Road Structure Assessment Module for RADAN-NT processing system”, North Salem 2001. [GSSI, 2001]

GSSI - “RADAN for windows, RADACT processing system, user’s manual”, North Salem 1996. [GSSI, 1996]

Hall, J. – “Rolling Wheel Deflectometer – for highways pavements” – Status of research and development, USA, 1999 [Hall, J.;1999]

Hall, K and Correa, C –“Effects of Subsurface Drainage on Performance of Asphalt and Concrete Pavements”, NCHRP Report 499, Transport research Board, Washington, D.C., 2003 [Hall, K and Correa, C, 2003]

-
- Hausmann, L.D.; Tutumluer, E. and Barenberg, E.J. – “Neural Network Algorithms for the Correction of Concrete Slab Stresses from Linear Elastic Layered Programs, Preprint n° 970540, 76th Meeting of Transportation Research Board, Washington, D.C., 1997;
- Hecht-Nielsen, R. - “Neurocomputing”, Addison-Wesley, New York, 1989. [Hecht-Nielsen, R.; 1991]
- Hicks, R. G.; Seeds, S. B. and Peshkin, D.G. – “Selecting a preventive maintenance treatment for flexible pavements”, Presentation for Foundation for Pavement Preservation, 1999. [Hicks, R. G. *et al*; 1999]
- Highways Agency – “Design Manual for Roads and Bridges” Structural Assessment Methods, HA 72/94 Volume 7, Section 3, The stationary office, London, U.K. 1994. [Highways Agency, 1994]
- Highways Agency – “Design Manual for Roads and Bridges” Structural Assessment Methods, HD 29/94, The stationary office, London 2001 [Highways Agency, 2001].
- Hildebrand, G.; Rasmussen, S.; Andrés, R. “Development of a Laser Based High Speed Deflectograph” Non-destructive Testing of Pavement and Backcalculation of Moduli: Third Volume, ASTM STP 1375, 1999. [Hildebrand, G *et al*, 1999].
- Hopfield, J.J. and Tank, D.W. – “*Neural* computation of decision in optimization problems”, Biological Cybernetics, Vol.52,1985. [Hopfield, J.J.; Tank, D.W.; 1985].
- Hopman, P.C.; - “Concept manual VEROAD” Version 1.5 – Netherlands pavement Consultant, Utrecht 1998. [Hopman, P.C.; 1998]
- Hopman, P.C.; Pronk, A.C.; Kunst, P.A.J.C., Molenaar, A.A.A. and Molenaar, J.M.M. – “Application of the visco-elastic properties of asphalt concrete” – 7th International Conference on Asphalt Pavements, Nottingham, 1992.
- Houben, L.J.M.; Vogelzang, C.H. and Dommelen, A.E. van – “LINTRACK Rutting Research Project – ALT Testing Program” 6th International Conference on the Bearing Capacity of Roads, Railways and Airfields (BCRA), Lisbon, 2002. [Houben, L.J.M. *et al*; 2002]
- ICAO – “Aerodrome Design Manual – Part 3 – Pavements”2nd Ed. 1983. [ICAO; 1983]

Intrator, N. – “Artificial Neural Networks” – Machine Learning, Foundations: Lecture 8, Spring, Summer 2003/4 – School of Mathematical Sciences Tel Aviv, downloaded in 2004. [http://www.math.tau.ac.il/~nin/Courses/ML04/scribe_ANNB.pdf] [Intrator, N.; 2004]

Ioannides, A.M. – “Concrete pavement backcalculation using *ILLI-BACK 3.0* “Non-destructive Testing of Pavement and Backcalculation of Moduli: Second Volume, ASTM STP 1198, 1994. [Ioannides, A.M.; 1994]

Ioannides, A.M.; Alexander, D.R., Hammons, M.I. and Davis, C.M. – “Application of Artificial Neural Networks to Concrete Pavement Joint Evaluation”. Transportation Research Record n° 1540, Washington, D.C., U.S.A., 1996. [Ioannides, A.M. *et al*; 1996]

Irwin, L.H. “Backcalculation: An overview and perspective” FWD / Backcalculation Workshop 3 – 6th International Conference on the Bearing Capacity of Roads, Railways and Airfields - BCRA 2002, Cascais, 2002. [Irwin, L.H.; 2002]

JAE – “Catálogo de Degradações dos Pavimentos Rodoviários Flexíveis” – 2^a versão Junta Autónoma de Estradas, Lisboa, 1997. [JAE, 1997] (in Portuguese)

JAE – “Manual de Concepção de Pavimentos para a Rede Rodoviária Nacional” Junta Autónoma de Estradas, Lisboa, 1995. [JAE, 1995] (in Portuguese)

Jaselskis, E.J.; Grigas, J. and Brilingas, A. – “Dielectric properties of asphalt pavement”. Journal of Materials in Civil Engineering, September-October; 2003. [Jaselskis, E.J. *et al*; 2003]

Johnson R. - “A Rolling Weight Deflectometer for Quantitative Pavement Measurements” TP-367, QUEST Integrated, USA, 1995. [<http://www.qi2.com/rwdorig.html>] [Johnson, R.; 1995]

Johnson, A.M. – “Best Practice Handbook on Asphalt Pavement Maintenance” – Report N° MN/RC – 2000-04, U.S.A, 2000. [Johnson, A.M.; 2000]

Kameyama, S.; Himeno, K.; Kasahara, A. and Maruyama, T. – “Backcalculation of Pavement Layer Moduli Using Genetic Algorithms” 8th International Conference On Asphalt Pavements, Ann Arbor, 1998 [Kameyama, S *et al*, 1998]

Kaseko, M.S.; Lo, Z.P. and Ritchie, S.G. – “Comparison of Traditional and Neural Classifiers for Pavement Crack Detection”, Journal of Transportation Engineering, ASCE, Vol 120, n° 4, July/August 1994. [Kaseko, M.S. *et al*; 1994]

Kenedy, C.K.; Fevre, P. and Clark, C.S. - “Pavement Deflection Equipment for Measurement in the United Kingdom” TRRL Report 834, Transport and Road Research Laboratory, UK, 1978. [Kenedy, C.K. *et al*, 1978].

Kerr, A.D. – “ Elastic and visco-elastic foundations models. Journal of Applied Mechanics, ASME, 1964

Kestler, M.A. – “Current and Proposed Practices for Non-destructive Highway Pavement Testing” Special Report N° 97-28 US Army Corps of Engineer, 1997 (http://www.crrel.usace.army.mil/techpub/CRREL_Reports/reports/SR97_28.pdf) [Kestler, M.A.; 1997]

Khazanovich, L. – “Dynamic analysis of FWD test results for rigid pavements”1999. Non-destructive Testing of Pavement and Backcalculation of Moduli: Third Volume, ASTM STP 1375, 1999.

Khazanovich, L. - “Finite Element Analysis of Curling of Slabs on Pasternak Foundation”, 16th ASCE Engineering Mechanics Conference, July 16-18, Seattle 2003.

Khazanovich, L. and Roesler, J. – “DIPLOBACK: A Neural-Networks_Based Backcalculation Program for Composite Pavements”. Transportation Research Record n° 1570, Washington, D.C., U.S.A., 1997. [Khazanovich, L.; Roesler, J; 1997].

Kim, Y. and Kim R. – “Prediction of Layer Moduli from Falling Weight Deflectometer and Surface Wave Measurements Using Artificial Neural Network”. Transportation Research Record n° 1639, Washington, D.C., U.S.A., 1998. [Kim, Y.; Kim R.; 1998]

King, R.W.P. and Smith, G.S.; “Antennas in matter”, Mit press, 1981

King,M.L. – “Locating a subsurface oil leak using Ground Penetrating Radar” (http://www.geosurvey.co.nz/Subsurface_oil_leak_GPR.pdf). downloaded 2004. [King,M.L., dld 2004]

Kohonen, T. – “Self Organized Formation of Topologically Correct Feature Maps”. *Biological Cybernetics*, Vol. 43; 1982. [Kohonen, T.; 1982]

Koivo, H.N. – “NEURAL NETWORKS: Basics using MATLAB Neural Network Toolbox”. (<http://www.control.hut.fi/Kurssit/AS-74.115/Material/Nn2000.pdf>), 2000. [Koivo, H.N; 2000]

Kopperman, S.; Tiller, G. and Tseng, M.; - “ELSYM 5, Interactive Microcomputer Version – User’s Manual”, Report n° FHWA-RD-85, Georgetown Pike, U.S.A., 1985. [Kopperman, S. *et al*, 1985]

LCPC – “French Design Manual for Pavements”, Laboratoire Central des Ponts et Chaussées, Paris, 1997. [LCPC, 1997]

LCPC – “Auscultation – Road Evaluation, downloaded 2004. (<http://perso.wanadoo.fr/r-et-//AUSCULT.htm>); (in French). [LCPC, 2004]

Lebas, M.; Peybernard, J. and Carta, V. – “*Méthode de traitement des enregistrements de mesures de densité en continu*”, Bulletin de Liaison des Laboratoires de Ponts et Chaussées, 114, Juillet/Août; 1981. (in French) [Lebas, M. *et al*; 1981]

Lenngren C A – “Rolling Deflectometer meter data strategy dos and don'ts” Proceedings of 5th International Conference on the Bearing Capacity of Roads and Airfields, Norway, 1998. [Lenngren C A, 1998]

Lima, H.; Quaresma, L. and Fonseca, E. – “Caracterização do Factor de Agresividade do tráfego de Veículos Pesados em Portugal” Rel. Proc° 092/16/12991, LNEC, Lisboa, 1999. (in Portuguese) [Lima, H. *et al*; 1999]

Lin, T. – “Neural Network: The solution to true AI” (<http://home.ipoline.com/~timlin/neural/NeuralNetwork>). [Lin, T.; 2002]

Lo, J.Y. and Floyd, C.E. – “Application of Artificial Neural Networks for Diagnosis of Breast Cancer”. Evolutionary programming and neural networks applied to breast cancer research (<http://garage.cps.msu.edu/cec99/specialSessions/land.html>). Downloaded in 2004.

LTPP – “Phase I: Validation of guidelines for k-value selection and concrete pavement performance prediction) – Publication no. FHWA-RD-96-198, McLean, 1997. [LTPP, 1997]

Lytton, R.L. – “Characterising Asphalt Pavement for Performance”. Paper No 00-2878, 2000. [Lytton, R.L.; 2000]

Marcelino, J. – “Application of neural networks in geotechnical engineering” Proc. “3rd International Workshop of Applications of Computational Mechanics in Geotechnical Engineering”, Porto, September 1998. [Marcelino, J.;1998]

Marcelino, J. – “Modelling of collapse and creep in embankments”, - Ph.D. thesis, Lisbon 1996. (in Portuguese). [Marcelino, J.;1996]

Marchand, J.P., Dauzats, M., Lichtenstein, H. and Kobisch, R. – “*Quelque Formule Utiles por le Calcul des Chaussées sur Petites Calculatrices Programmables*”, Bulletin de Liason des Laboratoires de Ponts et Chaussées, 114, Juillet/Août; 1981. (in French) [Marchand, J.P. et al; 1981]

Maser, K et al.; “Ground Penetrating Radar Surveys to Characterize Pavement Layer Thickness Variation at GPS Sites” Transport Research Board, 72nd Annual Meeting. Washington, D.C., 1993. [Maser, K et al; 1993]

Maser, K. and Scullion, T.; “Automated Pavement Subsurface Profiling Using Radar: Case Studies of Four Experimental Field Sites”. TRR 1344, Transport Research Board, Washington, D.C., 1992. [Maser, K. and Scullion, T.; 1992]

Masri, S., Smyth, A., Chassiakos, A., Caughey, T. and Hunter, N. – “Application of Neural Networks for detection of changes in nonlinear systems”. ASCE Journal of Engineering Mechanics 126, 1999;

Meier, R.; Alexander, D.R. and Freeman, R.B. – “Using Artificial Neural Networks as a Forward Approach to Backcalculation”. Transportation Research Record n° 1570, Washington, D.C., U.S.A., 1997. [Meier, R. et al; 1997]

Meier, R.W. and Rix, G.J. – “Backcalculation of flexible pavement moduli using artificial neural networks”, TRR No. 1448, TRB, National Research Council, Washington, D.C. 1994. [Meyer, R.W. and Rix, G.J.; 1994]

Meier, R.W. and Tutumluer, E. – “Uses of Artificial Neural Networks in the Mechanistic-Empirical Design of Flexible Pavements”, Proceedings of the International Workshop on

Artificial Intelligence and Mathematical Methods in Pavement and Geomechanical Systems, Florida, USA, 1998. [Meyer, R.W.; Tutumluer, E.; 1998]

Meier, R.W. and Tutumluer, E. – “Uses of artificial neural networks in the mechanistic-empirical design of flexible pavements”, Paper submitted for the International Workshop on Artificial Intelligence and Mathematical Methods in Pavement and Geomechanical Engineering System, June 1998. [Meier, R.W. and Tutumluer, E. ; 1998]

Meier, R.W.; Alexander, D.R.; and Freeman R – “A Forward Approach to Backcalculation Using Artificial Neuronal Networks” Transportation Research Board 76th Annual Meeting Paper N° 970235, 1997. [Meier, R.W *et al*; 1997]

Meier, R.W.; Marshall, C. – “Genetic Algorithms Coupled with Neural Networks Present New Possibilities for Backcalculation”. FWD / Backcalculation Workshop 3 – 6th International Conference on the Bearing Capacity of Roads, Railways and Airfields - BCRA 2002, Cascais, 2002. [Meier, R.W *et al*; 2002]

Mesnil-Adelée, M.; Peybernard, J – “*Traitement automatique des résultats de mesures en continu – Application aux mesures de déflexion*”, Bulletin de Liaison des Laboratoires de Ponts et Chaussées, 130, Mars/Avril, 1984. [Mesnil-Adelée, M.; Peybernard, J.; 1984].

Miller, A; Blott, B. and Hames, T. – “Review of Neural Network Applications in Medical Imaging and Signal Processing Medical and Biological Engineering and Computing” (1992) (<http://www.openclinical.org/neuralnetworksrefs.html>). Downloaded in 2004.

MINCAD Systems – “CIRCLY 4 – User Manual” Mincad Systems, Australia, 1999. [MINCAD Systems, 1999]

Mogas, J. and Pinelo, A. – “Avaliação das Características Superficiais dos Pavimentos das Pistas dos Aeroportos de Lisboa, Porto e Faro”. LNEC- Rel. Proc° 92/1/8569, Lisbon, 1986 [Mogas, J. and Pinelo, A.; 1986]

Montgomery, D.C – "Design and Analysis of Experiments" – Fifth Edition, 2000

Montgomery, D.C – "Introduction to statistical quality control" – Third Edition, 1996.

Montgomery, D.C. and Runger, G.C. – "Applied statistics and probability for engineers" – Second Edition, 1999

Moody, J. and Darken, C. – “Fast Learning in Networks of Locally-Tuned Processing Units”. *Neural Computation*, Vol 1., 1989. [Moody, J.; Darken, C.; 1989]

MOPU – “Secciones de Firme” Instrucción 6.1-I.C. y 6.2-I.C., Ministerio de Obras Publicas y Urbanismo, Madrid, 1990] [MOPU, 1990]

Najjar, Y.M. and Basheer, I.A. – “Modelling the Durability of Aggregate Used in Concrete Pavement Construction: A Neuro-Reliability-Based Approach, Final Report KS-97-3, Kansas Department of Transportation, Topeka, U.S.A., 1997. [Najjar, Y.M.; Basheer, I.A.; 1997].

NATO – “Pavement Evaluation and Reporting Strength of NATO Airfields (PAVERS)” NATO STANDARD, Draft, 2000. [NATO; 2000]

Nave, R – “Electromagnetic wave concepts” dtd 2004. [<http://hyperphysics.phy-astr.gsu.edu/hbase/waves/emwavecon.html#c1>]

NPMA – “Pavement Surface Condition Field Rating Manual for Asphalt Pavements” – Northwest Pavement Management Association, U.S.A., 1999 [NPMA, 1999]

OECD – “Full Scale Pavement Test” Proceedeings of Concluding Conference – Force Project, France, 1991. [OECD; 1991]

Oliveira, M.M.P and Coelho, M.J. – “Aqueduto das Águas Livres, Lisbon – Geophysical Auscultation by Ground Penetrating Radar” - LNEC – Report Proc 054/533/1117, Lisbon, December 1994. (in Portuguese) [Oliveira, M.M.P; Coelho, M.J.;1994]

Ovik, J., Birgisson, B. and Newcomb, D – "Characterizing Seasonal Variations in Flexible Pavement Material Properties" TRR 1684 – Issues in the Design of New Rehabilitated Pavements - Transport Research Board, Washington, D.C; 1999. [Ovik, J. *et al*; 1999]

Pan, G. and Atluri, S.N. – “Dynamic response of finite size elastic runways subjected to moving loads: a coupled BEM/FEM approach”. *International Journal of Numerical methods in Engineering*; 1995. [www.sciencedirect.com]

Pan, G; Okada, H. and Atluri, S.N. – “Nonlinear transient dynamic analysis of soil-pavement interaction under moving load: a coupled BEM/FEM approach” *Engineering Analysis Bound Elements* 1994 [www.sciencedirect.com]

PARIS - "Performance Analysis of Road Infrastructure", Final Report, European Commission, Brussels, 1999. [PARIS; 1999]

Park, D.; Buch, N. and Chatti, K. – "Effective Layer Temperature Prediction Model and Temperature Correction Via Falling Weight Deflectometer Deflections" – TRR 1764 – Assessing and Evaluating Pavements, Transport Research Board, Washington, D.C. 2001. [Park, D *et al*; 2001].

Park, S. and Kim, R. – "Temperature Correction of Backcalculated Moduli and Deflections Using Linear Viscoelasticity and Time- Temperature Superposition" – TRR 1570 – Pavement Research Issues, Transport Research Board, Washington, D.C. 1997. [Park, S.; Kim, R.; 1997].

Parry, N.S.; Davis, J.L. and Rossiter, J.R. – "GPR Systems for Roads and Bridges". Proc. Of the Fourth International Conference on GPR, Rovaniemi, Finland, 1992.

Pei, J. and Smyth, A.W. – "A near-parametrized neural network approach for modelling non-linear hysteretic systems". 16th ASCE Engineering Mechanics Conference, July 16-18, University of Washington, Seattle, 2003. [Pei, J.; Smyth, A.W.; 2003]

Peng, J.; Li, Z. and Ma, B. – "Neural Network analysis of chloride diffusion in concrete". Journal of Materials in Civil Engineering, July/August 2002.

Penumadu, D.; Jin-Nan, L.; Chameau, J.L. and Arumugan, S. – "Rate-Dependent Behaviour of Clays Using Neural Networks". Proceedings of the 13th Conference of the International Society for Soil Mechanics and Foundation Engineering, Oxford and IBH Publishing Co., U.K. 1994. [Penumadu, D. *et al*; 1994]

Pereira, O.A. – "Determinação das Características Estruturais de Pavimentos a Partir da Linha de Influência Obtida em Ensaios de Carga com Pneu" – Thesis presented for obtaining the Specialist of LNEC degree. Lisbon 1969. [Pereira, O. A.; 1969]

PIARC – "Automated pavement Cracking Assessment Equipment – State of the Art" World Road Association – Technical committee on Surface Characteristics (C1), 2003 [PIARC, 2003]

Picado Santos, L. – "Consideração da Temperatura no Dimensionamento de Pavimentos Rodoviários Flexíveis" – Ph.D. Theses, Coimbra 1994 [Picado Santos, L.; 1994]

-
- Pinelo, A.M. – “Projecto e observação de pavimentos rodoviários”, Reseach program, Infrastructure Department, LNEC, Lisbon 1991. [Pinelo, A.M.; 1991]
- Powell, W.D.; Potter, J.F.; Mayhew, H.C. and Nunn, M.E. – “The Structural Design of Bituminous Roads” 1984 [Powell, W.D. *et al*; 1984]
- Prakas, S. – “Soil Dynamics”- Mc Graw-Hill, 1981. [Prakas, S.; 1981]
- Quaresma, L.M. – “Estudos relativos a pavimentos semi-rígidos. Dimensionamento e observação”. Thesis presented for the expert degree, LNEC, 1992. (in Portuguese) [Quaresma, L.M.; 1992].
- Ramos, C.M. – “Drenagem em Vias de Comunicação” Mestrado em Transportes, Instituto Superior Técnico, Lisboa. 2004. (in Portuguese) [Ramos, C.M.; 2004].
- Rmeili, E. and Scullion T. – “Detecting stripping in asphalt concrete layers using Ground Penetrating Radar. Transportation Research Record 1568, TRB, National Research Council, Washington D.C., 1997 [Rmeili, E. and Scullion T.;1997]
- Road Research Laboratory – “A Guide to the Structural Design of Pavements for New Roads” Road Note nº 29, 3rd Edition, London, 1970. [Road Research Laboratory, 1970]
- Roberts, C.A. and Attoh-Okine, N.O. – “Comparative Analysis of Two Artificial Neural Networks using Pavement Performance Prediction”. Computer Aided Civil and Infrastructure Engineering, Vol.13, nº 5, U.S.A., 1998. [Roberts, C.A.; Attoh-Okine, N.O.; 1998]
- Rohde, G.T. – “The mechanistic analysis of pavement deflections on subgrades varying in stiffness with depth”, Ph.D. Thesis, Department of Civil Engineering, Texas A&M University, Texas, 1990. [Rohde, G.T; 1990]
- Rohde, G.T. and Scullion, T – “MODULUS 4 – Expansion and validation of the MODULUS Backcalculation System” Research Report 1123-3, Texas, 1990. [Rohde, G.T. and Scullion, T; 1990]
- Rohde, G.T.; Yang, W. and Smith, R.E. – “Inclusion of depth to a rigid layer in determining pavement layer properties” 3rd International Conference on BCRA, Trondheim, 1990. [Rohde, G.T. *et al*; 1990]

Rumelhart, D.E.; Hinton, G.E. and Williams, R.J. – “Learning Internal Representations by Error Propagations”. Parallel distributed processing, Vol1. Cambridge, 1986. [Rumelhart, D.E. *et al*, 1986]

Saarenketo, T.– “Ground Penetrating Radar applications in road design and construction in Finnish Lapland”, Geological Survey of Finland, Special paper 15, 1992. [Saarenketo, T.; 1992]

Saarenketo, T; – “Using Ground Penetrating Radar and dielectric probe measurements in pavement quality control”, paper submitted for Presentation and publication at 1997 Annual Meeting of the Transportation Research Board, Washington, D.C., U.S.A., 1996. [Saarenketo, T.; 1996]

Sabbatinni, R.M.E. – “Neural Networks for Classification and Pattern Recognition of Biological Signals”. (<http://www.ibiblio.org/pub/academic/medicine/brazil-mirror/neuralnets/NIB-papers/biosignal.txt>). Downloaded in 2004.

Saim, R. and Sousa, J.B. – “Utilização e Verificação de Correlações Obtidas a Partir do Cone de Penetração Dinâmico em Portugal”. 1º Congresso Rodoviário Português, Lisbon, 2000. (in Portuguese) [Saim, R.; Sousa, J.B.; 2000].

Saldanha, P - “Methods of measurement for the structural condition of pavement”, downloaded 2004. (<http://www.civil.port.ac.uk/projects/hmaint/struct.htm>)

Salt Institute - “Deicing Salt and Corrosion” <http://www.saltinstitute.org>.

Saraiva, J.M. and Ebecken, N.F. – “Aplicação de redes neuronais artificiais no estudo da confinabilidade estrutural”. Revista Internacional de Métodos Numéricos para Cálculo y Diseño en Ingeniería, Vol.14,2, 1996.

Sayers, M. and Karamilhas, S. – “The little book of profiling”;1998. [Sayers M and Karamilhas, S.;1998].

Scullion, T– “Implementation of the Texas Ground Penetrating Radar system”, FHWA/TX-92/1233-1, Texas, 1994. [Scullion, T.; 1994]

Scullion, T and Saarenketo, T. – “ Implementation of ground penetrating radar technology in asphalt pavement testing” – Ninth International conference on Asphalt Pavements, Copenhagen, Denmark [Scullion, T.; Saarenketo, T.; 2002]

Scullion, T and Saarenketo, T. – “Using Suction and Dielectric measurements as Performance Indicators for Aggregate Base Material”, Transportation Research Record 1577, 1997. [Scullion, T.; Saarenketo, T.; 1997]

Scullion, T; Lau, C.L. and Chen, Y. – “Implementation of Ground Penetrating Radar System”, Texas Transportation Institute FHWA/TX-92/1233-1; 1992. [Scullion, T. *et al*; 1992]

Shekharan, A.R. – “Assesment of Relative Contribution of Input Variables on Pavement Performance Prediction by Artificial Neural Networks”. Paper prepared for presentation, annual meeting, Transportation Research Board, Washingto, D.C., 1999. [Shekharan, A.R.; 1999]

SHELL – “BISAR P.C. – User’s Manual”. Shell International Petroleum Company, London, U.K., 1995. [SHELL, 1995]

Shi, X.P.; Fwa, T.F. and Tan, S.A. – “Warping Stress in Concrete Pavements on Pasternak Foundation”, ASCE, TE6 (119), Reston, USA, 1993.

Shook, J.; Finn, F.; Witczak, M. and Monismith, C. – “Thickness Design of Asphalt Pavements – The Asphalt Institute Method”, Proceedings of the Fifth International Conference on Structural Design of Asphalt Pavements, Delft, The Netherlands, 1982. [Shook, J. *et al*; 1982]

SHRP – “Distress Identification Manual for long-term pavement performance program” – Federal Highway Administration Publication n° FHWA-RD-03-031 Georgetown Pike, 2003 [SHRP, 2003]

SHRP; “Ground penetrating radar surveys to characterise pavement layer thickness variations at GPS sites” – SHRP-P-397 – Washington, D.C. 1994. [SHRP, 2003]

Simonin, J.M. – “Evaluation of radar systems used for monitoring pavement layer thickness”; Bulletin des Laboratoires des Ponts et Chaussées - 238 - Mai June 2002; pp 51-60, 2002 <http://www.lcpc.fr/fr/sources/blpc/index238uk.dml> [Simonin, J.M. 2002]

Smith, K.L.; Titus-Glover, L. and Evans, L.D. –“Pavement Smoothness Index Relationship” - Federal Highway Administration Publication n° FHWA-RD-02-057 Washington, D.C., 2002. [Smith, K. L. *et al.*; 2002]

Sohn, H.; Worden, K. and Farrar, C. - “Statistical damage classification under changing environmental and operational conditions”. Journal of Intelligent Materials Systems and Structures 13, 2003;

Sorensen, A. – “Seismic Transducers for Monitoring FWD Deflections” Dynatest International, Denmark, 2004 (<http://www.dynatest.com/gallery/papers/seismic.htm>) [Sorensen, A.; 2004]

Specht, D.F. – “A General Regression Neural Network”. IEEE Transaction on Neural Networks, Vol.2, N° 6, 1991. [Specht, D.F.; 1991]

Statistica, Inc. – “Statistica for Windows” – Computer program manual, Tulsa 1998. <http://www.statsoft.com/textbook/stneunet.html>. [Statistica, Inc.; 1998]

Stergiou, C. and Siganos, D. – “Neural Networks” Report, Surveys and Presentations in Information Systems Engineering (SURPRISE) 96 Journal Imperial College London, downloaded in 2004. [http://www.doc.ic.ac.uk/~nd/surprise_96/journal/vol4/cs11/report.html] [Stergiou, C.; Siganos, D.; 2004]

Stet, M.; Thewessen; B. and Verbeek, J. – “Structural Assessment of Flexible and Rigid Airfield Pavement” FWD / Backcalculation Workshop 3 – 6th International Conference on the Bearing Capacity of Roads, Railways and Airfields - BCRA 2002, Cascais, 2002. [Stet, M *et al.*; 2002]

Stet, M; Beuving, E and Thewessen; B – 1998 – “Dutch Structural Evaluation Method for Jointed Airfield Pavements” – Fifth International Conference on the Bearing Capacity of Roads and Airfields – vol.1 pg 161-170 - Trondheim, Norway [STET, M *et al.*;1998]

Stubstad, R. N.; Lukanen, E. O.; Richter, C. A.; Baltzer S. – “Calculation of AC layer temperatures from FWD field data”, 5th International Conference on the Bearing Capacity of Roads and Airfields, Trondheim, July 1998. [Stubstad, R.N. *et al.*; 1998].

Terzi, S. and Salatan, M - “Modeling The Deflection Basin By Genetic Algorithms Approach” <http://www.ijci.org/volume1/ijci1-1/P038.pdf> , 2003.

-
- Theodorakopoulos, D.D. – “Dynamic Analysis of a Poroelastic Half-Plane Soil Medium Under Moving Loads”, Science Direct webpage (<http://www.sciencedirect.com/web-editions>), 2003. [Theodorakopoulos, D.D.; 2003]
- Tholen. O. – “Falling Weight Deflectometer – A Device for Bearing Capacity Measurement: Properties and Performance” – Ph.D. Thesis – Department of Highway Engineering Royal Institute of Technology – Stockholm, 1980 [Tholen, O.; 1980]
- Timm, D.; Birgisson, B. and Newcomb D – " Development of Mechanistic- Empirical Pavement Design in Minnesota" TRR 1629 Design and Rehabilitation of Pavements Transport Research Board, Washington, D.C. 1998. [Timm, D. *et al*; 1998].
- Tong, F. and Liu, X.L. – “On Training Sample Selection for Artificial Neural Networks using Number-Theoretic Methods”. The Forth International Conference on Engineering Computational Tecnology”; Lisbon, 2004.
- TRB - “Effects of Subsurface Drainage on Performance of Asphalt and Concrete Pavements” – NCHRP Report 499 –TRB, National Academy Press Washington, D.C. 2003.
- TRB - “Ground penetrating radar for evaluation subsurface conditions for transportation facilities” – NCHRP Synthesis 255 –TRB, National Academy Press Washington, D.C. 1998. [TRB, 1998]
- TRB – “Use of Artificial Neural Networks in Geomechanical and Pavement Systems”. Transportation Research Circular Number E-C012. Transportation Research Board, Washington, D.C. 1999. [TRB, 1999]
- Tutumler, E. and Seyhan, U. – “Neural Network Modeling of Anisotropic Aggregate Behaviour from Repeated Load Triaxial Tests”. Transportation Research Record n° 1615, Washington, D.C., U.S.A., 1998. [Tutumler, E.; Seyhan, U.; 1998]
- Tutumluer, E. and Meier, R.W. – „ Attempt at Resilient Modulus Modelling Using Artificial Neural Networks“. Transportation Research Record 1540, Washington, D.C., USA ,1996.
- Uddin, W. – “Finite Element Modelling and Simulation of FWD Dynamic Load Tests”. FWD / Backcalculation Workshop 3 – 6th International Conference on the Bearing Capacity of Roads, Railways and Airfields - BCRA 2002, Cascais, 2002. [.; 2002]

Uddin, W., Hudson, W.R and Stroke II, K.H. – “A structural evaluation methodology for pavements based on dynamic deflections”, Research Report 3987-1, CTR, Texas, 1986. [Uddin, W. *et al*, 1985]

Uddin, W., Meyer, A.H. and Hudson, W.R. – “Rigid Bottom Considerations for Nondestructive evaluation of Pavements” – Transportation Research Record 1070, Washington, D.C., 1986. [Uddin, W. *et al*, 1986]

Ullidtz, P. – “Analytical Tools for Design of Flexible Pavements” –Keynote – International Society for Asphalt Pavements (ISAP), - 9th International conference on Asphalt Pavements, Copenhagen, 2002. [Ullidtz, P.; 2002]

Ullidtz, P. – “Modelling flexible pavement response and performance” –Technical University of Denmark, 1998. [Ullidtz, P; 1998]

Ullidtz, P. – “Pavement Analysis” –Technical University of Denmark, Lyngby, 1997. [Ullidtz, P; 1987]

Ulriksen P. – “Application of impulse radar to civil engineering” – Lund University of Technology, Doctoral Thesis, Lund, 1982 [Ulriksen, P.; 1982],

US Army Engineer – “Portable Seismic Pavement Analyzer” – Fact sheet, 1999 (<http://pavement.wes.army.mil/factsheets/portable.pdf>) [US Army Engineer, 1999]

Uzan, J.; Witczak, M.W.; Scullion, T. and Lytton, R.L. – “Development and Validation of Realistic Pavement Response Models”. 7th International Conference of Asphalt Pavements, Nottingham, U.K., 1992. [Uzan, J. *et al*; 1992]

Van Cauwelaert, F. – “Coefficients of Deformation of an Anisotropic Body”, Jurnal of the Engineering Mechanics Division, American Society of Civil Engineers, 1977. [Van Cauwelaert, F; 1977].

Van Gorp, C.A.P.M. – “Characterisation of Seasonal Influences on Asphalt Pavements with the use of Falling Weight Deflectometer”. Ph.D. Thesis, Delft, the Netherlands, 1995. [Van Gorp, C.A.P.M.; 1995]

- Van Leest, A.J.– “Pavement surveying with Euroradar: High speed measurements of layer thickness and defects, experiences on roads and airfields in Holland”- 5th International Conference on the Bearing Capacity of Roads and Airfields. [Van Leest, A.J.;1998].
- Wambold, C.J; Antle, C.E.; Henry, J.J. and Rado, Z; - “International PIARC experiment to compare and harmonise texture and skid resistance measurements, PIARC, 1995. [Wambold, C.J *et al*; 1995]
- Wang, K.C.P., Nallamothe, S. and Elliot, R.P. – “Classification of Pavement Surface Distress with an Embedded Neural Net Chip”. Manuals and Reports on Engineering Practice, ASCE, 1998. [Wang, K.C.P. *et al*; 1998]
- Wasserman, P. D. – “Neural Computing: Theory and Practice” Van Nostrand Reinhold, New York, 1989. [Wasserman, P. D.; 1989].
- Westergaard, H.M.S. – “New formulas for stress in concrete pavements of airfields”, ASCE, 1947. [Westergaard, H.M.; 1947].
- White, D.W.; Haddock, J.E.; Hand, A.J.T and Fang, H. – “Contribution of Pavement Structural Layers to Rutting of Mix Asphalt Pavements”. National Cooperative Highway Research Program (NCHRP) Report 468, Washington, D.C., 2002. [White, D.W. *et al*; 2002]
- Wimsatt, A.J., Ragsdale, J., Scullion, T. and Servos,S - “Use of Seismic Pavement Analyser in Monitoring Degradation of Flexible Pavements Under Texas Mobile Load Simulator (A Case Study)”, Transportation Research Board (TRB) 77th annual meeting, Washington, D.C., 1998 [Wimsatt, A.J *et al*; 1998]
- WSDOT Pavement guide – downloaded 2004 (http://hotmix.ce.washington.edu/wsdot_web/Modules/04_design_parameters/04-2_body.htm#r-value) [WSDOT; 2004]
- Yoder, E.J.; and Witczak, M.W. – “Principles of Pavement Design”, 2nd Edition, John Wiley and Sons, Inc., 1975. [Yoder, E.J.; and Witczak, M.W.; 1975]
- You, Z. and Buttlar, W.G. – “Discrete Element Modelling to Predict the Modulus of Asphalt Concrete Mixtures” – Journal of Materials in Civil Engineering ASCE March/April 2004,. [You, Z. and Buttlar, W.G; 2004]
- Zengal, M. – “A discrete element study of the resilient behaviour of granular materials” – 16th ASCE Engineering Mechanics Conference, Seattle, 2003. [Zengal, M.; 2003]

Zhang, W and Ullidtz,P; - “Estimation of the plastic strain in the pavement subgrade and the pavement functional condition” <http://www.ctt.dtu.dk/group/rtm/Performance-350.pdf> (c3)
[Zhang, W and Ullidtz, P; 2004]

Zhang, W. and Macdonald, R. – “Response and performance of a test pavement to one Freeze-Tow Cycle”, Danish Road Institute, Report 102, Copenhagen, 2000. [Zhang, W. and Macdonald, R.; 2000]

Zhang, W. and Ullidtz, P. – “Back-calculation of pavement layer moduli and forward calculation of stresses and strains”, ISAP, Copenhagen, 2002. [Zhang, W. and Ullidtz, P.; 2002]

Annex 1 - Current FWD analysis programs

Results of a Questionnaire issued by COST336
[COST 336, 2002]

		UCESLAB	PAVERS	BAP	EVERCALC 5.0	CARE
	Input requirements and method of operation					
1	Pavement Type (rigid, flexible, both)	Rigid	Flexible	Flexible	Flexible	Flexible
2	Analysis Method (static or dynamic)	Static	Static	Static	Static	Static
3	Maximum number of geophones	9	7	9	10	9
4	Measurement format (Dynatest F20)	n/a	n/a		Dynatest Edition+C61 20	Both F20 and F25
5	Analyses all test points or statistically representative test points	n/a	n/a		User selected (all or individual test locations)	Sas desired
6	Maximum number of independent layers	1: slab on grade	4	5	5	4
7	Seed Moduli required (Yes/No)	The method uses the static Young's modulus of the Cement Concrete as a fixed input. It must be determined by resonance measurements. In fact the program backcalculates the slab support conditions of interior and edge.	Yes	Yes	Yes, if more than 3 layers are specified	Yes
8	Layer Modulus Constraints (required, optional)	n/a	Optional	Required	Optional	Optional
9	Ability to fix modulus (yes, no)	n/a	Yes	Yes	Yes	Yes
10	Layer interface analysis (Fixed or variable friction)	n/a	TEMPUS	Fixed friction	Fixed	Fixed or total slip
11	Convergence Criteria (root mean square, sum of squares, absolute sum)	Manually controlled iterative technique (trial-and-error)	Manually controlled iterative technique (trial-and-error)	Sum of squares	Root mean square	Choice of: 1) root mean square of relative deviations; 2) root mean square of absolute deviations;
12	Convergence Criteria (percent, mils or microns)	n/a	n/a	Percent	Percent	
13	Forward calculation method (Multi layered linear elastic)	Slab on Pasternak or Winkler foundation	Linear elastic (isotropic)	Multilayered	Multilayered linear elastic	Multilayered linear elastic
14	Forward analysis program (WESDEF)	Van Cauwelaert	Van Cauwelaert (improved WESDEF)	BISTRO	Weslea	WESDEF
15	Layer Stiffness calculation method (bowl matching)	Bowl matching: E concrete and H fixed; varying K and G foundation parameters)	Matching: E varying, H	Bowl matching	Bowl matching	Bowl matching

		UCESLAB	PAVERS	BAP	EVERCALC 5.0	CARE
16	Subgrade modeling:					
	-semi-infinite (Y/N)	n/a	Yes	Yes	Yes	Yes
	-stiff layer at depth (Y/N)	n/a	No	Yes	Yes	No
	- other	Slab on Pasternak or Winkler foundation; backcalculation of interior and slab edge positions. The latter requires the load transfer as an extra input parameter	n/a			
17	For rigid, what parameters? (e.g. load transfer, K values at corners)	Young's modulus concrete and poisson ratio, deflection bowl, plate thickness, load transfer deflection ratio (edge only)	n/a			
	Output Possibilities					
18	Output file format (formatted ASCII., ASCII comma delimited)	All options possible; also printable	All options possible; also printable	Formatted ASCII	ASCII comma delimited, formatted ASCII	Database for residual life analysis module
19	Layer stiffness moduli at test temp (Y/N)	n/a	Yes	Yes	Yes, for asphalt layer	Yes
20	Layer stiffness moduli at standard temp (Y/N)	n/a, rigid	E-T mix relations	No	Yes, for asphalt layer	Yes
21	Is standard temp fixed or variable, if fixed, what is it (20 C)	n/a	Variable load time and temperature		User specified	Variable depending on air temperature acc. To SPDM
22	Temperature correction approach (none, fixed, variable)	n/a	Shell E-T	None	Fixed	Variable acc.to chosen stiffness characteristic
23	Stresses and strains (fixed or user defined positions)	Stresses at user defined positions	All options possible		User defined positions	Fixed positions
24	Residual lives (fixed or userdefined method)	Yes, fatigue law and airplane loads can either be selected from database or can be user defined; lateral distribution of aircraft traffic is included	Yes, fatigue law and airplane loads can either be selected from database or can be user defined; lateral distribution of aircraft traffic is included		Not used in analysis	Semi-fixed but user can define fatigue and stiffness graphs, temperature, speed, design load and such
25	Overlay thickness (Fixed or user defined method)	No	No		Not used in analysis	Semi-fixed but user can define fatigue and stiffness graphs, temperature, speed, design load and such
26	Goodness of fit (percent error between measured and predicted bowls)	Yes	Yes	Percent error	Percent error between measured and predicted	2% considered good; 2-5% as dubious, more than 5% bad
27	Batch processing (backcalculation) of multiple FWD files (Yes/No)	No	No	Yes	Batch processing	

		CANUV	BOUSDEF	MODCOMP 5	UMPED	PEDD	MICHBACK
	Input requirements and method of operation						
1	Pavement Type (rigid, flexible, both)	Flexible	Primarily for flexible, but it has been used successfully for rigid	Both	Rigid and flexible both; composite; unpaved	Rigid and flexible both; composite	Flexible
2	Analysis Method (static or dynamic)	Static	Static	Static	Static analysis	Static (dynamic analysis option being developed)	Static
3	Maximum number of geophones	7	7	Up to 12 geophones, up to 8 load levels	7; minimum 4; FWD, Dynaflect	7 or more; minimum 4; FWD, Dynaflect	10
4	Measurement format (Dynatest F20)	KUAB .DAT	User input	Any	Dynatest standard or manual data entry	Dynatest KUAB, PRI standard or manual entry	KUAB, ASCII
5	Analyses all test points or statistically representative test points	All test points	All test points	User controlled	All points and all drops; peak or history data	All points and all drops; peak or history data	Both
6	Maximum number of independent layers	3: one asphalt layer (from all asphalt layers), subbase (bound or unbound) and subgrade	5	up to 12 layers (max. 5 or 6 unknown layers recommended)	4	4	4
7	Seed Moduli required (Yes/No)	Yes (user defined)	Yes	Yes	No; auto predicted by program; input allowed	No; auto predicted by program; input not allowed	Yes, but internally generated
8	Layer Modulus Constraints (required, optional)	Optional	Required	Internal to program	Optional; default shown	Not required; only layer material type required	Optional
9	Ability to fix modulus (yes, no)	No	Yes	Yes, can fix layer moduli or K1 and k2 parameters.	Yes, optional	Not allowed	Yes
10	Layer interface analysis (Fixed or variable friction)	Fixed	Fixed	Fixed	Fixed	Fixed	Fixed
11	Convergence Criteria (root mean square, sum of squares, absolute sum)		Absolute sum	RMS error reported, but not a convergence criterion	Minimum absolute difference	Minimum absolute difference	Root mean square
12	Convergence Criteria (percent, mils or microns)	Percent	Percent	Percent, mils or microns as well as rate of change of moduli	Percent	Percent	Percent
13	Forward calculation method (Multi layered linear elastic)	Multilayered linear elastic	Multilayered linear elastic	Multilayered linear or nonlinear elastic	Multilayered linear elastic	Multilayered linear elastic	Multilayered linear elastic
14	Forward analysis program (WESDEF)	OPMEKO (results nearly to BISTRO)	Boussinesq theory and MET	CHEVLAY 2 (corrected version)	PAVRAN (based upon ELSYM5)	PAVRAN (based upon ELSYM5)	Enhanced Chevron
15	Layer Stiffness calculation method (bowl matching)	Bowl matching	Bowl matching	Iterative, deflection matching	Deterministic equations and bowl matching	Deterministic equations and bowl matching	Bowl matching

STRUCTURAL EVALUATION OF FLEXIBLE PAVEMENTS USING NON-DESTRUCTIVE TESTS

		CANUV	BOUSDEF	MODCOMP 5	UMPED	PEDD	MICHBACK
16	Subgrade modeling:						
	-semi-infinite (Y/N)	Yes	Yes	Yes	Yes	Yes	Yes, optional
	-stiff layer at depth (Y/N)	No	Can be fixed by user	Yes	Yes	Yes	Yes, optional
	- other			Internal routine to predict stiff layer depth	Option to create a rigid bottom	Option to create a rigid bottom	
17	For rigid, what parameters? (e.g. load transfer, K values at corners)			Moduli of all layers (interior slab model)	E only	E; K at mid slab, interior	
	Output Possibilities						
18	Output file format (formatted ASCII, ASCII comma delimited)	ASCII, DBF	ASCII	Formatted ASCII, user specified amount of output	Text	Text	Formatted ASCII
19	Layer stiffness moduli at test temp (Y/N)	Yes	Does not correct for temp	Yes	Yes	Yes	Yes
20	Layer stiffness moduli at standard temp (Y/N)	Yes	Does not correct for temp	No	Yes	Yes	Yes
21	Is standard temp fixed or variable, if fixed, what is it (20 C)	Fixed (11 C)	Does not correct for temp		Variable; default 21 C (70 F)	Variable; default 21 C (70 F)	Fixed at 20 C
22	Temperature correction approach (none, fixed, variable)	Fixed	Does not correct for temp		Variable; default available	Variable; default available	Fixed statistical
23	Stresses and strains (fixed or user defined positions)	Fixed at the bottom of stiff layers	Does not calculate	Use NELAPAV for forward calculations at user-defined positions using MODCOMP models.	User defined positions; default available	User defined positions (loads/responses); default	Fixed
24	Residual lives (fixed or userdefined method)	Fixed	Does not calculate	Ditto	No; only modulus backcalculation	AASHTO equations; modulus backcalculation	
25	Overlay thickness (Fixed or user defined method)	Fixed	Does not calculate	Ditto	No	Yes; AASHATO equations; modulus backcalculation	User defined
26	Goodness of fit (percent error between measured and predicted bowls)	Percent error between measured and calculated bowl	Percent error	RMS error, plus interpretive comments	Maximum % error 10% cycle 1; 20% later	Maximum % error 10% cycle 1; 20% later	Yes
27	Batch processing (backcalculation) of multiple FWD files (Yes/No)	Yes	No	Yes, unlimited number	Yes	No; one data file at a time	No

		MFPDS	DAPS	EFROMD2	ELMOD	MODULUS 5.0	SIDMOD
	Input requirements and method of operation						
1	Pavement Type (rigid, flexible, both)	Flexible	Both	Flexible	Both	Both	Both
2	Analysis Method (static or dynamic)	Static	Static	Static	Static	Static	Static
3	Maximum number of geophones		9	User's input (unrestricted)	15	7 or less	10
4	Measurement format (Dynatest F20)	KUAB, ASCII	F20+others as required	Link with Excel input sheets	All Dynatest file formats	Any Dynatest	Dynatest.F25
5	Analyses all test points or statistically representative test points	Both	All good bowls	Link with Excel output sheets	All test points	All points	All test points
6	Maximum number of independent layers	4	4	User's input (maximum 12 layers)	5	4	Cannot exceed n° of deflection, works best for 3 unknowns
7	Seed Moduli required (Yes/No)	Yes, but internally generated	No	Yes	No	Subgrade	Yes
8	Layer Modulus Constraints (required, optional)	Optional	No	Required/Optional	Optional	Required	Required
9	Ability to fix modulus (yes, no)	Yes	No	Yes	Yes	Yes	Yes
10	Layer interface analysis (Fixed or variable friction)	Fixed	Fixed	Fixed/variable	Fixed	Fixed	Fixed
11	Convergence Criteria (root mean square, sum of squares, absolute sum)	Root mean square	RMS	Error Function = $\{\text{Sum} [\text{weight} \cdot (1 - \text{estimated deflection}/\text{actual deflection})]^2 / \text{Sum} [\text{weight}^2]\}^{0,5}$	RMS (either mils, microns, or %)	Weighted Absolute Sum	Modulus Tolerance
12	Convergence Criteria (percent, mils or microns)	Percent	Percent	Percent	Any	Percent	Percent
13	Forward calculation method (Multi layered linear elastic)	Multilayered linear elastic	Multilayered linear elastic	Multilayered linear elastic	Odemark-Boussinesq (method of equivalent thicknesses)	Multilayered elastic	Multilayered linear elastic
14	Forward analysis program (WESDEF)	Enhanced Chevron	ELSYS	CIRCLY	None but WESDEF can be used to calibrate MET results	Weslea	BISAR for flexible, FEM & Spline semi-analysis method for rigid
15	Layer Stiffness calculation method (bowl matching)	Bowl matching	Singular Value Dicomposition	Bowl matching	Bowl matching or radius of curvature	Bowl matching	Bowl matching

STRUCTURAL EVALUATION OF FLEXIBLE PAVEMENTS USING NON-DESTRUCTIVE TESTS

		MFPDS	DAPS	EFROMD2	ELMOD	MODULUS 5.0	SIDMOD
16	Subgrade modeling:		Single Layer with Rock Depth				
	-semi-infinite (Y/N)	Yes, optional	Available	Yes	Yes	Optional	Yes
	-stiff layer at depth (Y/N)	Yes, optional	Available	Yes	Yes	Yes	Yes
	- other			Nonlinear elastic	Nonlinear stress softening	User input	Can backcalculate the depth of the stiff layer
17	For rigid, what parameters? (e.g. load transfer, K values at corners)				K midslab, K joints, K corners, load transfer (%)	E moduli only	E for slab, E or K for subgrade
	Output Possibilities						
18	Output file format (formatted ASCII, ASCII comma delimited)	Formatted ASCII and ASCII comma delimited	ASCII and EXCEL compatible	Formatted ASCII	ASCII comma delimited	ASCII	Formatted ASCII
19	Layer stiffness moduli at test temp (Y/N)	Yes	Yes	Yes	Yes	Yes	Yes
20	Layer stiffness moduli at standard temp (Y/N)	Yes	No	No (link with Excel design sheets)	No	No	Yes
21	Is standard temp fixed or variable, if fixed, what is it (20 C)	Fixed at 20 C	n/a	As above	Variable	No	20 C
22	Temperature correction approach (none, fixed, variable)	Statistical and thermodynamic	None	As above	Variable	External	Variable
23	Stresses and strains (fixed or user defined positions)	Fixed	Calculated	As above	Fixed	No	User defined positions
24	Residual lives (fixed or userdefined method)			As above	User defined	Fixed	Fixed
25	Overlay thickness (Fixed or user defined method)	User defined		As above	User defined	No	Not finished
26	Goodness of fit (percent error between measured and predicted bowls)	Yes	Reported	Percent error between measured and predicted	RMS, measured vs. calculated bowls	Yes	Percent error between measured and predicted bowls
27	Batch processing (backcalculation) of multiple FWD files (Yes/No)	No	Available	Yes	Yes (for backcalculation but not remaining life/overlay requirements)	No	No

ANNEX 2 – ANN performance (sensitivity to input variations)

Results obtained for the average difference between the target moduli and the ANN response

Road Pavement

h3 data	ANN:var	E1			E2			E3			legend average error Er
		0	-%	+%	0	-%	+%	0	-%	+%	
Trained: hvar	A1:2-5%	0	-%	+%	0	-%	+%	0	-%	+%	
Tested: hvar	D0	4%	12%	12%	4%	8%	8%	3%	4%	3%	
	D3	4%	6%	5%	4%	7%	6%	3%	5%	4%	
	D6	4%	4%	4%	4%	4%	4%	3%	4%	3%	
	h1	4%	11%	12%	4%	7%	8%	3%	3%	3%	
	h2	4%	4%	5%	4%	4%	5%	3%	3%	3%	
Trained: hvar	A1:10%										
Tested: hvar	D0	4%	56%	39%	4%	30%	30%	3%	17%	5%	
	D3	4%	21%	15%	4%	23%	40%	3%	38%	20%	
	D6	4%	7%	6%	4%	8%	8%	3%	9%	11%	
	h1	4%	12%	12%	4%	7%	9%	3%	3%	3%	
	h2	4%	5%	5%	4%	7%	7%	3%	4%	3%	
Trained: 1.25m	A2:2-5%										
Tested: hvar	D0	11%	15%	16%	22%	22%	25%	22%	21%	22%	
	D3	11%	12%	11%	22%	23%	22%	22%	22%	22%	
	D6	11%	12%	11%	22%	22%	22%	22%	22%	22%	
	h1	11%	16%	15%	22%	25%	22%	22%	22%	21%	
	h2	11%	12%	11%	22%	25%	22%	22%	22%	21%	
Trained: 2.00m	A3:2-5%										
Tested: hvar	D0	16%	24%	15%	25%	27%	25%	27%	27%	27%	
	D3	16%	15%	16%	25%	25%	26%	27%	27%	27%	
	D6	16%	16%	16%	25%	25%	25%	27%	28%	27%	
	h1	16%	27%	14%	25%	24%	28%	27%	27%	27%	
	h2	16%	15%	16%	25%	25%	26%	27%	27%	27%	

Airport Pavement

h3 data	ANN:var	E1			E2			E3			E4		
		0	-%	+%	0	-%	+%	0	-%	+%	0	-	+
Trained: hvar	B1:2-5%												
Tested: hvar	D0	4%	10%	11%	5%	21%	20%	4%	9%	7%			
	D3	4%	6%	6%	5%	16%	17%	4%	10%	10%			
	D6	4%	4%	5%	5%	7%	7%	4%	6%	7%			
	h1	4%	5%	6%	5%	14%	16%	4%	5%	6%			
	h2	4%	4%	4%	5%	5%	6%	4%	4%	4%			
Trained: hvar	B1:10%												
Tested: hvar	D0	4%	50%	40%	5%	59%	75%	4%	29%	20%			
	D3	4%	24%	21%	5%	42%	48%	4%	27%	25%			
	D6	4%	12%	9%	5%	22%	18%	4%	15%	14%			
	h1	4%	9%	10%	5%	28%	29%	4%	7%	9%			
	h2	4%	4%	4%	5%	7%	8%	4%	5%	5%			
Trained: 1.20m	B2a:2-5%												
Tesed: hvar	D0	3%	7%	10%	13%	10%	24%	13%	13%	13%			
	D3	3%	6%	4%	13%	20%	9%	13%	13%	13%			
	D6	3%	4%	6%	13%	9%	21%	13%	12%	14%			
	h1	3%	5%	7%	13%	23%	9%	13%	13%	13%			
	h2	3%	4%	3%	13%	16%	11%	13%	13%	13%			
Trained: 1.20m	B2b-2%												
Tested: 1.20m	D0	2%	8%	10%	5%	9%	21%	2%	2%	2%			
	D3	2%	5%	3%	5%	15%	5%	2%	2%	1%			
	D6	2%	3%	5%	5%	6%	17%	2%	2%	3%			
	h1	2%	5%	7%	5%	18%	7%	2%	2%	1%			
	h2	2%	2%	2%	5%	9%	4%	2%	2%	1%			
Trained: 1.20m	B2c-10%												
Tested: 1.20m	D0	2%	41%	33%	5%	42%	65%	2%	9%	4%			
	D3	2%	19%	16%	5%	51%	29%	2%	3%	4%			
	D6	2%	14%	17%	5%	33%	54%	2%	13%	8%			
	h1	2%	11%	12%	5%	32%	18%	2%	3%	2%			
	h2	2%	3%	2%	5%	12%	5%	2%	2%	1%			
Trained: 2.0m	B3-2%												
Tested: hvar	D0	4%	10%	9%	15%	23%	15%	17%	18%	17%			
	D3	4%	5%	6%	15%	14%	20%	17%	17%	17%			
	D6	4%	5%	5%	15%	22%	15%	17%	19%	16%			
	h1	4%	7%	7%	15%	15%	23%	17%	17%	18%			
	h2	4%	4%	4%	15%	14%	17%	17%	17%	17%			
Trained: 1.20m	B4-2%												
Tested: 1.20m	D0	3%	28%	23%	8%	34%	45%	3%	6%	6%	2%	3%	3%
	D3	3%	7%	6%	8%	19%	25%	3%	14%	13%	2%	3%	3%
	D6	3%	6%	6%	8%	25%	19%	3%	9%	9%	2%	3%	3%
	h1	3%	4%	4%	8%	21%	16%	3%	4%	5%	2%	2%	2%
	h2	3%	3%	3%	8%	9%	8%	3%	4%	4%	2%	2%	2%
	h3	3%	3%	3%	8%	8%	10%	3%	4%	5%	2%	2%	2%

legend
average error Er

<10% 10-25% >25%

ANNEX 3 – Case study results

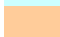
Average difference between the measured deflections
and the calculated based on ANN pavement structure

Case study

	location	D0	D1	D2	D3	D4	D5	D6
Zone 1	50	6%	10%	8%	9%	10%	10%	4%
	125	-4%	-5%	-1%	-2%	0%	6%	5%
	200	1%	1%	1%	2%	0%	1%	-5%
	275	9%	11%	21%	20%	26%	34%	40%
	350	-2%	-2%	-5%	-5%	-8%	-10%	-10%
	425	-1%	-2%	-1%	-1%	-1%	0%	-1%
	500	-1%	-2%	-3%	0%	3%	7%	3%
	575	-3%	0%	0%	1%	4%	11%	14%
	650	-5%	-3%	4%	0%	7%	15%	17%
	725	14%	19%	21%	25%	29%	37%	34%
average error		4%	4%	5%	4%	6%	11%	11%
zone 2	800	2%	1%	2%	3%	6%	6%	-3%
	875	3%	4%	9%	8%	11%	16%	13%
	950	6%	9%	14%	23%	38%	41%	16%
	1025	-2%	3%	0%	2%	1%	6%	3%
	1100	4%	2%	3%	6%	6%	5%	-11%
	1175	18%	22%	23%	26%	32%	39%	30%
	1250	-9%	-9%	-7%	-7%	-6%	-3%	-16%
	1325	19%	28%	49%	64%	109%	153%	176%
	1400	-2%	6%	14%	28%	52%	78%	84%
	1475	2%	9%	18%	32%	57%	87%	107%
	1550	-5%	-5%	-2%	-1%	2%	4%	-13%
	1625	2%	2%	6%	5%	8%	13%	7%
	1700	6%	4%	4%	6%	4%	3%	-5%
	1775	32%	34%	54%	66%	94%	121%	129%
	1850	6%	5%	5%	6%	4%	3%	-8%
	1925	2%	2%	3%	5%	5%	4%	-12%
	2000	4%	7%	6%	7%	7%	11%	8%
	2075	8%	8%	11%	18%	24%	28%	10%
	2150	-4%	-6%	-2%	-2%	-1%	1%	-15%
	2225	3%	2%	5%	8%	12%	14%	-7%
2300	45%	55%	70%	87%	125%	152%	131%	
2375	7%	4%	4%	5%	2%	0%	-10%	
average error		5%	5%	5%	7%	9%	10%	10%

legend:

 - relative error < 5%

 - outliers

bold - average error per zone without the outliers